

The role of glycosyltransferase 61 and BAHD genes
in determining ferulate & *para*-coumarate content
of the cell walls of the Poaceae

Lucy Sarah Hyde

Doctor of Philosophy

University of York

Biology

September 2016

Abstract

Lignocellulosic biomass, composed largely of plant cell walls, of economically important cereal crops is remarkably recalcitrant to digestion, both in second generation biofuel production and ruminant nutrition applications. Ferulic acid (FA) esterified to arabinoxylan (AX) forms oxidatively-linked dimers and oligomers which cross-link polysaccharide chains. FA is also a nucleation site for lignin formation. These cross-links are major inhibitors of enzymatic digestion, and therefore FA is a key target for improving the digestibility of grass cell walls. Also, *para*-coumaric acid (*p*CA) esterified to AX may be involved in the polymerisation of lignin.

Despite the importance of cell wall-bound hydroxycinnamic acids, many of the genes and enzymes responsible for the esterification of *p*CA and FA to AX remain to be elucidated. The BAHD and glycosyltransferase (GT)61 gene families have previously been identified as likely to be involved in the process (Mitchell et al., 2007). Here, the role of candidate genes within the BAHD and GT61 families in *p*CA and FA esterification to AX is investigated in the model organism *Brachypodium distachyon* (Brachypodium).

Jasmonic acid induced large increases in cell wall-esterified *p*CA, and moderate increases in FA and FA dimer in Brachypodium callus, accompanied by up-regulation of genes within the BAHD and GT61 families. Furthermore, transformation of Brachypodium with RNAi constructs designed to knock-down expression of paralogues *BdGT61.9p1* and *BdGT61.9p2* resulted in decreased cell wall-esterified FA. Overexpression of *BdGT61.9p1* in Brachypodium resulted in a small increase in the 8-8-coupled FA dimer. These findings complemented the existing body of evidence for the involvement of genes within the BAHD and GT61 families in hydroxycinnamic acid esterification to AX.

Table of Contents

Abstract.....	2
Table of contents.....	3
List of Figures.....	8
List of Tables.....	12
Acknowledgements.....	13
Declaration.....	15
Chapter 1. General Introduction	17
1.1 The Poaceae and the commelinid monocots	17
1.2 Second generation liquid biofuels	18
1.3 Ruminant nutrition.....	19
1.4 Cell walls	19
1.5 Xylan structure	21
1.6 Cell wall-bound hydroxycinnamic acids (HCAs)	25
1.6.1 Cell wall-bound ferulic acid (FA)	25
1.6.2 Cell wall-bound ferulic acid (FA) dimers.....	26
1.6.3 FA cross-link to lignin.....	29
1.6.4 FA cross-linking in digestibility.....	30
1.6.5 Cell wall-bound <i>para</i> -coumaric acid (<i>pCA</i>).....	30
1.6.6 Cell wall-bound sinapic acid	31
1.7 Glucurono- and arabinoxylan synthesis	32
1.7.1 Discovery of xylan synthesis genes.....	32
1.7.2 Synthesis of the β -(1-4)-xylan backbone	33
1.7.3 Dicot GX side chain synthesis.....	34
1.7.4 Arabinoxylan (AX) synthesis in the Poaceae.....	34
1.7.5 Conservation of <i>IRX</i> genes.....	36
1.7.6 The xylan synthase complex	36

1.8	FA synthesis genes.....	39
1.8.1	BAHD acyl transferases in feruloylation.....	39
1.8.2	Glycosyltransferase 61 family in feruloylation	42
1.9	Brachypodium	46
1.10	Project aims.....	48
Chapter 2. General Materials and Methods		49
2.1	Chemicals and reagents.....	49
2.2	Plant growth and harvest	49
2.3	Tissue preparation	49
2.4	Alcohol insoluble residue (AIR) preparation	49
2.5	Destarching of alcohol insoluble residue	50
2.6	Matrix polysaccharides extraction and analysis	51
2.7	Crystalline cellulose extraction and analysis.....	51
2.8	Lignin extraction and analysis	52
2.9	Silica analysis.....	52
2.10	Saccharification.....	53
2.11	Cell wall-bound phenolic acid extraction.....	53
2.12	High performance liquid chromatography (HPLC).....	54
2.13	Standard cloning procedure	55
2.14	Agrobacterium transformation	55
2.15	Callus generation	56
2.16	Brachypodium transformation.....	56
2.17	DNA isolation	57
2.18	Quantitative PCR (qPCR) to determine zygosity	58
2.19	RNA isolation	58
2.20	Western blotting.....	60
2.21	Microscopy	61

Chapter 3. The Effect of Mechanical Stress on Cell Wall Composition in <i>Brachypodium distachyon</i>	62
3.1 Introduction.....	62
3.2 Chapter 3 specific methods	66
3.2.1 Plant growth.....	66
3.2.2 Mechanical stress.....	66
3.2.3 Overview of mechanical stress experiments.....	66
3.2.4 Statistics.....	70
3.3 Results	71
3.3.1 Plant growth.....	71
3.3.2 Cell wall-bound phenolic acids.....	72
3.3.3 Cell wall monosaccharides and lignin	74
3.3.4 Silica	74
3.3.5 Digestibility.....	77
3.4 Discussion.....	79
3.4.1 Stem length	79
3.4.2 Cell wall-bound FA and FA dimers	79
3.4.3 Lignin	81
3.4.4 Cell wall monosaccharides	81
3.4.5 Silica	83
3.4.6 Digestibility.....	84
3.4.7 Conclusion	84
Chapter 4. Methyl-Jasmonate Induces Increased Wall-Bound Ferulic Acid and <i>p</i> -Coumaric Acid and Expression of BAHD and GT61 Family Arabinoxylan Synthesising Genes in <i>Brachypodium distachyon</i> Callus.....	86
4.1 Introduction.....	86
4.2 Chapter 4 specific methods	90
4.2.1 <i>Brachypodium</i> hydroponics.....	90

4.2.2	Callus generation and growth	90
4.2.3	Preparation of methyl-jasmonate stock solutions	91
4.2.4	Brachypodium callus experiments.....	91
4.2.5	Mild acid hydrolysis	92
4.2.6	Statistics.....	92
4.2.7	RNA sequencing.....	93
4.3	Results.....	95
4.3.1	Brachypodium seedlings: hydroponics experiment	95
4.3.2	Brachypodium callus: JA concentration experiment	97
4.3.3	Cell wall-bound pCA and FA	97
4.3.4	Cell wall polysaccharides	100
4.3.5	Mild acid hydrolysis	102
4.3.6	Brachypodium Callus 50 μ M meJA time course experiment.....	103
4.3.7	Cell wall composition	103
4.3.8	RNA-seq transcriptome.....	107
4.3.9	Cell wall genes	107
4.4	Discussion.....	115
4.4.1	Cell wall-bound pCA and FA	115
4.4.2	Cell wall genes	117
4.4.3	BAHD and GT61 family genes.....	118
4.4.4	Conclusion	119
Chapter 5. Effects of Glycosyltransferase (GT)61.9 Overexpression and RNAi on Cell Wall Composition, and an Investigation of the Expression Driven by Upstream Regions from the two GT61.9 Paralogues, in <i>Brachypodium distachyon</i>		
5.1	Introduction.....	121
5.2	Chapter 5 specific methods	125
5.2.1	Phylogenetic tree construction.....	125

5.2.2	Vector design of <i>GT61.9p1</i> overexpression construct.....	126
5.2.3	Vector design of <i>GT61.9p1</i> and <i>p2</i> RNAi construct.....	127
5.2.4	Brachypodium transformation.....	130
5.2.5	Determination of zygoty	130
5.2.6	Experimental design	131
5.2.7	Analyses of <i>GT61.9</i> overexpression and RNAi lines	131
5.2.8	Statistics.....	131
5.2.9	<i>GT61.9p1</i> and <i>p2</i> promoter-GFP fusion experiment.....	132
5.2.10	Analyses of <i>GT61.9p1</i> and <i>p2</i> promoter-GFP fusion.....	134
5.3	Results.....	135
5.3.1	Phylogenetic tree of the GT61 family	135
5.3.2	Overexpression of <i>GT61.9p1</i> in Brachypodium.....	135
5.3.3	RNAi knockdown of <i>GT61.9p1</i> and <i>p2</i> in Brachypodium.....	143
5.3.4	Expression patterns of <i>GT61.9p1</i> and <i>p2</i> in Brachypodium	149
5.4	Discussion.....	154
Chapter 6. General Discussion		159
6.1	Summary of results.....	159
6.2	BAHDs and GT61s in FA and <i>pCA</i> esterification to arabinoxylan.....	160
6.3	Functional redundancy with the BAHD and GT61 families.....	162
6.4	The difficulty in studying cell wall-bound FA and <i>pCA</i>	164
6.5	Brachypodium as a model organism for the grasses	165
6.6	Further work	165
6.7	Concluding remarks.....	167
Appendices.....		168
Appendix A Expression of genes within the GT61 and BAHD families in rice root and shoot when treated with jasmonic acid.....		168

Appendix B The effect of jasmonic acid on cell wall-bound ferulic acid dimers in root and shoot of hydroponically grown <i>Brachypodium distachyon</i>	169
Appendix C The effect of 17 d treatment with increasing concentrations of methyl-jasmonate on individual cell wall-bound ferulic acid dimer isomers in <i>Brachypodium distachyon</i> callus.....	170
Appendix D The effect of 1-8 d treatment with 50 μ M methyl-jasmonate on cell wall-bound ferulic acid dimer isomers in <i>Brachypodium distachyon</i> callus.....	171
Appendix E Venn diagram showing counts of differentially expressed genes (DEGs) with 50 μ M meJA or a mock control for 1, 2, 4 or 8 d.....	172
Appendix F Changes in gene expression of upregulated cell wall synthesis genes after 1, 2, 4 or 8 d treatment with 50 μ M meJA in <i>Brachypodium distachyon</i> callus	173
Appendix G Changes in gene expression of downregulated cell wall synthesis genes after 1, 2, 4 or 8 d treatment with 50 μ M meJA in <i>Brachypodium distachyon</i> callus.....	174
Appendix H Comparison of the effect of jasmonic acid on gene expression profiles of selected genes in <i>Brachypodium distachyon</i> callus, rice shoot and root.....	175
Appendix I Gene expression data highlighting the differences in gene expression of <i>Brachypodium distachyon</i> paralogues GT61.9p1 (Bradi1g06560) and p2 (Bradi3g11337).....	177
Appendix J RNAi sequence designed to simultaneously knock down the expression of GT61.9p1 and GT61.9p2 in <i>Brachypodium distachyon</i>	178
Appendix K Phylogenetic tree of GT61 family genes showing bootstrap values.....	179
Appendix L An example of using qPCR to determine zygosity.....	180
Definitions	181
References.....	184

List of Figures

Figure 1.1 Schematic representation of xylan side chain variation in dicots and grasses.	24
Figure 1.2 Schematic representation of known cell wall-bound HCAs associated with arabinoxylan and lignin	27
Figure 1.3 Mechanism of peroxidase- and H ₂ O ₂ -mediated dimerisation of FA into the five possible isomers found in plant cell walls.....	28
Figure 1.4 Phylogenetic tree of two clades within the BAHD family which are differentially expressed in monocot and dicot species and therefore are candidates for AX feruloylation	41
Figure 1.5 Phylogenetic tree of rice, wheat, <i>Brachypodium</i> and <i>Arabidopsis GT61</i> genes	43
Figure 1.6 Two models for the role of BAHD acyltransferases and glycosyltransferase (GT)61.9 enzymes in the synthesis of hydroxycinnamic acid (HCA) side chain synthesis of arabinoxylan (AX) in grasses.....	45
Figure 3.1. Experimental design of mechanical stress treatment of <i>Brachypodium distachyon</i>	68
Figure 3.2 The effect of 3 weeks of mechanical stress on stem length and internode number in <i>Brachypodium distachyon</i>	71
Figure 3.3 The effect of 4 weeks of mechanical stress on relative wall-bound ferulic acid (FA) and <i>para</i> -coumaric acid (<i>pCA</i>) in <i>Brachypodium distachyon</i> tissues.....	73
Figure 3.4 The effect of 1 week of mechanical stress on wall-bound hydroxycinnamic acids (HCAs): ferulic acid (FA), FA dimer and <i>para</i> -coumaric acid (<i>pCA</i>) in young <i>Brachypodium distachyon</i> stem and leaf tissue	73
Figure 3.5 The effect of 3 weeks of mechanical stress on monosaccharide concentrations in <i>Brachypodium distachyon</i> tissues	75
Figure 3.6 The effect of 3 weeks mechanical stress on lignin content in <i>Brachypodium distachyon</i> tissues.	76
Figure 3.7 The effect of 4 weeks or 3 weeks mechanical stress on silica content in <i>Brachypodium distachyon</i> stem and leaf.....	76

Figure 3.8 The effect of 4 weeks or 3 weeks mechanical stress on saccharification potential in <i>Brachypodium distachyon</i> stem and leaf.....	78
Figure 4.1 The effect of 24 h or 48 h treatment with 100 μ M (\pm)-jasmonic acid (JA) on <i>para</i> -coumaric acid (pCA) and ferulic acid (FA) monomer and dimer (\pm SE) in hydroponically grown <i>Brachypodium distachyon</i> seedling roots and shoots.....	96
Figure 4.2 The effect of 17 d treatment with increasing concentrations of methyl-jasmonate on <i>para</i> -coumaric acid (pCA) and ferulic acid (FA) monomer and dimer in <i>Brachypodium distachyon</i> callus	99
Figure 4.3 Monosaccharide concentrations of destarched alcohol insoluble residue (AIR) in <i>Brachypodium distachyon</i> callus after 17 d treatment with varying concentrations of methyl-jasmonate	101
Figure 4.4 The effect of 1, 2, 4 and 8 d treatment with 50 μ M methyl-jasmonate (meJA) on <i>para</i> -coumaric acid (pCA) and ferulic acid (FA) monomer and dimers in <i>Brachypodium distachyon</i> callus cell walls	105
Figure 4.5 The effect of 50 μ M methyl-jasmonate (meJA) on cell wall monosaccharides and lignin in <i>Brachypodium distachyon</i> callus destarched AIR (alcohol insoluble residue) after 1, 2, 4 and 8 d treatment.....	106
Figure 4.6 Mapped and unmapped reads in <i>Brachypodium distachyon</i> callus RNA sequencing analysis.....	109
Figure 4.7 MDS plot showing clustering of RNA sequencing samples of <i>Brachypodium distachyon</i> treated with 50 μ M meJA for 24 h, 48 h, 4 d or 8 d, compared to a mock control.....	110
Figure 4.8 List of top 20 represented Gene Ontology (GO) terms for each GO category (cellular process, molecular function and biological process) and no. of sequences associated, for DEGs with meJA treatment in <i>Brachypodium distachyon</i> callus treated with 50 μ M meJA and sampled at 1, 2, 4 and 8 d.	111
Figure 4.9 Heat map of cell wall differentially expressed genes (DEGs) with meJA treatment.....	112
Figure 4.10 Kyoto Encyclopedia of Genes and Genomes (KEGG) analysis of differentially expressed genes with 50 μ M meJA treatment in <i>Brachypodium distachyon</i> callus, and schematic diagram of differentially expressed genes in the phenylpropanoid synthesis pathway)	114

Figure 5.1 Protein alignment of <i>Brachypodium distachyon</i> paralogous genes <i>Bradi1g06560</i> (<i>GT61.9p1</i> here) and <i>Bradi3g11337</i> (<i>GT61.9p2</i> here) with rice gene <i>OsXAX1</i>	123
Figure 5.2 A schematic diagram (not to scale) of the construct ordered from Genscript®, USA, to be used for overexpression of <i>GT61.9p1</i> in <i>Brachypodium distachyon</i>	126
Figure 5.3 A diagram of the A224p6i-U-Gusi master vector used for transformation of <i>Brachypodium distachyon</i>	128
Figure 5.4 A schematic diagram of the cloning procedure used to create vector <i>pUbi::GT61.9p1-Myc</i>	129
Figure 5.5 A schematic diagram of the cloning procedure used to create vector <i>pIRX5::GT61.9p1-Myc</i>	129
Figure 5.6 Photographs of <i>Brachypodium distachyon</i> transformation procedure....	130
Figure 5.7 A schematic representation of the cloning procedure used to create vectors <i>pGT61.9p1::GFP</i> , <i>pGT61.9p2::GFP</i> , and <i>pUbi::GFP</i>	133
Figure 5.8 Phylogenetic tree of GT61 family genes.....	136
Figure 5.9 Gel electrophoresis image showing positive incorporation of the <i>pUBI::GT61.9p1-Myc</i> transgene into <i>Brachypodium</i> genomic DNA (gDNA)	137
Figure 5.10 Western blot assay of transgenic Ubi::GT61.9-Myc overexpression <i>Brachypodium</i> lines.....	137
Figure 5.11 Ferulic acid (FA) monomer and total dimers (\pm SE) in stem (top) and leaf (bottom) of five <i>Brachypodium distachyon</i> lines overexpressing <i>GT61.9p1</i> , driven by the maize ubiquitin promoter.	140
Figure 5.12 Ferulic acid dimers (\pm SE) in stem (top) and leaf (bottom) of five <i>GT61.9p1</i> overexpression lines, (expression driven by the maize ubiquitin promoter) in <i>Brachypodium distachyon</i>	141
Figure 5.13 Monosaccharide concentrations of transgenic <i>Brachypodium</i> lines which overexpress <i>GT61.9p1</i> (<i>Bradi1g06560</i>) under constitutive expression of the maize ubiquitin promoter, compared to null segregants	142
Figure 5.14 Ferulic acid (FA) monomer and dimer in stem and leaf of five <i>Brachypodium</i> RNAi lines transformed with a construct designed to knock down	

expression of <i>GT61.9p1</i> and <i>GT61.9p2</i> simultaneously, driven by the maize ubiquitin promoter	145
Figure 5.15 Ferulic acid dimers in stem and leaf of five Brachypodium RNAi lines transformed with a construct designed to knock down expression of <i>GT61.9p1</i> and <i>GT61.9p2</i> simultaneously, driven by the maize ubiquitin promoter	146
Figure 5.16 Ferulic acid (FA) monomer and dimer in leaf and stem of five Brachypodium RNAi lines transformed with a construct designed to knock down expression of <i>GT61.9p1</i> and <i>GT61.9p2</i> simultaneously, driven by the <i>IRX5</i> promoter	147
Figure 5.17 Ferulic acid dimers in stem and leaf of five Brachypodium RNAi lines transformed with a construct designed to knock down expression of <i>GT61.9p1</i> and <i>GT61.9p2</i> simultaneously, driven by the <i>IRX5</i> promoter	148
Figure 5.18 Visualisation of GFP in GFP-promoter fusion transgenic Brachypodium seedling (2.5 month old) leaves	150
Figure 5.19 Confocal microscopy images of the middle section of the root. Differences in expression of the promoter regions (1500 bp upstream of start codon) of <i>GT61.9</i> paralogues <i>p1</i> and <i>p2</i> in Brachypodium root. Promoter regions are fused to GFP in transgenic Brachypodium	151
Figure 5.20 Confocal microscopy images of a section of the bottom (nearest the tip) quarter of the root. Differences in expression of the promoter regions (1500 bp upstream of start codon) of <i>GT61.9</i> paralogues <i>p1</i> and <i>p2</i> in Brachypodium root. Promoter regions are fused to GFP in transgenic Brachypodium	152
Figure 5.21 Confocal microscopy images of the root tip. Differences in expression of the promoter regions (1500 bp upstream of start codon) of <i>GT61.9</i> paralogues <i>p1</i> and <i>p2</i> in Brachypodium root. Promoter regions are fused to GFP in transgenic Brachypodium	153

List of Tables

Table 1.1 Known arabinoxylan (AX) synthesis genes in dicots and monocots.	37
Table 3.1 Summary of experiments on the effect of mechanical stress on <i>Brachypodium distachyon</i> cell walls.....	69
Table 4.1 The mean percentage of hydroxycinnamic acids associated with the supernatant or pellet fraction of <i>Brachypodium distachyon</i> callus destarched AIR (alcohol insoluble residue) which was subjected to mild transfluoroacetic acid (TFA) (0.05 M) hydrolysis after 7 d treatment with methyl-jasmonate (meJA).	102
Table 4.2 The average proportion of the dry weight of alcohol insoluble residue (AIR), and destarched AIR, in control and 50 μ M meJA treated <i>Brachypodium</i> callus samples	103
Table 4.3 Changes in gene expression of statistically significant upregulated candidate genes for <i>para</i> -coumaric and ferulic acid esterification to arabinoxylan after 1, 2, 4 or 8 d treatment with 50 μ M meJA compared to a mock control, in <i>Brachypodium distachyon</i> callus	113

Acknowledgements

There are a large number of people that I wish to thank for providing support and assistance throughout this PhD project, without whom it could not have been completed. I am grateful for the funding for this project, provided by the BBSRC.

Foremost, thank you to my main supervisor Rowan Mitchell, who has provided guidance and support throughout this project, and has shared his extensive knowledge and interesting theories on ferulic acid esterification in grass cell walls with me. Also thanks, of course, to Jackie Freeman for invaluable support in the lab, and to Till Pellny, for “Till’s top tips” and for never letting me have a calculator to do sums.

I am grateful to my supervisor at York university, Simon McQueen-Mason, for invaluable guidance on my project. Also, my sincere thanks to Richard Waites, Frans Maathuis, Steve Thomas and Fred Beaudoin who have taken time out of their busy schedules to provide feedback on my written work and for their helpful suggestions on the direction of my project.

Two of my biggest thanks should go to the Rothamsted glass house staff for taking such good care of my plants, mainly Jill, Steve, Fiona, Anthony and Helen but many others behind the scenes, and to the lab 115 technicians who have rotated over the years, but mainly Ian who has been around for the longest and was always friendly and helpful.

Thank you to Steve Powers for assistance with statistics, Kirsty Halsey and Smita Kurup for assistance with capturing microscopy images, Steve Hanley for carrying out RNA sequencing, and David Hughes, Alberto Vangelism and Keywan-Hassani-Pak for assistance with RNA sequencing analysis. Thank you to Leo Gomez

and Rachael Hallam for assistance with monosaccharide, lignin, silica and cellulose analysis during time spent working in Simon's lab at York.

Thank you also to the members of the Rothamsted cell wall group: Peter Shewry, Mark Wilkinson, Alison Lovegrove, Ondrej Kosik, Suzanne Harris and Amy Plummer, and visiting workers Matt Sinnott and Carolin Kramer.

During my project I was surrounded with very smart friends and colleagues in the lab, all of whom were genuinely always available to help when I was stuck on something. Thanks to: my bench mate Hongtao for assistance with proteins; Michaela for help with RNA; Theresia, for the constant stream of biscuits whilst writing my thesis and for her numerous contributions to the first line of my methods chapter; Belinda, for being an unofficial mentor throughout my PhD; and Ondrej, for our competitions extracting phenolic acids and for sharing his wealth of knowledge of carbohydrate biochemistry with me.

Thank you to all the Rothamsted students for making my time at Rothamsted so enjoyable, for much needed coffee breaks and for Friday nights at the Pavilion: Beth, Sofia, Joe, Will, Joe and Aislinn. Thanks especially to SJ for keeping me company during all the late nights writing our theses together.

Thank you to my best friends Charlotte and Diana for all the insults, hilarious times and lots of wine.

Thank you Kasra, for coming to England.

Thank you to my brother Matthew and his wife Jenna, who inspired me to do a PhD; my sister Rachel; my dad; and my mum, who passed on her love for the English language to me, which I could not have written this thesis without, and without whom I would not be me.

Declaration

I declare that this thesis is a presentation of original work and I am the sole author. This work has not previously been presented for an award at this, or any other, University. All sources are acknowledged as References

Chapter 1. General Introduction

1.1 The Poaceae and the commelinid monocots

The Poaceae (also known as grasses, formerly named the Gramineae) are an extraordinarily successful family of plants which fall within the commelinids. The commelinids represent a clade within the monocots which diverged 90-120 million years ago and comprise orders Arecales (palms), Commelinales (spiderwort, water hyacinth), Zingiberales (gingers, banana) and Poales (grasses, rushes and bromeliads); the Poaceae are the largest family within the Poales order (APG IV, 2016).

The Poaceae evolved 55-70 million years ago and diverged from dicotyledonous plants and other commelinid monocots (Kellogg, 2001). The group collectively describes 10,000 species in over 600 genera (Eckardt, 2004), and their success is evident in that grasslands cover 40% of the Earth's terrestrial surface (excluding Antarctica and Greenland), and are found on every continent (World Resources Institute, 2000). Out of these grasslands have emerged modern cereal crops; for example, 10,000 years ago saw the first cultivation of wheat, which aided the transition from a hunter-gatherer lifestyle to settled agriculture, a major cultural milestone (Shewry, 2009). Today, the grasses are hugely environmentally and economically important. They are consistently the leading crop species produced globally (tonnes per year), including sugarcane (1st), maize (2nd), rice (3rd), wheat (4th), barley (11th), and sorghum, millet and oats (FAO, 2013), and also include emerging bioenergy crops such as switchgrass and miscanthus (APG IV, 2016). Grasses represent a major portion of global human nutrition, most notably through direct human consumption (Shewry, 2009), but also indirectly through forages fed to ruminants, and have attracted attention in the biofuel industry as feedstocks for bioethanol production (Jung et al., 2012).

1.2 Second generation liquid biofuels

Global warming due to greenhouse gas emissions is increasing at an alarming rate and current predictions are in the range of 2-4 °C warming by the year 2100. Thus, there is an international drive to limit the increase in global temperature to 2 °C, relative to pre-industrial levels. The transport sector is responsible for 23% of total CO₂ emissions worldwide (IPCC, 2014), and there is therefore a demand for a carbon-neutral fuel to replace petroleum based fuels, such as bioethanol to replace petrol. First generation bioethanol is sourced from starch from the grain of cereal crops such as maize, or sucrose from crops such as sugarcane, and is currently blended with petroleum, by up to 25% in Brazil (Socol et al., 2010). However, utilising both food crops and arable agricultural land for bioethanol production has led to a strain on the rising global demand for food, and has increased global food prices (Marriott et al., 2016).

Second generation liquid biofuel technology was developed in response to a rising global demand for a carbon-neutral fuel from a non-food plant resource. In contrast to first generation fuels, second generation biofuels utilise lignocellulosic feedstocks from non-food agricultural by-products such as wheat, barley and rice straw, sugarcane bagasse, maize and sorghum stover, or dedicated bioenergy crops such as miscanthus or switchgrass. Such feedstocks are predominantly composed of cell wall material, comprising polysaccharides and lignin, which is enzymatically digested to release individual monosaccharides, and further fermented to produce bioethanol (Nigam and Singh, 2011). Many globally important crops such as sugarcane, maize, rice and wheat belong to the Poaceae family of commelinid monocots, which have distinct cell walls from dicots and other monocots. The cell walls of the Poaceae are remarkably recalcitrant to enzymatic digestion (Grabber, 2005). Thus, digestion of the long chain polysaccharides to produce usable sugars from the cell wall is

currently expensive and time consuming due to the complex interactions between polysaccharides and lignin (Jung et al., 2012, Grabber, 2005). Current pretreatments for digestion of cell wall polymers involve high pressures, high temperatures and toxic chemicals, which are costly and generate chemical wastes. Thus, second generation bioethanol is not currently suitable for commercial production (Kumar et al., 2009, Nigam and Singh, 2011). Increasing the digestibility of lignocellulosic biomass will have significant impact in this sector.

1.3 Ruminant nutrition

Ruminants, including important agricultural livestock such as cattle, goats and sheep, have a specialised multi-compartment gut able to digest plant cell wall polysaccharides and ferment the products of digestion into short-chain fatty acids. Grass cell walls make up the main portion of ruminant nutrition whose diet consists of forage grasses or hay, as ruminants are able to digest the polysaccharides of the cell wall with the aid of gut microorganisms (Jung et al., 2012). However, it has been found that up to one third of cell wall material is indigestible by the microorganisms (Wilson and Mertens, 1995). Increased cell wall digestibility may have beneficial effects on ruminant nutrition; for example, higher digestibility is positively correlated with increased milk production in cows (Jung et al., 2011).

1.4 Cell walls

Cell walls are a complex, often recalcitrant network of polymers, which create the 'plant skeleton'. The major function of cell walls has, in the past, been described as providing structural support. However, far from being a static structure whose function lies solely in structural support, the cell wall is now understood as a dynamic, changing extracellular matrix, which is key in responding to environmental

changes and providing developmental cues. The interaction between the polymers of the cell wall in different tissues and at different developmental stages is key to controlling cell expansion and cell shape, and protecting against pathogen attack. As the barrier between cells in plants, the wall is also important in cell signalling (Carpita and McCann, 2000). The basic components of the cell wall are cellulose, hemicellulose, pectin, protein and in some wall types, lignin (Bacic et al., 1988), and are bound together to create a structurally integral framework which creates a physical and chemical barrier to enzymatic attack and therefore to digestibility (Grabber, 2005).

Cell wall composition varies between species, tissue and even on opposite sides of the same cell. Cell walls can be grouped into non-lignified primary cell walls and lignified secondary cell walls. Primary cell walls are deposited by expanding cells during cell growth, and lignified secondary cell walls are formed in some tissues such as the sclerenchyma or xylem, after cell expansion has ceased, to provide structural reinforcement (Carpita and McCann, 2000). Secondary cell walls contain more cellulose and hemicellulose, and less pectin and protein than primary walls, and primary cell walls are devoid of lignin (Bacic et al., 1988). Lignified tissues are major inhibitors of saccharification in bioethanol production (Grabber, 2005).

The composition of the cell walls of the commelinid monocots is distinct from that of dicots, and therefore primary cell walls can be further grouped into Type I and Type II cell walls, depending on the major hemicellulose present. Type I primary cell walls of dicots and non-commelinid monocots comprise xyloglucan as the major hemicellulose, and little xylan, whereas the major hemicellulose of the type II primary cell walls of the commelinids is arabinoxylan (Scheller and Ulvskov, 2010).

1.5 Xylan structure

Xylans are a structurally diverse group of cell wall polysaccharides, which seemingly evolved in the ancestor of land plants and modern Charophyte green algae (Popper et al., 2011, Mikkelsen et al., 2014). Xylans consist of a β -(1-4)-xylopyranose (Xyl) backbone, which is decorated by substitutions that vary between taxa and between tissues within the same plant. The xylan of commelinid monocot cell walls, including that of the grasses, is unique in structure with important features that distinguish it from the xylan of dicots and other monocots (**Figure 1.1**).

Dicot xylan is prevalent in the secondary cell wall, where it comprises around 30% of the wall (Scheller and Ulvskov, 2010). The xylan of dicots is commonly named glucuronoxytan (GX) due to its main substitutions of α -(1-2)-glucuronic acid (GlcA) and α -(1-2)-4-*O*-methyl glucuronic acid (meGlcA), which decorate the polysaccharide backbone. Dicot xylan may also be decorated by (1-2)- or (1-3)-*O*-acetyl substitutions, and may have small amounts of α -(1-2)-arabinofuranose. The reducing end of dicot xylan contains a conserved tetrasaccharide: β -Xyl-(1,4)- β -Xyl-(1,3)- α -rhamnose (Rha)-(1,2)- α -galacturonic acid (GalA)-(1,4)-Xyl (Scheller and Ulvskov, 2010).

The xylan of the commelinid monocots, including the Poaceae, comprises approximately 40% of the cell walls of vegetative tissues (Scheller and Ulvskov, 2010) and can represent up to 70% of the cell walls of starchy endosperm of cereals, such as wheat and barley (Bacic and Stone, 1981). In contrast to dicots, the xylan of the commelinid monocots has many more numerous and varied substitutions which decorate the backbone. The major decoration of commelinid monocot xylan is α -(1-3)-arabinofuranose (Ara), and hence is named arabinoxylan (AX). Arabinose (Ara) substitutions on AX can also be α -(1-2)-linked to the xylan backbone, or may di-substitute xylose at the C-2 and C-3 position, as is common in starchy endosperm

of wheat (Bacic and Stone, 1981). A unique and important feature of the AX of the commelinids is that α -(1-3)-linked arabinose residues may be further substituted on the C-5 position by ferulic acid (FA) or *para*-coumaric acid (*p*CA; **section 1.6**). The AX of commelinids may also be substituted by α -(1-2)-GlcA and its 4-*O*-methyl derivative as in dicots, as is common in vegetative tissues, and may therefore also be referred to as (glucurono)arabinoxylan (GAX). Further, C-2- and C-3-linked acetyl groups may decorate the backbone (Scheller and Ulvskov, 2010, Fincher, 2009, York and O'Neill, 2008, Vogel, 2008, Burton and Fincher, 2012). In addition to these common substitutions, AX may also have other less abundant substitutions, such as 2-*O*- β -Xyl-(5-*O*-feruloyl)-Ara (Wende and Fry, 1997), which may be further substituted on Xyl by (1-4)-galactopyranose (Gal) (Saulnier et al., 1995), and Ara-(1-2)-Ara-(1-3) (Verbruggen et al., 1998).

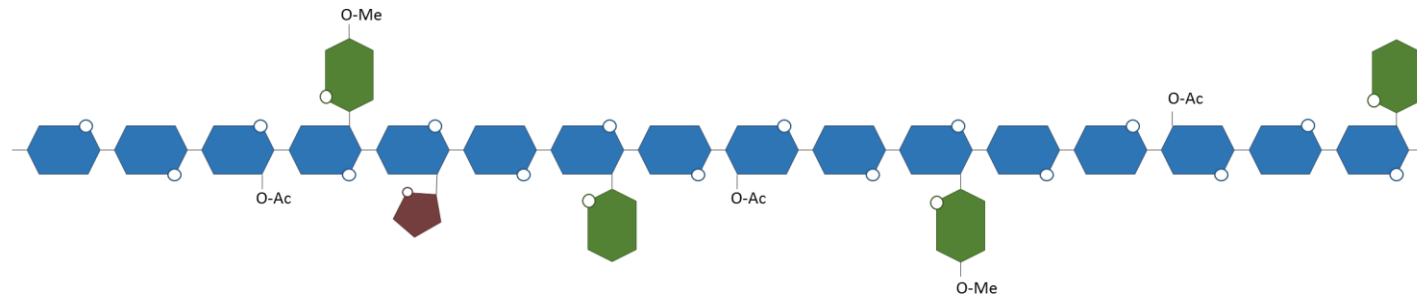
The degree of substitution of xylan varies greatly between species and tissue. The (Me)GlcA:Xyl ratio of dicot GX is usually in the range of 1:4-1:16. This is in contrast to the highly branched (G)AX of the grasses, where the backbone, on average, has one substitution for every two backbone xylose residues, although regions of up to 6-9 unoccupied xylose sugars may be present. The substitution rate of AX in the starchy endosperm is also very high, where the Ara:Xyl ratio is 1:2-1:5 (Ebringerova, 2006, Fincher, 2009). There is some evidence that xylan may have a repeating structure; in wheat, co-immunoprecipitation was used to isolate a xylan synthase complex which produced two distinct oligosaccharides when digested, suggesting a regular structure (Zeng et al., 2010). However, Bromley et al. (2013) described major (GlcA:Xyl ratio = 1:6-1:26) and minor (GlcA:Xyl ratio = 1:5-1:7) GX domains in *Arabidopsis thaliana* (*Arabidopsis*), which did not seem to have a regular structure.

Xylans provide structural support to the load-bearing cellulose microfibrils. The degree, and type, of xylan substitution is important in conferring its interaction with

cellulose and other wall components, as unbranched regions of xylan allow steric alignment with cellulose, allowing hydrogen bond formation between them (Ebringerova and Heinze, 2000, Burton and Fincher, 2012, Busse-Wicher et al., 2016). Substitutions of xylans may also be important in protecting the polymer from being enzymatically degraded (Ebringerova and Heinze, 2000, Izydorzyc and Biliaderis, 1995, Van Craeyveld et al., 2009), particularly FA substitutions (**section 1.6.4**).

In recent years, some xylans have been discovered that contain unusual branching patterns. The highly branched heteroxylan of *Plantago ovata* (psyllium) and *Arabidopsis thaliana* (Arabidopsis) seed mucilage have attracted interest. Although this mucilage xylan contains the common β -(1-4)-Xyl backbone, both psyllium and Arabidopsis mucilage heteroxylan backbones are substituted by up to 45% (Voiniciuc et al., 2015, Van Craeyveld et al., 2009). Psyllium mucilage heteroxylan contains mono-, di- or tri-saccharide decorations comprised of Ara and Xyl, which occur frequently along the backbone (Fischer et al., 2004, Guo et al., 2008). Arabidopsis seed mucilage may contain Xyl substitutions along the backbone and few Glc or Ara substitutions (Voiniciuc et al., 2015). These unusual xylans may be useful in identifying xylan synthesis genes (Jensen et al., 2013), although they do not contain ferulic acid.

a) Dicot glucuronoxylan



- Glycosidic bond (-O-)
- Xylopyranose
- Arabinofuranose
- Glucuronic acid
- O-Me O-Methyl
- O-Ac O-Acetyl
- pCA* *para*-coumaric acid
- FA Ferulic acid

b) Grass arabinoxylan

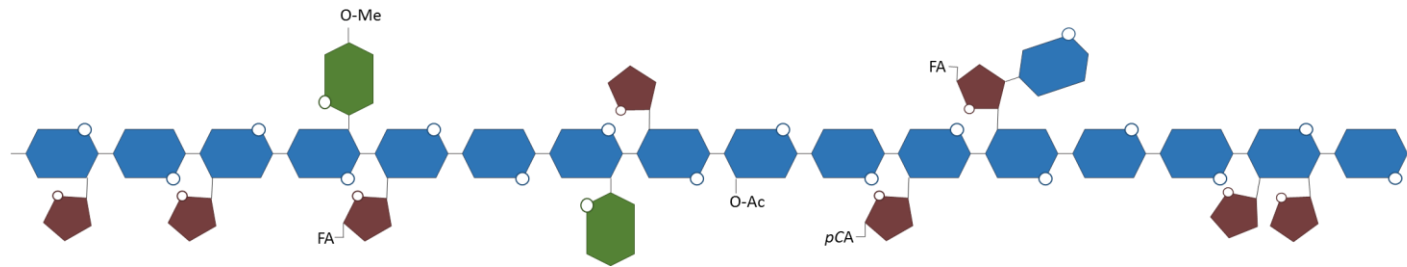


Figure 1.1 Schematic representation of xylan side chain variation in dicots and grasses.

1.6 Cell wall-bound hydroxycinnamic acids (HCAs)

Cell wall-bound hydroxycinnamic acids (HCAs) are ferulic acid (FA), *para*-coumaric acid (*p*CA) and sinapic acid (SA). HCAs are synthesised in the phenylpropanoid pathway from cinnamic acid (Ralph, 2010, Buanafina, 2009), and are known to be incorporated into the cell wall through esterification to arabinoxylan, or coupling with lignin monomers (Ralph, 2010).

1.6.1 Cell wall-bound ferulic acid (FA)

Ferulic acid (FA) is an integral component of the cell walls of the commelinid monocots, including the grasses, and is an important factor in cell wall digestibility (**section 1.6.4**). It occurs as a component on side chains of AX, where it is ester linked at the C-5 position on (1-3)-Ara substitutions (Fincher, 2009, Scheller and Ulvskov, 2010, Buanafina, 2009). The feruloylation of AX is a highly specific, enzymatically controlled process, which occurs at the site of AX synthesis in the Golgi involving an FA-CoA precursor (Myton and Fry, 1994, Meyer et al., 1991), and may also occur at the cell wall involving an unknown FA precursor (Mastrangelo et al., 2009).

FA has long been recognised as an integral cell wall component of the grasses. Given its similarity to monolignols, FA was first thought to be solely associated with lignin in secondary cell walls (Brown, 1966), however was later shown to be esterified to an unknown polysaccharide in compounds isolated from cell wall material by both cellulase digestion and mild acidolysis (Hartley, 1972, Whitmore, 1974). Further, Harris and Hartley (1976) showed that FA was present in unligified primary cell walls of many grass species using ultraviolet fluorescence microscopy. FA was first shown to be esterified to the O-5 position of Ara in grass cell walls by Smith and Hartley (1983), who isolated and characterised FA-Ara-Xyl using cellulase digestion

of the cell walls in many tissues of Poaceous species including straw, leaves, flour and bran of barley, Italian ryegrass and wheat. Carbohydrate esters of AX-esterified FA have since been identified in several species using mild acid or Driselase hydrolysis to release the compounds. Poaceous species in which AX-esterified FA has been identified in addition to wheat, barley and Italian ryegrass include maize, sugarcane, wild rice, blue fescue (*Festuca arundinacea*), the common grass *Cynodon dactylon* (Ishii, 1997) and bamboo (Ishii and Hiroi, 1990). Also, AX-esterified FA is found in other commelinid monocots, including pineapple (clade Poales, Smith and Harris, 2001), banana (clade Zingiberales, de Ascensao and Dubery, 2003), and Chinese water chestnut (clade Poales, Parr et al., 1996). Ferulic acid is almost exclusively found esterified to AX in the Poaceae, however there is a lone report of a feruloylated xyloglucan compound isolated from bamboo (Ishii et al., 1990).

Cell wall-bound ferulates are most abundant in the commelinid monocots, however they have also been found in some Caryophyllales dicot species, such as spinach (Fry, 1982), sugar-beet (Colquhoun et al., 1994, Kroon and Williamson, 1996) and quinoa (Renard et al., 1999). In dicots, FA is linked to the arabinose (3-*O*-linked) and galactose (6-*O*-linked) residues of pectin, as opposed to the arabinose residues of AX as in grasses (Buanafina, 2009). Ferulic acid has also been found in very small quantities in the cell walls of tobacco (Merali et al., 2007), carrot (Parr et al., 1997), asparagus (Rodriguez-Arcos et al., 2004) and gymnosperms (Carnachan and Harris, 2000), suggesting it may be present in all vascular plant cell walls in low amounts.

1.6.2 Cell wall-bound ferulic acid (FA) dimers

While most of the interactions between cell wall polysaccharides are mediated by hydrogen bonding, FA is of great importance in grass cell walls as it is uniquely able to covalently cross-link polysaccharides through the formation of oxidatively-linked

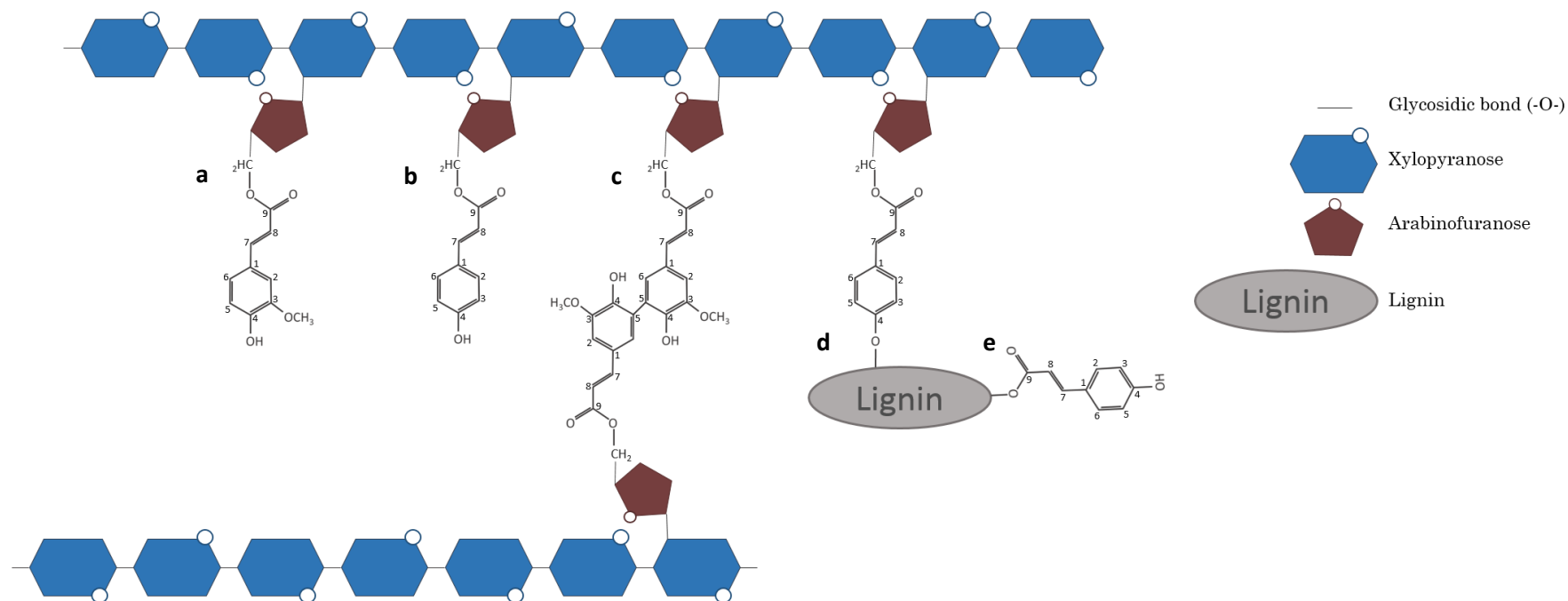


Figure 1.2 Schematic representation of known cell wall-bound HCAs associated with arabinoxylan and lignin. a) C5-linked ferulic acid (FA) on C3-linked arabinose side chains of arabinoxylan (AX); b) C5-linked *para*-coumaric acid (*p*CA) on C3-linked arabinose side chains of AX; c) FA 5-5 coupled dimer cross-linking two AX polysaccharide chains; d) FA cross-link to lignin; e) *p*CA esterified to lignin.

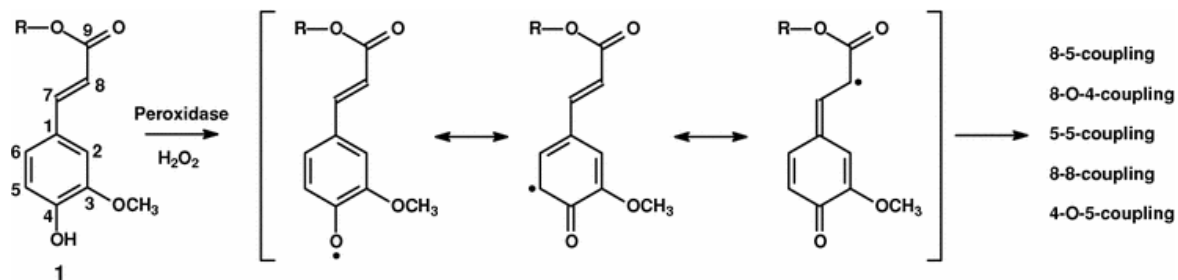


Figure 1.3 Mechanism of peroxidase- and H₂O₂-mediated dimerisation of FA into the five possible isomers found in plant cell walls. Figure obtained from Bunzel (2010).

diferulate bridges (**Figure 1.2**). The first FA dimer to be identified was the 5-5-coupled dimer in wheat seeds (Markwalder and Neukom, 1976), then thought to be the only product of diferulate coupling. Thus, prior to the discovery of the other diferulate isomers, the 5-5-coupled dimer was referred to simply as diferulate, and total FA dimers were largely underestimated by up to 20 times (Hatfield et al., 1999, Ralph et al., 1994). Eighteen years later, Ralph et al. (1994) identified a range of five dehydrodiferulate isomers (8-O-4, 8-5, 8-8, 5-5 and 4-O-5), which were possible to synthesise *in vitro* through H₂O₂ free-radical coupling mechanisms (**Figure 1.3**). Four of these dimers (8-O-4, 8-5, 8-8 and 5-5) were identified *in planta* in various grasses, such as corn, cocksfoot and switchgrass (Ralph et al., 1994), and the 4-O-5-coupled dimer was later identified as present in small amounts in the cell walls of cereal crops such as corn and wheat (Bunzel et al., 2000). Evidence that FA dimers cross-link AX chains comes from the isolation and characterisation of Ara-FA-FA-Ara bridges (Ishii, 1991, Saulnier and Thibault, 1999, Allerdings et al., 2005). More recently, evidence for a variety of cell wall-bound FA dehydrotrimers and dehydrotetramers has been reported, which raises the possibility that multiple polysaccharide chains may be cross-linked by FA (Rouau et al., 2003, Bunzel et al., 2006, Fry et al., 2000, Dobberstein and Bunzel, 2010a).

The formation of FA cross-links is not enzymatically controlled, but rather takes place through free radical coupling mediated by peroxidase oxidation reactions, which use H₂O₂ as a cofactor (Grabber et al., 1995, Burr and Fry, 2009, Wallace and Fry, 1995). Isolated maize primary cell walls containing endogenous peroxidases show increased FA dimerisation when treated with H₂O₂ (Grabber et al., 1995, Fry et al., 2000), in addition, younger cell suspension cultures showed extensive FA-coupling at the Golgi, which shifted to *in muro* coupling in older cultures (Fry et al., 2000). The type of dehydrodiferulate isomer that is formed in the cell wall is largely due the steric positioning of two or more FA monomers within the complex network of polysaccharides in the cell wall (Ralph et al., 2004).

1.6.3 FA cross-link to lignin

Another important feature of cell wall-bound FA in grasses is their integral interactions with lignin through ether or C-C bonds. In 1972, Hartley speculated that the interaction between the distinct lignin and the polysaccharide networks within the cell wall may be cross-linked by FA (Hartley, 1972). FA was later shown to be etherified to lignin in wheat straw (Scalbert et al., 1985), and Iiyama et al. (1990) found that some FA that was etherified to lignin was also esterified to AX, thereby demonstrating Hartley's original hypothesis. Further, ferulate that has already dimerised can also cross-link to lignin (Grabber et al., 2000). Crucially, FA can also form covalent linkages with monolignols coniferyl alcohol and sinapyl alcohol through the same radical coupling reactions that occurs during FA dimer coupling (**Figure 1.3**). This finding demonstrated that ferulate linked to AX does not just bind to lignin, but acts as a nucleation site for lignin polymerisation (Ralph et al., 1995, Jacquet et al., 1995, Grabber et al., 2002).

1.6.4 FA cross-linking in digestibility

Cell wall-bound FA cross-linking, between two or more AX polysaccharides through dimer formation, and between AX and lignin in grass cell walls, is one of the main inhibitors of digestibility in applications such as second generation liquid biofuel production and ruminant nutrition (**section 1.2, section 1.3**; Grabber, 2005, Buanafina, 2009, de Oliveira et al., 2015).

FA dimer formation is implicated in cessation of cell wall expansion and cell growth in plant development, and may therefore be a factor which controls the size and shape of cells (MacAdam and Grabber, 2002). In addition, FA dimers inhibit pathogen invasion, both by forming a physical barrier to pathogen invasion, and by limiting digestion of the cell wall by hydrolysing enzymes released by the pathogen (Bily et al., 2003, Grabber et al., 1998a).

Cell wall digestibility is negatively correlated with both FA dimerisation and with lignin concentration (Grabber, 2005). In primary cell walls devoid of lignin, an increase in FA dimerisation stimulated by H₂O₂ resulted in a 30% decrease in cell wall sugars that were hydrolysed after 3 h digestion (Grabber et al., 1998a). Further, in an artificially lignified environment, reduced FA-lignin cross linking resulted in significantly increased digestibility (Grabber et al., 1998b). Thus, there has been keen interest in the reduction of FA in lignocellulosic biomass to improve the digestibility of cell walls (Dhugga, 2007).

1.6.5 Cell wall-bound *para*-coumaric acid (*pCA*)

pCA is also esterified to the O-5 position on α -(1-3)-Ara of AX, although to a lesser extent than FA (Mueller-Harvey and Hartley, 1986), however, the majority of cell wall-bound *pCA* is ester-linked to lignin (Bartley et al., 2013). *pCA* has not been shown to dimerise or cross-link *in vivo* (Hatfield et al., 1999), rather, *pCA* monolignol

ester conjugates are formed intracellularly by an enzyme in the BAHD acyl transferase family: *p*-coumaroyl CoA:monolignol transferase (PMT). The conjugates are then transported to the cell wall and incorporated into the growing lignin polymer (Petrik et al., 2014, Withers et al., 2012). The function of *p*CA in the plant cell wall remains largely unknown. There is growing evidence that *p*CA esterified to lignin is involved in the lignin polymerisation process, in which it readily forms free radicals, but preferentially transfers the unpaired electron to other more stable phenols, such as sinapyl alcohol. This hypothesis was first suggested by Takahama et al. (1996), and was later evidenced *in vitro* using peroxidases extracted from maize cell walls (Hatfield et al., 2008). However, the mechanism remains to be proven *in planta*. *p*CA esterified on arabinoxylan has an as yet unknown function. It has been suggested that total cell wall-bound hydroxycinnamates, including *p*CA, are involved in resistance against pathogens (Santiago et al., 2006, Santiago et al., 2008), however, at present there is little direct evidence supporting a role for *p*CA in defence.

1.6.6 Cell wall-bound sinapic acid

Sinapic acid has been isolated from cell wall fractions of cereals, such as wheat, maize, rice and barley, but does not appear to be universal in the grasses as it was not found in oat or millet (Bunzel et al., 2003). At present, the cell wall polymer to which sinapic acid is acylated is unknown. However, there is some evidence that it is associated with cell wall polysaccharides (Bunzel et al., 2002). Sinapic acid has been suggested to have an analogous function to FA in cross-linking components of grass cell walls, due to the existence of dehydrosinapic acid and sinapate-ferulate heterodimers in cereal grains (Bunzel et al., 2003).

1.7 Glucurono- and arabinoxylan synthesis

AX synthesis is localised at the Golgi membrane, as is most non-cellulosic cell wall polysaccharide synthesis (Scheller and Ulvskov, 2010). Sugars activated with uridine diphosphate (UDP) are transferred to the growing polysaccharide chain by glycosyltransferases. AX is then transported to the cell wall, in vesicles, to be deposited. Glycosyltransferases (GTs) that have currently been identified in AX synthesis are in the families GT8, GT43, GT47, GT61 (Rennie and Scheller, 2014).

1.7.1 Discovery of xylan synthesis genes

The first plant cell wall synthesis enzymes to be identified were the cellulose synthase (*CesA*) enzymes (Pear et al., 1996). Since then, the genes and enzymes responsible for the synthesis of other cell wall polysaccharides have begun to be elucidated, including those responsible for xylan synthesis, although many more remain to be discovered. AX is synthesised at the Golgi and transported to the cell wall via vesicles and deposited, therefore xylan synthases are integral membrane proteins which are localised at the Golgi membrane (Rennie and Scheller, 2014). The *Arabidopsis* irregular xylem T-DNA insertion mutants have been influential in identifying xylan synthase genes (Brown et al., 2007), as have large scale comparative gene expression studies and co-expression studies (Pellny et al., 2012, Jensen et al., 2013, Mitchell et al., 2007, Molinari et al., 2013). Known glucurono- and arabino-xylan (GX and AX) synthase genes are summarised in **Table 1**.

Mitchell et al. (2007) identified candidate genes for AX synthesis, using a novel comparative bioinformatics approach, based on the hypothesis that orthologous genes for AX synthesis were likely to be more highly expressed in grasses than in dicotyledonous species. Specific clades within the GT43, GT47, GT61 and Pfam PF02458 (now known as BAHD) families were the most likely to encode the enzymes

that synthesise AX and its side chains. Concurrent to this study, the first xylan synthesis genes were beginning to be elucidated in Arabidopsis mutants (Pena et al., 2007, Brown et al., 2007), which confirmed the predictions of Mitchell et al. (2007).

1.7.2 Synthesis of the β -(1-4)-xylan backbone

The first β -(1-4)-Xyl backbone genes to be discovered were *IRREGULAR XYLEM (IRX)9* (Pena et al., 2007, Brown et al., 2007, Lee et al., 2007a), *IRX10* (Brown et al., 2009, Wu et al., 2009) and *IRX14* (Brown et al., 2007), the gene products of which belong to the glycosyltransferase (GT)43 and GT47 families of enzymes. These genes were identified in T-DNA insertion mutant lines characterised by a collapsed xylem and reduced cell wall xylose. As xylem tissue is composed mainly of GX rich secondary cell walls, these enzymes were predicted to be associated with GX synthesis. The mutant plants had decreased GX chain length and the proteins were shown to have β -(1-4)-Xyl transferase (XylT) activity in microsomal membranes (Brown et al., 2007, Brown et al., 2009). Recently, the *in vivo* XylT activity of *IRX10* from family GT47 was unambiguously confirmed using a bioluminescent assay (Urbanowicz et al., 2014) and heterologous expression in yeast (Jensen et al., 2014). Closely related homologues of these genes were later identified; namely, *IRX9-L*, *IRX10-L* and *IRX14-L* (Keppler and Showalter, 2010, Wu et al., 2010, Wu et al., 2009), which have functional redundancy to their equivalent homologue. Recently, *IRX15* and *IRX15-L* have been identified as also having a role in xylan biosynthesis, although their exact function remains to be discovered (Jensen et al., 2011, Brown et al., 2011). The role of the functionally redundant homologous pairs of genes is unknown, although it has been suggested that each pair may be differentially expressed in the primary and secondary cell walls (Mortimer et al., 2015, Chiniquy et al., 2013).

1.7.3 Dicot GX side chain synthesis

Genes *FRA8/IRX7* (Brown et al., 2007, Zhong et al., 2005), *IRX8* (Pena et al., 2007, Brown et al., 2007, Persson et al., 2007), *PARVUS* (Brown et al., 2007, Lee et al., 2007b) and *F8H* (Lee et al., 2009) are implicated in the synthesis of the dicot-specific GX reducing end tetrasaccharide (**section 1.5**), which may be a “primer” involved in elongation of the polysaccharide chain.

Recently, the proteins that synthesise the GlcA and 4-*O*-meGlcA side chain substitutions on GX were discovered in Arabidopsis mutants lacking these decorations on the backbone. The genes were named *GlucUronic acid substitution of Xylan (GUX)* (Mortimer et al., 2010). GUX1, 2, 3 and 4 have been shown to exhibit GlcAT activity onto xylooligomers in microsomal membranes and are differentially expressed in pith, xylem and interfascicular fiber (Lee et al., 2012, Rennie et al., 2012). GUX1 and 2 have been shown to substitute GX in two distinct domains (Bromley et al., 2013, Busse-Wicher et al., 2016). In addition, Arabidopsis genes *eskimo1/TBL29* (Urbanowicz et al., 2014, Yuan et al., 2013), *TBL3* and *TBL31* (Yuan et al., 2015) have been shown to catalyse the addition of O-acetyl groups to xylan *in vitro*.

1.7.4 Arabinoxylan (AX) synthesis in the Poaceae

AX synthesis of the grasses remains poorly understood despite their global economic and nutritional significance and the dominance of AX in grass cell walls. In wheat, Lovegrove et al. (2013) reported that RNAi suppression of the wheat *irx9* and *irx10* orthologue, *TaGT43_2* and *TaGT47_2* resulted in a reduction in total AX, with decreased AX chain length, but increased arabinosyl substitution. Additionally, Zeng et al. (2010) showed AX synthase activity in wheat microsomes of a GT43-4 (IRX14 orthologue), GT47-13 (IRX10 orthologue) and GT75-4 complex. In rice, Zhang et al.

(2014) reported that the orthologue of *irx10*, *OsGT47A*, rescued the phenotype of the *Arabidopsis irx10/irx10-L* double mutant, and Chiniquy et al. (2013) showed that rice genes *OsIRX9*, *OsIRX9-L* and *OsIRX14*, rescued the phenotypes of their equivalent orthologous mutants in *Arabidopsis*. These results suggest that the genes for β -(1-4)-Xyl backbone synthesis are conserved in the Poaceae.

Additionally, the enzymes which catalyse the synthesis of some AX side chains in the grasses have recently been described. GT61 family genes *XAT1* and *XAT2* have been characterised as adding the α -(1-3)-Ara substitutions on AX in the grasses (Anders et al., 2012). In this study, RNAi knock down of *TaXAT1* in wheat resulted in greatly decreased α -(1-3)-Ara substitution of AX. Furthermore, heterologous expression of wheat *TaXAT2*, and its rice homologues, *OsXAT2* and *OsXAT3*, in *Arabidopsis* wild type and *gux* mutants (**section 1.7.3**) resulted in Ara decorations on (G)X, where these substitutions are usually absent. Furthermore, Chiniquy et al. (2012) described the reduction of Xyl on the grass-specific β -(1-2)-Xyl-(5-*O*-feruloyl)- α -(1-3)-Ara-substitution of AX in rice mutant *xax1*. Thus, the authors suggested that XAX1 was a xylosyl transferase, however, the mutants also showed significantly reduced cell wall-bound FA and *pCA*, which suggests that XAX1 may be a feruloyl-arabinosyl or coumaroyl-arabinosyl transferase (**section 1.8.2**). Also, overexpression of BAHD acyl transferase family gene *OsAT10* resulted in a large increase in AX-esterfied *pCA* and is therefore involved in *pCA* substitution on AX (Bartley et al., 2013). Despite these recent advances, many of the enzymes involved in addition of grass-specific side chains to AX remain to be discovered; in particular, the genes responsible for the addition of FA-Ara side chains to AX, which are important in cell wall digestibility (**section 1.6.4**), are still unknown.

1.7.5 Conservation of *IRX* genes

The *IRX* genes have been shown to be functionally conserved in other species, such as poplar, cotton, willow, asparagus and plantago (Ratke et al., 2015, Wan et al., 2014, Zeng et al., 2016, Jensen et al., 2014). Interestingly, genes orthologous to *IRX9-L*, *IRX10* and *IRX14*, responsible for synthesis of the β -(1-4)-Xyl backbone, are also conserved in mosses and spike mosses (Hornblad et al., 2013, Harholt et al., 2012) and orthologues of *IRX10/IRX10-L*, *IRX7/FRA8* and *IRX8* involved in synthesising the Xyl backbone, and the dicot-specific reducing end tetrasaccharide have been identified in the charophyte green algae (Mikkelsen et al., 2014), showing conservation throughout land plant evolution.

1.7.6 The xylan synthase complex

The concept of a xylan synthase complex was suggested as early as the *irx* genes were discovered (Brown et al., 2007). Later, Zeng et al. (2010) provided empirical evidence that TaGT43-4 (*IRX14* orthologue), TaGT47-13, (*IRX10* orthologue) and an uncharacterised putative Ara mutase (*Arap* to *Araf*) in the GT75 family, TaGT75-4 co-immunoprecipitate. The interaction between *IRX14* and *IRX10* was expected, however the addition of GT75 to the Golgi localised complex was surprising, as the rice orthologue, UAM1 has previously been shown to catalyse *Arap* to *Araf* in the cytosol (Konishi et al., 2007). The purified complex had xylosyl transferase, arabinosyltransferase, and glucuronosyltransferase activities (Zeng et al., 2010). Site directed mutagenesis of the catalytic sites of *IRX9*, *IRX9L*, and *IRX14* showed that the catalytic site was not essential for the function of the protein, and *IRX14* function was dependant on substrate binding, but not on catalytic site activity in *Arabidopsis* (Ren et al., 2014). Jiang et al. (2016) provide evidence to support this as the *IRX14* wheat orthologue (TaGT43-4) was shown to have a role in anchoring the complex to organelle membranes. More recently, Zeng et al. (2016) reported that asparagus (non-

Table 1.1 Known arabinoxylan (AX) synthesis genes in dicots and monocots. Asterisks represent two genes which may be involved in hydroxycinnamic acid addition to AX.

Locus	Gene name	Orthologue	Gene family	Species	Activity	Reference
Dicots						
<i>At2g37090</i>	<i>IRX9</i>		GT43			Brown et al. (2007), Pena et al. (2007), Lee et al. (2007a) Wu et al. (2010)
<i>At1g27600</i>	<i>IRX9-L</i>		GT43			Wu et al. (2010), Mortimer et al. (2015)
<i>At1g27440</i>	<i>IRX10</i>		GT47	Arabidopsis	xylosyl transferase, β -(1-4)-Xyl backbone	Brown et al. (2009), Wu et al. (2009), Jensen et al. (2014), Wu et al. (2010), Urbanowicz et al. (2014)
<i>At5g61840</i>	<i>IRX10-L</i>		GT47			Brown et al. (2009), Wu et al. (2009), Wu et al. (2010), Mortimer et al. (2015)
<i>At4g36890</i>	<i>IRX14</i>		GT43			Brown et al. (2007) Keppler et al. (2010), Wu et al. (2010), Mortimer et al. (2015)
<i>At5g67230</i>	<i>IRX14-L</i>		GT43			Keppler et al. (2010), Wu et al. (2010)
<i>At2g28110</i>	<i>IRX7/FRA8</i>		GT47			Brown et al. (2007), Zhong et al. (2005)
<i>At5g22940</i>	<i>F8H</i>		GT47	Arabidopsis	dicot reducing end tetrasaccharide	Lee et al. (2009)
<i>At5g54690</i>	<i>IRX8</i>		GT8			Brown et al. (2007), Pena et al. (2007), Persson et al. (2007)
<i>At1g19300</i>	<i>PARVUS</i>		GT8			Brown et al. (2007), Lee et al. (2007b)
<i>At3g50220</i>	<i>IRX15</i>		DUF579	Arabidopsis	unknown function	Jensen et al. (2011), Brown et al. (2011)
<i>At5g67210</i>	<i>IRX15-L</i>					Jensen et al. (2011), Brown et al. (2011)
<i>At3g18660</i>	<i>GUX1</i>		GT8	Arabidopsis	glucuronic acid transferase, (me)GlcA substitution	Mortimer et al. (2010), Lee et al. (2012), Rennie et al. (2012), Bromley et al. (2013), Mortimer et al. (2015)
<i>At4g33330</i>	<i>GUX2</i>		GT8			Mortimer et al. (2010), Rennie et al. (2012), Bromley et al. (2013), Mortimer et al. (2015)
<i>At1g77130</i>	<i>GUX3</i>		GT8			Mortimer et al. (2015)
<i>At1g54940</i>	<i>GUX4</i>		GT9			Rennie et al. (2012)
<i>At3g10320</i>	<i>MUC1₂₁</i>		GT61 clade B	Arabidopsis	Xylan side chain synthesis, specific expression in Arabidopsis mucilage, unknown activity	Voiniciuc et al. (2015)
<i>At3g55990</i>	<i>ESK1/TBL29</i>		DUF231	Arabidopsis	<i>O</i> -2 and <i>O</i> -3 acetylation substitutions	Yuan et al. (2013), Urbanowicz et al. (2014)
<i>At5g01360</i>	<i>TBL3</i>				<i>O</i> -3 acetylation substitutions	Yuan et al. (2015)
<i>At1g73140</i>	<i>TBL31</i>				<i>O</i> -3 acetylation substitutions	Yuan et al. (2015)

Locus	Gene name	Orthologue	Gene family	Species	Activity	Reference
Commelinid monocots						
	<i>TaGT43_2</i>	<i>Atirx9</i>	GT43	wheat		Lovegrove et al. (2013)
	<i>TaGT47_2</i>	<i>Atirx 10</i>	GT47	wheat		Lovegrove et al. (2013)
<i>LOC_Os07g49370</i>	<i>OsIRX9</i>	<i>Atirx9</i>	GT43	rice	xylosyl transferase, β-(1-4)-Xyl backbone	Chiniquy et al. (2013)
<i>LOC_Os01g48440</i>	<i>OsIRX9-L</i>	<i>Atirx9-L</i>	GT43	rice		Chiniquy et al. (2013)
<i>LOC_Os06g47340</i>	<i>OsIRX14</i>	<i>Atirx14</i>	GT43	rice		Chiniquy et al. (2013)
<i>Os0g0926600</i>	<i>OsGT47A</i>	<i>Atirx10</i>	GT47	rice		Zhang et al. (2014)
	<i>TaGT47-13</i>	<i>Atirx10</i>	GT47			
	<i>TaGT43-4</i>	<i>Atirx14</i>	GT43	wheat	xylan synthase complex	Zeng et al. (2010), Jiang et al. (2016)
	<i>TaGT75-4</i>		GT75			
	<i>XAT1</i>			wheat		
	<i>XAT2</i>		GT61 clade A	wheat, rice	arabinosyl transferase activity, (1-3)-Ara substitutions	Anders et al. (2012)
<i>LOC_Os02g22480</i>	<i>OsXAT2</i>			rice		
<i>LOC_Os03g37010</i>	<i>OsXAT3</i>			rice		
<i>LOC_Os02g22380</i>	<i>XAX1*</i>		GT61 clade A	rice	xylosyl-arabinosyl transferase/ feruloyl- arabinosyl transferase?	Chiniquy et al. (2012)
<i>LOC_Os06g39390</i>	<i>OsAt10*</i>		BAHD	rice	p-coumaroyl CoA transferase, <i>pCA</i> side chain	Bartley et al., 2013
<i>LOC_Os03g40270</i>	<i>OsUAM1</i>		GT75		UDP-Arap to UDP-Araf mutase	Konishi et al. (2007)
<i>LOC_Os07g41360</i>	<i>OsUAM3</i>		GT75	rice	UDP-Arap to UDP-Araf mutase	

commelinid monocot) genes *AoIRX9*, *AoIRX10* and *AoIRX14* interact to form a xylan synthase complex, which is localised at the Golgi membrane when heterologously expressed in *Nicotiana benthamiana*. The xylan synthase appears to be assembled at the endoplasmic reticulum, and transported to the Golgi (Jiang et al., 2016). GUX or GT61 enzymes, which are xylan side chain (me)GlcA and Ara transferases, have hitherto not been shown to be incorporated into the xylan synthase complex.

1.8 FA synthesis genes

Despite the recent advances in identification of AX synthesis genes of the grasses, the genes responsible for the addition of important FA-Ara side chains to AX are still unknown. Mitchell et al. (2007) predicted that genes in the GT61 and BAHD acyl transferase families would be involved in the process. In particular, genes in a clade within the BAHD Pfam family PF02458 were the most differentially expressed acyl transferases between monocots and dicots and are therefore strongly implicated in the feruloylation of AX. In addition, genes within the GT61 family were highly co-expressed with the BAHDs (Mitchell et al., 2007, Molinari et al., 2013) and are therefore likely to also be involved in the feruloylation of AX.

1.8.1 BAHD acyl transferases in feruloylation

The BAHD superfamily of acyltransferases is a large group containing the functional Pfam domain PF02458 and is localised to the cytoplasm (D'Auria, 2006). A clade within this family has been predicted to be involved in the addition of HCAs to AX by Mitchell et al. (2007), and hence was coined the “Mitchell clade” (Bartley et al., 2013). This clade showed differential expression between monocot and dicot species (Mitchell et al., 2007).

Two enzymes within the Mitchell clade have been functionally characterised. The first is a cytoplasmic *p*-coumaroyl monolignol transferase (PMT, Petrik et al., 2014, Withers et al., 2012). The second is a *p*-coumaroyl coenzyme A acyltransferase involved in the addition of *p*CA to AX (Bartley et al., 2013).

The role of BAHDs in feruloylation remains elusive, however two BAHD genes have been shown to localise with a QTL for the feruloylation of AX in maize (Barriere et al., 2012). Also RNAi suppression of *Bd2g43520* (*BAHD5/BDAT1*, **Figure 1.4**), which is highly expressed in leaves of *Brachypodium distachyon* (Brachypodium) throughout development (Molinari et al., 2013), resulted in decreased cell wall-bound FA in Brachypodium (Buanafina et al., 2016), however this effect was not replicated in rice (Piston et al., 2010). Piston et al. (2010) also tested the role of other BAHD genes within the Mitchell clade and found a modest 19% reduction in cell wall-bound FA in stem, supporting the role of the clade in feruloylation.

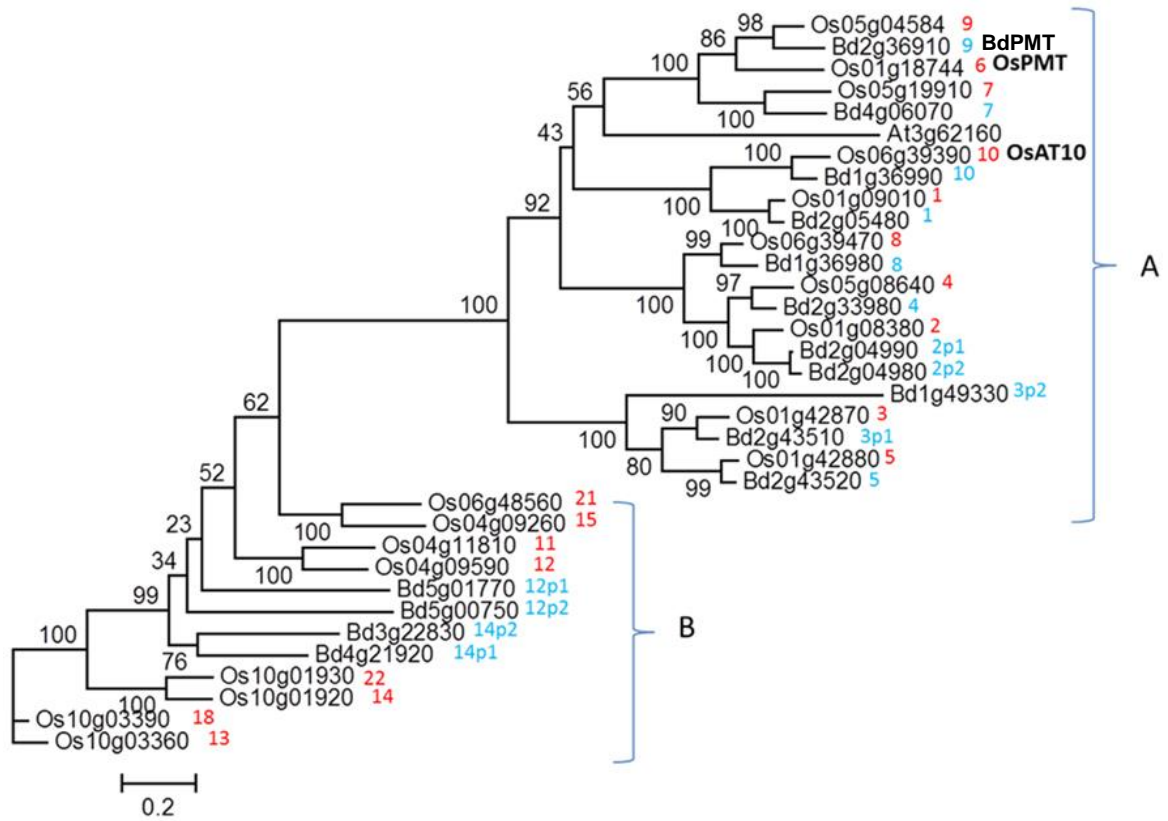


Figure 1.4 Phylogenetic tree of two clades within the BAHD family which are differentially expressed in monocot and dicot species and therefore are candidates for AX feruloylation. The tree shows rice, *Brachypodium distachyon*, and *Arabidopsis* genes within the clades. Genes are arbitrarily numbered. The figure highlights characterised genes *OsPMT*, *BdPMT* and *OsAT10*. Figure sourced from Molinari et al. (2013).

1.8.2 Glycosyltransferase 61 family in feruloylation

Glycosyltransferase (GT)61 family (**Figure 1.5**) enzymes are type II GTs; most of which contain a single transmembrane domain, and all of which contain an inverting catalytic domain of unknown function (PF04566). All GT61 enzymes are predicted to be localised at the Golgi, where AX is synthesised, and this has been evidenced for some GT61s (Anders et al., 2012, Chiniquy et al., 2012). The GT61 family can be divided into three clades (**Figure 1.5**; Anders et al., 2012).

Some clade A enzymes TaXAT1, TaXAT2, OsXAT2 and OsXAT3 have been characterised as α -(1,3)-arabinosyl transferases (Anders et al., 2012). If the substrate for feruloylation is an activated form of FA-Ara, this suggests that the candidate for feruloylation of AX may be in the GT61 family. Additionally, a clade B Arabidopsis GT61 was shown to be involved in xylan synthesis in Arabidopsis mucilage; the biochemical activity of the enzyme remains uncharacterised, however the mutant GT61 had reduced Xyl decoration attached directly to the backbone in a unique mucilage xylan, and therefore may be a xylosyl transferase (Voiniciuc et al., 2015). Clade C is distantly related to Clades A and B; a representative from Clade C was shown to have β -(1,2)-XylT activity involved in protein glycosylation in Arabidopsis (Bencur et al., 2005).

Additionally, Chiniquy et al. (2012) characterised the *xax1* mutant. The authors proposed that XAX1 is a xylosyltransferase, which adds a xylose residue to an unferuloylated arabinose on arabinoxylan, which is subsequently feruloylated. However, feruloylation has been shown to occur at the Golgi (Myton and Fry, 1994). Also, the wheat orthologue of *XAX1*, *TaGT61.9* is highly expressed in starchy endosperm in wheat, where the proposed linkage is not found. Additionally, the

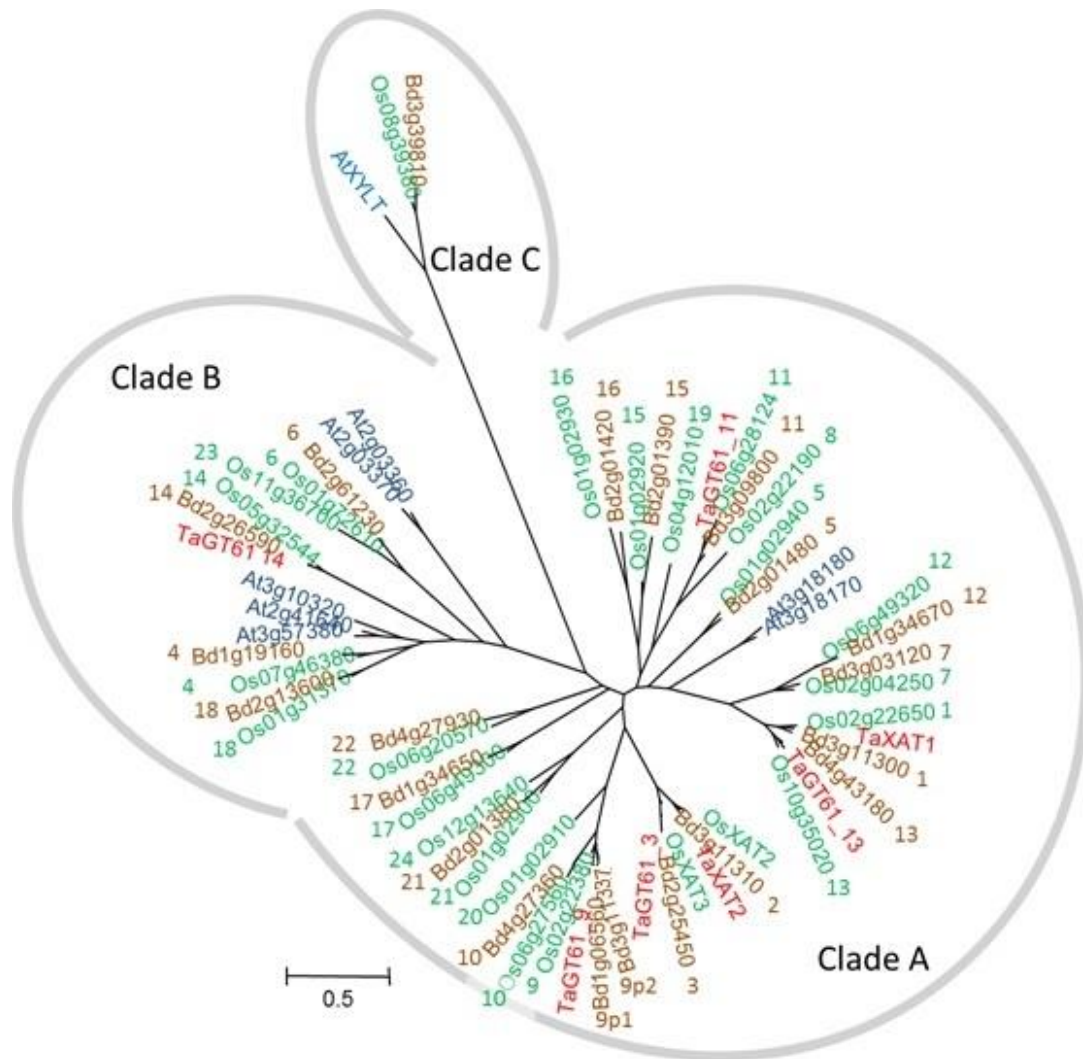
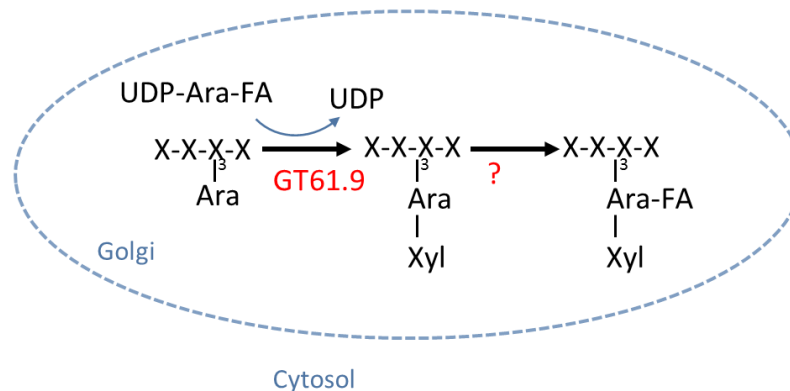


Figure 1.5 Phylogenetic tree of rice, wheat, Brachypodium and Arabidopsis *GT61* genes. Genes are arbitrarily numbered depending on sequence similarity. Only highly expressed wheat genes are included.

Brachypodium orthologues of *XAX1*, *BdGT61.9p1* and *BdGT61.9p2*, are coexpressed with the candidate genes within the BAHD acyl-coA transferase family (**Figure 1.4**), suggesting involvement of these proteins in feruloylation (Molinari et al., 2013), and there is strong evidence that BAHD genes are responsible for addition of *p*CA to arabinose (Bartley et al., 2013). BAHD proteins are localised to the cytosol (confirmed by analysis of GFP fusion proteins for TaBAHD1, 2 and 3, Dr. Jackie Freeman, unpublished) where UDP-arabinofuranose is made before being transported to the Golgi (Konishi et al., 2007). These findings support the hypothesis that GT61.9 is a feruloyl-arabinoxyl transferases that is responsible for the addition of feruloylated and/or coumaroylated Ara side chains to the Xyl backbone on AX. In this model, the loss of the Xyl linkage observed by Chiniquy et al. (2012) is explicable as the loss of the feruloylated Ara would in turn result in decreased available sites for the addition of (1-2)-linked Xyl residues. Thus, there are currently two competing models for the function of *XAX1/GT61.9* (**Figure 1.6**).

Chiniquy et al. (2012) model:



Our model:

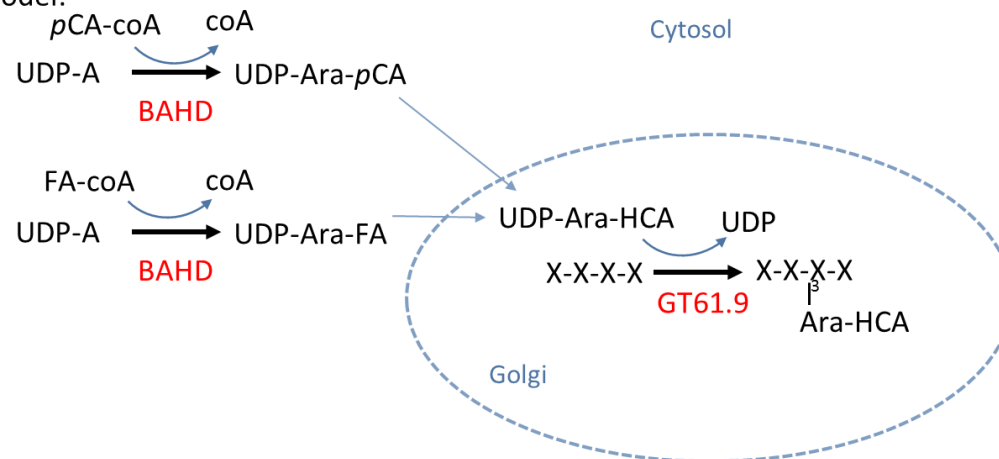


Figure 1.6 Two models for the role of BAHD acyltransferases and glycosyltransferase (GT)61.9 enzymes in the synthesis of hydroxycinnamic acid (HCA) side chain synthesis of arabinoxylan (AX) in grasses. BAHD enzymes are postulated to catalyse HCA-coA to uridine diphosphate (UDP)-arabinose (Ara) in the cytoplasm. There are two competing theories for the function of GT61.9. Chiniquy et al. (2012) propose that GT61.9 is a xylosyl (Xyl) transferase which catalyses the addition of a unique Xyl side chain of AX, whereas the alternative model proposes GT61.9 is a feruloyl- and/or coumaroyl-arabinosyl transferase.

1.9 Brachypodium

Historically, the dicotyledonous species *Arabidopsis thaliana* (*Arabidopsis*) has been the leading model organism for plants. However, the *Arabidopsis* genome is distantly related to the Poaceae (Draper et al., 2001) and the difference between monocot and dicot cell walls renders *Arabidopsis* a poor model for grass cell wall research.

Brachypodium distachyon (*Brachypodium*) is a small grass in the Poaceae family (subfamily Pooideae), and is closely related to the major cereal crops. Out of the 'big 3' cereal crops, maize, rice and wheat (Shewry, 2009), *Brachypodium* is most closely related to wheat, deriving from a common ancestor approximately 35 million years ago (Girin et al., 2014), however it is still closely related to rice and maize (Opanowicz et al., 2008). There are around 30 inbred lines of *Brachypodium*, created from a collection of natural accessions collected by the USDA National Plant Germplasm System (Garvin et al., 2008), of which the most widely used is inbred line Bd21.

Brachypodium has all the important characteristics of a good model organism, including a small genome of 272 Mb on 5 chromosomes, which has been fully sequenced from the inbred line Bd21 (International *Brachypodium* Initiative, 2010) and is available online (www.phytozome.net), and has an available microarray (Brkljacic et al., 2011). *Brachypodium* also has a short life cycle of 10-18 weeks, small growth height of 20 cm and simple growth requirements (Draper et al., 2001, Opanowicz et al., 2008, Vain, 2011). Furthermore, it is routinely transformable using an *Agrobacterium*-mediated method (Vogel and Hill, 2008). Additionally, there is a large number of available T-DNA insertion mutants for *Brachypodium* from the United States Department of Energy Joint Genome Institute (DOE JGI), which currently holds 23,649 lines (<http://jgi.doe.gov/our-science/science-programs/plant-genomics/brachypodium/brachypodium-t-dna-collection/>), and two available

Targeting Induced Local Lesions in Genomes (TILLING) populations from INRA in Versailles and the Boyce Thompson Institute (Brkljacic et al., 2011). Unfortunately, no plants carrying deletion-of-function mutations in the *BdGT61* genes of interest for AX synthesis are available. All things considered, Brachypodium provides an ideal model organism for the study of grasses and their unique cell walls, especially in transformation studies.

1.10 Project aims

In summary, FA is an integral and important component of grass cell walls, which cross-links polysaccharide chains and is a nucleation site for lignin polymerisation. Further, FA is a key target for improving the digestibility of grass and cereal cell walls in second generation biofuel and ruminant nutrition applications. Despite its importance, the genes and enzymes responsible for the addition of FA and *pCA* to AX remain elusive, but candidate genes have been described in the BAHD and GT61 families of enzymes (Mitchell et al., 2007). Rice knock-out mutants for a GT61 enzyme (*xax1*, named *GT61.9* here, resulted in decreased AX-esterified FA and *pCA* (Chiniquy et al., 2012), and therefore may be responsible for the addition of FA and/or *pCA* to AX, although the authors described *GT61.9* as a xylosyl transferase. *Brachypodium* provides an ideal model organism for the grasses in order to study the genetics of the esterification of FA on AX. Identifying these genes could be exploited for improved cell wall digestibility.

With this in mind, the aims of this project were to:

1. Identify an environmental factor (mechanical stress or jasmonic acid) which induced increased cell wall-bound FA and/or *pCA* (**Chapter 3 and 4**).
2. Identify changes in transcript levels of genes within the BAHD and GT61 families that corresponded to increased FA and/or *pCA* (**Chapter 4**).
3. Distinguish between two competing theories for the function of *GT61.9* in FA and/or *pCA* esterification to AX, using overexpression and RNAi knock-down in *Brachypodium* (**Chapter 5**).
4. Investigate the differential expression of two paralogues of *GT61.9* in *Brachypodium* tissues (**Chapter 5**).

Chapter 2. General Materials and Methods

2.1 Chemicals and reagents

Chemicals and reagents were sourced from Sigma-Aldrich®, UK, unless otherwise stated.

2.2 Plant growth and harvest

Brachypodium distachyon, inbred line Bd21 (Brachypodium), was used in all experiments. Germination and growth of Brachypodium is described in the chapter specific methods. Material was harvested directly into liquid nitrogen and stored at -80 °C.

2.3 Tissue preparation

Tissue was ground to a fine powder in liquid nitrogen using a Spex SamplePrep Freezer/Mill®, or by hand in liquid nitrogen using a pestle and mortar. Ground plant material was freeze dried and stored at room temperature until use in subsequent analyses, unless otherwise stated.

2.4 Alcohol insoluble residue (AIR) preparation

AIR preparation method 1: Tissue (20-50 mg) was washed with 2 ml phenol, 2 ml chloroform:methanol (2:1), and 1.5 ml ethanol. Samples were vortexed thoroughly, and centrifuged (>10,000 g, 20 min) to recover the pellet after each wash. The resulting pellet was air dried for 2 h.

AIR preparation method 2: AIR was prepared using a method slightly modified from Goubet et al. (2009). Tissue (100 mg) was washed successively with 2 ml volumes of aqueous solutions of 100% (v/v) ethanol, chloroform:methanol (1:1), 65% (v/v) ethanol,

80% (v/v) ethanol and 100% (v/v) ethanol. Samples were vortexed, and centrifuged (2000 g, 20 min) during each wash, to recover the pellet. AIR was dried at 60 °C overnight.

2.5 Destarching of alcohol insoluble residue

Destarching method 1: Starch was removed from the AIR using a method slightly modified from Harholt et al. (2006). AIR prepared using ‘AIR preparation method 1’ (**section 2.4**) was suspended in 1.5 ml 10 mM potassium phosphate buffer, pH 6.5, 1 mM CaCl₂, 0.05% (w/v) NaN₃, preheated to 95 °C. After 30 s, 1 unit/ml α-amylase (*Bacillus licheniformis*, Sigma-Aldrich®) was added and samples were incubated at 85 °C, for 15 min. The destarched AIR was collected by centrifugation (>10,000 g, 20 min), and washed thrice with 1 ml ethanol. Samples were vortexed, and centrifuged at (>10,000 g, 10 min) during each wash, to recover the pellet. Destarched AIR was dried at 60 °C under vacuum.

Destarching method 2: Destarching was performed using a method slightly modified from Englyst et al. (1994). AIR was prepared using ‘AIR preparation method 2’ (**section 2.4**). AIR (10 mg ± 0.20 mg) was suspended in 1 ml 0.1 M sodium acetate buffer, pH 5.2, with 1.25% (v/v) α-amylase (*Bacillus licheniformis*, Sigma-Aldrich®). Samples were incubated at 85 °C, for 1 h, with shaking. A volume of 5 µl pullulanase (*Bacillus acidopullulyticus*, Sigma-Aldrich®) was added, and samples were incubated at 50 °C, for 30 min, with shaking. Polysaccharides were precipitated in 1.3 ml cold ethanol for 1 h on ice, and pelleted by centrifugation (10,000 g, 4 °C, 10 min). The pelleted polysaccharides were washed with 1 ml 70% (v/v) aqueous ethanol thrice. Samples were vortexed, and centrifuged (16,000 g, 5 min), during each wash, to recover the pellet. Destarched AIR was dried at 40 °C under vacuum.

2.6 Matrix polysaccharides extraction and analysis

Matrix polysaccharides were analysed as previously described by Jones et al. (2003). Tissue (5 mg) was treated with 0.5 ml 2 M trifluoroacetic acid (TFA), and oxygen was removed by flushing with argon. Samples were hydrolysed at 100 °C, for 4 h, with mixing at regular intervals. TFA was evaporated under vacuum. The resulting pellet was washed twice in 500 µl isopropanol, and dried under vacuum. The pellet was resuspended in 200 µl ELGA water and samples were centrifuged (>10,000 g, 5 min). The supernatant was analysed for reducing sugars by high performance anion-exchange chromatography. Monosaccharides were separated on a Dionex CarboPac PA20 (3 x 150 mm), using H₂O (solution A), 200 mM sodium hydroxide (solution B) and 0.1 M sodium hydroxide, 0.5 M sodium acetate (solution C) as the mobile phase, with the following gradient elution program: 0-5 min, linear gradient from 100% A to 99% A, 1% B; 5-22 min, linear gradient to 47.5% A, 22.5% C, 30% D; 22-30.1 min, linear gradient to 100% B; 30.1-37 min, 99% A, 1% B; 37-39 min; 100% A. The flow rate was maintained at 0.5 ml min⁻¹. Peaks were identified and quantified compared to runs of known standards. The pellet was used to determine crystalline cellulose content of the sample (**section 2.7**).

2.7 Crystalline cellulose extraction and analysis

Crystalline cellulose was analysed using a method modified from Viles and Silverman (1949). The pellet obtained from the matrix polysaccharides extraction (**section 2.6**) was washed in 1.5 ml water once, and in 1.5 ml acetone thrice. Samples were vortexed, and centrifuged (10,000 g, 5 min), during each wash. The resulting pellet was air dried at room temperature. Cellulose was hydrolysed in 72% (w/v) aqueous sulphuric acid, at room temp, for 4 h, and then in 3.2% (w/v) aqueous sulphuric acid, at 120 °C, for 4 h. Samples were centrifuged

(>10,000 g, 5 min), and 40 µl of the supernatant was diluted with 360 µl water. The sample was added to 800 µl sulphuric acid with 2 mg/ml anthrone reagent. The samples were heated at 80 °C for 30 min. Absorbance was read at 620 nm on a 96-well optical plate (200 µl/ well). Glucose concentration was determined by comparison of absorbance to glucose standards.

2.8 Lignin extraction and analysis

Lignin was analysed using a method modified from Foster et al. (2010). Tissue (5 mg) was treated with 250 µl glacial acetic acid:acetyl bromide (3:1), at 50 °C, for 3 h, thrice mixed by vortex in the final hour. A volume of 1 ml 2 M NaOH and 175 µl 0.5 M hydroxylamine was added and made up to 5 ml total volume with glacial acetic acid. The samples were diluted, 1 in 10, with glacial acetic acid, and A_{280} was measured. The percentage of acetyl bromide soluble lignin (ABSL) was determined using equation 1, with the coefficient = 17.75, pathlength = 1, and volume = 5 ml.

Equation 1
$$\text{ABSL (\%)} = \left(\frac{\text{ABS}_{280}}{\text{coefficient}} \times \text{pathlength} \right) \times \left(\frac{\text{volume (ml)} \times 100\%}{\text{biomass (g)}} \right)$$

2.9 Silica analysis

Silica concentration was determined using X-ray fluorescence spectrometry as previously described by Reidinger et al. (2012). Ground, freeze-dried tissue was compressed into a dense pellet, under high pressure, using a manual hydraulic press. Silicon concentration was determined using a portable P-XRF instrument (Niton XL3t900 GOLDD Analyser, Thermo Scientific) using settings as previously described. Silica content (SiO_2) was determined as a function of silicon (Si) molecular weight using equation 2. Samples were analysed in duplicate and averaged.

Equation 2
$$\text{Si (\%)} \times 2.14 = \text{SiO}_2(\%)$$

2.10 Saccharification

Saccharification was performed by Rachael Hallam, York University, as described by Gomez et al. (2011), using a specialised automated platform. To summarise, 4 mg sample was pre-treated with 350 µl water at 90 °C for 30 min, rinsed with 25 mM sodium acetate buffer five times, and hydrolysed at 50 °C for 8 h with 250 µl Celluclast (Novozyme):water (1:4). The hydrolysate was treated with 1 M NaOH and a solution containing 0.43 mg/ml MBTH and 0.14 mg/ml DTT in 25 mM sodium acetate buffer. Reducing sugars were determined by measuring A_{620} after addition of an oxidising reagent (0.2% (w/v) $\text{NH}_4\text{Fe}(\text{SO}_4)_2$, 0.2% (w/v) sulfamic acid, 0.1% (v/v) HCl), and by comparison to the absorbance of known standards.

2.11 Cell wall-bound phenolic acid extraction

Cell wall-esterified phenolic acids were extracted using a method slightly modified from Li et al. (2008). Exactly 10 mg \pm 0.20 mg tissue was washed with 1 ml 80% (v/v) aqueous ethanol. The samples were vortexed, sonicated for 10 min, heated at 80 °C for 15 min and centrifuged (5000 g, 15 min) to recover the pellet. The wash was carried out thrice, without heating on the second and third washes. A volume of 20 µl 3,5-dichloro-4-hydroxybenzoic acid (15 mg/ml) internal standard was added and samples were hydrolysed with 800 µl 2 M NaOH for 16-18 h in the dark. The samples were centrifuged (5000 g, 15 min) and the supernatant was acidified to a pH below 2 with 220 µl 12 M HCl (Fisher Scientific). Phenolic acids were extracted into 800 µl ethyl acetate (Fisher Scientific) thrice; on each extraction the upper phase was collected after centrifugation (16,000 g, 5 min) and pooled, before being dried under vacuum. The extracted phenolic acids were stored at either -20 °C or 4 °C before separation and quantification by High Performance Liquid Chromatography (HPLC, **section 2.12**).

2.12 High performance liquid chromatography (HPLC)

All chemicals used were of HPLC quality where available. Phenolic acids were resuspended in 1 ml 50% (v/v) aqueous methanol (Fisher Scientific), 2% (v/v) aqueous acetic acid (Fisher Scientific) for plant material, and 100 μ l 2% (v/v) aqueous acetic acid for callus material, for analysis by HPLC.

Phenolic acids were quantified using a Shimadzu Prominence high-performance liquid chromatograph with a photo-diode array detector. Phenolic acids were separated on a Kinetex Phenyl-Hexyl reverse phase UPLC column (150 x 4.6 mm, 5 μ m), maintained at 30 °C, using acetonitrile (Fisher Scientific) (solution A) and 2% aqueous acetic acid (Solution B) as the mobile phase, with the following gradient elution program: 0-12 min, linear gradient from 100% B to 30% B; 12-14 min, isocratic 30% B; 14-14.1 min, linear gradient from 30% B to 100% B; 14.1-18 min, isocratic 100% B followed by 2 min post-run at 100% B. The flow rate was maintained at 2 ml min⁻¹. The injection volume was 20 μ l. Quantitation was by integration of peak areas of absorbance at 280 nm relative to internal standard peak area. Peaks were identified by retention times of pure standards and by published absorbance spectra (Waldron et al., 1996, Dobberstein and Bunzel, 2010b). Ferulic acid (FA) and *para*-coumaric acid (*p*CA) concentration was calculated by reference to calibrations generated using known amounts of commercial standards (Sigma-Aldrich®). Amounts of *cis*- and *trans*-FA were summed to give total monomeric FA. Diferulic acid (diFA) concentrations were calculated using relative response factors (RRFs, relative to FA) generated by using known amounts of pure diFA (8-8-, 8-5-, 5-5-, 8-O-4- and 8-5 benzofuran- (8-5 BF)-coupled) provided by John Ralph and Fachuang Lu (Great Lakes Bioenergy Institute, University of Wisconsin, Madison, USA). diFA8-O-4 and diFA8-5 BF are reported together where peaks failed to fully separate on the chromatograph.

2.13 Standard cloning procedure

Plasmids were digested using Promega enzymes and buffers, following the manufacturer's instructions. The digestion products were separated on 1% agarose (Fisher Scientific) TAE gels (4.84 g/l Trizma[®] base, 1.14 ml/l glacial acetic acid, 2 ml/l 0.5 M EDTA, pH 8.0), containing ethidium bromide (0.5 µg/ml) to allow visualisation on a UV transilluminator (GelDoc-It^{®2} Imager, Ultra-Violet Products Ltd, Cambridge). Bands of DNA were extracted from the gel using the Wizard[®] SV Gel and PCR Clean-Up System (Promega), following the manufacturer's instructions. Ligation was performed using T4 DNA Ligase (NEB), following the manufacturer's instructions. The ligation product was transformed into competent *Escherichia coli* DH5α (homemade) or JM109 (Promega) cells and plated onto 2xYT agar (Fisher Scientific) with selection (300 µg/ml streptomycin and 100 µg/ml spectinomycin), and incubated at 37 °C. Individual colonies were picked and cultured in 2xYT agar broth with selection, at 37 °C with shaking. Plasmids were extracted from cells using the GeneJET Plasmid Miniprep Kit (Thermo Scientific), following the manufacturer's instructions. Sequencing by Eurofins sequencing service (Eurofins Genomics, Germany) confirmed the plasmid sequence.

2.14 Agrobacterium transformation

Agrobacterium tumefaciens, genotype AGL1 (Agrobacterium) was transformed with the construct of interest using electroporation. Two µl of 30 ng/µl plasmid was added to 50 µl AGL1 Agrobacterium. Electroporation was applied at 2.5 kV, 400 Ω and 25 µF, and the transformed cells were immediately mixed with 1 ml ice-cold SOC media and subsequently incubated at 28 °C for 2 h. The Agrobacterium culture was plated onto LB media (1% (w/v) tryptone, 0.5% (w/v) yeast extract, 1% (w/v) NaCl, 1.5% (w/v) Bacto[™] Agar (Fisher Scientific)), containing 300 µg/ml streptomycin,

100 µg/ml spectinomycin, 25 µg/ml rifampicin (Melford), and 100 µg/ml carbenicillin (Melford). Plates were incubated at 28 °C. Transformed *Agrobacterium* was either stored at -80 °C in glycerol stocks, or directly plated onto MG/L media (5 g/l tryptone (Oxoid Ltd), 2.5 g/l yeast extract (Oxoid Ltd), 5 g/l NaCl, 5 g/l mannitol (Acros Organics), 0.1 g/l MgSO₄, 0.25 g/l K₂HPO₄ (Fisher Scientific), 1.2 g/l glutamic acid, 1.5% (w/v) Bacto™ Agar (Fisher Scientific), pH 7.2) for *Brachypodium* transformation.

2.15 Callus generation

Callus was generated as described by Vogel and Hill (2008). *Brachypodium* was grown in the glasshouse at 20/20 °C day/night temperature, with a 16/8 h light/dark cycle provided by natural light, with supplementary lighting. Plants were vernalised 1 week after sowing, for 3 weeks at 6 °C, 8/16 h light/dark cycle. Immature seeds were harvested from 2-3 month old plants and the lemma was removed. Seeds were surface sterilised in 10% household bleach for 5 min, and washed with sterile water thrice. Immature embryos were removed from sterilised seeds by dissection, and were transferred to callus induction media (CIM; 4.43 g/l LS salts (Duchefa Biochemie), 30 g/l sucrose (Fisher Scientific), 0.6 mg/l CuSO₄, 2.5 mg/ml 2,4-D, 0.2% (w/v) Phytigel™, pH 5.8). The embryos were incubated at 28 °C in the dark to generate callus, which was subcultured every 2-3 weeks to generate a sufficient quantity.

2.16 *Brachypodium* transformation

Brachypodium callus was transformed as described by Vogel and Hill (2008), using an *Agrobacterium* mediated method. *Agrobacterium* was suspended in a liquid CIM suspension (CIM as per **section 2.15**, without Phytigel™ gelling agent, with

200 μ M acetosyringone and 10 μ l/ml 10% Synperonic PE/F68), to an OD₆₀₀ of 0.6. Brachypodium calli (50 pieces per 20 ml suspension) were added and were co-cultivated with the Agrobacterium for 5 min. Co-cultivated calli were placed onto a 7 cm Whatman filter paper disc, and dried in the dark at 22 °C for 3 d. Callus pieces were transferred to CIM plates with 150 mg/l Timentin and 60 mg/l hygromycin selection, and incubated in the dark at 28 °C for one week, and then on fresh media for 2 weeks. Healthy callus was transferred to regeneration media (4.43 g/l LS salts, 30 g/l maltose (Melford), 0.2% (w/v) Phytigel™, pH 5.8), with 0.2 mg/l Kinetin (Duchefa Biochemie), 150 mg/l timentin and 60 mg/l hygromycin selection. Shoots were generated at 22 °C, 16/8 h light/dark cycle, and then transferred to pots containing MS media (4.42 g/l MS salts plus vitamins, 30 g/l sucrose, 0.2% (w/v) Phytigel™, pH 5.7) until plants were large enough to transfer to soil.

2.17 DNA isolation

Plant tissue was harvested, frozen at -80 °C, freeze-dried, and ground to a powder using a Spex Sampleprep 2010 Geno/Grinder®. The ground material was extracted into 500 μ l DNA extraction buffer (100 mM Tris-HCl, pH 7.0, 250 mM NaCl, 25 mM EDTA, 0.5% SDS), and centrifuged (16,000 g, 5 min). A volume of 350 μ l isopropanol was added to an equal volume of the supernatant and mixed. Samples were centrifuged (16,000 g, 5 min) and the supernatant was discarded. A volume of 900 μ l 70% (v/v) aqueous ethanol was added to the pellet and samples were incubated at room temperature for 1 h with shaking, and centrifuged (16,000 g, 5 min) and the supernatant was discarded. The DNA pellet was dried under vacuum, and gently resuspended in 40 μ l nuclease-free water by incubating at room temperature for 1 h, with shaking. DNA concentration was determined on a NanoDrop 1000 Spectrophotometer (Thermo Scientific).

2.18 Quantitative PCR (qPCR) to determine zygosity

Genomic DNA was extracted as described in **section 2.17**. Quantitative PCR (qPCR) was carried out on a Roche LightCycler® 96 System, in a 96-well plate. Reaction mixtures contained 4 µl FastStart Essential DNA Green Master (Roche), 3 µl primer mix (400 nM F primer, 400 nM R primer) and 1 µl DNA per well (1-500 ng/µl). Primers were: F 5'GTGCAGGTCGATCTTAGCAGG and R 5'AGTCCTCTTCAGAAATGAGCTTTTG (for amplification of overexpression constructs *Ubi::GT61.9p1-Myc* and *IRX5::GT61.9p1-Myc*), and F 5'CGCAAGACAATGACCGCTATG and R 5'CCAATCCGACGCCTCCTTATA (for amplification of the housekeeping gene ubiquitin). Cycling conditions were 95 °C for 10 min, 40 x (95 °C for 20 s, 60 °C for 15 s, 72 °C for 15 s). As a quality control measure, a melting curve was created using an increasing temperature gradient (95 °C for 5 s, 70 °C increasing to 95 °C, 40 °C for 30 s). Two technical replicates per sample were averaged. Amplification of the overexpression construct fragment was standardised to amplification of the housekeeping gene fragment using equation 3 (where C_q = quantitation cycle). Homozygous plants were determined as those with double the zygosity value of heterozygous plants.

Equation 3 Zygosity value = $\frac{2^{-\text{gene of interest (C}_q\text{)}}}{2^{-\text{housekeeping gene (C}_q\text{)}}$

2.19 RNA isolation

Pine Tree RNA Isolation Method: RNA was extracted as described by (Chang et al., 1993). Tissue (10-50 mg) was suspended in 500 µl-1 ml RNA extraction buffer (2% (w/v) hexadecyltrimethylammonium bromide (CTAB), 2% (w/v) polyvinylpyrrolidone K 30 (PVP), 100 mM Tris-HCl (pH 8.0),

25 mM EDTA, 2 M NaCl, 0.5 g/l spermidine, 2% (v/v) β -mercaptoethanol), warmed to 65 °C. Extraction was carried out twice with an equal volume of chloroform:isoamyl alcohol. The aqueous phase was recovered following centrifugation (16,000 g, 15 min) after each extraction. RNA was precipitated by the addition of 10/32 of the volume 8 M LiCl and incubated on ice, overnight. Samples were centrifuged (20,000 g, 4 °C, 30 min) to pellet the precipitated RNA. The pellet was resuspended in 500 μ l SSE buffer (1 M LiCl, 0.5% SDS, 10 mM Tris-HCl (pH 8.0), 1 mM EDTA (pH 8.0), warmed to 65 °C), by incubation at room temperature for 30 min, with shaking. An equal volume of chloroform:isoamyl alcohol was added and the aqueous phase was recovered after mixing by vortexing and centrifugation (20,000 g, 4 °C, 30 min). Two volumes of ethanol were added, and samples were incubated at 80 °C for 30 min, and at 20 °C for 1-24 h. The samples were centrifuged (20,000 g, 4 °C, 20 min) and the resulting pellet was dried under vacuum. RNA was resuspended in nuclease free water.

TRIzol RNA isolation method: Tissue was prepared as described in **section 2.3**, without freeze-drying, and stored at -80 °C. Around 10-50 mg fresh tissue was suspended in 1 ml TRI Reagent[®] and then centrifuged (12,000 g, 4 °C, 10 min). The supernatant was added to 200 μ l chloroform, and incubated at room temperature for 2-3 min. The samples were centrifuged (10,000 g, 4 °C, 15 min). To the upper phase, $\frac{1}{2}$ volume of isopropanol, and an equal volume of 0.8 M aqueous sodium citrate, 1.2 M aqueous NaCl was added. The samples were incubated at room temperature for 10 min, and centrifuged (10,000 g, 4 °C, 10 min). The pelleted RNA was washed with 1 ml 75% (v/v) aqueous ethanol (vortexed, centrifuged 10,000 g, 4 °C, 10 min), and evaporated to dryness under vacuum. RNA was resuspended in nuclease free water. RNA concentration was determined on a NanoDrop 1000 Spectrophotometer (Thermo Scientific).

2.20 Western blotting

Protein was extracted from samples flash-frozen in liquid nitrogen and ground by hand, or freeze-dried and ground in a Spex SamplePrep 2010 Geno/Grinder®.

Samples were suspended in an aqueous solution containing NuPAGE® LDS Sample Buffer (4x) and NuPAGE® reducing agent (10x) (Life Technologies), diluted to 1x from stock. Samples were vortexed and heated at 70 °C for 10 min, cooled on ice and centrifuged (16,000 g, 5 min). A volume of 5 µl (stem samples) or 20 µl (leaf samples) of the supernatant was run on SDS-PAGE gels (NuPAGE™ Novex™ 4-12% Bis-Tris Protein Gel) using 1 x NuPAGE® MOPS SDS running buffer (Life Technologies) at 50-60 V for 30 min, and then at 200 V for 60 min.

To visualise proteins, the gels were fixed in an aqueous solution containing 10% (v/v) acetic acid, 10% (v/v) methanol for 15 min, stained in 80% (v/v) aqueous Brilliant Blue G according to manufacturers instructions, and destained with distilled water.

To Western blot the protein gel, the Life Technologies iBlot system was used, following the manufacturer's instructions. The resulting nitrocellulose blot was blocked in Tris Tween Buffered Saline (TTBS; 5 mM Trizma®.HCl, 28 mM NaCl, pH 7.5, 0.05% TWEEN® 20) containing 5% milk protein (Marvel Original), at 4 °C, overnight. The blot was incubated first with mouse monoclonal anti-c-Myc antibody (Life Technologies), at 4 °C overnight, and then with goat anti-mouse IgG secondary antibody, Alexa Fluor® 488 conjugate (Thermo Fisher Scientific), at room temperature, for 2 h. Antibodies were diluted to 0.2 µl/ml (primary antibody) and 0.12 µl/ml (secondary antibody) in TTBS with 1% (w/v) Bovine Serum Albumin (BSA) before use. Blots were washed in TTBS between each incubation. Immunoreactivity was visualised using 5 ml Pierce® ECL Western Blotting Substrate (Thermo

Scientific) and exposure to Amersham Hyperfilm™ ECL (GE Healthcare Life Sciences).

2.21 Microscopy

Green fluorescent protein (GFP) was visualised using a Zeiss 780 LSM confocal microscope. GFP was excited under a 488 nm laser, and detected at 499-556 nm.

Chapter 3. The Effect of Mechanical Stress on Cell Wall Composition in *Brachypodium distachyon*

3.1 Introduction

Environmental mechanical stresses to plants are in the form of wind, rain, hail or disturbance by animals, humans or machinery, and often result in dramatic yield loss (Biddington, 1986, Mitchell, 1996, Jaffe and Forbes, 1993, Braam, 2005). Mechanical stress has become increasingly relevant in urban plant growth and in agriculture where invasive practices are used (Mitchell, 1996). The effect of mechanical stress, which may be seismomorphogenic (stress by shaking; Mitchell et al., 1975) or thigmomorphogenic (stress by touch or wind; Jaffe, 1973), on plant morphology is well characterised as a dramatic reduction of internode length and leaf elongation, accompanied by an increase in stem diameter (Biddington, 1986, Mitchell, 1996). These morphological changes are thought to be adaptive, and improve tolerance to abiotic and biotic stresses (Braam, 2005, Chehab et al., 2012).

The signalling mechanisms involved in the mechanical stress response involve an initial and rapid influx of cytosolic calcium (Jones and Mitchell, 1989, Knight et al., 1992), calcium-activated calmodulin (calcium binding signalling molecule) upregulation (Braam and Davis, 1990), and generation of reactive oxygen species (ROS; Yahraus et al., 1995). Downstream, the signalling hormone ethylene has long been associated with the mechanical stress response, although it only accounts for increased radial growth of the stem, and not the decrease in internode elongation that is typically observed in the mechanical stress response (Biro and Jaffe, 1984). Auxin and ABA have also been implicated in the mechanical stress pathway (Erner and Jaffe, 1982), and more recently jasmonic acid (JA) has been shown to be required

in the mechanical stress response (Chehab et al., 2012). Interactions between hormones and downstream signalling remain to be elucidated.

Cell wall polysaccharides are affected by mechanical stress in differing plant families. Woody plants develop specialised secondary cell walls termed 'reaction wood' in response to bending due to gravitational forces or wind. Reaction wood manifests in angiosperms such as *Populus sp.* as an alternative cell wall layer, the 'G-layer', which has increased crystalline cellulose, and decreased matrix polysaccharides and lignin on the upper side of the branch, termed tension wood (Andersson-Gunneras et al., 2006). In gymnosperms, reaction wood manifests as increased lignin on the underside of the branch (Yamashita et al., 2007), the purpose of which is to upright a tilted stem. In cactus, specialised cell walls are reported to form at joints, in response to bending stress, which are thicker and have more lignin (Kahn-Jetter et al., 2000).

There is limited knowledge of the effect of mechanical stress on the cell wall of herbaceous plants, although Verhertbruggen et al. (2013) reported that pectic arabinan side chains may increase in response to mechanical stress in *Arabidopsis*. Additionally, Lee et al. (2005) report that only 22 cell wall modifying genes are upregulated in response to mechanical perturbation in *Arabidopsis*, including cellulose synthase, pectin esterases, arabinogalactan protein and expansin and extensin proteins. Reports on the direct effect of mechanical stress in the Poaceae are scarce.

Hydroxycinnamic acids ferulic- and *para*-coumaric acid (FA and *p*CA), which are ester-linked to arabinoxylan (AX) in grass cell walls, are of interest in abiotic stresses. Cell wall-bound FA may dimerise to form covalently bonded AX bridges, or may form ether or C-C bridges which links AX to lignin. These cross-links function in strengthening or hardening of certain tissues, and in the cessation of cell expansion. The function of AX-linked *p*CA remains poorly understood, but has been implicated

in plant defence (Santiago et al., 2008, **Chapter 1.6.5**). There is some evidence that wall-bound FA may be inducible in response to some abiotic stresses, such as salt stress (Uddin et al., 2014), and drought stress (Vuletic et al., 2014), however, the effect of mechanical stress on FA and *p*CA in grass cell walls is unknown. FA mediated cross-links are formed by peroxidase-mediated chemical reactions which generate ROS such as H₂O₂ (Hatfield et al., 1999). It is therefore possible that the ROS burst caused by mechanical stress and other abiotic stresses induces increased cell wall-bound FA dimerisation and cross-links to lignin.

Lodging in cereals reduces grain yield and is caused by mechanical stresses such as wind and rain (Berry et al., 2004). Therefore, physiological changes induced by mechanical stress, such as reduced growth and increased stem diameter are likely to be traits associated with increased lodging resistance. Additionally, genetic traits associated with differences in lodging resistance include lignin (Flint-Garcia et al., 2003) and cellulose (Kashiwagi et al., 2016). FA cross-linking has been shown to be a trait associated with lodging resistance, as shown in barley (Travis et al., 1996).

Arabinoxylan may also be involved in stem strength, as xylan synthesis mutants have been shown to have greatly reduced stem strength which is approximately 40% of that of wild type (Chiniquy et al., 2013). Additionally, increased arabinose substitutions on AX, possibly caused by increased transcript levels *OsXAT2* and *3* genes, are negatively correlated with lodging in rice mutants, which may be due to the interaction between AX and cellulose (Li et al., 2015).

An increased understanding of environmental factors which affect feruloylation and other features of grass cell walls, and how they affect key traits such as recalcitrance and lodging resistance, will be influential in breeding new elite cultivars. Further, an easily applied environmental treatment which induces changes in feruloylation could

be exploited to study the associated changes in transcripts and proteins, to investigate mechanisms controlling this key trait.

Due to the current limited knowledge of the effect of mechanical stress on the plant cell wall, and the speculated role of FA in the stress response, the aims of the experiments in this chapter were to investigate the effect of thigmomorphogenic mechanical stress on biochemical changes in the cell wall composition of *Brachypodium*, and to determine whether mechanical stress induced increases in AX-linked HCAs.

3.2 Chapter 3 specific methods

3.2.1 Plant growth

Brachypodium was grown in the glasshouse at 25/20 °C, 16/8 h light/dark cycle with supplementary lighting, after 2 weeks of vernalisation at 6 °C, 8/16 h light/dark cycle.

3.2.2 Mechanical stress

At the time specified in **Table 3.1**, plants were moved to a mechanical stress treatment with a moving metal bar that brushed the plants at 1 brush/min, at a speed of 0.1 m/s, or to a control treatment without brushing (**Figure 3.1**, mechanical stress device designed and constructed at Rothamsted Research, UK). Upon completion of the stress period (**Table 3.1**), leaf and stem material was harvested as described in **Chapter 2.2** and plant material for analysis was prepared as described in **Chapter 2.3**.

3.2.3 Overview of mechanical stress experiments

The pilot study was performed to analyse the cell wall-bound phenolic acid composition of Brachypodium after 4 weeks mechanical stress. In this experiment, four biological replicates of ten plants each were analysed for phenolic acids (three technical replicates), silica (no technical replication) and saccharification (four technical replicates) as described in **Chapter 2.11-2.12**, **2.9** and **Chapter 2.10 (Table 3.1)**. Mechanically stressed plants were compared to controls of four biological replicates of ten plants each, which were grown alongside the mechanically stressed plants but without brushing (**Figure 3.1**, **Table 3.1**).

Experiment two (exp. 2) was performed to analyse total cell-wall composition of mechanically stressed Brachypodium. During experiment two, two biological

replicates of ten plants per treatment were randomly assigned in a statistical design. These plants were harvested after 1 week of stress and labelled 'young tissue'. Cell wall-bound phenolic acids were analysed in duplicate as described in **Chapter 2.11** and **Chapter 2.12** in young tissue. The remaining plants were grown for 22 or 23 d, with continuous stress except for an unintentional 5 d stress-free period from days 8-12 (inclusive). Stem heights and internode number of 60 plants per treatment were measured and averaged. Two biological replicates (trays) of 30 plants were analysed for cell wall components lignin, cellulose and matrix polysaccharides in triplicate and averaged, as described in **Chapter 2.8**, **Chapter 2.7** and **Chapter 2.6** respectively, and for silica as described in **Chapter 2.9**. During exp. 2, tillers were removed from plants every 3-4 d to create uniform, comparable plants (**Table 3.1**). Mechanically stressed plants were compared to an equal number of untreated control plants, which were grown alongside the mechanically stressed plants but without brushing (**Figure 3.1**, **Table 3.1**).

A



B



Figure 3.1. Experimental design of mechanical stress treatment of *Brachypodium distachyon*. Plants were divided into A) a control treatment group, or B) a mechanical stress treatment group with a moving metal bar to administer stress treatment.

Table 3.1 Summary of experiments on the effect of mechanical stress on *Brachypodium distachyon* cell walls (MS = mechanical stress).

Experiment name	Start of treatment (plant age, d)	Biological Replication	Days of mechanical stress	Tillers removed	Analyses
Exp. 1 (Pilot)	41	MS: 4 reps of 10 plants	28	No	Phenolic acids, silica, saccharification
		Controls: 4 reps of 10 plants	0		
Exp. 2 young plants	35	MS: 2 reps of 10 plants	7	Yes	Phenolic acids
		Controls: 2 reps of 10 plants	0		
Exp. 2 developed plants	35	MS: 2 reps of 30 plants	Rep 1: 22 Rep 2: 23 stress-free period days 8-12 (inclusive)	Yes	Stem height, lignin, cellulose, matrix polysaccharides, silica, saccharification
		Controls: 2 reps of 30 plants	0		

3.2.4 Statistics

Outlying values were discounted as per Grubbs' outliers test. Student's t-test (two-tailed distribution, assuming equal variance), was applied to the pilot experiment and stem height measurements data using Microsoft Excel 2010.

Analysis of variance (ANOVA) was applied to the data from exp. 2, taking account of the 2 d of measurement as blocks and the number of technical replicate observations per sample, and testing the main effects and interaction between two factors: treatment and tissue (F-tests). Means in relevant statistically significant ($p < 0.05$, F-test) terms from the ANOVA are interpreted using the standard error of the difference (SED) between means on the residual degrees of freedom (df), invoking a least significant difference (LSD) at the 5% level of significance. Where mean figures are presented in the text as a main effect of treatment, the figure presented is the average of values across the two tissues measured: leaf and stem. Assistance with statistical analyses was provided by Stephen Powers, Rothamsted Research.

3.3 Results

3.3.1 Plant growth

Brachypodium plants were mechanically stressed for 3-4 weeks using a moving metal bar. Plants that were stressed exhibited stunted growth compared to the control treatment. After 3 weeks of mechanical stress (exp. 2, developed plants, **Table 3.1**) the stem height of mechanically stressed plants was 28% lower than controls, reduced from 12.8 cm in control samples to 9.2 cm in mechanically stressed plants. The number of internodes remained constant between mechanically stressed plants and the controls (**Figure 3.2**).



	Control	Mechancially stressed
Stem length (cm, mean)	12.8 (\pm 0.07)	9.2 (\pm 0.06)
Internode no. (mode)	6	6

Figure 3.2 The effect of 3 weeks of mechanical stress on stem length (\pm SE) and internode number in *Brachypodium distachyon*.

3.3.2 Cell wall-bound phenolic acids

Cell wall-bound *p*CA, FA monomer and FA dimers were measured in 10 week old *Brachypodium* leaf and stem after 4 weeks of mechanical stress treatment and compared to a non-stressed control group (exp. 1, **Table 3.1**). There was no significant difference in cell wall-bound *p*CA or FA monomer in *Brachypodium* leaf or stem after 4 weeks of mechanical stress, compared to the non-stressed controls. However, cell wall-bound FA dimers in mechanically stressed leaf tissue were 28% greater than controls ($p < 0.044$, F-test for interaction between factors treatment and tissue: means = 1.00 (control leaf), 1.25 (stress leaf); SED 0.038 on 24 df, (**Figure 3.3**).

Since mature tissue in the 10 week old plants evaluated may already be coumaroylated and feruloylated to the maximum extent, particularly in stem tissue, the effect of mechanical stress on phenolic acids was also measured in young *Brachypodium* leaf and stem tissue (6 weeks old, exp. 2 young plants, **Table 3.1**) after 1 week of mechanical stress treatment. In this experiment, there was no significant difference in cell wall-bound *p*CA or FA dimers between mechanically stressed *Brachypodium* and the controls. However, there was a main statistically significant effect of mechanical stress on cell wall-bound FA monomer, which was 7.7% and 8.6% greater than the controls in mechanically stressed stem and leaf respectively ($p = 0.001$, F-test for main effect of treatment in stem and leaf tissue: means = 2.22 (control), 2.40 (stress); SED 0.037 on 11 df). In young *Brachypodium* leaves, FA dimer also increased by 16%, although this was not statistically significant (**Figure 3.4**). Finally, there was a small 5% increase in *p*CA in leaf (not statistically significant).

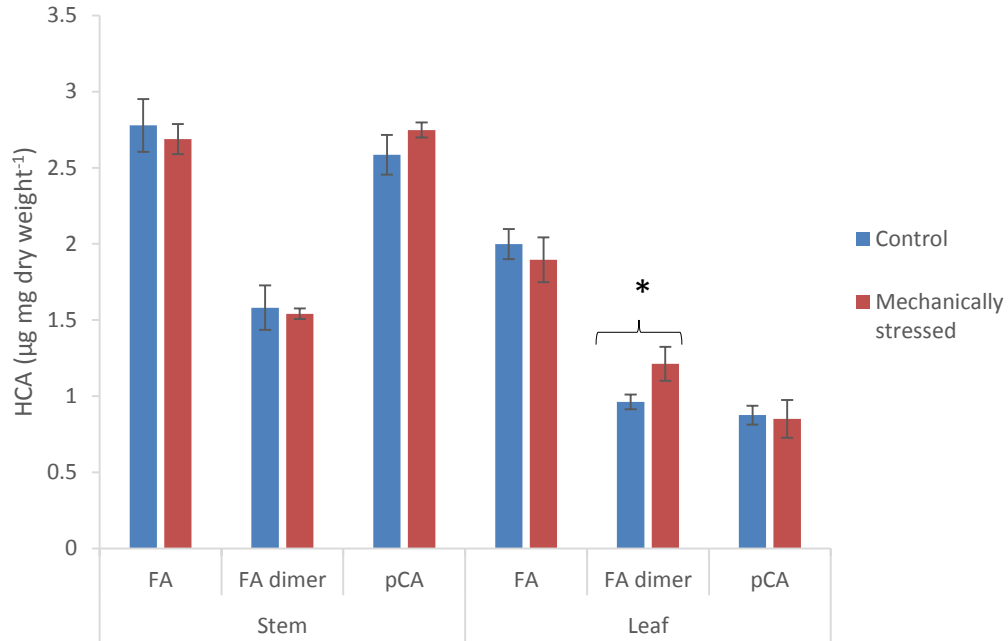


Figure 3.3 The effect of 4 weeks of mechanical stress on relative wall-bound ferulic acid (FA) and *para*-coumaric acid (*pCA*) (\pm SE) in *Brachypodium distachyon* tissues. FA dimers are the sum of diF8-8, diF8-5, diF8-5 benzofuran, diF5-5 and diF8-O-4. Analyses were performed on material from ‘exp. 1’ (**Table 3.1**). Asterisk represents significant difference ($p < 0.05$, LSD) between control and treatment.

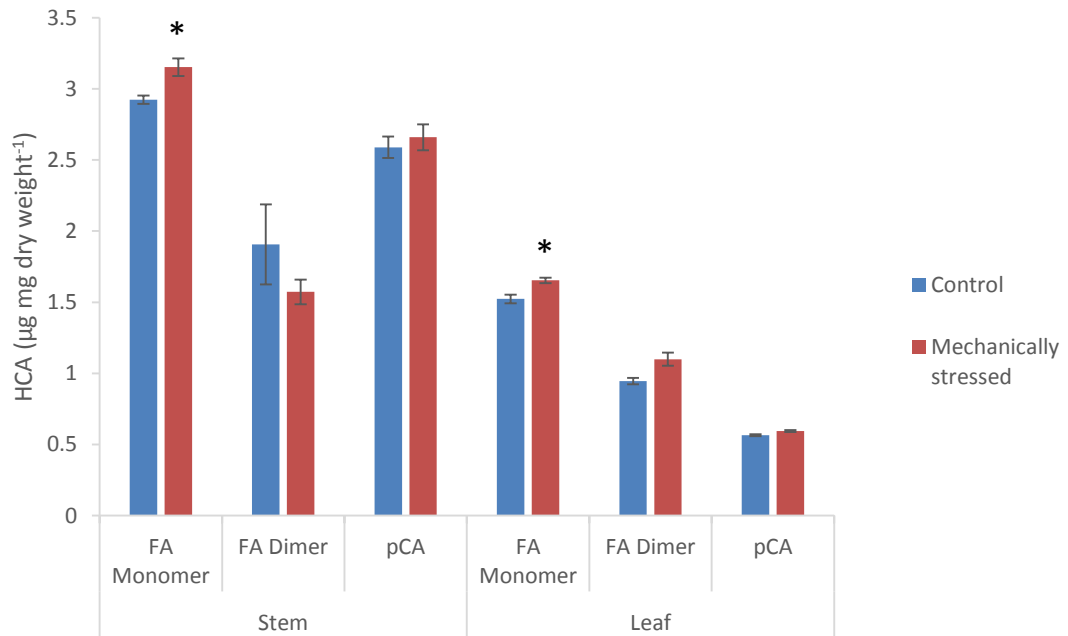


Figure 3.4 The effect of 1 week of mechanical stress on wall-bound hydroxycinnamic acids (HCAs): ferulic acid (FA), FA dimer and *para*-coumaric acid (*pCA*) in young *Brachypodium distachyon* stem and leaf tissue (\pm SE). FA dimers are the sum of diF8-8, diF8-5, diF8-5 benzofuran, diF5-5 and diF8-O-4. Analyses were performed on material from ‘exp. 2 young plants’ (**Table 3.1**). Asterisks represent significant difference ($p < 0.05$, F-test) between control and treatment for main effect of treatment.

3.3.3 Cell wall monosaccharides and lignin

A comprehensive analysis of cell wall components was performed on 8 week old mechanically stressed *Brachypodium* compared to a non-stressed control group (exp. 2, developed plants, **Table 3.1**, **Figure 3.5**). Glucose in the cellulose cell wall fraction, neutral sugars in the hemicellulose cell wall fraction, lignin and silica were measured, and the majority of mechanical stress-induced changes in the cell wall were found in leaf tissue.

There was a significant interaction between treatment and tissue for xylose ($p = 0.015$, F-test), arabinose ($p = 0.006$, F-test), galactose ($p = 0.012$, F-test), and mannose ($p = 0.011$, F-test). Cell wall sugars that were statistically significantly greater ($p < 0.05$, LSD) in mechanically stressed leaves than the control group were xylose (29%), arabinose (43%), galactose (27%) and mannose (46%). Glucose in the cellulose fraction of mechanically stressed leaves was also 31% greater than the controls, although this was not statistically significant. Notably, mannose in mechanically stressed stem was 21% less than control ($p < 0.05$, LSD, **Figure 3.5**). Acetyl-bromide lignin was also slightly greater in both stem and leaf by 5% and 3.5% respectively, although this was not quite statistically significant at 5% ($p = 0.06$, F-test, main effect of treatment, **Figure 3.6**).

3.3.4 Silica

Silica was measured in *Brachypodium* leaf and stem in the pilot study (exp. 1, 4 weeks of mechanical stress), and in exp. 2 (3 weeks of mechanical stress, **Table 3.1**). In both experiments, silica in mechanically stressed tissue was significantly greater than the non-stressed controls in stem and leaf. In exp. 1, silica was approximately 30% greater in mechanically stressed samples than in controls, in both leaf and stem tissues ($p < 0.001$, F-test for main effect of treatment: means = 1.64 (control),

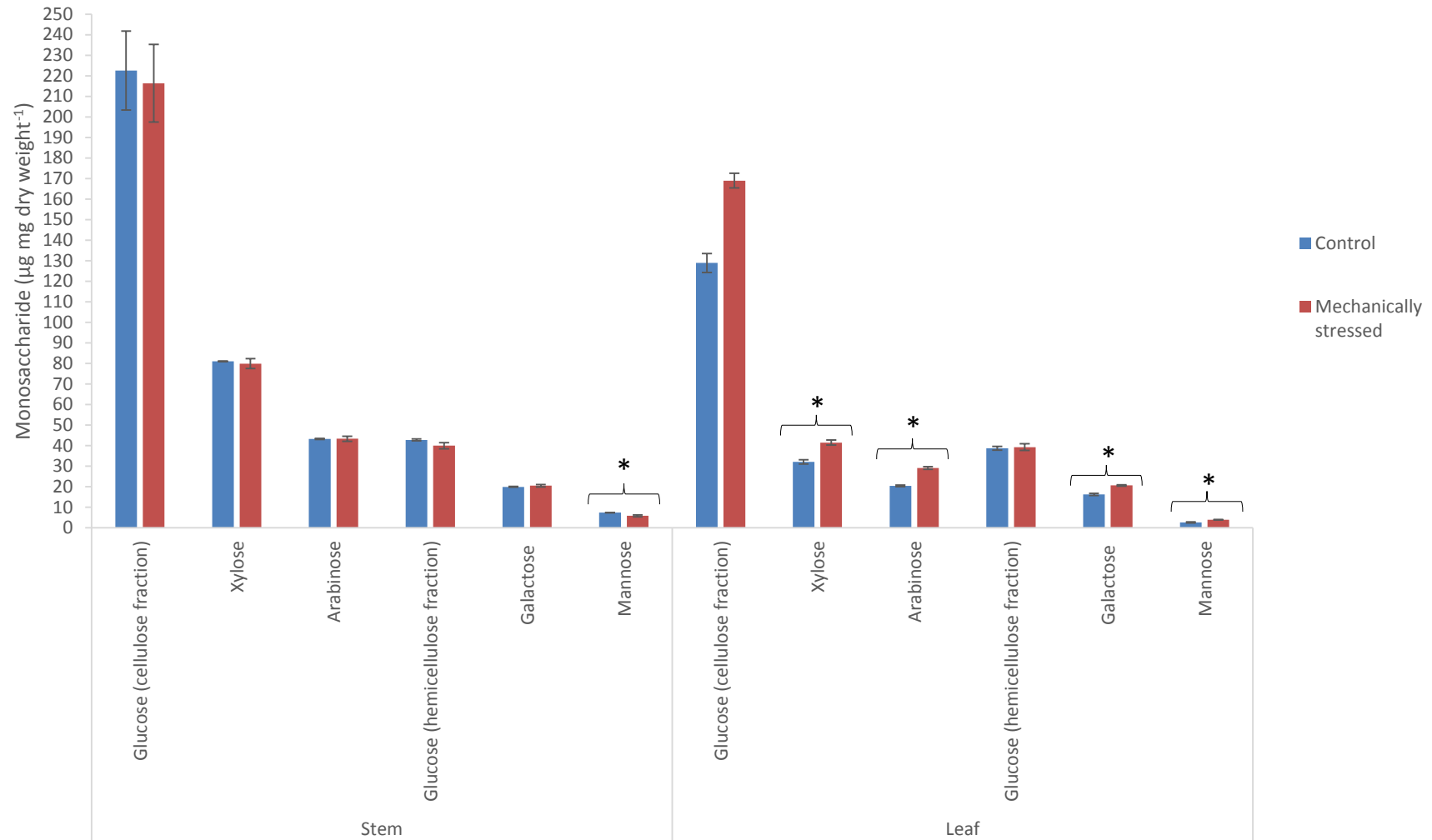


Figure 3.5 The effect of 3 weeks of mechanical stress on monosaccharide concentrations (\pm SE) in *Brachypodium distachyon* tissues. Analysis was performed on material from ‘experiment 2 developed plants’ (Table 3.1). Asterisks represent statistically significant difference ($p < 0.05$, LSD) between treatment and control groups.

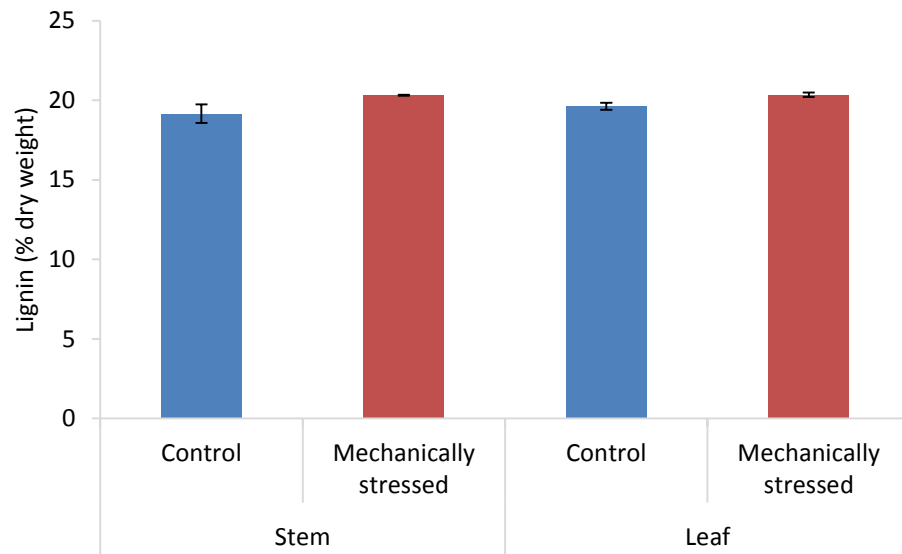


Figure 3.6 The effect of 3 weeks mechanical stress on lignin content (\pm SE) in *Brachypodium distachyon* tissues. Analysis was performed on material from ‘experiment 2 developed plants’ (Table 3.1).

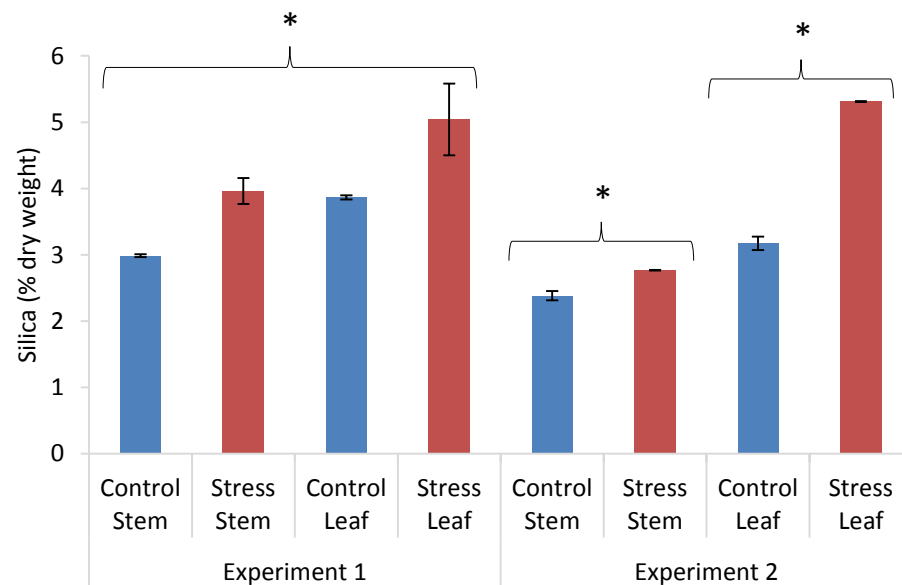


Figure 3.7 The effect of 4 weeks (experiment 1) or 3 weeks (experiment 2) mechanical stress on silica content (\pm SE) in *Brachypodium distachyon* stem and leaf. Analyses were performed on material from pilot experiment (exp. 1) or experiment 2 developed plants (exp. 2, Table 3.1). Asterisks represent statistically significant difference between treatment and control groups for main effect of treatment (exp. 1, $p < 0.05$, F-test) or interaction effect (exp. 2, $p < 0.05$, LSD) between treatment and tissue.

2.10 (stress); SED 0.097 on 25 df). Similarly, in exp. 2, there was an interaction effect between treatment and tissue for silica ($p < 0.001$, F-test), where silica was 16% greater than controls in mechanically stressed stem, and 67% greater than controls in mechanically stressed leaves ($p < 0.05$, LSD, **Figure 3.7**).

3.3.5 Digestibility

Saccharification analysis was performed on *Brachypodium* stem and leaf material from exp. 1 (4 weeks of mechanical stress) and exp. 2 (3 weeks of mechanical stress, **Table 3.1**), respectively. There was a significant main effect of treatment in exp. 1, where 14% and 3% less sugars were released from mechanically stressed leaf and stem tissue, respectively, than from the control samples ($p = 0.002$, F-test for main effect of treatment: means = 76.96 (control), 71.15 (stress); SED 1.821 on 50 df). In exp. 2, there was a trend towards greater recalcitrance to digestion in mechanically stressed samples than in the control samples, however, this was not statistically significant ($p = 0.091$, F test for main effect of treatment). In exp. 2, 12-14% fewer sugars were released from mechanically stressed stem and leaf tissue than the controls (**Figure 3.8**).

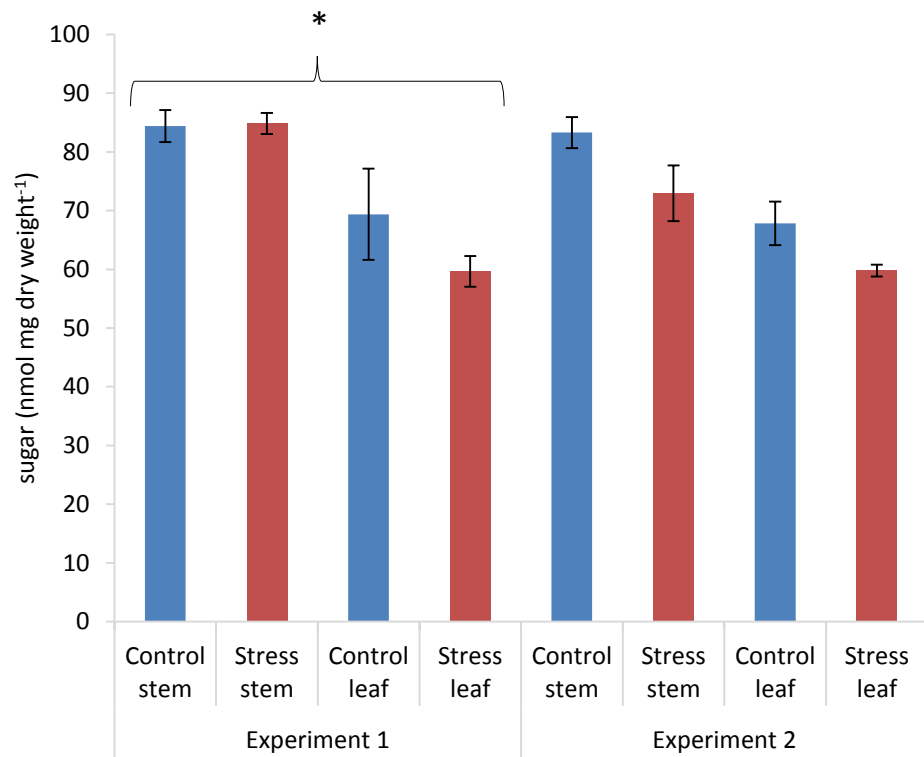


Figure 3.8 The effect of 4 weeks (exp. 1) or 3 weeks (exp. 2) mechanical stress on saccharification potential (\pm SE) in *Brachypodium distachyon* stem and leaf. Analyses were performed on material from pilot experiment (exp. 1) or experiment 2 developed plants (exp. 2, **Table 3.1**). Asterisk represents statistically significant difference ($p < 0.05$, F-test) for the main effect of treatment.

3.4 Discussion

3.4.1 Stem length

Mechanically stressed *Brachypodium* exhibited a dwarfed phenotype, characterised by a 28% reduction in stem length compared to the non-stressed controls, whilst retaining an equal number of internodes as the control group (**Figure 3.2**). This is a well-documented result in many species, including grasses (Biddington, 1986, Mitchell, 1996), and is in accordance with the findings of Jaffe (1973), who reported that grass species rye, barley and maize have reduced biomass of 28-42% after 11 d of thigmomorphogenic perturbation. This mechanical stress-induced dwarfed phenotype was suggested by Suge (1978), and later confirmed by Lange and Lange (2015), to be related to the growth hormone gibberellin, and was caused by induced gibberellin catabolism. In *Arabidopsis*, this phenotype was rescued by exogenous gibberellin application (Lange and Lange, 2015). The mechanical stress applied here may replicate harsh wind or rain, trampling, or invasive farming practices. The effect of mechanical stress is often overlooked as it usually occurs simultaneously with other abiotic stresses; these results show the extent to which mechanical stress, in the absence of other abiotic stresses, affects plant growth. Despite the dramatic morphological changes induced by mechanical stress, the effect on the grass cell wall is poorly understood.

3.4.2 Cell wall-bound FA and FA dimers

A 4-week period of mechanical stress did not affect cell wall-bound FA monomer or FA dimer in stem tissue of 10 week old *Brachypodium* (**Figure 3.3**). This result was somewhat surprising given the putative role of FA dimerisation in cessation of cell growth and increased stem strength (Buanafina, 2009). Further, FA monomer and

dimer are reported to increase as a result of other abiotic stresses, such as salt stress in maize (Uddin et al., 2014). After 4 weeks of mechanical stress, any increases in cell wall-bound FA in stem tissue may be undetectable as cell walls may already be feruloylated to the maximum extent, and therefore, stems of 6 week old *Brachypodium* after 1 week of mechanical stress were analysed; here, monomeric FA increased by 8% (**Figure 3.4**). These results are consistent with Uddin et al. (2014), who report that the effect of salt stress on FA was larger in elongating tissue in maize.

In *Brachypodium* leaf, monomeric and dimeric FA increased by 9% and 13% respectively after 1 week of mechanical stress (**Figure 3.4**), and FA dimers increased by 28% after 4 weeks of mechanical stress (**Figure 3.3**). Cell wall FA cross-links via dimerisation, or C-C or ether bonds to lignin, are formed by a peroxidase-mediated oxidative chemical reaction; the increases in FA dimer seen here are therefore consistent with ROS release into the cell wall induced by mechanical stress, which has been shown previously (Yahraus et al., 1995). Plant modifications in response to mechanical stress are thought to be largely adaptive, as plants conditioned to mechanical stresses are able to withstand further mechanical stress (Braam, 2005), and are able to resist biotic stresses (Chehab et al., 2012). Cell wall-bound FA dimers act as a physical barrier, which strengthens the cell wall and decreases enzymatic digestion (Buanafina, 2009). The increases in cell wall-bound FA shown here may therefore be a physical defence to withstand further abiotic stress, or to prepare the plant for biotic attack by pathogens, insect herbivores, or ruminant grazing. Additionally, FA is a nucleation site for lignin polymerisation (Ralph et al., 1995) in the cell wall, suggesting FA may have a role in increasing the lignin content of the cell wall as a defence mechanism. Finally, it is also possible that FA cross-linking may be involved in the cessation of cell expansion, contributing to the dwarfed

phenotype of mechanically stressed plants, possibly as a mechanism to resist further stresses or lodging (**Figure 3.2**).

3.4.3 Lignin

Acetyl-bromide lignin was found to marginally increase in leaf and stem in response to 3 weeks mechanical stress, by 3.5% and 5% respectively (**Figure 3.6**); although, the effect was not quite statistically significant. The majority of *pCA* is associated with lignin in secondary cell walls of *Brachypodium* (Petrik et al., 2014), and therefore the increased lignin was consistent with the 5% increase in *pCA* in young *Brachypodium* leaves. It was also surprising to note that leaf and stem material were found to have equal amounts of lignin in the range of 19-20% of biomass (**Figure 3.6**), whereas it has previously been reported that expanding *Brachypodium* leaves contain 5.3% lignin of alcohol insoluble residue (AIR), and that sheath and stem contain 11% and 12% lignin of AIR respectively (Rancour et al., 2012). Here, labelled stem material is a 'stem-enriched' fraction containing sheath and stem. Although the acetyl-bromide method was used to measure lignin in both studies, here, lignin was measured as a percentage of dry weight as opposed to as a percentage of AIR. Proteins are known to interfere with absorbance spectra and therefore this may explain the disparity in measured lignin here compared to previous studies. In any case, marginal increases in lignin seen here in mechanically stressed *Brachypodium* cell walls are inconclusive.

3.4.4 Cell wall monosaccharides

The majority of the effects of 3 weeks mechanical stress on monosaccharides in *Brachypodium* cell walls were observed in leaf tissue. Similar increases were found in glucose in the cellulose fraction (31%), xylose (29%), and galactose (27%) in leaf as a result of mechanical stress, and larger increases in arabinose (43%) and mannose

(46%) were found. Monosaccharides in stem tissues were mostly not affected (**Figure 3.5**). Although the increase in glucose (cellulose fraction) was not statistically significant, this may have been due to the low biological replication; this could be clarified in further experiments with increased biological replication.

AX is the most abundant hemicellulose in grass cell walls, typically constituting 20-40% of wall mass (Scheller and Ulvskov, 2010). Therefore, increases in xylose and arabinose and xylose were assumed to be increases in AX in response to mechanical stress. Similarly, increases in galactose and mannose suggest an increase in galactomannan polysaccharides in response to mechanical stress. Increased glucose in the cellulose fraction is in accordance with Lee et al. (2005), who report that cellulose synthase genes are upregulated in response to touch in the dicotyledonous model organism *Arabidopsis*. As cell wall components are reported as a percentage of dry weight, an overall expansion of the cell wall cannot be ruled out as a cause of the increases of cell wall monosaccharides. However, it is also possible that increases in cellulose, AX and galactomannan are advantageous adaptations to mechanical stress. As arabinose increased to a greater extent than xylose (14% greater increase in arabinose than xylose), this may indicate increased decoration of AX by arabinose in mechanically stressed leaves. Increased arabinose side chains on AX have previously been reported to be associated with decreased crystalline cellulose through hydrogen bonding between AX arabinose side chains and cellulose, and thereby increase resistance to lodging in rice (Li et al., 2015). Similarly, mannose increased to a greater extent than galactose (19% greater increase in mannose than galactose) and therefore may indicate increased decoration of galactomannan. Interestingly, salt stress was also found to induce increased arabinose and galactose in maize (Uddin et al., 2014), suggesting a role of AX and galactomannan in the stress response in grasses. In dicots, increased arabinan side chains on pectin have previously been

reported to be induced in response to mechanical stress (Verhertbruggen et al., 2013), which may have a similar function as the increases in hemicelluloses seen here in grasses. The authors also reported that mutations in *ARAD1* and *ARAD2* (GT47 family) arabinan synthase genes partially rescued the decreased internode elongation phenotype of Arabidopsis, suggesting that increased arabinan is important in mechanical stress-induced morphological changes in dicots. Speculatively, the changes seen in leaves here may be a mechanism of increasing tissue flexibility through interactions between hemicellulose and cellulose components, as a mechanism to withstand further stresses.

3.4.5 Silica

In this study, silica (SiO_2) increased in stem and leaf of *Brachypodium*, in both exp. 1 and 2, after 4 weeks and 3 weeks of mechanical stress respectively, ranging from 16-67% greater silica than the controls (**Figure 3.7**). Silica is taken up from the soil and deposited on the epidermis of tissues throughout the plant as a hydrated, amorphous polymer (Ma, 2004), and may interact directly with cell wall polymers (Guerriero et al., 2016). This is the first report of a direct effect of thigmomorphogenic mechanical stress on silica in grasses, however, increased silica due to the mechanical stress of flowing water has been shown previously in aquatic macrophytes (Schoelynck et al., 2015), and silica in grasses has previously been reported to be inducible by the biotic stresses of herbivore grazing (Massey et al., 2007). Wall-bound silica has previously been shown to confer increased strength and support, and may have a role in abiotic stress resistance and protection against lodging due to increased stiffness (Ma and Yamaji, 2006). These results therefore support a role of silica as an adaptive defence mechanism against further stresses in response to mechanical stress.

3.4.6 Digestibility

Saccharification is a measure of the propensity of material to release sugars from the cell wall by a specific method. Here, mechanically stressed *Brachypodium* leaf and stem exhibited lower saccharification potential than the controls in two experiments, ranging from 3-14% less sugars released (**Figure 3.8**). The decrease in released sugars reflects a change in the composition of the cell walls, although it is unclear whether this was due to the small increase in lignin or the increase in cellulose and hemicelluloses, and the physical interactions of these polysaccharides. It is also possible that increased silica physically inhibited saccharification by physical inhibition of enzymes binding to the polysaccharide substrate. The effect of environmental mechanical stresses such as wind and rain, and anthropogenic factors such as invasive farming practices, on the saccharification potential of grasses is relevant in applications such as second generation liquid biofuel production.

3.4.7 Conclusion

This study investigated the response in *Brachypodium* cell walls and changes in plant morphology when treated with continual mechanical stress throughout early and vegetative growth. An extensive investigation into the effect of mechanical stress on grass cell walls is presented, which, prior to this study, was largely unknown. Tissue- and growth stage-dependant increases are reported in cellulose, arabinoxylan, galactomannan and silica. Cell wall-bound FA and FA dimers are shown to increase in young tissues and in leaf.

These novel cell wall adaptations in *Brachypodium* appear to be species and tissue specific. While some studies report plants that have cell walls with higher crystalline cellulose, with low amounts of lignin are well adapted to mechanical stress, as in tension wood (Andersson-Gunneras et al., 2006), other reports suggest that plants

develop high levels of lignin as an adaptation to mechanical stress (Yamashita et al., 2007, Kahn-Jetter et al., 2000). In the dicotyledonous model Arabidopsis, cellulose synthase has been shown to be upregulated in response to touch, as well as cell wall hydrolyases and extensins and expansins (Lee et al., 2005).

The cell wall acts as the first physical barrier to withstand stresses, and therefore the mechanically induced changes in the cell walls of *Brachypodium* presented in this study speculatively may act as a strengthening defence mechanism against further mechanical stress. Interactions between cellulose and hemicelluloses, and increased arabinose substitutions of AX may be important in increasing cell wall flexibility. Further, plants sensing touch may be important in the plant defence against biotic attack or herbivores. These findings contribute to an increased understanding of factors affecting saccharification and selecting for these cell wall factors may be of interest in breeding for lodging resistance.

The effect of mechanical stress on cell wall-bound FA in these experiments was small, and was well within the range of values of unstressed plants at a later developmental stage. Mechanical stress as an environmental treatment is therefore not suitable as a means of investigation into the genetic control of cell wall-bound ferulate.

Chapter 4. Methyl-Jasmonate Induces Increased Wall-Bound Ferulic Acid and *p*-Coumaric Acid and Expression of BAHD and GT61 Family Arabinoxylan Synthesising Genes in *Brachypodium distachyon* Callus

4.1 Introduction

Jasmonic acid (JA) is a lipid derived phytohormone and signalling molecule involved in plant development, including inducing viable pollen production, leaf senescence, tuber formation, tendril coiling and fruit ripening, and inhibiting root growth and photosynthesis at certain developmental stages. Furthermore, JA is induced in biotic and abiotic stress responses, including wounding by herbivores, and in response to pathogen or insect elicitors. JA orchestrates a complex signalling cascade, involving cross-talk with other hormones such as ethylene, abscisic acid and salicylic acid, which activates transcription factors controlling defence genes, such as protease inhibitors, terpenoids, phytoalexins, flavonoid and sesquiterpenoid biosynthesis enzymes and antifungal proteins (Creelman and Mullet, 1995, Avanci et al., 2010, Wasternack and Hause, 2013).

The effects of JA signalling are often studied by the exogenous application of methyl-JA (meJA), which is cleaved by meJA-esterase to JA *in planta* (Wu et al., 2008). Activation of JA responsive genes requires conversion of JA to its bioactive isoleucine conjugate (JA-Ile). JA-Ile binds to the Skp1-Cullin-F-box (SCF)^{CO11} E3 ubiquitin ligase complex, triggering the degradation of JAZ transcriptional repressor proteins, which normally repress MYC2 transcription factor activity in the nucleus. Activated MYC2 controls the expression of JA-responsive genes (Thines et al., 2007,

Chini et al., 2007, Lee et al., 2013). JA-responsive genes are extensive in number and function. Some studies have reported the effects of exogenously applied meJA on global transcription in both dicots and monocots. Pauwels et al. (2008) reported that 6 h meJA treatment induced differential expression of 495 genes in cell suspension cultures of the dicotyledonous model organism *Arabidopsis*. Other studies have reported the effect of meJA on global transcription in the Poaceae. Yang et al. (2015) reported that meJA induced up- and down- regulation (≥ 2 -fold change) of 1,216 and 1,530 genes respectively in maize. Further, Salzman et al. (2005) reported that meJA induced upregulated and downregulated expression (> 1.5 fold) of 2980 and 1842 genes respectively in *Sorghum*. Additionally, public expression database RiceXPro provides useful information on global transcription changes in rice after treatment with various hormones, including JA (Sato et al., 2013).

Relatively few studies have reported changes to the cell wall as a direct result of JA. A well-documented effect of JA is increased cell wall class III peroxidases, which generate reactive oxygen species (ROS) such as hydrogen peroxide (H_2O_2). ROS result in increased phenolic cross-linking within the cell wall. In the Poaceae, this includes increased lignification and increased ferulic acid (FA) dimerisation, creating a physical barrier to pathogen invasion and leading to increased pathogen resistance (Almagro et al., 2009). Increased expression of cell wall genes in response to exogenously applied JA, such as cellulose synthases, have been reported in global gene expression studies (Salzman et al., 2005), however, the resulting biochemical changes in the cell wall have not, to my knowledge, been quantified.

The distinct cell walls of the commelinid monocots, including the Poaceae, comprise arabinoxylan (AX) as the major non-cellulosic component. The AX of grasses differs in structure from dicot xylan in that a large amount of arabinofuranose residues decorate the xylopyranose backbone at the C-2 and C-3 positions. C-3 linked

arabinofuranose residues can be esterified on the O-5 position by hydroxycinnamic acids (HCAs): FA or *para*-coumaric acid (*pCA*). AX-esterified FA forms covalently-linked dimers, which increase cell wall recalcitrance to enzymatic digestion (Hatfield et al., 1999), and are a nucleation site for lignin formation (Ralph et al., 1995), whereas AX-esterified *pCA* residues have an unknown function (**Chapter 1.6.5**). There have been few studies on the effect of JA on the levels of these grass-specific features of cell walls. Indirect evidence for a possible relationship was found in a study of cellulose-deficient cell walls of maize cell suspension cultures that revealed an increase in AX branching, FA monomer, FA dimer, and *pCA*; these increases were correlated with an increase in JA pathway signalling genes (Melida et al., 2015). However, whether the effect on the cell wall was due to increased JA remains unclear. Additionally, Lee et al. (1997) reported an apparent increase in cell wall-bound FA and *pCA* in barley as a direct response to JA, although, the effect was inconsistent, so evidence for this effect remains scarce.

Despite the importance of FA and *pCA* in the plant cell wall, the mechanism by which these phenolic acids become ester-linked to AX remains unclear. Very few of the genes involved have been characterised, although genes within the BAHD and GT61 gene families have been predicted by Mitchell et al. (2007) to be involved in the process (**Chapter 1.8**). One gene that has been identified is *OsAT10* in the BAHD gene family, which has been shown to be required for *pCA* ester-linked to AX in rice (Bartley et al., 2013). Evidence from public expression database RiceXPro shows that JA induces increased expression in many of the genes in the BAHD and GT61 candidate families in rice seedlings (Sato et al., 2013, **Appendix A**). Thus, we hypothesised that JA may induce increased esterification of FA and *pCA* on AX and therefore may provide a system in which to study associated changes in gene expression of *BAHD* and *GT61* genes.

The aim of the experiments in this chapter were to study the effect of JA on the cell walls of the Poaceae using the model organism *Brachypodium distachyon*. Changes in cell wall polysaccharides and lignin were measured, together with associated changes in FA and pCA, and are discussed in relation to global- and candidate-gene expression changes.

4.2 Chapter 4 specific methods

4.2.1 Brachypodium hydroponics

Brachypodium seeds were surface sterilised with 10% household bleach for 5 min, and rinsed four times with sterile water. Sterilised seeds were germinated aseptically on blue roll in the dark overnight at 4 °C, and subsequently incubated at room temperature for 5 d, and were kept moist with sterile water. Seedlings were then stored at 4 °C for 2 d to halt growth, and from 8 d were grown hydroponically with aeration in G7 Magenta vessels, in nutrient solution comprised of 1.5 mM Ca(NO₃)₂, 5 mM KNO₃, 2 mM NaNO₃, 1 mM MgSO₄, 1 mM KH₂PO₄, 25 µM FeEDTA, 160 nM CuCl₂, 9.2 µM H₃BO₃, 3.6 µM MnCl₂, 16 nM Na₂MoO₄, 5 µM KCl, and 8 µM ZnCl₂, at pH 5.8, with 0.5 g MES hydrate per litre to stabilise pH. The nutrient solution was replaced with fresh solution every 2 d. Plants were grown in a controlled-environment growth room at 25/20 °C day/night temperature, with a 16-h-light/8-h-dark cycle, 150 µmol m⁻² s⁻¹ light intensity, 60 % humidity, and 380 ppm CO₂. At 18 d, the nutrient solution was replaced with a nutrient solution containing 100 µM (±)-jasmonic acid, 0.02% DMSO, or without jasmonic acid for the mock control group. Three biological replicates of two pots, with four plants per pot, were harvested into liquid nitrogen after 24 h or 48 h treatment and ground in a pestle and mortar in liquid nitrogen, and freeze dried. Phenolic acids were analysed as described in **Chapter 2.11**. Two technical replicate samples of shoot material were analysed, but only one technical replicate of root material.

4.2.2 Callus generation and growth

Brachypodium callus was generated on CIM, as described in **Chapter 2.15**.

4.2.3 Preparation of methyl-jasmonate stock solutions

Stock solutions of 1 mM, 5 mM, 10 mM, 50 mM and 100 mM methyl jasmonate (meJA) in ethanol, were prepared. The mock control solution was ethanol.

4.2.4 Brachypodium callus experiments

Callus Experiment 1: Brachypodium calli were subcultured onto plates of CIM containing increasing concentrations of methyl jasmonate: 1 μ M, 5 μ M, 10 μ M, 50 μ M, 100 μ M meJA and a mock control. Nine calli per plate (plate = one biological replicate) and 3 biological replicates per treatment were analysed and averaged. Callus material was analysed for phenolic acid composition, as described in **Chapter 2.11**, on a dry weight basis.

Callus Experiment 2: Brachypodium calli were subcultured onto plates of CIM containing increasing concentrations of methyl jasmonate as in experiment 1. Sixteen calli per plate (plate = one biological replicate) and four biological replicates per treatment were analysed and averaged for phenolic acid composition on a dry weight basis, as in experiment 1. For all other analyses, three biological replicates per treatment were prepared using 'AIR preparation method 1' (**Chapter 2.4**) and 'destarching method 1' (**Chapter 2.5**). Matrix monosaccharides (**Chapter 2.6**) and cellulose (**Chapter 2.7**) were analysed as previously described.

Callus Experiment 3: Brachypodium calli were transferred onto plates of CIM containing 50 μ M meJA, or a mock control solution. Samples were taken at 24 h, 48 h, 4 d and 8 d. Four biological replicates were harvested per treatment at each timepoint. Each biological replicate consisted of three plates (each containing 36 calli) that were pooled. Material was prepared using AIR preparation method 'AIR preparation method 2' (**Chapter 2.4**) and 'destarching method 2' (**Chapter 2.5**), and was analysed for phenolic acid composition (**Chapter 2.11**), lignin (**Chapter 2.8**),

matrix monosaccharides (**section 2.6**), and cellulose (**Chapter 2.7**) as previously described. RNA was extracted using the TRIzol RNA isolation method (**Chapter 2.12**).

4.2.5 Mild acid hydrolysis

AIR was prepared by washing *Brachypodium* callus tissue with 1 ml 80% (v/v) aqueous ethanol. The samples were vortexed, sonicated for 10 min, heated at 80 °C for 15 min and centrifuged (5000 g, 15 min) to recover the pellet. The wash was washed twice more, without heating on the second and third washes. The pellet was then washed in 1 ml CHCl₃:MeOH (1:1) (vortexed, centrifuged 10,000 g, 10 min), and dried under vacuum at 40 °C. Starch was then removed following destarching method 2 (chapter 2.5), except polysaccharides were precipitated for 30 min. The dry pellet was incubated in 0.05 M trifluoroacetic acid (TFA) (0.6 ml) at 100 °C for 4 h, with shaking. Samples were centrifuged (10,000 g, 10 min). A volume of 500 µl supernatant was dried under vacuum at 40 °C. The pellet was washed thrice with 1 ml water (vortex, centrifuge 16,000 g, 5 min), and dried under vacuum at 40 °C. Internal standard was added and phenolic acids were released by alkaline hydrolysis, then extracted, as described in **Chapter 2.11**.

4.2.6 Statistics

The GenStat (17th edition, VSN International Ltd, Hemel Hempstead, UK) statistical package was used for analysis. Assistance with statistical analyses was provided by Stephen Powers, Rothamsted Research.

Analysis of Variance (ANOVA) was applied to the data to test the main effects and interactions between the factors of JA treatment and time (hydroponics experiment and callus exp. 3), or to test the effect of concentration and whether there was

evidence of a linear and non-linear dose response (callus exp. 1 and 2), using F-tests. Appropriate means and standard error of the difference (SED) values on the residual degrees of freedom (df) from the ANOVA were output and compared using the least significant difference (LSD) at the 5% level of significance. Where mean values are presented in the text to illustrate the main effect of jasmonic acid over time, the figure presented is the average of the sampled time points. A natural log transformation was used for phenolic data in ‘callus experiment 2’ to account for heterogeneity of variance.

4.2.7 RNA sequencing

RNA sequencing (RNA-seq) was carried out by Steve Hanley, Rothamsted Research, on an Ion Proton™ System. Libraries were made using the Ion Total RNA-Seq Kit v2, templates were prepared using the Ion PI™ Template OT2 200 Kit V2 and were sequenced using the Ion PI™ Sequencing 200 Kit v2 with an Ion PI™ Chip Kit v2. All sequencing equipment and reagents were from Thermo Fisher Scientific and used following the manufacturer’s instructions.

Sequencing reads were analysed using Galaxy software (Giardine et al., 2005). Reads were mapped to the *Brachypodium distachyon v3.1* reference transcriptome from Phytozome 11.0 (Goodstein et al., 2012) with one representative splice variant per gene (file “Bdistachyon_314_v3.1.transcript_primaryTranscriptOnly.fa”). Comparison with an earlier reference Genebuild 2010-02-Brachy 1.2, showed that the transcript for candidate gene *BdBAHD04*, *Bradi2g33980.1* was replaced by a transcript from the opposite strand, *Bradi2g33977.1* in v3. However, the strand-specific Ion Torrent reads all mapped to the strand in the v1.2 gene model, hence the *Bradi2g33977.1* sequence was manually replaced with *Bradi2g33980.1* in the reference, and this was used for all results reported here. Reads less than 30bp were removed using the

Trimmomatic tool, mapped to the reference transcriptome with BWA-MEM, and percentage mapped reads were obtained using Flagstat. Mapped reads were quantified using eXpress, and tables of effective counts and FPKM (fragments per kilobase of transcript per million mapped reads) were created using Merge eXpress. For global analysis: ANOVA was applied on effective counts, performed in RStudio using the EdgeR package, taking account of the 4 biological replicates per sample. This analysis tested for the main effects and interaction between the two factors treatment and time, at the $p = < 0.05$ significance level corrected for multiple testing using Benjamini-Hochberg false discovery rate, after filtering for genes with counts per million (cpm) > 1 in 3 samples or more. Genes significantly affected by treatment were analysed using the Terra-BLASTN tool on a Dechypher platform. Significantly differentially expressed genes (DEGs) for the treatment ANOVA factor were annotated with Gene Ontology (GO) terms against the Gene Ontology Consortium database (Ashburner et al., 2000), and with Kyoto Encyclopedia of Genes and Genomes (KEGG) pathways (Kanehisa et al., 2016), using Blast2GO software with default parameters (Conesa et al., 2005).

For cell wall genes analysis: A count of 484 cell wall genes were identified and ANOVA was performed as above on only these genes to determine differentially expressed cell wall genes.

4.3 Results

4.3.1 Brachypodium seedlings: hydroponics experiment

There was no statistically significant effect of 100 μM (\pm)-JA on total cell wall-bound FA (monomer plus dimers) or *p*CA in 19 and 20 d old, hydroponically grown, Brachypodium seedling root or shoot tissue. Cell wall-bound FA monomer was approximately 2/3 of total wall-bound FA, and wall-bound FA dimers (diF8-8, diF8-5, diF8-5 benzofuran, diF5-5 and diF8-O-4) constituted 1/3 of total wall-bound FA, in roots and shoots. In shoot tissue, there was no change in the ratio of wall-bound FA monomer to wall-bound FA dimers, however, in root tissue, some moderate effects of JA were observed. In root, cell wall-bound FA monomer was 14% less than the control samples after 24 h JA treatment, and 7% less than the control samples after 48 h treatment ($p = 0.003$, F-test for the main effect of JA over time: means = 2.91 (+ JA), 3.27 (- JA); SED = 0.077 on 7 df; **Figure 4.1**). Cell wall-bound FA dimers were 18% greater than the control samples after 24 h JA treatment, and 13% greater than the control samples after 48 h ($p = 0.037$, F-test for the main effect of JA over time: means = 0.55 (+ JA), 0.47 (- JA); SED = 0.095 on 7 df; **Figure 4.1**). Notably, major dimers diF8-O-4 and diF8-5 benzofuran were 18% and 9% greater than the control respectively after 24 h treatment, and 15% and 17% greater than the control respectively after 48 h JA treatment in root (diF8-O-4: $p = 0.003$, F-test for the main effect of JA over time: means = 0.55 (+ JA), 0.47 (- JA); SED = 0.017 on 7 df; diF8-5: $p = 0.002$, F-test for the main effect of JA over time: means = 0.43 (+ JA), 0.38 (- JA); SED = 0.103 on 7 df; **Appendix B**). Further, FA dimer diF5-5 was 40% greater than the control in root after 48 h JA treatment ($p = 0.008$, F-test for the main effect of JA over time: means = 0.36 (+ JA), 0.28 (- JA); SED = 0.200 on 7 df; **Appendix B**). Dimers diF8-8 and diF8-5 were not statistically different from the control.

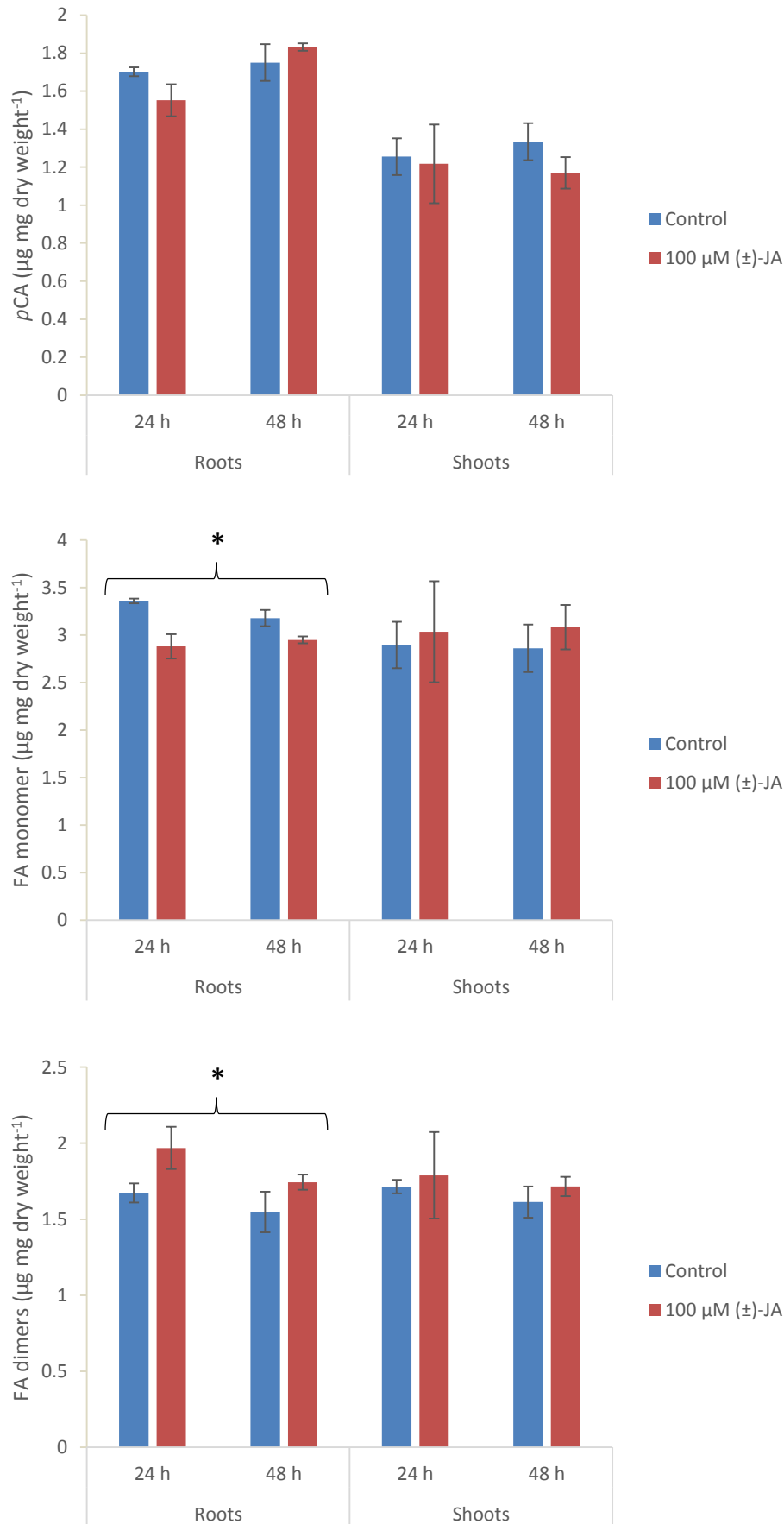


Figure 4.1 The effect of 24 h or 48 h treatment with 100 μM (\pm)-jasmonic acid (JA) on *para*-coumaric acid (pCA) and ferulic acid (FA) monomer and dimer (\pm SE) in hydroponically grown *Brachypodium distachyon* seedling roots and shoots. FA dimers are the sum of diF8-8, diF8-5, diF8-5 benzofuran, diF5-5 and diF8-O-4. Asterisks represent statistically significant differences between control and (\pm)-JA treated samples for the main effect of treatment.

4.3.2 Brachypodium callus: JA concentration experiment

The amount of cell wall-bound FA was assumed to be underestimated in lignified plant tissues, as AX-bound FA ether linked to lignin will not be released by the alkaline hydrolysis treatment used here, and there is currently no method of releasing FA cross-linked to lignin by C-C bonds. Additionally, lignin-linked *p*CA in Brachypodium plant tissues may have masked any effect on AX-linked *p*CA. For these reasons it was decided to repeat the experiments testing the effect of JA on cell wall-bound FA and *p*CA using callus tissue, in which the cell walls are dominated by primary cell walls with low lignin content (Rancour et al., 2012).

4.3.3 Cell wall-bound *p*CA and FA

Two repeated experiments (callus exp. 1 and exp. 2, **section 4.2.4**) were carried out to investigate the effect of increasing concentrations of meJA (1 μ M – 100 μ M) on Brachypodium callus cell walls.

Cell wall-bound *p*CA was dramatically greater than the control samples in Brachypodium callus, when treated with 1 μ M – 100 μ M meJA for 17 d, having accounted for linear and non-linear trends in the response ($p < 0.001$, exp. 1 and exp. 2, F-tests). Cell wall-bound *p*CA was 8-fold ($p < 0.05$, LSD) greater than the control with 50 μ M meJA treatment in exp. 1 (no significant difference with 1 μ M, 5 μ M or 10 μ M meJA treatment). However, cell wall-bound *p*CA was 3-fold greater ($p < 0.05$, LSD) than the control with 1 μ M meJA treatment in experiment 2. At 100 μ M meJA, cell wall-bound *p*CA showed a dramatic 10-fold increase ($p < 0.05$, LSD) in experiment 1, and 5.5-fold increase ($p < 0.05$, LSD) in experiment 2 compared to the control (**Figure 4.2**).

Additionally, cell wall-bound FA monomer was significantly greater after 1 μM – 100 μM meJA treatment for 17 d, compared to the control, in *Brachypodium* callus ($p = 0.004$, exp.1; $p < 0.001$, exp. 2, F-tests). There was evidence of a statistically significant linear ($p < 0.001$, exp.1; $p < 0.022$, exp.2, F-tests), and non-linear ($p < 0.034$, exp.1; $p < 0.001$, exp.2, F-tests) effect of increasing concentrations of meJA on cell wall-bound FA monomer. A dose of 1 μM meJA was sufficient to induce a statistically significant effect on cell wall-bound FA monomer ($p < 0.05$, LSD; exp. 1 and exp. 2), which was 19% and 32% greater than the control in experiment 1 and 2 respectively. At 100 μM meJA concentration, cell wall-bound FA monomer was 42% greater than the control in both exp. 1 and exp. 2 ($p < 0.05$, LSD; **Figure 4.2**).

Total cell wall-bound FA dimers were significantly greater after 1 μM – 100 μM meJA treatment for 17 d, compared to the control ($p < 0.001$, exp.1 and exp. 2, F-tests). There was evidence of a statistically significant linear ($p < 0.001$, exp.1 and exp.2, F-tests), and non-linear ($p = 0.002$, exp. 2, F-test) effect of increasing concentrations of meJA on cell wall-bound total FA dimers. At 1 μM meJA treatment, wall-bound FA dimers were ~30% greater than the control in the two experiments ($p < 0.05$, LSD, exp.1 and exp. 2), and at 100 μM meJA treatment, wall-bound FA dimers were 76% and 350% greater than the control in exp. 1 and exp. 2 respectively ($p < 0.05$, LSD, exp. 1 and exp. 2; **Figure 4.2**). At 50 μM and 100 μM meJA, amounts of each of the five dimers that were measured were significantly greater than in the control samples ($p < 0.05$, LSD; **Appendix C**). No FA or pCA were detected in the media that the callus was grown on (data not shown).

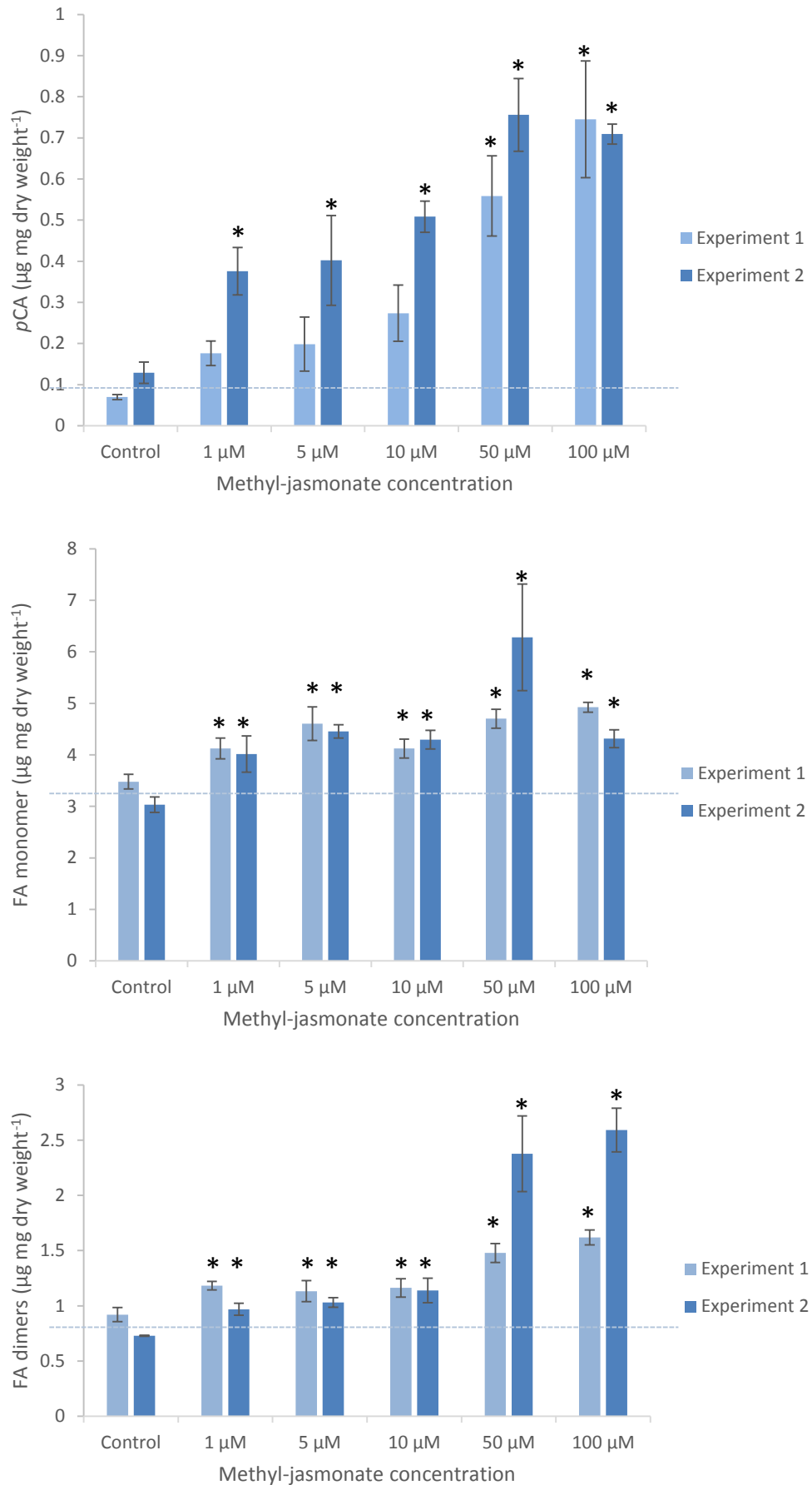


Figure 4.2 The effect of 17 d treatment with increasing concentrations of methyl-jasmonate on *para*-coumaric acid (*p*CA) and ferulic acid (FA) monomer and dimer (\pm SE) in *Brachypodium distachyon* callus, in two experiments (callus experiments 1 & 2). FA dimers are the sum of diF8-8, diF8-5, diF8-5 benzofuran, diF5-5 and diF8-O-4. Asterisks represent statistically significant differences between control and methyl-jasmonate samples ($p < 0.05$, LSD). Dotted lines symbolise average value for controls

4.3.4 Cell wall polysaccharides

Cell wall sugars were analysed in callus exp. 2 (**section 4.2.4**), after 17 d treatment with 1 μM meJA – 100 μM meJA. Some cell wall sugars were greater than control samples with differing concentrations of meJA. A dose of 10 μM meJA induced a statistically significant ($p < 0.05$) increase in glucose (cellulose) and galactose compared to control samples, whereas 50 μM meJA was required to induce a statistically significant increase in xylose, and 100 μM meJA induce a statistically significant increase in arabinose compared to controls. At 100 μM meJA treatment, the concentration of xylose, arabinose, and galactose in the hemicellulose fraction were 63%, 76% and 140% greater than control samples respectively, as a proportion of AIR ($p < 0.05$, LSD). Likewise, glucose (cellulose) was double the amount of the control samples when treated with 100 μM meJA, as a proportion of AIR ($p < 0.05$, LSD). No statistically significant change was observed in glucose (hemicellulose), mannose, galacturonic acid or glucuronic acid when treated with meJA, although notably hemicellulose-associated glucose was consistently 20-30% lower than the control (**Figure 4.3**).

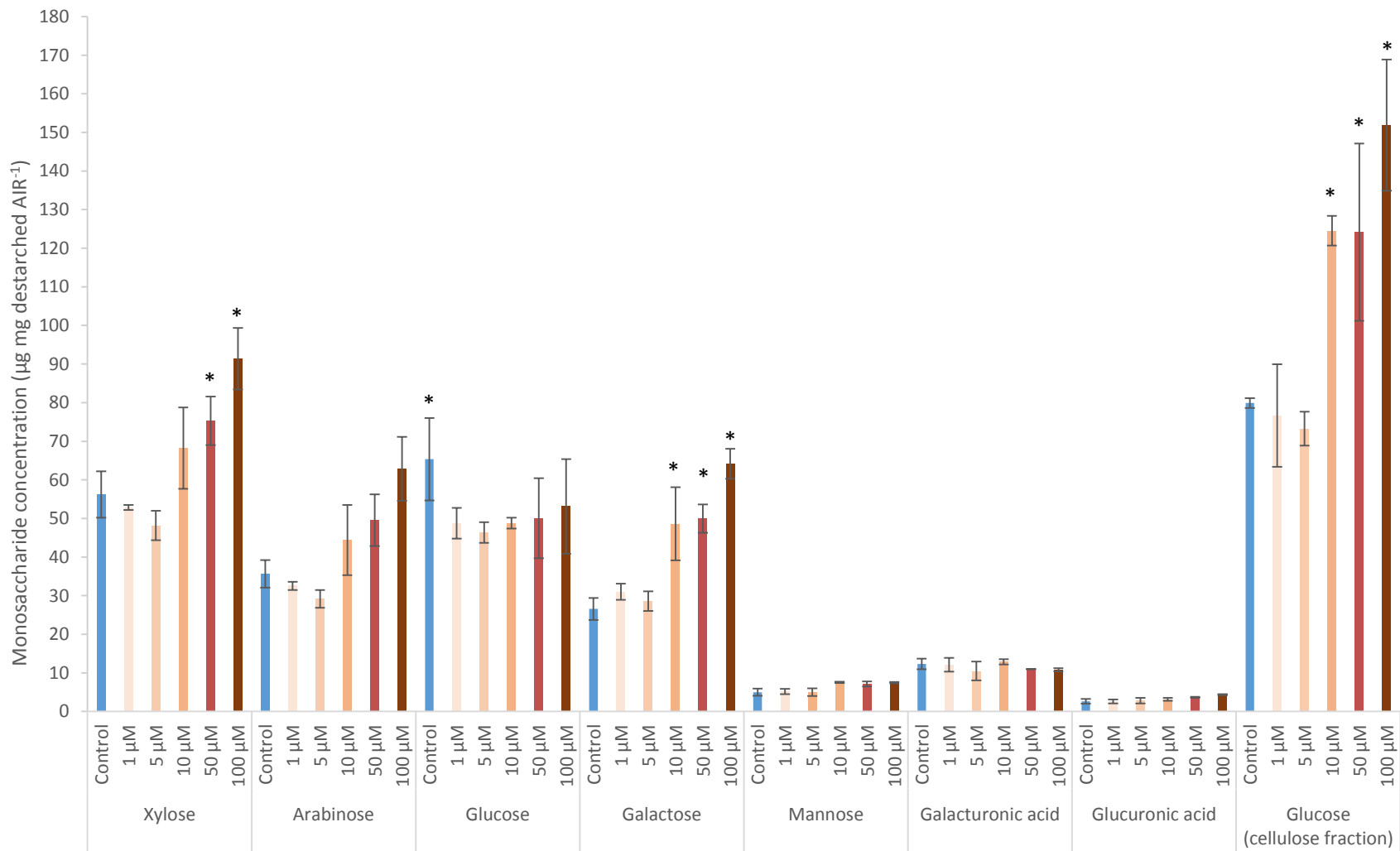


Figure 4.3 Monosaccharide concentrations \pm SE in the hemicellulose fraction (xylose, arabinose, glucose, galactose, mannose, galacturonic acid, glucuronic acid) and glucose in the cellulose fraction of destarched alcohol insoluble residue (AIR) in *Brachypodium distachyon* callus after 17 d treatment with varying concentrations of methyl-jasmonate (1 μ M, 5 μ M, 10 μ M, 50 μ M and 100 μ M, callus experiment 2). Asterisks represent statistically significant differences between control and meJA treatment ($p < 0.05$, LSD).

4.3.5 Mild acid hydrolysis

To determine the proportions of *p*CA ester to lignin and to AX in *Brachypodium* callus tissue, cell wall-bound *p*CA and FA were released by mild acid hydrolysis as previously described (Petrik et al., 2014, Bartley et al., 2013). The mild acid hydrolysis treatment preferentially hydrolyses the glycosidic Ara-Xyl bond, releasing AX side chains, including ester-linked HCAs, into the supernatant. HCAs cross-linked to lignin remain in the pellet. Application of mild acid hydrolysis to meJA treated callus and control samples showed that 93% of total *p*CA was found in the supernatant for both (**Table 4.1**), indicating that the majority of *p*CA was ester linked to AX in this tissue. As expected, around 90% of total measured FA was in the supernatant. FA does not occur ester-linked to lignin, however around 10% of total FA was found in the pellet, which suggests that incomplete hydrolysis took place. The remaining 7% of *p*CA in the pellet was therefore likely to be AX-linked, and it was concluded that it is most likely that there is no *p*CA ester-linked to lignin in *Brachypodium* callus tissue.

Table 4.1 The mean percentage of hydroxycinnamic acids associated with the supernatant or pellet fraction of *Brachypodium distachyon* callus destarched AIR (alcohol insoluble residue) which was subjected to mild transfluoroacetic acid (TFA) (0.05 M) hydrolysis after 7 d treatment with methyl-jasmonate (meJA).

	Supernatant		Pellet	
	Control	meJA	Control	meJA
<i>p</i> CA (% of total)	93.0	93.0	7.0	7.0
FA monomer (% of total)	89.3	90.9	10.7	9.1
FA dimer (% of total)	88.6	93.0	11.4	7.0

4.3.6 Brachypodium Callus 50 μ M meJA time course experiment

Having established the effects of JA on Brachypodium callus cell walls, it was decided to compare the timing of these effects with changes in the transcriptome. Calli were treated with 50 μ M meJA and sampled at 24 h, 48 h, 4 d and 8 d (callus exp. 3, **section 4.2.4**).

4.3.7 Cell wall composition

To determine whether previously observed changes in cell wall-bound *p*CA and FA (**Figure 4.2**) were due simply to an increase in proportion of dry weight of the cell wall, AIR, destarched AIR, and total dry weight of callus were determined. The proportion of dry weight as AIR was approximately 40%, and as destarched AIR was approximately 20%, and was unaffected by meJA treatment (**Table 4.2**).

Table 4.2 The average proportion of the dry weight (\pm SE) of alcohol insoluble residue (AIR), and destarched AIR, in control and 50 μ M meJA treated Brachypodium callus samples. Data obtained in callus exp. 3.

	AIR (% of dw)		Destarched AIR (% of dw)	
	control	meJA	control	meJA
24 h	39.5 (\pm 0.8)	40.9 (\pm 0.6)	18.6 (\pm 0.8)	18.5 (\pm 3)
48 h	40.9 (\pm 0.5)	42.2 (\pm 0.7)	22.2 (\pm 0.7)	22.3 (\pm 0.6)
4 d	40.8 (\pm 0.7)	41.5 (\pm 0.5)	20.5 (\pm 0.8)	21.3 (\pm 0.5)
8 d	40.3 (\pm 1.1)	41.4 (\pm 0.8)	20.6 (\pm 1.1)	21.5 (\pm 0.8)

Wall-bound *p*CA accumulated rapidly in Brachypodium callus when treated with 50 μ M meJA, showing a significant main effect of meJA treatment over time ($p < 0.001$, F-test: means = 0.18 (- JA), 0.33 (+ JA); SED = 0.022 on 23 df). *p*CA was 50% greater than the control samples after 24 h, and continued to accumulate, increasing significantly to 2 fold greater than the control by day 8 of treatment ($p < 0.05$, LSD). Additionally, there was a significant main effect of meJA treatment

over time on cell wall-bound FA monomer in *Brachypodium* callus ($p = 0.03$, F-test: means = 4.31 (- JA), 4.63 (+ JA); SED = 0.133 on 23 df). Cell wall-bound FA monomer in samples treated with meJA remained 5-9% greater than the control over 1 - 8 d treatment. There was also a significant main effect of meJA for wall-bound FA dimers, which were 12% greater than the control after 8 d meJA treatment ($p = 0.018$, F-test: means = 2.01 (- JA), 2.31 (+ JA); SED = 0.118 on 23 df; **Figure 4.4**). Individual dimers diF8-O-4 ($p = 0.007$, F-test), diF5-5 ($p = 0.048$, F-test) and diF8-5 ($p = 0.023$, F-test) showed a statistically significant main effect of meJA, whereas dimers diF8-5 benzofuran and diF8-8 remained unaffected (**Appendix D**).

Glucose in the hemicellulose fraction was 10% lower than the control after 4 d 50 μM meJA treatment and was 25% lower after 8 d treatment in *Brachypodium* callus ($p = 0.016$, F-test for the main effect of meJA, over time: means = 45.3 (+ JA) 51.6 (- JA); SED = 2.44 on 24 df). There was no significant change in hemicellulose associated xylose, arabinose, galactose, galacturonic acid, mannose or glucuronic acid, or in glucose extracted from the hemicellulose fraction after 8 d of treatment with 50 μM meJA.

Lignin showed an interaction effect between treatment and time in *Brachypodium* callus treated with meJA for 1 – 8 d ($p = 0.023$, F-test). Lignin concentration in destarched AIR was 40% greater than in controls after 8 d 50 μM meJA treatment, increasing to 95 $\mu\text{g mg}^{-1}$ at 8 d ($p < 0.05$, LSD), although notably lignin concentration in controls was highly variable, with a maximum lignin concentration of 98 $\mu\text{g mg}^{-1}$ at 4 d and varied by 30 $\mu\text{g mg}^{-1}$ across the four time points measured (**Figure 4.5**).

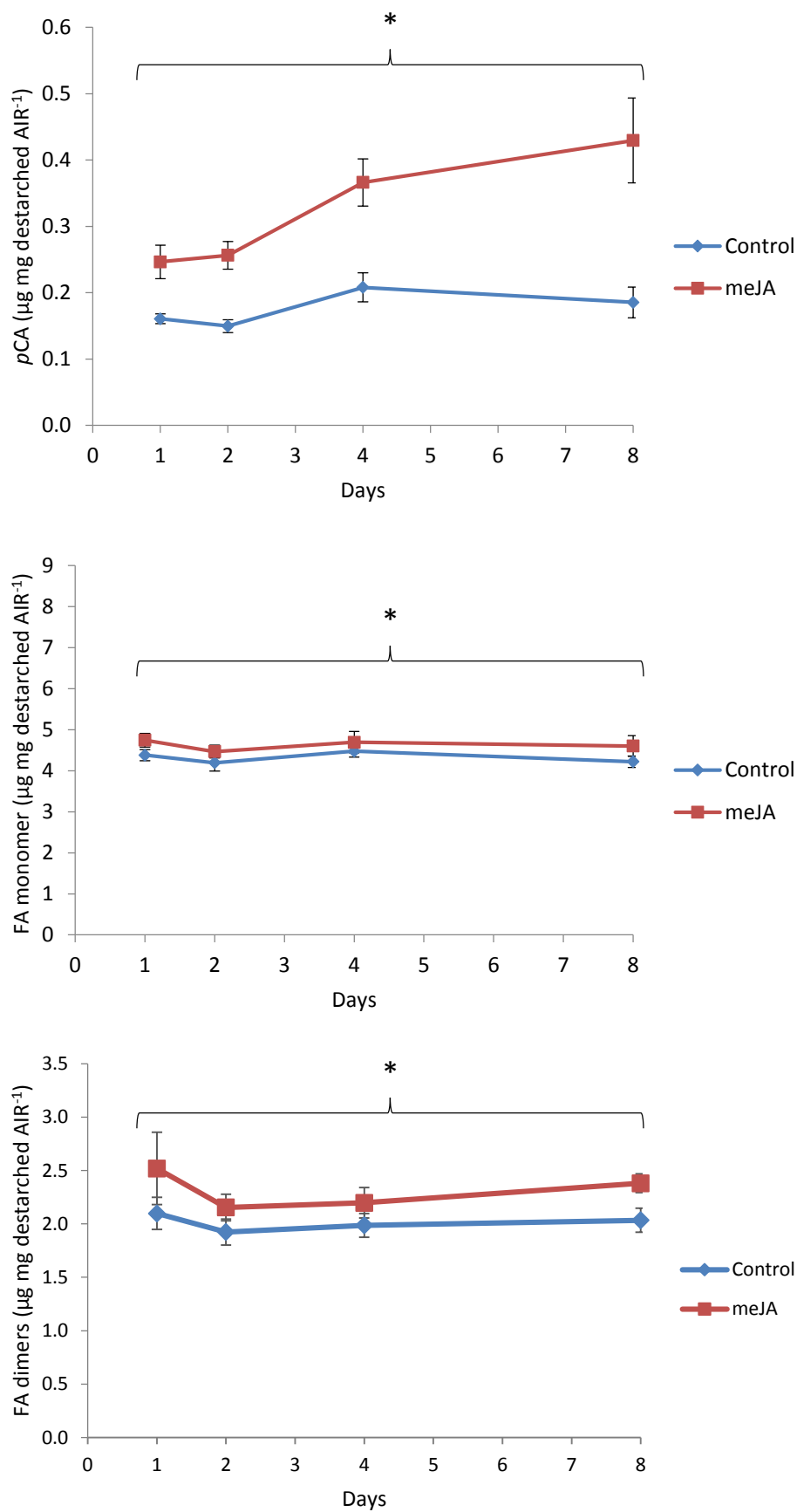


Figure 4.4 The effect of 1, 2, 4 and 8 d treatment with 50 μM methyl-jasmonate (meJA) on *para*-coumaric acid (pCA) and ferulic acid (FA) monomer and dimers (\pm SE) in *Brachypodium distachyon* callus cell walls (callus experiment 3). Analyses were of destarched alcohol insoluble residue (AIR). FA dimers are the sum of diF8-8, diF8-5, diF8-5 benzofuran, diF5-5 and diF8-O-4.

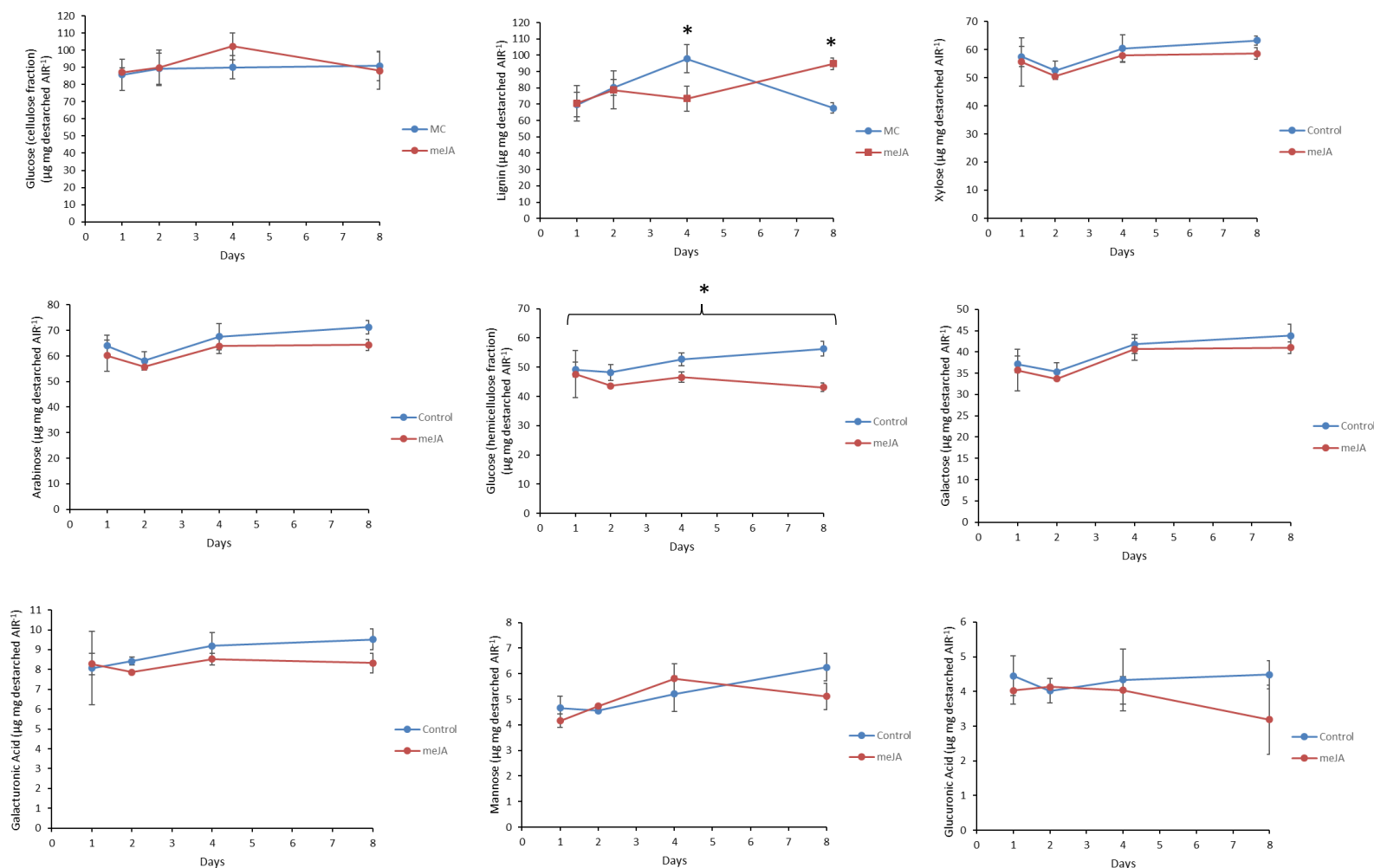


Figure 4.5 The effect of 50 μM methyl-jasmonate (meJA) on cell wall monosaccharides and lignin in *Brachypodium distachyon* callus destarched AIR (alcohol insoluble residue) after 1, 2, 4 and 8 d treatment (callus experiment 3). Glucose concentration in the cellulose fraction, lignin concentration after acetyl bromide treatment, and xylose, arabinose, glucose, galactose, galacturonic acid, mannose and glucuronic acid concentration in the hemicellulose fraction were measured. Error bars show \pm SE. Asterisks represent statistically significant difference between treatment and control groups for main effect of treatment ($p < 0.05$, F-tests) or interaction effect between treatment and tissue ($p < 0.05$, LSD).

4.3.8 RNA-seq transcriptome

RNA-seq returned between 3.1 - 11.2 million reads per sample, averaging 6.8 million reads. On average 93% of total reads were mapped to the reference (6.4 million reads (± 0.23 SE); **Figure 4.6**). The MDS plot of variation between samples showed that meJA treatment had a large effect on the variation between samples, whereas time resolved the variation to a lesser extent (**Figure 4.7**). EdgeR revealed 4508 differentially expressed genes (DEGs) for the ANOVA treatment factor, 1270 DEGs for the time factor, and 170 genes that showed an interaction effect between treatment and time (**Appendix E**). Within the DEGs for meJA treatment over time, 3377 genes were upregulated and 1131 genes were downregulated. The major represented Gene Ontology (GO) terms associated with these DEGs were integral membrane components (cellular process), ATP binding (molecular function) and oxidation-reduction process (biological function), although represented GO terms varied greatly, as expected given the diverse roles of JA *in planta*. Cell wall associated cellular process and biological function GO terms were amongst the top 20 represented terms (**Figure 4.8**). KEGG analysis predicts that enzymes in the phenylpropanoid pathway are differentially expressed with meJA treatment (**Figure 4.10**).

4.3.9 Cell wall genes

Forty cell wall-synthesis genes were significantly upregulated in response to 50 μ M meJA including genes from families GT2, GT4R, GT8, GT31, GT61, GT64, GT65 and GT77, BAHD genes and lignin synthesis genes (**Figure 4.9, Appendix F**). Twenty-eight genes were significantly downregulated, including genes from families GT2, GT8, GT31, GT37, GT47, GT48 and GT77, and extensins and an expansin (**Figure 4.9, Appendix G**).

Candidate genes for *pCA* and FA esterification to AX in the BAHD and GT61 families increased significantly in *Brachypodium* callus when treated with 50 μM meJA. Six BAHD family genes, including two paralogues of *BAHD2*, and eight GT61 family genes showed increased gene expression. Of the GT61 upregulated genes, 6 genes were from clade A, and 2 genes were from clade B (*Bradi2g61230* (*GT61_6*), *Bradi2g26590* (*GT61_14*), *Bradi2g04980* (*BAHD2p2*) and *Bradi2g01380* (*GT61_21*) showed the highest fold change in gene expression within their respective families, although overall gene expression was low, while *Bradi2g05480* (*BAHD 1*) showed the highest expression of the candidate genes with an average FPKM of 129 across 4 time points in the control samples, compared to 172 in meJA treated callus. *Bradi2g01480* (*GT61_5*) also showed relatively high expression within the BAHD and GT61 families, which had an average FPKM of 54 in the control samples and 65 in the meJA treated callus. (**Table 4.3, Appendix H**). The BAHD gene from the same Clade responsible for addition of *pCA* to lignin, *BdPMT* (Petrik et al., 2014), was not expressed in control or meJA treated samples (data not shown).

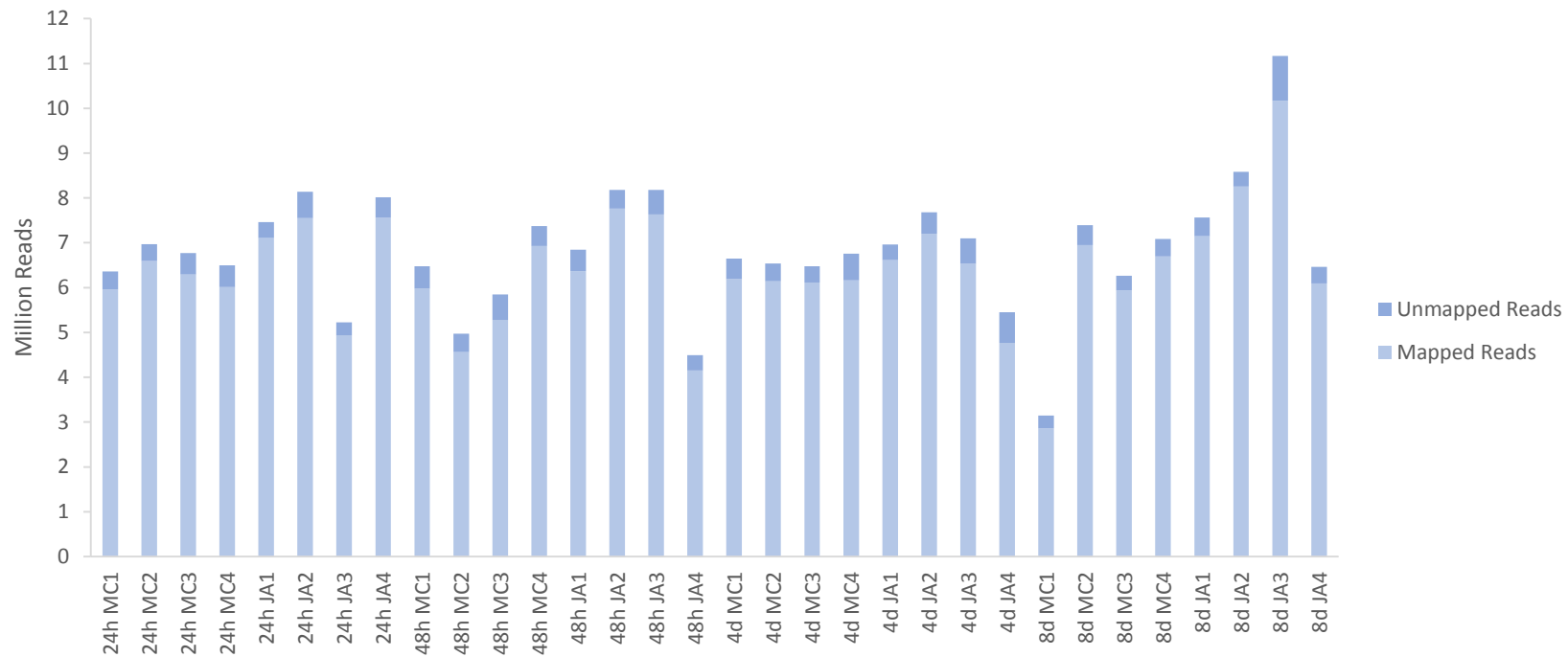


Figure 4.6 Mapped and unmapped reads in *Brachypodium distachyon* callus RNA sequencing analysis. Four replicates of +/- 50 μ M meJA at 24 h, 48 h, 4 d or 8 d treatment were analysed. Reads were mapped using BWA-MEM tool and mapping statistics were generated using the Flagstat tool in Galaxy software (Giardine et al., 2005).

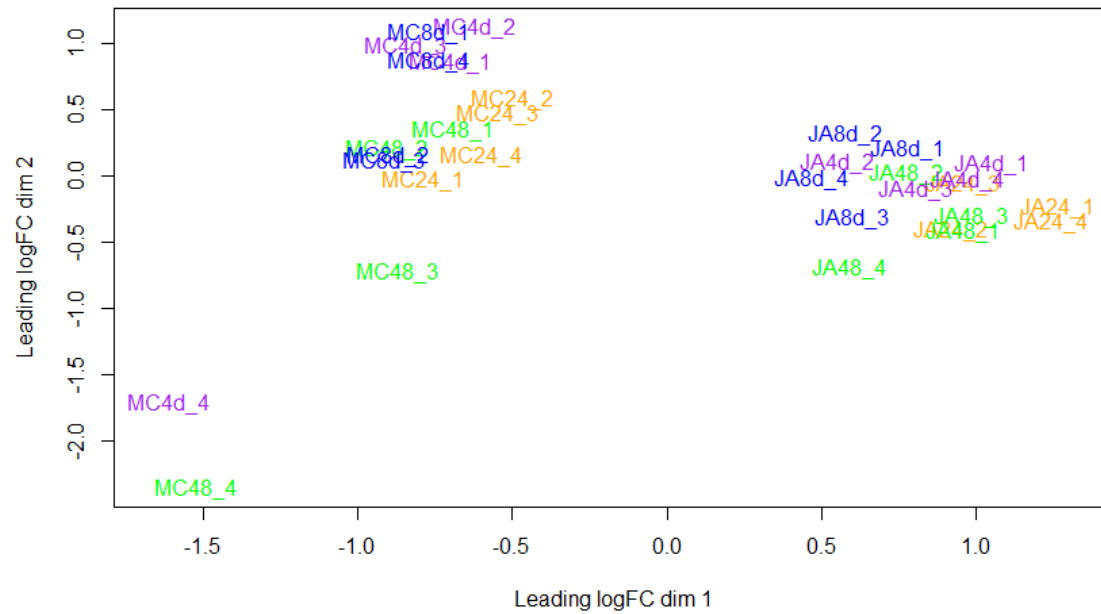


Figure 4.7 MDS plot showing clustering of RNA sequencing samples of *Brachypodium distachyon* treated with 50 μ M meJA (JA) for 24 h (orange), 48 h (green), 4 d (purple) or 8 d (blue), compared to a mock control (MC). Four biological replicates were analysed (1-4). Plot was generated in R Studio by calculating leading log fold change (FC) from effective counts of reads, for genes with cpm > 1 in 3 or more samples.

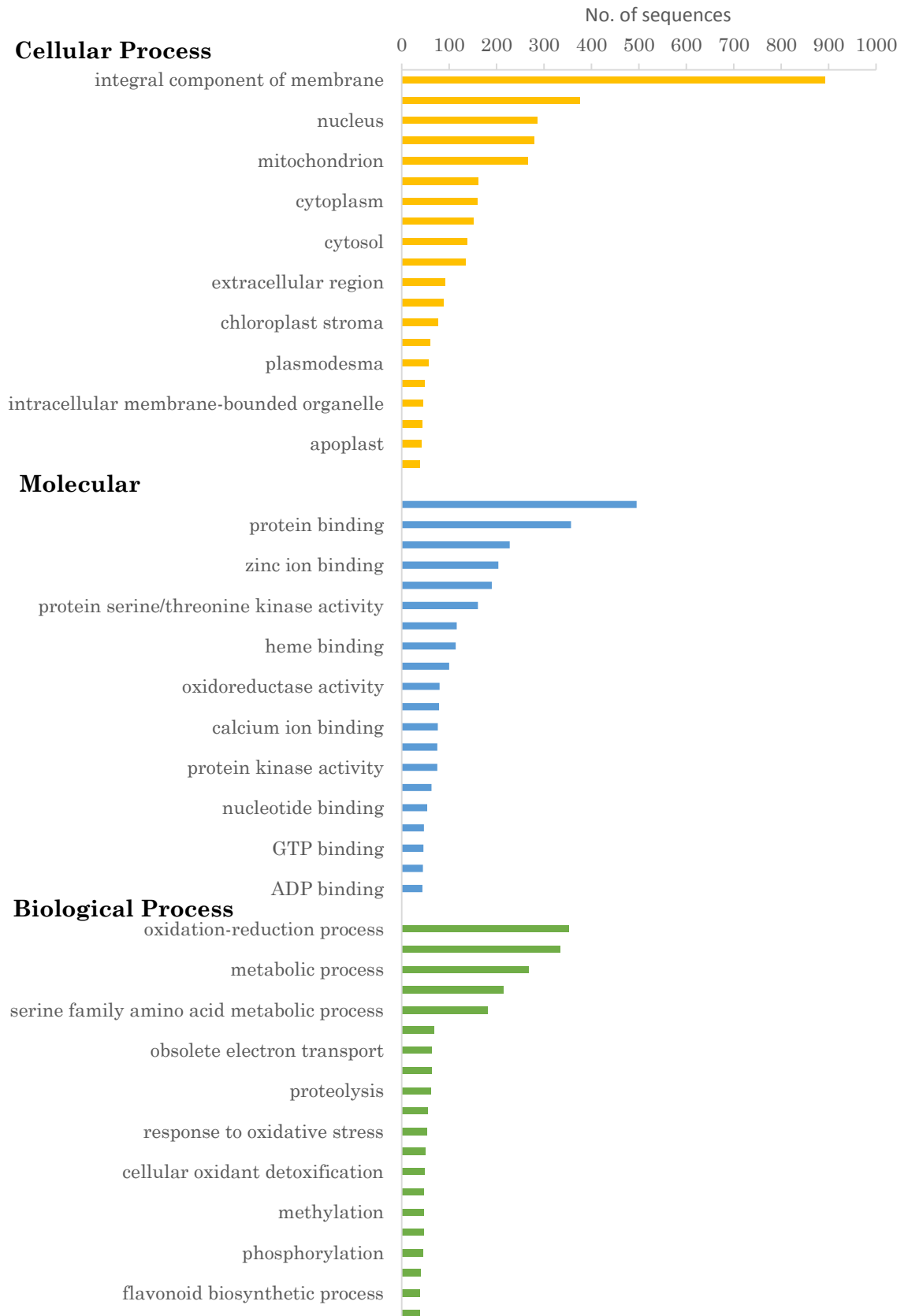


Figure 4.8 List of top 20 represented Gene Ontology (GO) terms for each GO category (cellular process, molecular function and biological process) and no. of sequences associated, for DEGs with meJA treatment in *Brachypodium distachyon* callus treated with 50 μ M meJA and sampled at 1, 2, 4 and 8 d.

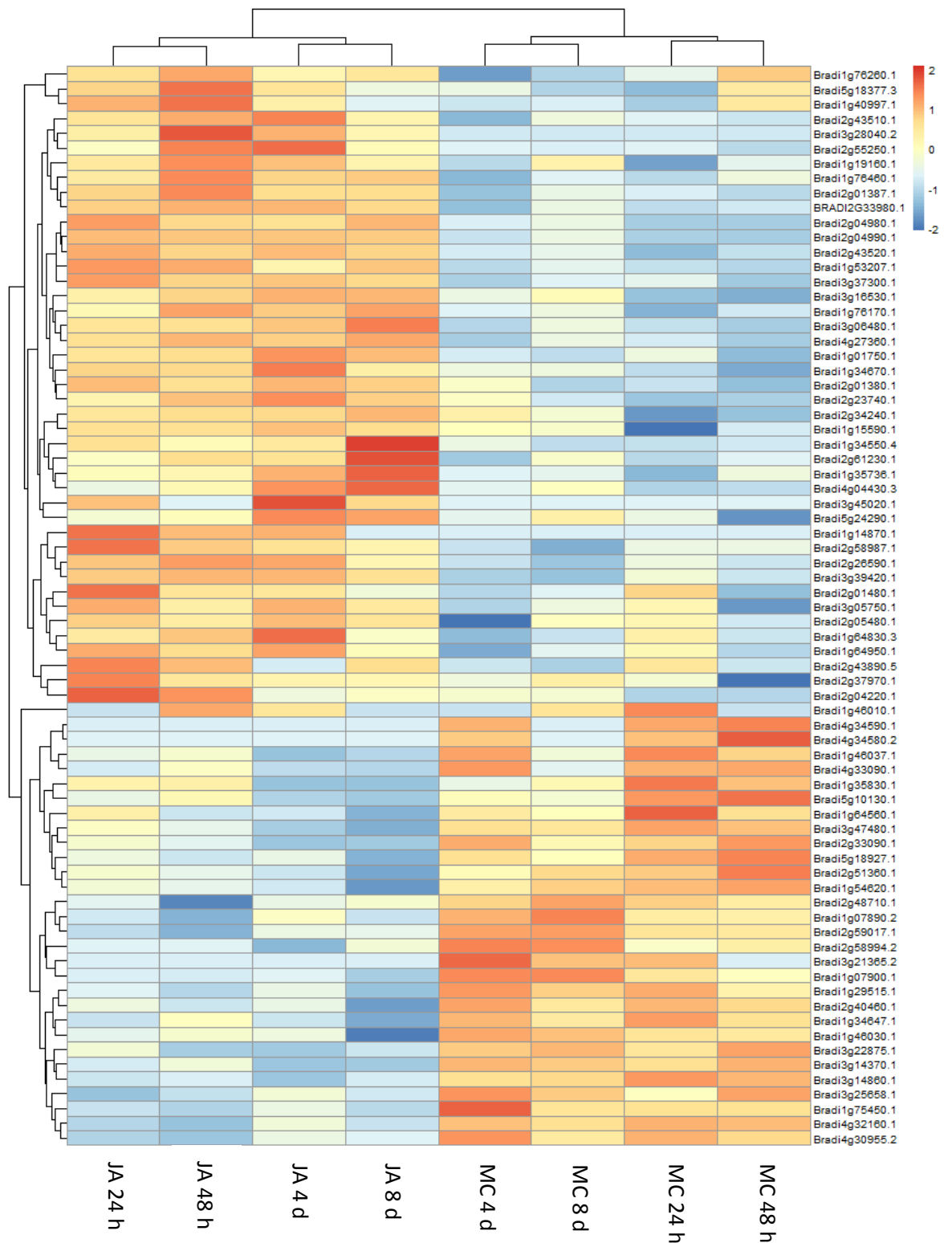


Figure 4.9 Heat map of cell wall differentially expressed genes (DEGs) with meJA treatment. Log cpm fitted values generated by EdgeR were used to generate heat map. *Brachypodium distachyon* callus samples were treated with 50 μ M meJA (JA) or a mock control (MC) treatment for 24 h, 48 h, 4 d or 8 d.

Table 4.3 Changes in gene expression of statistically significant upregulated candidate genes for *para*-coumaric and ferulic acid esterification to arabinoxylan after 1, 2, 4 or 8 d treatment with 50 μ M meJA compared to a mock control, in *Brachypodium distachyon* callus. Fold changes are based on FPKM values from an RNAseq experiment and *p*-values (ANOVA) are corrected for FDR Benjamini-Hochberg. Candidate genes are arbitrarily numbered according to their rice orthologues, p = paralogue. Genes are ordered within families by average fold change over 4 time points.

gene name	family	candidate	transcript abundance (FPKM)		24 h fold change	transcript abundance (FPKM)		48 h fold change	transcript abundance (FPKM)		4 d fold change	transcript abundance (FPKM)		8 d fold change	<i>p</i> -value
			24 h MC	24 h meJA		48 h MC	48 h meJA		4 d MC	4 d meJA		8 d MC	8 d meJA		
<i>Bradi2g04980</i>	BAHD Clade	BAHD2p2	0.3	2.0	774%	0.2	1.4	557%	0.4	1.2	300.2%	0.5	1.7	344.4%	2.26E-07
<i>Bradi2g04990</i>	BAHD Clade	BAHD2p1	1.1	6.1	536%	1.0	5.8	591%	1.4	5.8	421.8%	2.1	5.8	275.1%	2.49E-11
<i>Bradi2g33980</i>	BAHD Clade	BAHD4	21.4	37.7	176%	21.1	40.6	193%	20.0	40.3	201.4%	26.1	37.9	145.1%	2.51E-06
<i>Bradi2g43510</i>	BAHD Clade	BAHD3p1	19.7	25.1	128%	17.8	27.6	155%	18.1	29.3	161.8%	21.7	24.7	113.9%	3.13E-04
<i>Bradi2g05480</i>	BAHD Clade	BAHD1	146.9	172.8	118%	117.6	162.3	138%	103.2	179.7	174.1%	149.5	171.5	114.7%	3.63E-03
<i>Bradi2g43520</i>	BAHD Clade	BAHD5	21.6	30.4	140%	21.4	29.5	138%	24.1	30.1	124.9%	25.1	30.2	120.3%	3.36E-04
<i>Bradi2g01380</i>	GT family 61	GT61_21	0.3	1.2	458%	0.2	1.0	565%	0.5	1.3	250.8%	0.2	1.1	459.3%	1.95E-04
<i>Bradi1g34670</i>	GT family 61	GT61_12	1.2	2.1	187%	0.9	2.1	241%	1.5	2.6	182.7%	1.5	2.0	133.1%	1.45E-04
<i>Bradi4g27360</i>	GT family 61	GT61_10	20.6	31.1	151%	17.3	34.6	200%	19.1	32.8	171.5%	23.6	36.3	154.1%	1.33E-06
<i>Bradi2g01387</i>	GT family 61	GT61_15	25.8	39.0	151%	22.3	45.9	205%	23.2	38.9	167.7%	28.8	39.7	138.0%	2.69E-05
<i>Bradi2g61230</i>	GT family 61	GT61_6	3.1	4.2	135%	3.2	5.1	162%	3.1	4.9	160.1%	4.0	6.8	171.4%	3.67E-04
<i>Bradi2g26590</i>	GT family 61	GT61_14	13.4	17.7	132%	11.5	18.9	164%	12.7	18.6	146.7%	12.1	16.2	134.0%	4.34E-07
<i>Bradi1g19160</i>	GT family 61	GT61_18	13.2	19.2	145%	14.7	22.1	150%	15.1	20.8	137.7%	18.6	19.2	103.5%	4.24E-03
<i>Bradi2g01480</i>	GT family 61	GT61_5	61.4	70.5	115%	46.7	64.1	137%	52.9	64.3	121.5%	56.1	60.2	107.2%	1.71E-03

4.4 Discussion

4.4.1 Cell wall-bound *p*CA and FA

Ferulic acid (FA) is esterified to arabinoxylan (AX) in cell walls of the Poaceae, and is able to dimerise, and therefore covalently cross-link AX polysaccharides (Hatfield et al., 1999). In this study, 100 μ M (\pm)-jasmonic acid (JA) induced increased cell wall-bound FA dimers and induced decreased cell wall-bound FA monomer in *Brachypodium* seedling root tissue, while total FA remained stable (**Figure 4.1**). This may be attributable to free radical-generating class III peroxidases that are released into the cell wall downstream of jasmonic acid signalling. This has been evidenced directly in dock leaf (Moore et al., 2003), and as a response to insect herbivory in wheat (Shetty et al., 2003). Class III peroxidases in the cell wall create increased cross-linking through FA dimerisation, and increased lignin biosynthesis (Almagro et al., 2009). Indeed, in this study, an increase in lignin was found 8 d post 50 μ M meJA treatment in *Brachypodium* callus (**Figure 4.5**).

There was no significant effect of 100 μ M (\pm)-JA in cell wall-bound *p*CA, or total FA, in *Brachypodium* roots and shoots grown in hydroponics after 48 h (**Figure 4.1**). It is possible that insufficient cell wall synthesis occurred within the 48 h period studied, and therefore longer treatment with (\pm)-JA may have shown increased total HCAs. Indeed, resistance to infection has been shown to be acquired 2-3 d after wounding in *Rumex spp.* (Hatcher et al., 1994). Alternatively, FA and *p*CA cross-linked to lignin may be a complicating factor. Lignin typically comprises around 20% of *Brachypodium* plant cell walls (**Figure 3.6**), and ester-bonded FA residues on AX are a known nucleation site for lignin formation (Ralph et al., 1995). Cross-linking of FA residues to lignin via ether or C-C bonds may well have increased due to class III

peroxidase release into the cell wall. FA cross-linked to lignin by ether or C-C bonds would not be released by the alkaline-hydrolysis method used here, and therefore total FA may have been underestimated. Lignin also contains alkali-labile ester-linked *p*CA, which is 4 times the amount of *p*CA residues on AX in *Brachypodium* tissues (Petrik et al., 2014). The undifferentiated cells of callus generally have very little secondary cell wall, with half the amount of lignin as plant tissues (**Figure 4.5**). Although *Brachypodium* callus cell walls contained some lignin, the bound *p*CA in callus cell walls was almost entirely ester-bonded to AX, as shown by mild acidolysis, and this was not altered by JA treatment (**Table 4.1**). The amounts of *p*CA, FA and FA dimers, lignin and neutral sugars found in *Brachypodium* callus in this study were similar to those found by Rancour et al. (2012). Therefore, callus provided a useful system to study the effect of jasmonic acid on wall-bound hydroxycinnamic acids (HCAs).

Wall-bound *p*CA increased dramatically in methyl-jasmonate treated callus, increasing 5-10 fold after 17 d treatment with 100 μ M meJA (**Figure 4.2**). Although wall-bound *p*CA was greater than the control samples (50%) after 24 h meJA treatment, and was two-fold greater after 8 d treatment (**Figure 4.4**), lignin was only 40% greater than the control samples after 8 d meJA treatment (**Figure 4.5**). There was no evidence that AX was greater in meJA treated samples (**Figure 4.5**), hence, *p*CA increased per unit AX. Arabinoxylan *p*-coumaroylation was shown to be one of the first, and greatest, changes to the cell wall in response to meJA. The role of this linkage is unknown since it does not cross-link, although it has been hypothesised that *p*CA linked to lignin may promote lignin polymerisation (Boerjan et al., 2003, Hatfield et al., 2008), and it is possible that AX-linked *p*CA also has a role in lignin polymerisation. Alternatively, it could act as an inhibitor of AX digestion under biotic stress given the role of JA in the wounding response.

Total wall-bound FA was greater in meJA treated *Brachypodium* callus after 8 d treatment with 50 μ M meJA than in control samples; notably FA dimers were 12% greater than the control (**Figure 4.4**). As meJA did not affect the amount of arabinose or xylose in the callus cell walls, this experiment indicates that total FA per unit AX increased in response to jasmonic acid signalling. However, results of a separate experiment where callus tissue was treated for 17 d with 100 μ M meJA, and where AX was shown to increase, may not be consistent with this (**Figure 4.2**, **Figure 4.3**). Increased FA in response to meJA is not well documented, however the results of this study concur with Lee et al. (1997), who reported a 1-2 fold increase in wall-bound FA in JA-treated barley leaf segments after 48 h treatment. Increased wall-bound FA and FA dimers presumably fortifies the cell wall against insect or pathogen invasion due to its role in inhibition of digestion by cross-linking (Grabber et al., 1998a).

4.4.2 Cell wall genes

There was a large response to meJA in cell wall associated genes in the primary cell walls of *Brachypodium* callus, including upregulation of cellulose synthase genes (*CesAs*), *GT43* and *47* families, and lignin genes (**Appendix F**), although some *GT47* family genes were downregulated in response to meJA treatment (**Appendix G**). β -glucan synthesis *cellulose synthase-like* (*CSL*) genes were also downregulated (**Appendix G**). Consistent with this was decreased glucose in the hemicellulose fraction of meJA treated callus (**Figure 4.5**), suggesting a role for decreased β -glucan in response to JA. The distribution of GO terms that were assigned to differentially expressed genes showed that cell wall associated GO terms were among the top cellular processes that were affected by meJA. Furthermore, consistent with the increase in cell wall-bound pCA and FA (**Figure 4.4**), enzymes

within the phenylpropanoid pathway were differentially expressed with meJA treatment (**Figure 4.10**).

4.4.3 BAHD and GT61 family genes

Treatment with meJA for 24 h induced upregulation of *BAHD1*, *2p1*, *2p2*, *3p1*, *4* and *5* transcripts and *GT61.5*, *10*, *12*, *14*, *15*, *18* and *21* (clade A) and *GT61 6* and *14* (clade B) transcripts (**Table 4.3**). As cell wall-bound *pCA* and FA increased in the same time frame, the enzymes encoded by the upregulated BAHD and GT61 transcripts are implicated in synthesising cell wall-bound HCAs in *Brachypodium*. Gene expression profiles of these genes were similar to the response of their rice orthologues from experiments in rice seedlings in response to JA, as documented in the RiceXPro database (Sato et al., 2013) (**Appendix A, Appendix H**), verifying that the callus system is representative of the system *in planta*.

Mitchell et al. (2007) were the first to hypothesise that a clade within the BAHD acyltransferase family and two clades of the glycosyltransferase (GT)61 gene families were involved in arabinoxylan synthesis. Evidence that some BAHD genes are involved in the esterification of *pCA* to AX has since accumulated (Molinari et al., 2013, Piston et al., 2010); the best evidence for this is that *OsAT10* has been shown to esterify *pCA* to AX in rice (Bartley et al., 2013). The *Brachypodium* orthologue *bdBAHD10* was not expressed in control or meJA treated callus in this study, although *pCA* esterified to AX increased dramatically, suggesting functional redundancy within the BAHD family.

One gene within the same BAHD clade (*BdPMT*) has been shown to add *pCA* to lignin (Withers et al., 2012, Petrik et al., 2014). Cell wall-bound *pCA* in callus was found to be mostly or entirely linked to AX as opposed to lignin, as evidenced by mild acidolysis analysis (**Table 4.1**), and consistent with this was the absence of BAHD

acyltransferase *BdPMT* expression, which is responsible for all pCA linked to lignin in plant tissues (Petrik et al., 2014).

BAHD2p1 and *p2* genes showed the greatest upregulation in response to meJA in callus (**Table 4.3**), suggesting that these genes may be responsible for pCA linked to AX, whereas the other *BAHDs* which were upregulated to a lesser extent could be responsible for FA linked to AX, as FA increased to a lesser extent than pCA (**Figure 4.4**). To support this hypothesis, *BdBAHD5*, which was upregulated here, has previously been implicated in feruloylation of AX (Piston et al., 2010, Buanafina et al., 2016).

It has been shown that some GT61 clade A genes (*XAT 1, 2 & 3*) are arabinosyl transferases (Anders et al., 2012). As described in **Chapter 1.8.2**, it is hypothesised that *XAX1* and the Brachypodium orthologue, *BdGT61.9*, are similarly feruloyl/coumaryl arabinosyl transferases. Neither *GT61.9p1* nor *GT61.9p2* showed significant change in gene expression when treated with meJA. However, the closely related *GT61.10* showed an increase in gene expression after 24 h, rising to a 2-fold increase at 48 h (**Table 4.3**), and may be therefore functionally redundant with *GT61.9p1/p2*. AX-esterified FA is greater than AX-esterified pCA (Mueller-Harvey and Hartley, 1986); as *BAHD1* and *GT61.5* showed the highest relative expression of the *BAHD* and *GT61* genes which were upregulated, these genes are also good candidates for involvement in FA esterification. Conclusion

Treatment with meJA was found to increase arabinoxylan pCA and FA in the cell wall of Brachypodium callus, and increase FA cross-linking. It remains to be seen whether these increases contribute to greater cell wall recalcitrance and to acquired resistance to pests and pathogens. The expression of genes in the *BAHD* and *GT61* genes families increased in response to meJA in conjunction with increased pCA and FA, and therefore the experiments in this chapter have added to the existing

evidence that genes within these families are involved in feruloylation and coumaroylation on AX in grass cell walls. Candidate genes were also identified, such as *BAHD2*, for which there is strong evidence for involvement in *pCA* esterification to AX in the cell wall.

Chapter 5. Effects of Glycosyltransferase (GT)61.9 Overexpression and RNAi on Cell Wall Composition, and an Investigation of the Expression Driven by Upstream Regions from the two GT61.9 Paralogues, in *Brachypodium distachyon*.

5.1 Introduction

The unique cell walls of the Poaceae (grasses) comprise arabinoxylan (AX) as the major hemicellulose. Ferulic acid (FA) cross-linking in grasses are major inhibitors of enzymatic digestion in second generation biofuel and ruminant nutrition applications. Elucidating the genes involved in the esterification of FA, and the very similar phenolic molecule *para*-coumaric acid (*pCA*), to AX is of great interest in increasing the digestibility of grass cell walls (**Chapter 1.6.4**).

Despite the significance of FA in grass cell walls and the potential positive applications in biofuel production and ruminant nutrition, little is known about the mechanisms of FA and *pCA* esterification to AX, and very few of the genes involved have been identified. The BAHD acyl-coA transferase clade A (**Figure 1.4**) and the glycosyltransferase (GT) 61 family (**Figure 1.5**), have been predicted to be involved in the process by Mitchell et al. (2007), using a comparative bioinformatics approach. Subsequently, it was suggested that GT61 gene *OsXAX1* was responsible for β -(1,2)-xylosyl transferase activity of α -(1,3)-arabinose residues on AX in rice (Chiniquy et al., 2012). This study also found a marked decrease in both cell wall-bound FA and *pCA* in *xax1* knockout mutants of around half compared to wild type.

Other GT61 family genes, *TaXAT1* and *TaXAT2* in wheat and *OsXAT2* and *OsXAT3* in rice encode α -(1,3) arabinosyl transferases which catalyse the addition of arabinofuranose onto β -(1,4) xylose backbone of AX (Anders et al., 2012). Also, the wheat orthologue of *OsXAX1*, named *TaGT61.9* here, is highly expressed in starchy endosperm in wheat, where the feruloyl-AX β -1,2-xylosyl side chain is absent (Saulnier et al., 2007). Furthermore, *OsGT61.9* is strongly coexpressed with members of the BAHD acyl-coA transferase clade A, which are implicated in adding ferulic acid to arabinose in the cytosol (Molinari et al., 2013, Mitchell et al., 2007). Given this evidence, an alternative hypothesis for *GT61.9* function is that it encodes an enzyme with feruloyl-arabinosyl transferase and *p*-coumaroyl arabinosyl transferase activities (**Figure 1.6**).

A widely used model species for the study of grass cell walls is *Brachypodium distachyon* (Brachypodium), a more relevant model for the temperate grasses than rice, which has potential advantages for understanding the role of hydroxycinnamic acids (HCAs) on AX in determining digestibility of grass biomass. Orthologues of *XAX1* in Brachypodium are the paralogous genes *Bradi1g06560* and *Bradi3g1137*, named *GT61.9p1* and *p2* respectively here. The encoded proteins of *GT61.9p1* and *p2* show 77% and 79% identity with *OsXAX1* (**Figure 5.1**). *GT61.9p1* has been shown by qRT-PCR data to be more highly expressed in stems and roots in Brachypodium, and *GT61.9p2* more highly expressed in leaf (Mitchell lab, unpublished, **Appendix I**). However, little is known about the function and activity of the two *GT61.9* paralogues in Brachypodium.

The aims of the experiments in this chapter were to investigate the function and control of expression of the two *GT61.9* paralogues in Brachypodium using transformation approaches. In order to determine the role of *GT61.9* genes in determining AX feruloylation and *p*-coumaroylation, constructs designed to

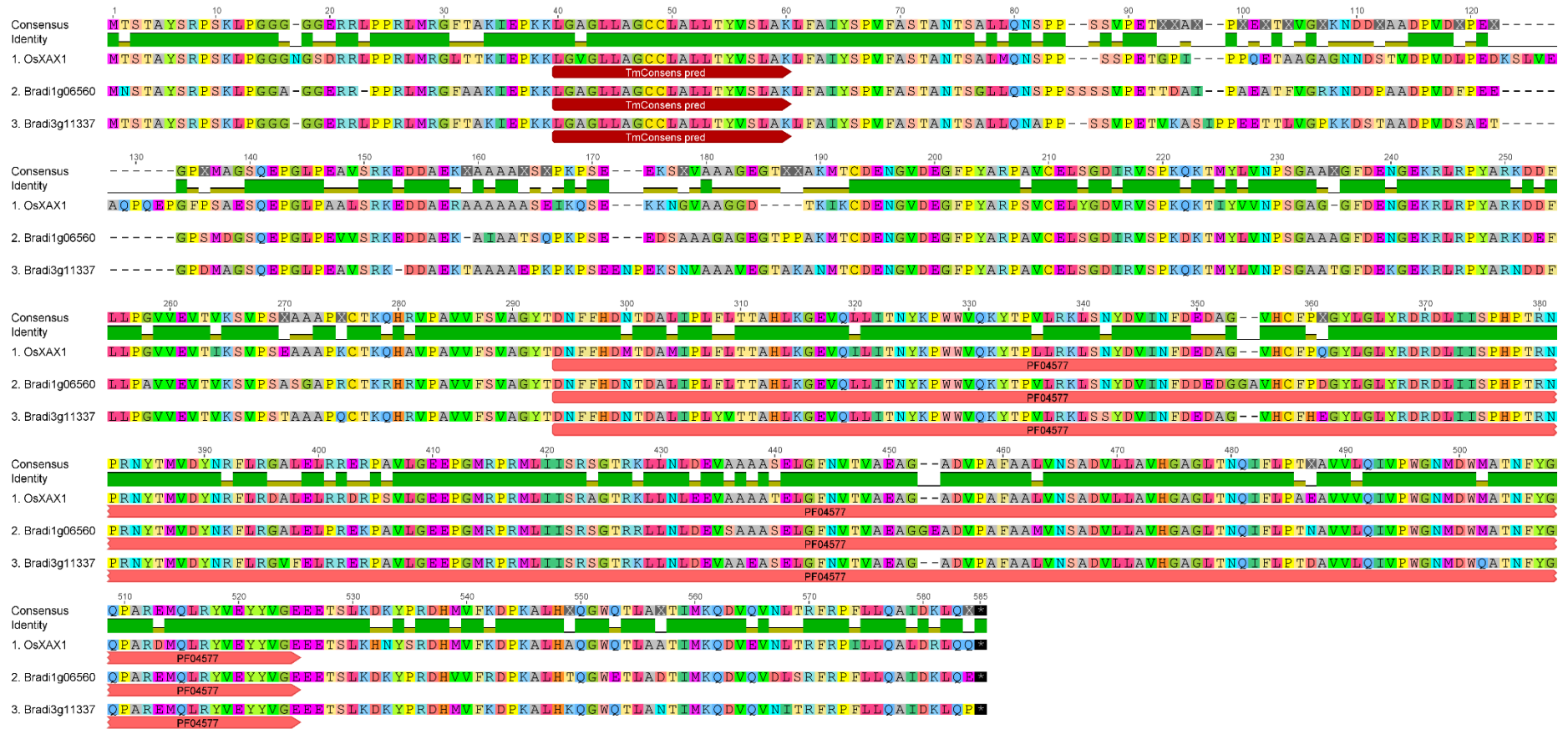


Figure 5.1 Protein alignment of *Brachypodium distachyon* paralogue genes *Bradi1g06560* (*GT61.9p1* here) and *Bradi3g11337* (*GT61.9p2* here) with rice gene *OsXAX1*. The alignment was created using Geneious software. The single transmembrane domain and the PF04577 functional domain are highlighted

overexpress and knock-down (RNA interference (RNAi)) the expression of two *GT61.9* paralogues were used to transform *Brachypodium*. It was anticipated that the knock-downs would replicate the result of *xax1* with decreased cell wall-bound HCAs, and overexpression lines may show increased cell wall-bound HCAs. Transgenic lines with such effects could be studied further to discriminate between competing hypotheses of the role of *GT61.9*, and also investigate effects on important traits such as digestibility. In order to investigate whether the differences in gene expression between the *GT61.9* paralogues observed from qRT-PCR in the Mitchell lab (unpublished, **Appendix I**) were attributable to their upstream promoter regions, GFP fusion transformants were analysed.

5.2 Chapter 5 specific methods

5.2.1 Phylogenetic tree construction

All protein sequences containing PFAM PF04577 domain, characteristic of the GT61 family, were downloaded from the JGI Phytozome 11 database (www.phytozome.net, Goodstein et al., 2012) for Arabidopsis, Brachypodium and rice. Three sequences (two Arabidopsis and one rice) which were distantly related to the others were excluded as they were the only sequences that were not included in the CAZy (www.cazy.org, Coutinho et al., 2003) list of GT61 proteins. Wheat protein sequences are not all available, so are not included in Phytozome11; a comprehensive set of wheat GT61 coding sequences compiled by Dr. Rowan Mitchell, Rothamsted Research from sequences cloned in the Cell Wall Group, IWGSC2 genomic sequences (Ensembl Plants, www.plants.ensembl.org, Hubbard et al., 2002) and wheat RNA-seq was used. To simplify the tree, only one homeologue from the three wheat sub-genomes was used, as these have >95% nucleotide sequence similarity. The set of GT61 protein sequences (8 Arabidopsis, 22 rice, 22 Brachypodium, 29 wheat) were aligned using MUSCLE (Edgar, 2004) in Geneious version 8 (Kearse et al., 2012), with default settings. The phylogenetic tree was generated using Phyml (Guindon and Gascuel, 2003) using the Whelan and Goldman (2001) model; proportion of invariable sites and gamma distribution parameters were optimised in an initial run at 0.012 and 0.893, respectively. These were then fixed at these values and topology and branch length were optimised in 100 bootstrap runs; the tree shown is the consensus tree with the number of bootstraps supporting branches shown.

5.2.2 Vector design of *GT61.9p1* overexpression construct

The *Bradi1g06560* (*GT61.9p1*) coding region CDS was obtained from the JGI Phytozome 11 database (<http://www.phytozome.net>, Goodstein et al., 2012). Silent transversion mutations were introduced into the CDS at base 579:C→G, 1143: C→G and 1269: C→G, to disrupt restriction sites. The stop codon, TAG, was replaced with

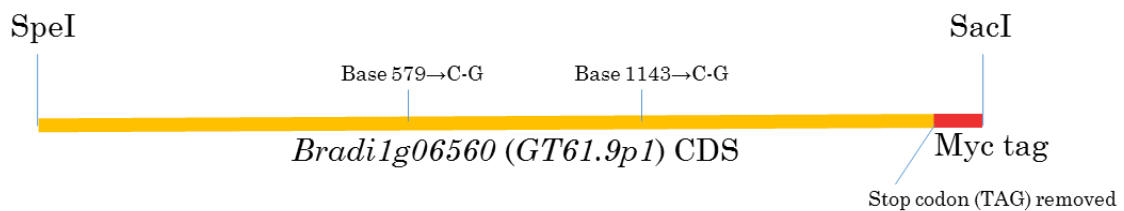


Figure 5.2 A schematic diagram (not to scale) of the construct ordered from Genscript®, USA, to be used for overexpression of *GT61.9p1* in *Brachypodium distachyon*.

the c-Myc epitope tag (5'GAGCAAAGCTCATTTCTGAAGAGGACTTG), and SpeI and SacI restriction sites were introduced at the 5' and 3' ends respectively (**Figure 5.2**). This construct was ordered cloned into the *pUC57* vector from Genscript®, USA.

Two vectors were created for overexpression of *GT61.9p1* driven by the maize ubiquitin promoter (*pUbi::GT61.9p1-Myc*) or the *IRX5* promoter (*pIRX5::GT61.9p1-Myc*). The maize ubiquitin promoter is well established. The *IRX5* promoter was chosen as suitable for driving expression in tissues synthesising secondary cell walls, which constitute the majority of final biomass and are therefore most relevant for digestibility applications. The *IRX5* promoter was identified by Dr. Rowan Mitchell as a 1,487 bp upstream region of *Bradi3g28350*, the orthologue of *IRX5* in *Arabidopsis*, which encodes a secondary-cell wall specific cellulose synthase. This *IRX5* promoter has been shown to drive strong expression in *Brachypodium* stems with a GUS reporter construct (Dr. Till Pellny, unpublished). The *Bradi1g06560-Myc* construct was inserted into the *A224p6i-U-Gusi* and *A224p6i-IRX5-Gusi* master

vectors (shown in **Figure 5.3**), using standard cloning procedures (**Chapter 2.13**) and according to the following cloning strategy. Plasmid *A224p6i-U-Gusi* was digested with SpeI and SacI to remove the GUS coding region (CDS), and *GT61.9p1* CDS (SpeI and SacI-digested from pUC57 vector) was inserted into the plasmid using SpeI and SacI sticky ends to create *pUbi::GT61.9p1-Myc* (**Figure 5.4**). Similarly, master plasmid *A224p6i-IRX5-Gusi* was used to create *pIRX5::GT61.9p1-Myc* (**Figure 5.5**).

5.2.3 Vector design of *GT61.9p1* and *p2* RNAi construct

Two RNAi vectors were designed and constructed by Dr. Till Pellny, Rothamsted Research. Vectors were designed to simultaneously knock down the expression of *GT61.9p1* (*Bradi1g06560*) and *GT61.9p2* (*Bradi3g11337*) in Brachypodium. The RNAi cassettes were constructed with inverted repeats of a sequence with a 90bp stretch of homology between *GT61.9p1* and *p2*, but only 14bp identity with closely related *GT61.10*, flanking the maize *Adh2* intron (sequence shown in **Appendix J**), and were under the control of the ubiquitin promoter (*pUbi::RNAi-GT61.9p1/p2*) or the *IRX5* promoter (*pIRX5::RNAi-GT61.9p1/p2*).

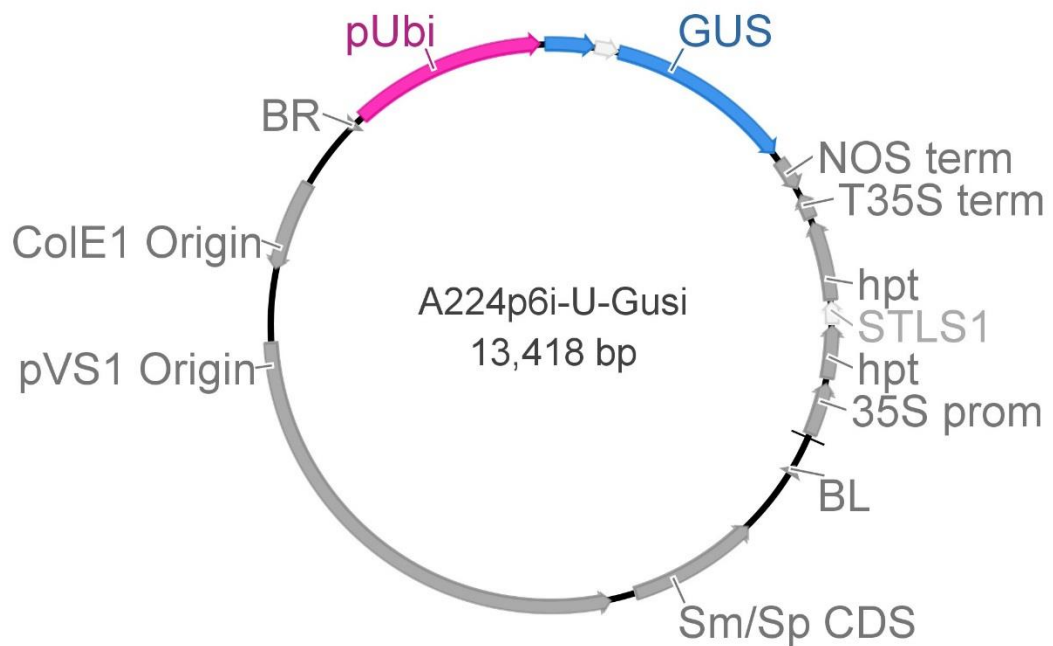


Figure 5.3 A diagram of the A224p6i-U-Gusi master vector used for transformation of *Brachypodium distachyon*. Features of the vector include the origins of replication for *Agrobacterium AGL1* (pVS1), and *Escherichia coli* (ColE1), and the streptomycin/spectinomycin resistance gene (Sm/Sp CDS). Inside the border sequences (BL and BR), the cauliflower mosaic virus (CaMV) 35S promoter drives expression of the hygromycin resistance gene (hpt), mediated by the potato ST-LS1 intron and terminated by the CaMV 35s terminator. The maize ubiquitin promoter (pUbi) drives expression of the GUS coding sequence (CDS), which was replaced with the CDS of *GT61.9p1* in this study, and terminated by the nopaline synthase (NOS) terminator.

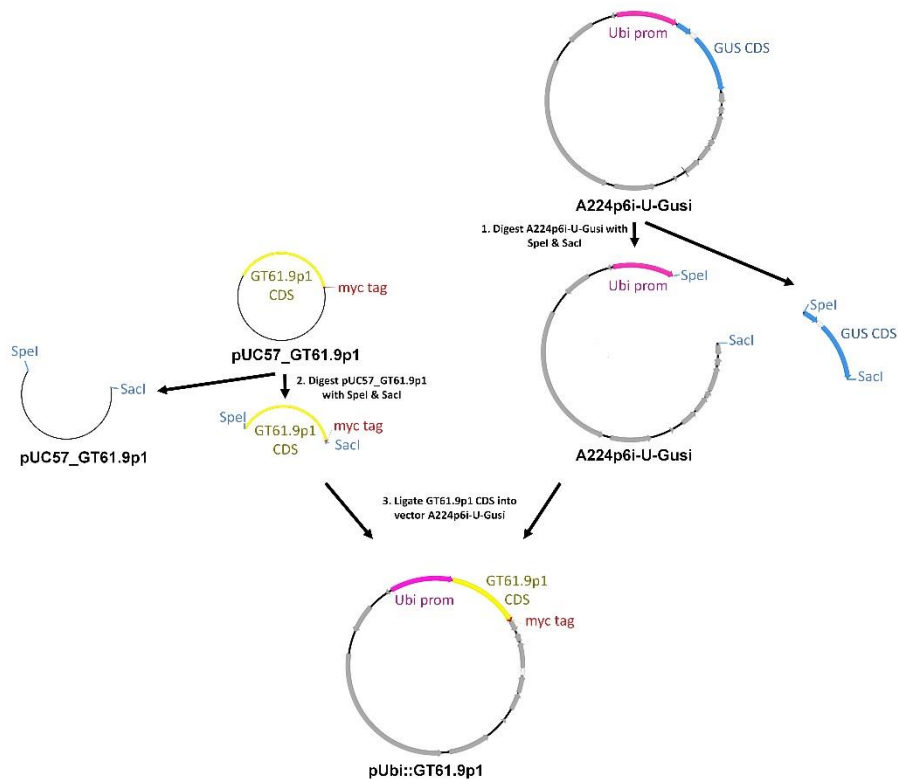


Figure 5.4 A schematic diagram of the cloning procedure used to create vector *pUbi::GT61.9p1-Myc*. Pink labels indicate the maize ubiquitin promoter, blue labels indicate the GUS coding region, and yellow labels represent the *Brachypodium distachyon* *GT61.9p1* coding region. Light blue labels show restriction site sticky ends.

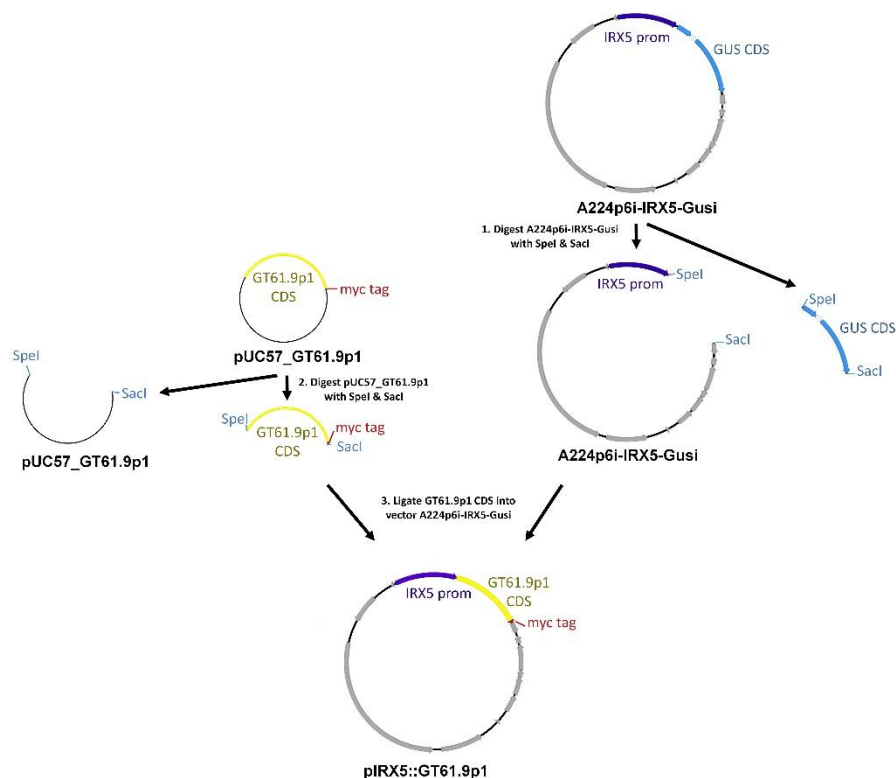


Figure 5.5 A schematic diagram of the cloning procedure used to create vector *pIRX5::GT61.9p1-Myc*. Purple labels indicate the *IRX5* secondary cell-wall specific promoter, blue labels indicate the GUS coding region, and yellow labels represent *Brachypodium distachyon* *GT61.9p1* coding region. Light blue labels show restriction site sticky ends.

5.2.4 Brachypodium transformation

Agrobacterium was transformed with overexpression constructs *pUbi::GT61.9p1-Myc* (section 5.2.2) and *pIRX5::GT61.9p1-Myc*, and RNAi constructs *pUbi::RNAi-GT61.9p1/p2* and *pIRX5::RNAi-GT61.9p1/p2* (section 5.2.3), as described in Chapter 2.14, and transgenic plants were generated as described in Chapter 2.16. Figure 5.6 depicts examples of the transformation procedure. T₀ and T₁ generations were grown in a glasshouse at 20/20 °C, 16/8 h light/dark cycle with supplementary lighting, with 2-4 weeks of vernalisation. T₂ generation seeds were grown as described in section 5.2.6 for analysis of phenolic acids.

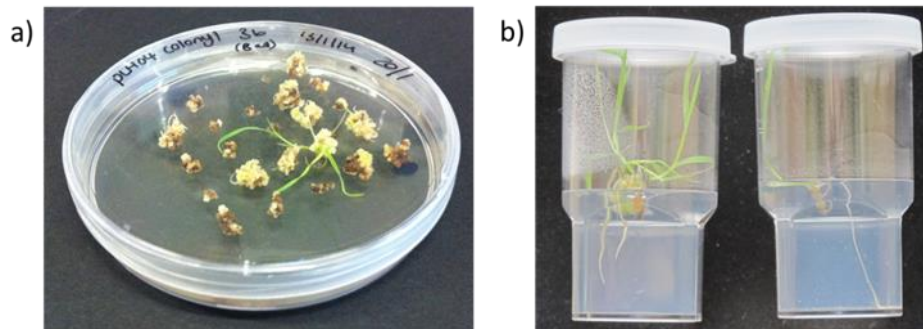


Figure 5.6 Photographs of *Brachypodium distachyon* transformation procedure, showing (a) callus on regeneration media containing hygromycin selection, showing generation of shoots, and (b) root generation of putative transformants on MS media under selection.

5.2.5 Determination of zygosity

Zygosity of T₂ generation plants was determined as described in Chapter 2.18.

5.2.6 Experimental design

Five independent lines from the T₂ generation were germinated and, when 20 days old, were grown in a statistically randomised paired block design, with positive transgenic plants paired with a null segregant. Four biological replicates were integrated into the block design. Plants were grown in a controlled environment cabinet at 24/20 °C, 20/4 h light/dark cycle, 65% humidity, 150 μmol m⁻² s⁻¹ photosynthetic photon flux. Plants were harvested after 4 weeks directly into liquid nitrogen (**Chapter 2.2**). It was observed that plants from the *pIRX5::GT61.9p1-Myc* experiment showed signs of disease.

5.2.7 Analyses of *GT61.9* overexpression and RNAi lines

Transformed *Brachypodium* lines (T₂) generation were verified as expressing the transgene using Western blot as described in **Chapter 2.20**, and were analysed for cell wall-bound phenolics as described in **Chapter 2.11 and 2.12**. Wall-bound sugars were analysed as described in **Chapter 2.6 and 2.7**.

5.2.8 Statistics

Outlying values were discounted as per Grubbs' outliers test. Analysis of variance (ANOVA) was applied to the data, taking account of the four biological replicates in the blocked experimental design, and testing the main effects of transgene (null or positive) and transgenic line using the F-test. Means in relevant statistically significant ($p < 0.05$, F-test) terms from the ANOVA were interpreted using the standard error of the difference (SED) between means on the residual degrees of freedom (df), invoking a least significant difference (LSD) at the 5% level of significance. Where mean values are presented in the text as a main effect of the transgene, the figure presented is the average across the lines that were analysed.

Line '2 hom' (homozygous segregants of *GT61.9* overexpression line 2) compared to its null segregant was analysed in an independent ANOVA as this line was grown in a separate tray to the other transgenic lines. Assistance with statistical analyses was provided by Stephen Powers, Rothamsted Research.

5.2.9 *GT61.9p1* and *p2* promoter-GFP fusion experiment

The promoter region of genes *Bradi1g06560* (*GT61.9p1*) and *Bradi3g11337* (*GT61.9p2*) were assigned as 1500 bp upstream of the start codon of the gene and obtained from EnsemblPlants (<http://plants.ensembl.org>, Kersey et al., 2016). Two constructs were designed and ordered from Genscript®, USA, in vector pUC57. *pUC57::GT61.9p1-GFP* consisted of the promoter region of *GT61.9p1*, fused in frame to the nuclear targeted *GFP* gene (*H2B-GFP*), with KpnI and SpeI restriction sites at the 5' and 3' ends of the promoter region, and a SacI restriction site at the 3' end of *H2B-GFP*. Base 272 was replaced (A-G) to avoid restriction sites. *pUC57::GT61.9p2-GFP* consisted of the promoter region of *GT61.9p2* with KpnI and SpeI restriction sites at the 5' and 3' ends respectively.

Three vectors were constructed containing the *H2B-GFP* coding region driven by either the promoter regions of *GT61.9p1*, *GT61.9p2*, or the maize ubiquitin promoter as a positive control, using standard cloning procedures (**Chapter 2.13**), as follows. Plasmid *A224p6i-U-Gusi* was digested with KpnI and SacI to remove the ubiquitin promoter and *GUS* coding region, and KpnI and SacI-digested *promGT61.9p1-H2B-GFP* was ligated into the plasmid using KpnI and SacI sticky ends to create *pGT61.9p1::H2B-GFP*. This plasmid was digested with KpnI and SpeI to remove the promoter, and the *GT61.9p2* promoter was inserted using KpnI and SpeI sticky ends, to create *pGT61.9p2::H2B-GFP*. The positive control plasmid *Ubi::H2B-GFP* was created by digesting plasmid *A224p6i-U-Gusi* with KpnI and SpeI

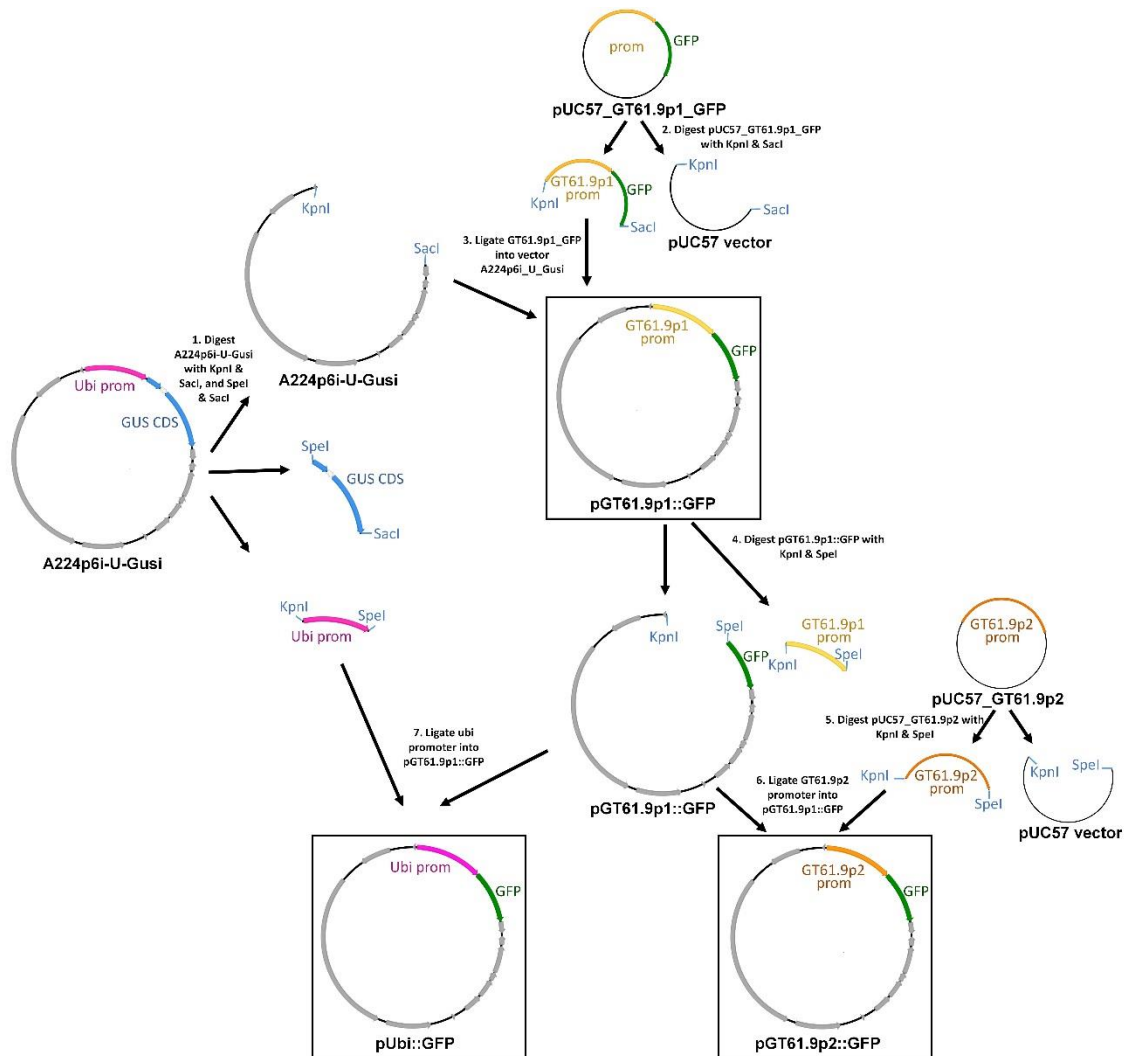


Figure 5.7 A schematic representation of the cloning procedure used to create vectors *pGT61.9p1::GFP*, *pGT61.9p2::GFP*, and *pUbi::GFP*. Pink labels indicate the maize ubiquitin promoter, green labels indicate the *H2B-GFP* coding region, blue labels indicate the GUS coding region, and yellow and orange labels indicate the *Brachypodium distachyon* *GT61.9p1* and *GT61.9p1* promoter regions (1500 bp upstream of the start codon) respectively. Light blue labels show restriction site sticky ends.

to remove the maize ubiquitin promoter and inserting into plasmid *pGT61.9p1::H2BGFP*, digested with KpnI and SpeI (**Figure 5.7**).

5.2.10 Analyses of *GT61.9p1* and *p2* promoter-GFP fusion

Brachypodium was transformed with promoter fusion vectors *pGT61.9p1::H2B-GFP*, *pGT61.9p1::H2B-GFP* and *Ubi::H2B-GFP* as described in **Chapter 2.14-2.16**. For analysis of leaves, T₁ or T₂ generation transgenic Brachypodium lines were grown in the glasshouse at 25/20 °C, 16/8 h light/dark cycle with supplementary lighting, after 2 weeks of vernalisation at 6 °C, 8/16 h light/dark cycle. For analysis of roots, Brachypodium seedlings were germinated on 0.5 x MS media (2.2 g/l (w/v) MS salts, 0.05% (w/v) MES, 0.5% (w/v) Phytigel™) and analysed when 4 days old. Green fluorescent protein (GFP) was visualised using a Zeiss 780 LSM confocal microscope as described in **Chapter 2.21**. At least two independent lines for each construct were analysed in 2.5 month old Brachypodium for leaf, or 4 day old seedlings for root. The root images were obtained with the assistance of the Rothamsted Research bioimaging department (Kirstie Halsey).

5.3 Results

5.3.1 Phylogenetic tree of the GT61 family

Reference sequences have been updated slightly since the phylogenetic tree of GT61 proteins shown in **Figure 1.5** was generated. Therefore, a new phylogenetic tree was generated to include all the species where there is direct evidence of function for a GT61 protein, namely rice, wheat, Arabidopsis and Brachypodium (**Figure 5.8, Appendix K**).

5.3.2 Overexpression of *GT61.9p1* in Brachypodium

Brachypodium was successfully transformed with overexpression constructs *pUBI::GT61.9p1-MYC* and *pIRX5::GT61.9p1-MYC*. Eighteen (*pUBI*) and fourteen (*pIRX5*) independent transgenic lines were generated, from a pool of 300 calli each, giving a transformation efficiency of 6% and 4.7% respectively. All of these lines were shown to be PCR positive, as exemplified in **Figure 5.9**, demonstrating successful selection on hygromycin. Four *pUBI::GT61.9p1-MYC* transgenic lines were assayed for the Myc antigen using Western blotting, for expected protein size 61 kDa and showed anti-c-Myc activity in stem and leaf (**Figure 5.10**), indicating expression of the transgene and its encoded protein in the assayed lines. Homozygous and heterozygous lines were identified by qPCR with genomic DNA as the template, as exemplified in **Appendix L**. In contrast to the predictions from the hypothesis, there was no difference in cell wall-bound FA monomer, total FA dimers, or *pCA* between *GT61.9* overexpression Brachypodium lines transformed with the *pUBI::GT61.9p1-MYC* construct, when compared to null segregants. The amounts of wall-bound FA monomer and dimers in leaf and stem remained constant across the transgenic lines measured. Total cell wall-bound FA (sum of monomer and dimers)

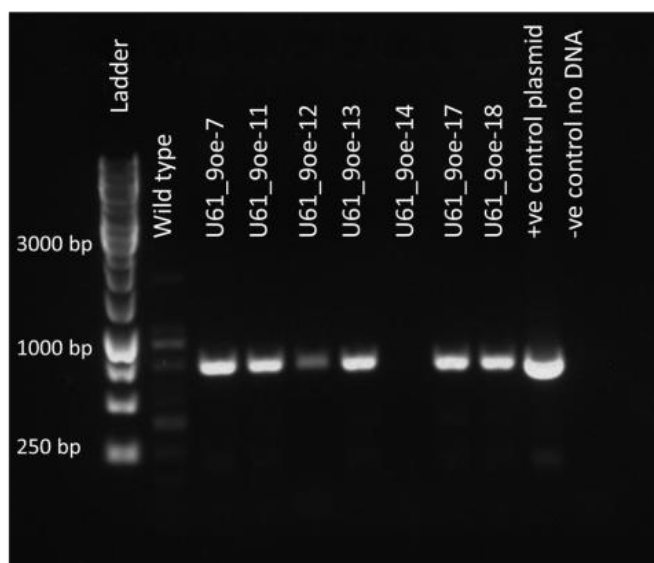


Figure 5.9 Gel electrophoresis image showing positive incorporation of the *pUBI::GT61.9p1-Myc* transgene into *Brachypodium* genomic DNA (gDNA). PCR was used to amplify a section of the transgene from template DNA extracted from leaves of primary transformants (T_0). Lines 7, 11, 12, 13, 14, 17 and 18 are shown and are representative of 18 transgenic lines generated. Control templates wild type *Brachypodium* DNA, a plasmid positive control and a no DNA negative control are also shown. gDNA from line 14 was re-extracted at a later date and was positive for the transgene.

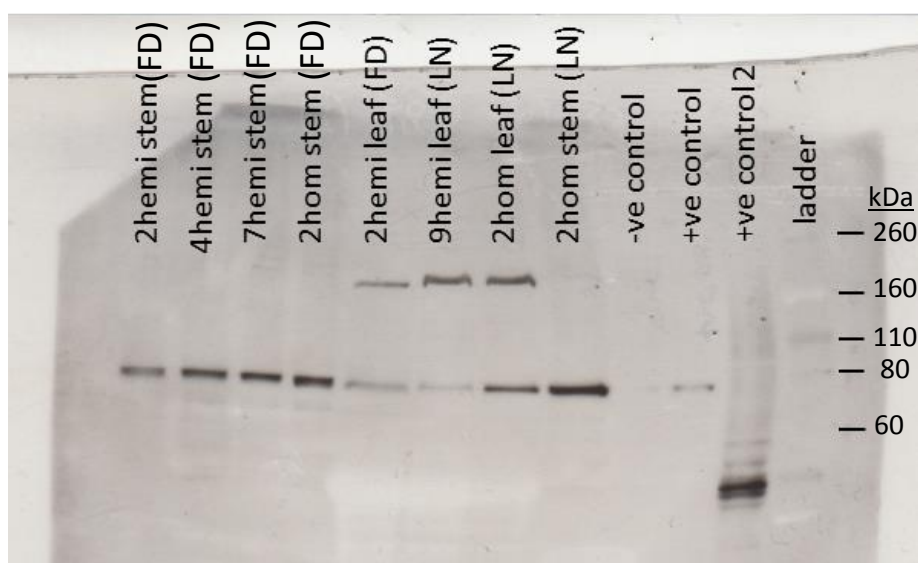


Figure 5.10 Western blot assay of transgenic *Ubi::GT61.9-Myc* overexpression *Brachypodium* lines. Expression of transgenic *GT61.9-Myc* is driven by the ubiquitin promoter (*Ubi*), and expression of *Myc* is visualised by detection of anti-c-Myc antibody activity. Transgenic lines 2, 4, 7 and 9 were analysed, which were either homozygous (hom) or hemizygous (hemi) for the transgene. Leaf or stem material collected from T_2 generation plants was either freeze dried (FD) or harvested directly into liquid nitrogen (LN). Controls: negative (-ve) control is a null segregant of transgenic line 2. Positive (+ve) controls are protein samples from transgenic line 2 (+ve control) and from a BAHD3-Myc fusion (predicted size 46.8 kDa) wheat overexpression line (+ve control 2) that have previously been shown to bind to the anti-C-Myc antibody.

ranged from 3.8-4.2 $\mu\text{g mg}^{-1}$, averaging 4 $\mu\text{g mg}^{-1}$ of dry weight in leaf, and ranged from 5.3 – 5.6 $\mu\text{g mg}^{-1}$, averaging 5.5 $\mu\text{g mg}^{-1}$ of dry weight in stem. Cell wall-bound *pCA* ranged from 1.1 - 1.2 $\mu\text{g mg}^{-1}$, averaging 1.5 $\mu\text{g mg}^{-1}$ of dry weight in leaf, and from 2.8 – 3.4 $\mu\text{g mg}^{-1}$, averaging 3.1 $\mu\text{g mg}^{-1}$ of dry weight in stem. These results indicate the reliability of the collected data. The level of FA in the homozygous segregants was equal to that of heterozygous plants. These findings were consistent across stem and leaf tissues (**Figure 5.11**). Some small but statistically significant changes were observed in individual dimers in *GT61.9p1* overexpression Brachypodium lines. In leaf, there was a significant main effect of the transgene across lines in diF8-8, which was 8% greater in *GT61.9* overexpression lines than in the null segregants ($p = 0.046$, F-test: means = 0.2585 (+), 0.2389 (-); SED = 0.00936 on 26 df), however, diF8-8 was not consistently less than the nulls in every line despite the fact that they all expressed the recombinant protein. In stem, diF5-5 was 5% more than the null segregant control in *GT61.9* overexpression line 5 ($p < 0.05$, LSD), but not in the other lines (**Figure 5.12**).

There were no statistically significant differences found between cell wall-bound sugars glucose (cellulose & hemicellulose fraction), xylose, arabinose, galactose, glucuronic acid, galacturonic acid, mannose and fucose for the main effect of the transgene across lines, with the exception of line '2', in which glucose (cellulose) in the transgenic line was significantly less than in the controls (**Figure 5.13**).

Another identical randomised block design experiment aimed to investigate phenolic content in Brachypodium transformed with overexpression of *GT61.9p1* driven by secondary cell wall promoter *pIRX5* (*pIRX5::GT61.9p1-MYC*) was carried out. This experiment was designed as an alternative to the *pUBI::GT61.9p1-MYC* experiment, to use in the possible event that ubiquitously expressing lines produced non-viable offspring. However, the plants acquired a disease phenotype during the experiment.

Therefore, phenolic content was not measured in these lines and, due to time constraints and given the generation and survival rate of lines which constitutively overexpressed *GT61.9p1* (see above), the experiment was not repeated and phenolic data was not collected from these lines.

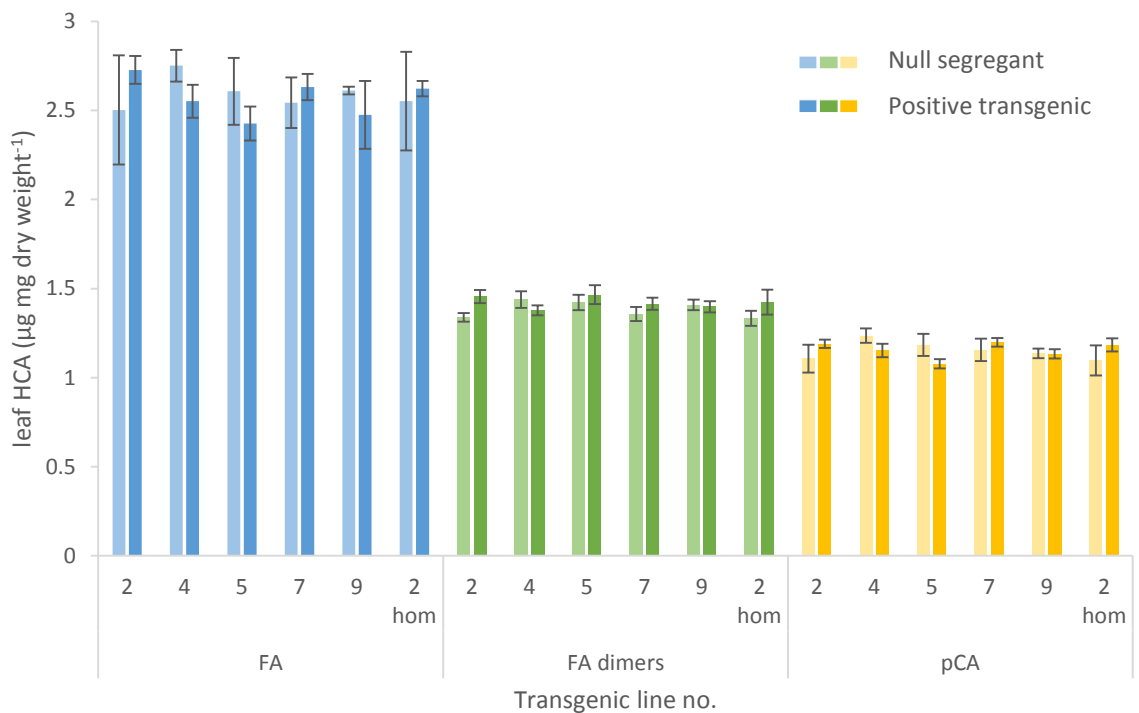
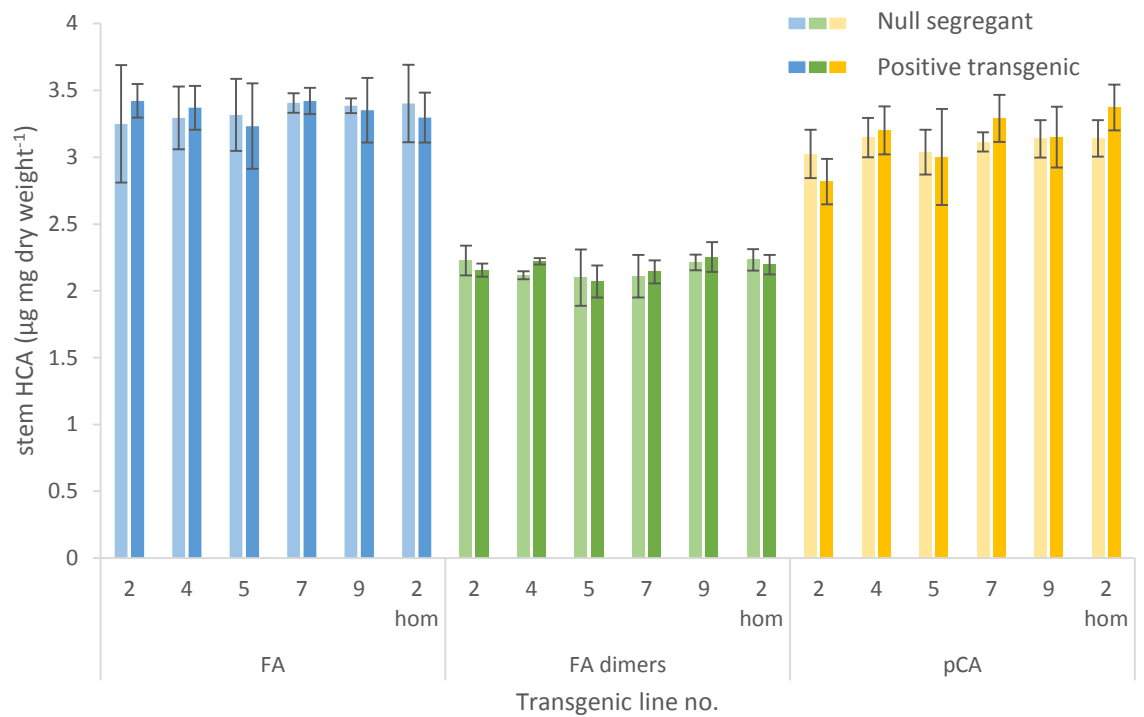


Figure 5.11 Ferulic acid (FA) monomer, total dimers and *para*-coumaric acid (\pm SE) in stem (top) and leaf (bottom) of five *Brachypodium distachyon* lines overexpressing *GT61.9p1*, driven by the maize ubiquitin promoter. Heterozygous lines (2, 4, 5, 7 and 9), and a homozygous segregant of line ‘2’ (2 hom) are shown and transgenic plants (dark blue, dark green and dark yellow) are compared to null segregants (light blue, light green and light yellow). FA dimer includes diF8-8, diF8-5 and diF8-5 benzofuran, diF5-5 and diF8-O-4.

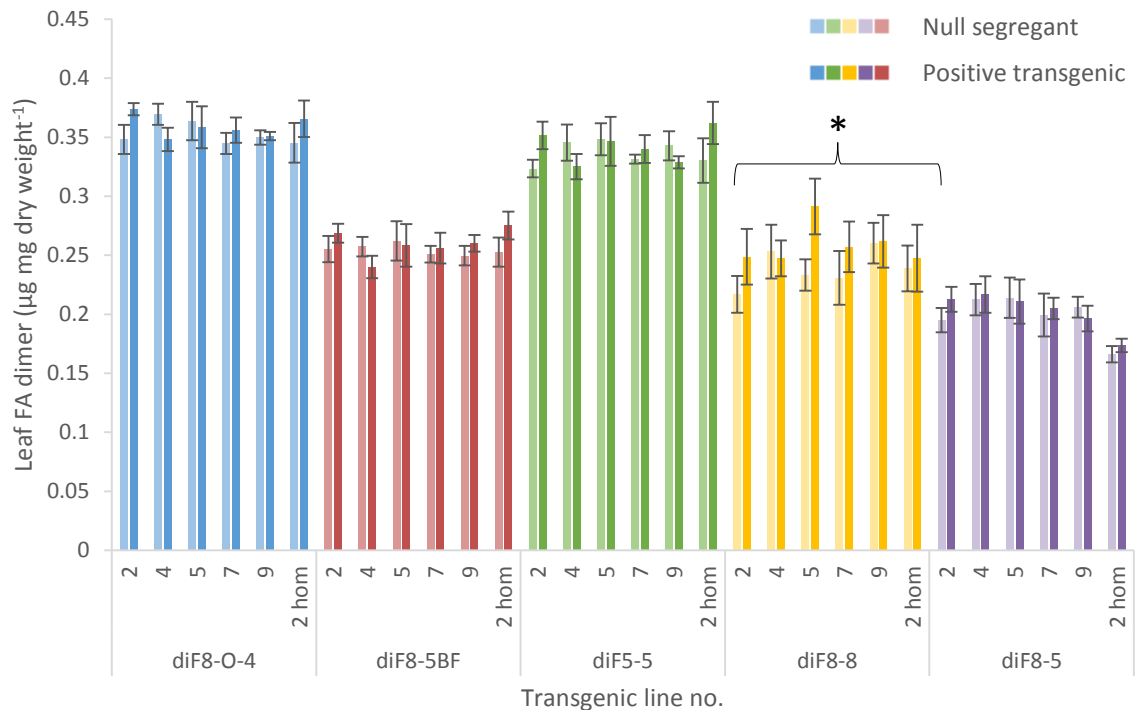
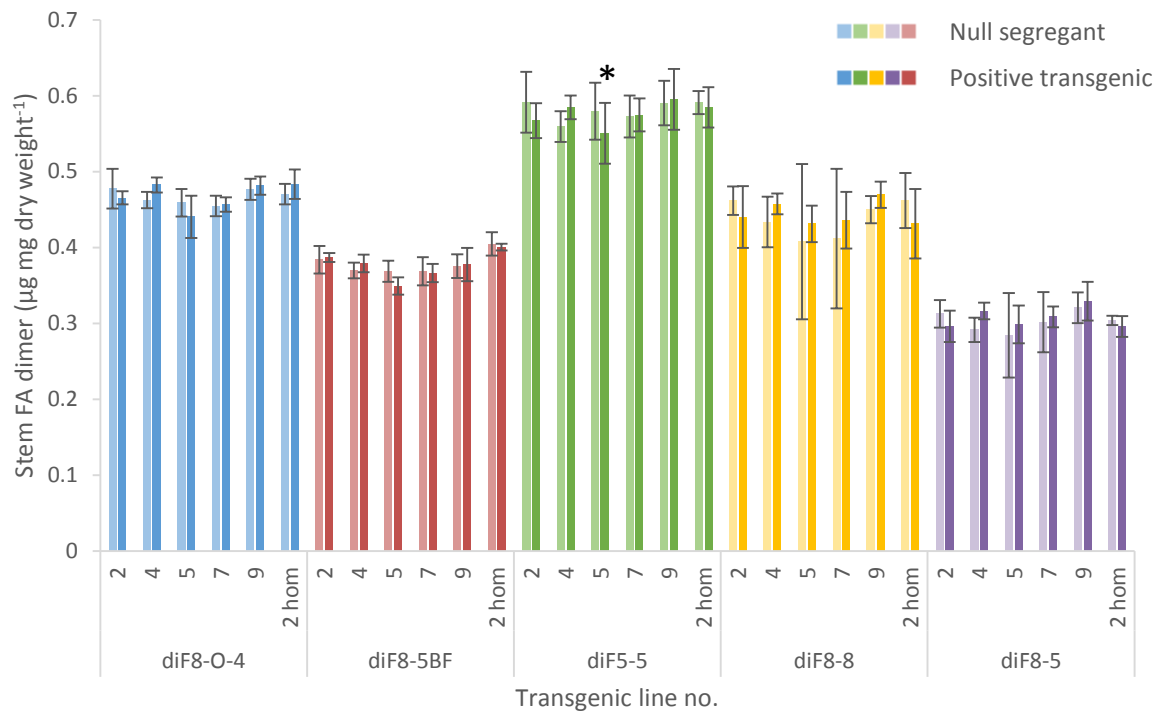


Figure 5.12 Ferulic acid dimers (\pm SE) in stem (top) and leaf (bottom) of five *GT61.9p1* overexpression lines, (expression driven by the maize ubiquitin promoter) in *Brachypodium distachyon*. Heterozygous lines (2, 4, 5, 7 and 9), and a homozygous segregant of line '2' (2 hom) are shown and transgenic plants (dark blue, dark green and dark yellow, dark purple, dark red) are compared to null segregants (light blue, light green and light yellow, light purple, light red). Asterisks indicate significant differences between transgenic lines and null segregants.

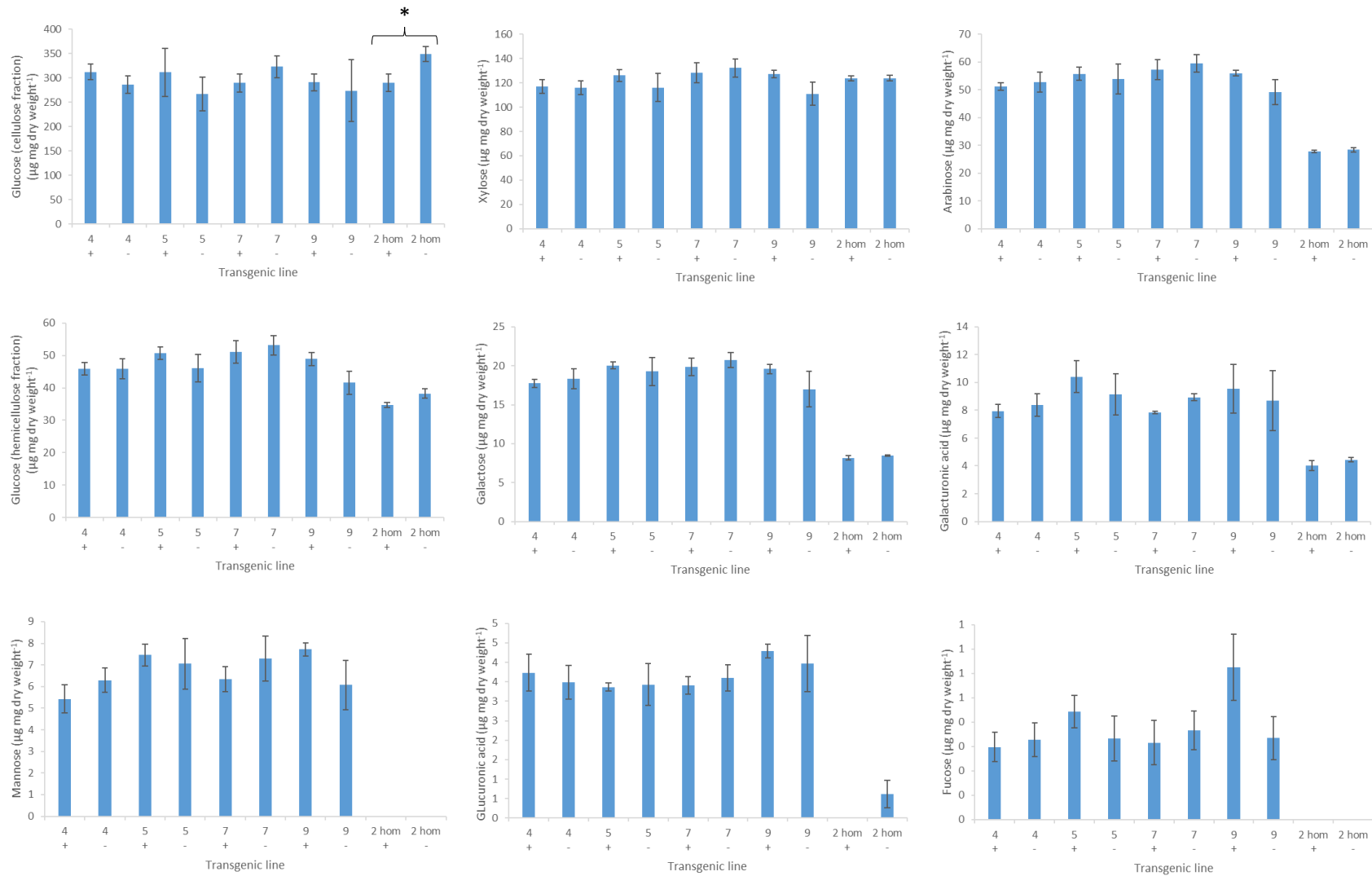


Figure 5.13 Monosaccharide concentrations of transgenic *Brachypodium* lines which overexpress (+) *GT61.9p1* (*Bradi1g06560*) under constitutive expression of the maize ubiquitin promoter, compared to null segregants (-). Error bars show \pm SE. Independent transgenic events are named transgenic lines 4, 5, 7, 9 (heterozygous) and line 2 hom (homozygous). The Asterisk indicates a significant difference between the transgenic line and null segregants

5.3.3 RNAi knockdown of *GT61.9p1* and *p2* in *Brachypodium*

RNAi lines designed to knock down the expression of *GT61.9* paralogues *p1* and *p2* were generated by Dr. Till Pellny, Rothamsted Research. Reduced expression was designed to be driven by the maize ubiquitin promoter (construct *pUbi::RNAi-GT61.9p1/p2*) and the *IRX5* secondary cell wall specific promoter (construct *pIRX5::RNAi-GT61.9p1/p2*), respectively. Five transgenic lines were analysed for phenolic content for each construct. RNAi lines were PCR positive for the transgene (data not shown).

Potential knock-down of *GT61.9* in *Brachypodium*, driven by the ubiquitin promoter, resulted in 4% less total FA (sum of monomer and dimers) in RNAi lines than the null controls in leaf tissue. Total FA decreased from 3.93 $\mu\text{g mg}^{-1}$ in null segregants, to 3.78 $\mu\text{g mg}^{-1}$ in positive *pUbi::RNAi-GT61.9p1/p2* lines ($p = 0.013$, F-test for main effect of the transgene; SED 0.0568 on 27 df; **Figure 5.14**). Cell wall-bound FA dimers diF8-O-4 and diF8-5BF decreased by 6% ($p = 0.005$, F-test for main effect of transgenic type (-/+ transgene): grand means = 0.6589 (-), 0.6190 (+); SED = 0.01292 on 27 df; **Figure 5.15**), which were measured together due to overlapping peaks on the HPLC chromatogram. In stem, there was no significant difference in total cell wall-bound FA (sum of monomer and dimers) between *pUbi::RNAi-GT61.9p1/p2* RNAi transgenics and null segregants, which ranged from 3 – 3.6 $\mu\text{g mg}^{-1}$, averaging 3.3 $\mu\text{g mg}^{-1}$ of dry weight (**Figure 5.14**). These data are consistent with the amounts of total FA in *GT61.9p1* overexpression lines (**Figure 5.11**).

Potential knock-down of *GT61.9* in *Brachypodium*, driven by the *IRX5* promoter showed significant decreases in total cell wall-bound FA dimers across all lines, and in cell wall-bound FA monomer in two lines across leaf and stem tissue. In stem, RNAi knock down lines had 6% less total cell wall-bound FA dimers than the null

controls ($p = 0.004$, F-test for main effect of transgenic type (-/+ transgene): means = 1.967 (-), 1.847 (+); SED = 0.0381 on 26 df, **Figure 5.16**). Individual FA dimers diF8-O-4 and diF8-5BF (summed) decreased by 5% in RNAi knock down lines ($p < 0.001$, F-test for main effect of transgenic type (-/+ transgene): means = 0.9438 (-), 0.8964 (+); SED = 0.1214 on 26 df), and diF5-5 decreased by 4% in individual knock down lines in stem ($p = 0.028$, F test for main effect of transgenic type (-/+ transgene): means = 0.5326 (-), 0.5123 (+); SED = 0.00872 on 26 df; **Figure 5.17**). Cell wall-bound FA monomer was also lower in RNAi knock down line 9 (9% reduction) and in line 22 (12% reduction), compared to null controls in stem ($p < 0.05$, LSD; **Figure 5.16**). In leaves of *pIRX5::RNAi-GT61.9p1/p2* knock down lines, there was some evidence of a main effect of transgenic type (-/+ transgene) on cell wall-bound FA dimers, which were 5% less than in the null controls in total across all lines ($p = 0.058$, F-test; means = 1.605 (-), 1.530 (+); SED = 0.0379 on 27 df; **Figure 5.16**). A significant 5% decrease in individual dimers diF8-O-4 and diF8-5BF contributed to this ($p = 0.047$, F-test, ANOVA main effect of transgenic type (-/+ transgene), grand means 0.7828 (-), 0.7463 (+), SED = 0.01754 on 27 df). Also, diF8-8 was 36% less in *IRX5* RNAi knock down line 21 than in the controls in leaf ($p < 0.05$, LSD), but not in the other lines (**Figure 5.17**). Cell wall-bound FA monomer was also lower in RNAi knock down line 22 (27% reduction), compared to null controls in leaf ($p < 0.05$, LSD, **Figure 5.16**).

There was no significant difference in *pCA* between the positive *pUbi::RNAi-GT61.9p1/p2* transformants or the *pIRX5::RNAi-GT61.9p1/p2* transformants and the null segregants. *pCA* ranged from 0.8 – 1.2 $\mu\text{g mg}^{-1}$, averaging 1.02 $\mu\text{g mg}^{-1}$ of dry weight in leaf, and from 3 – 3.6 $\mu\text{g mg}^{-1}$, averaging 3.3 $\mu\text{g mg}^{-1}$ of dry weight in stem across the transgenic lines (**Figure 5.14**, **Figure 5.16**). These data are consistent with the amounts of *pCA* in the overexpression lines (**Figure 5.11**).

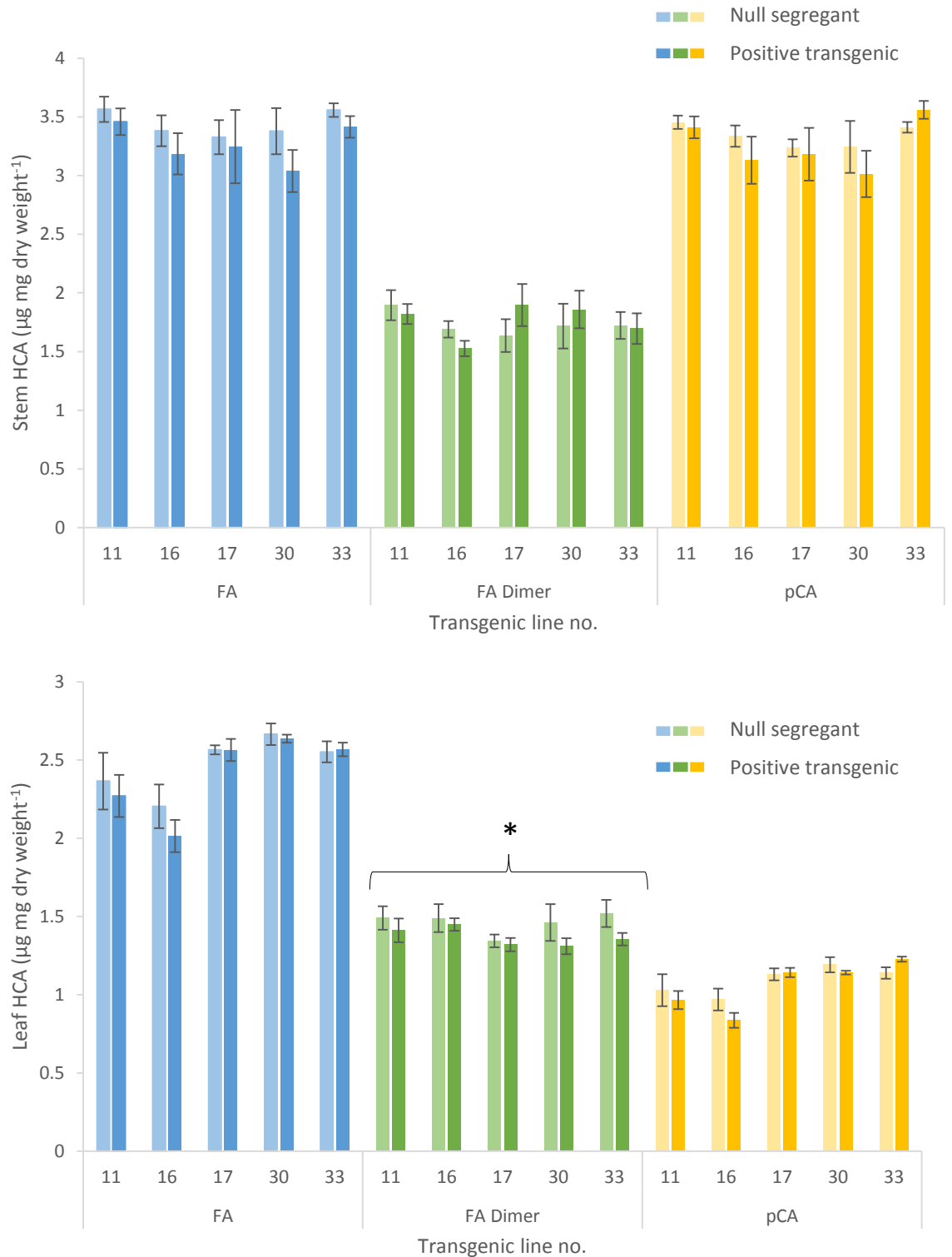


Figure 5.14 Ferulic acid (FA) monomer and dimer (\pm SE) in stem (top) and leaf (bottom) of five *Brachypodium* RNAi lines transformed with a construct designed to knock down expression of *GT61.9p1* and *GT61.9p2* simultaneously, driven by the maize ubiquitin promoter. Independent homozygous lines 11, 16, 17, 30 and 33 were analysed and transgenic plants (dark blue, dark green, dark yellow) were compared to null segregants (light blue, light green, light yellow). FA dimer includes diF8-8, diF8-5 and diF8-5 benzofuran, diF5-5 and diF8-O-4.

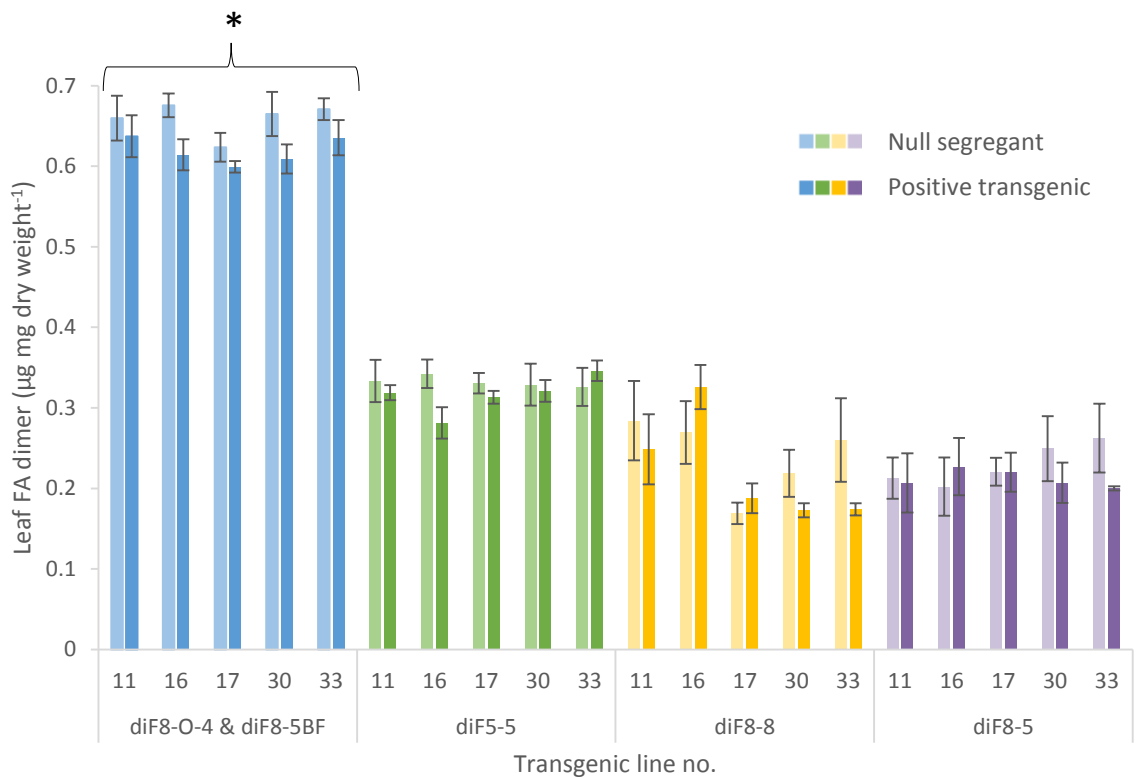
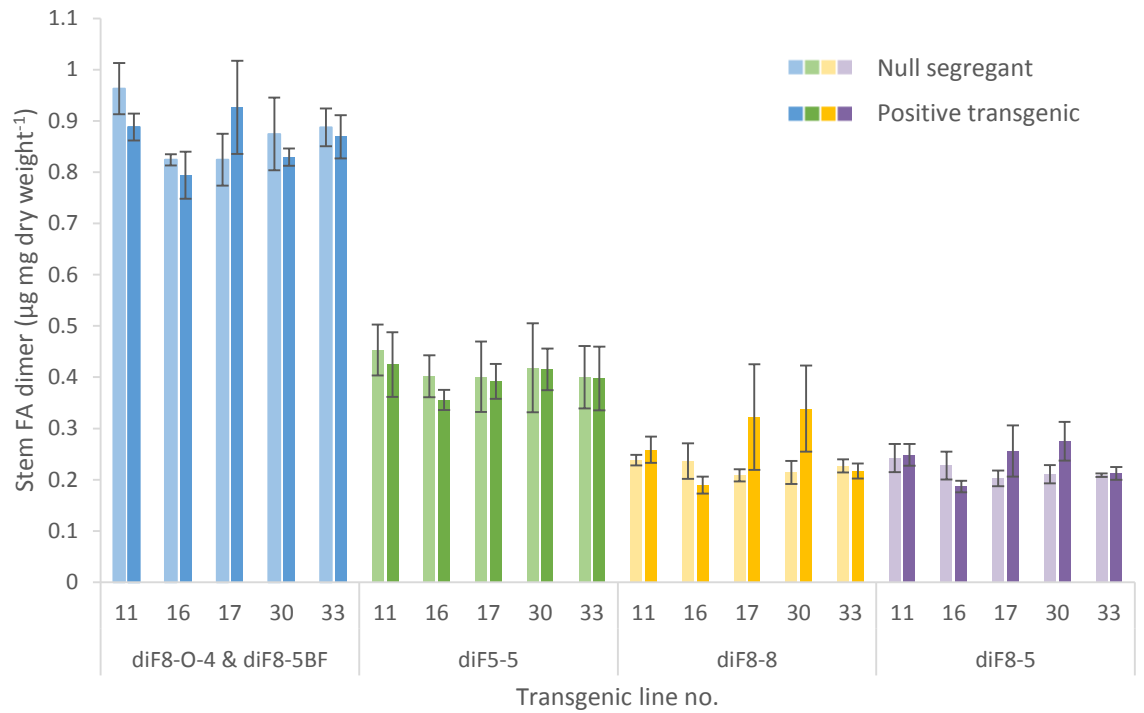


Figure 5.15 Ferulic acid dimers (\pm SE) in stem (top) and leaf (bottom) of five *Brachypodium* RNAi lines transformed with a construct designed to knock down expression of *GT61.9p1* and *GT61.9p2* simultaneously, driven by the maize ubiquitin promoter. Independent homozygous lines 11, 16, 17, 30 and 33 were analysed and transgenic plants (dark blue, dark green, dark yellow, dark purple) were compared to null segregants (light blue, light green, light yellow, light purple).

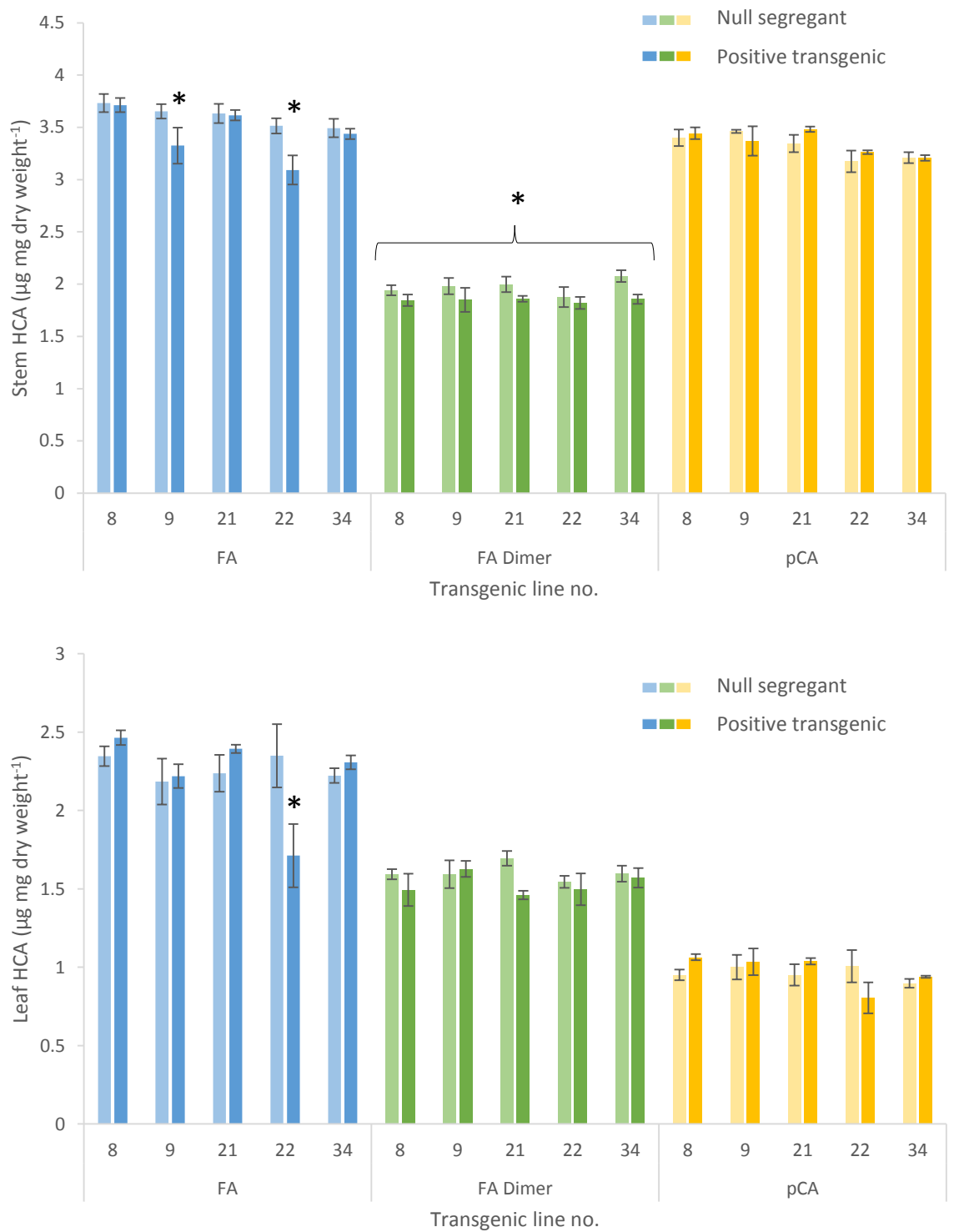


Figure 5.16 Ferulic acid (FA) monomer and dimer in leaf (top) and stem (bottom) of five *Brachypodium* RNAi lines transformed with a construct designed to knock down expression of *GT61.9p1* and *GT61.9p2* simultaneously, driven by the *IRX5* promoter. Independent homozygous lines 11, 16, 17, 30 and 33 were analysed and transgenic plants (+) were compared to null segregants (-). FA dimer includes diF8-8, diF8-5 and diF8-5 benzofuran, diF5-5 and diF8-O-4.

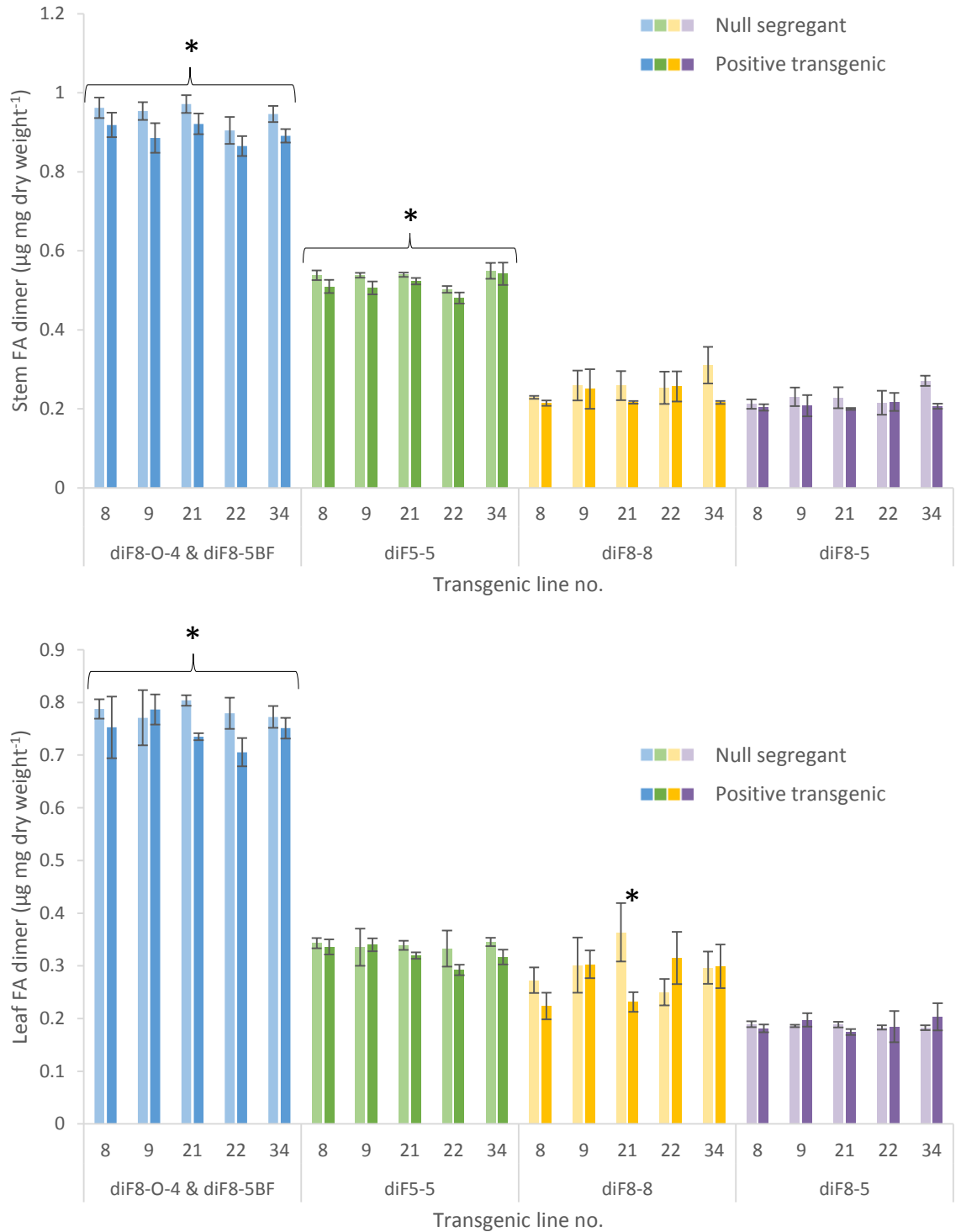
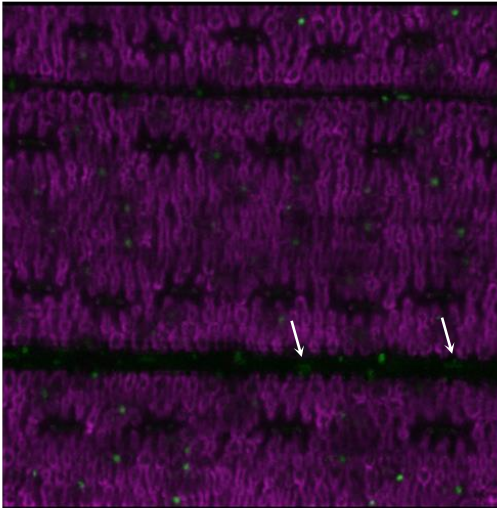


Figure 5.17 Ferulic acid dimers (\pm SE) in stem (top) and leaf (bottom) of five *Brachypodium* RNAi lines transformed with a construct designed to knock down expression of *GT61.9p1* and *GT61.9p2* simultaneously, driven by the *IRX5* promoter. Independent homozygous lines 11, 16, 17, 30 and 33 were analysed and transgenic plants (dark blue, dark green, dark yellow, dark purple) were compared to null segregants (light blue, light green, light yellow, light purple).

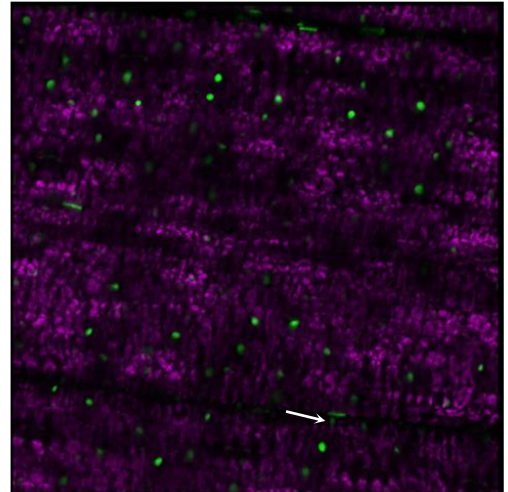
5.3.4 Expression patterns of *GT61.9p1* and *p2* in Brachypodium

Differences in expression patterns of the promoter regions (1500 bp upstream) of *GT61.9p1* and *p2* were visualised with fusion to GFP in Brachypodium. GFP was visualised using confocal microscopy. *GT61.9p2* was more highly expressed than *GT61.9p1* in 2.5 month old Brachypodium leaves. Expression of the *GT61.9p1* promoter was mainly in the vascular bundles and in some guard cells surrounding stomata, and was less in the bulliform cells. Expression of the *GT61.9p2* promoter was greater than that of *GT61.9p1* in leaf, and was expressed in many leaf cells, including all guard cells (**Figure 5.18**). In Brachypodium root, the *GT61.9p1* promoter showed expression in the top (furthest from the tip) section of the root, where GFP fluorescence was observed mostly in the epidermal layer, but not in the cortex or stele, although it is possible that GFP expression may have been present but too weak to observe in the inner root tissues (**Figure 5.19**). Expression of the *GT61.9p1* promoter ceased in the bottom (nearest the tip) one third to one quarter of the root (**Figure 5.20**, **Figure 5.21**). The *GT61.9p2* promoter showed greater expression than *GT61.9p1* in all root tissues. Expression of this promoter was observed along the full length of the root in most cells, including the epidermis, stele and cortex (**Figure 5.19**), some root hair cells (**Figure 5.20**), and the apical meristem and cap tissues at the root tip (**Figure 5.21**).

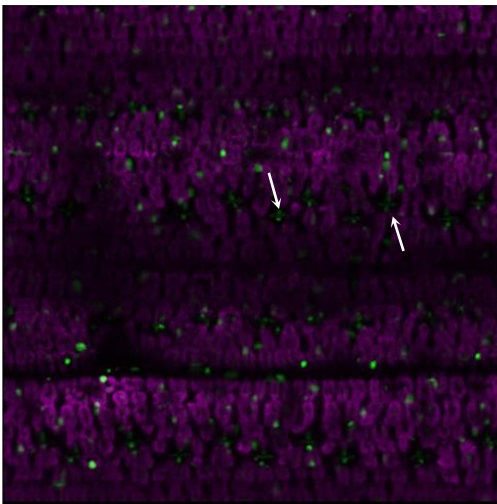
pGT61.9p1::GFP Line 1



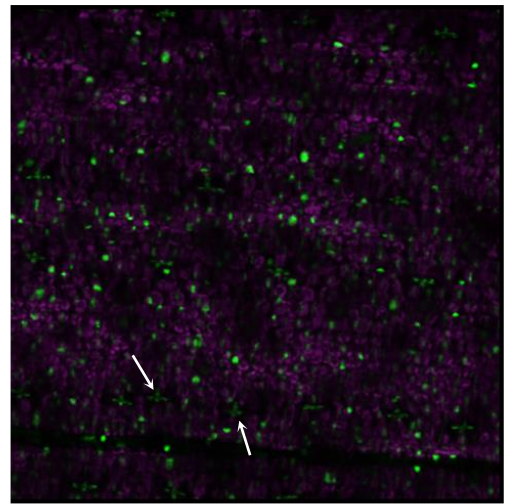
pGT61.9p1::GFP Line 2



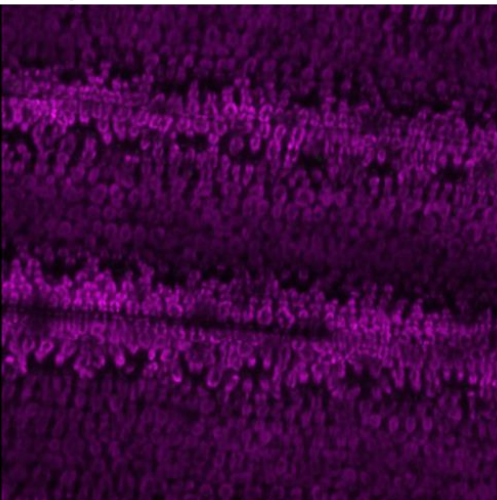
pGT61.9p2::GFP Line 1



pGT61.9p2::GFP Line 2



Negative control



Ubi::GFP

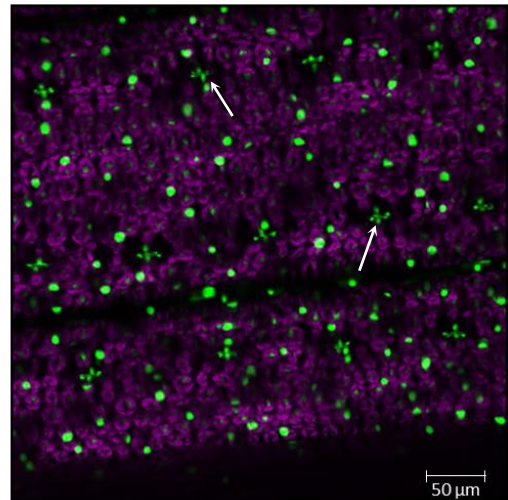
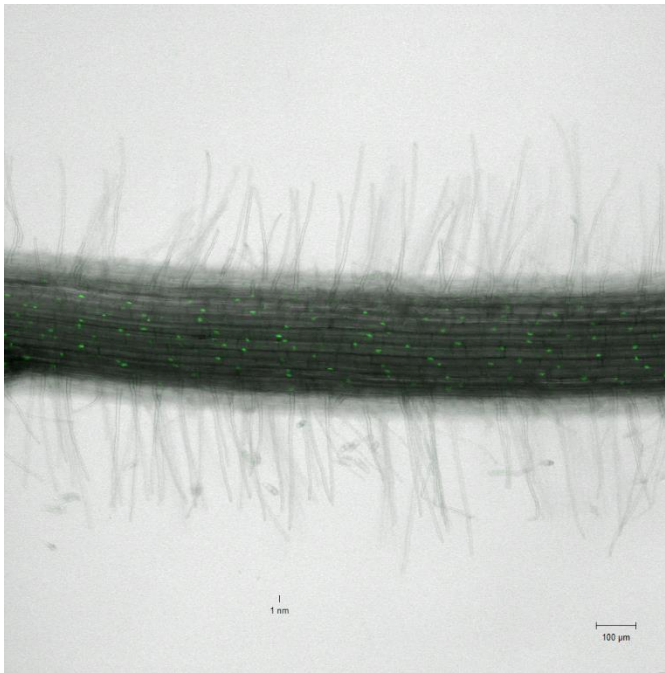
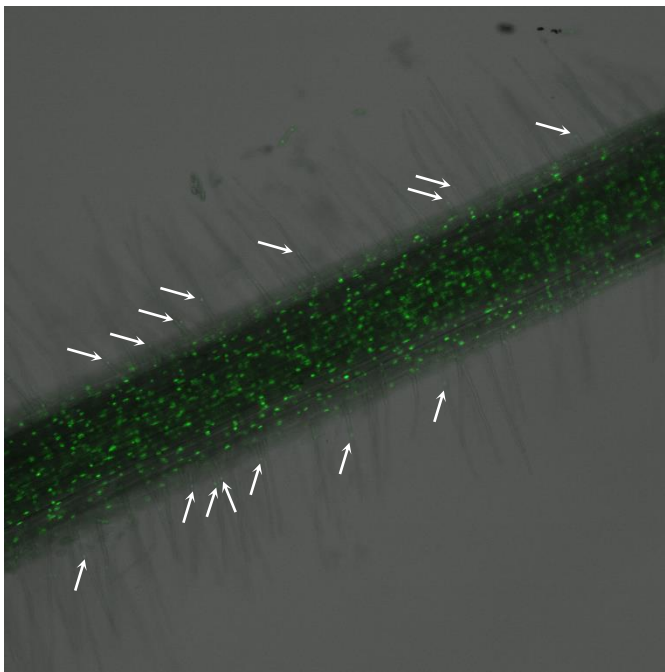


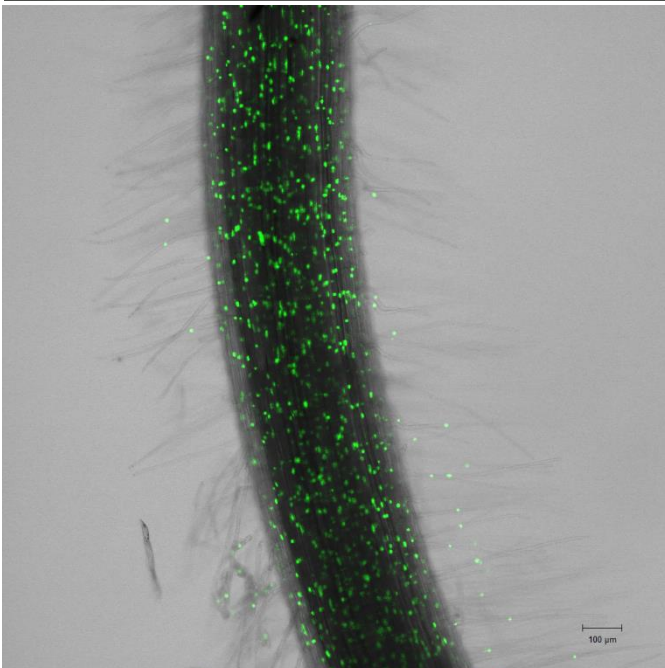
Figure 5.18 Visualisation of GFP in transgenic *Brachypodium* seedling (2.5 month old) leaves. Transgenes contain the promoter regions (1500 bp upstream of start codon) of *GT61.9* paralogue 1 (p1, *Bradi1g06560*) or paralogue 2 (*Bradi3g11337*, p2) fused to nuclear targeted GFP. Arrows point to GFP in stomatal guard cells.



pGT61.9p1::GFP

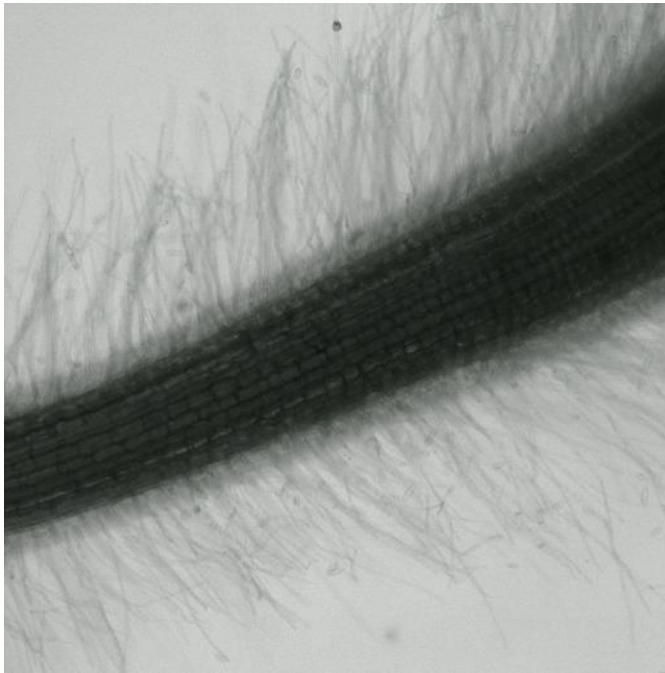


pGT61.9p2::GFP

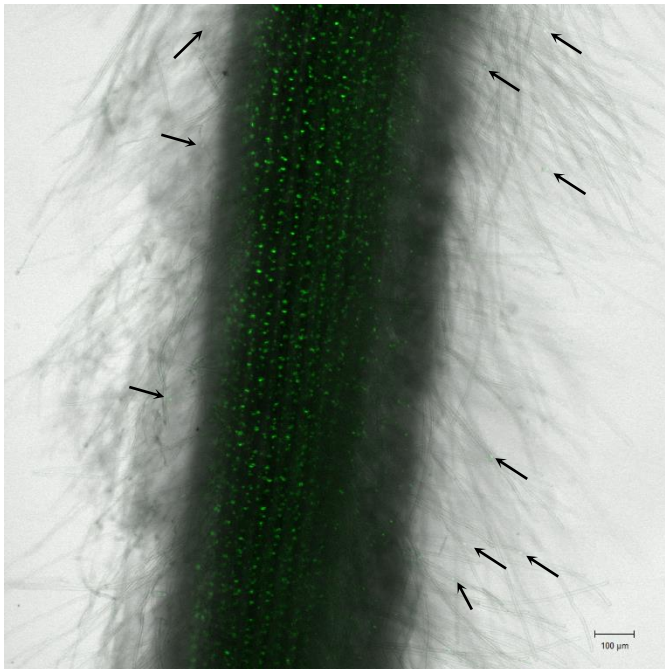


Ubi::GFP

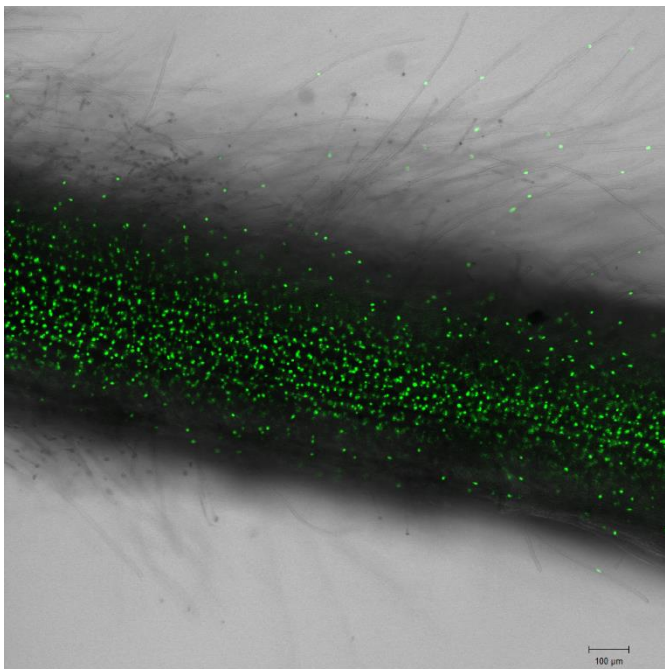
Figure 5.19 Confocal microscopy images of the middle section of the root. Differences in expression of the promoter regions (1500 bp upstream of start codon) of *GT61.9* paralogues *p1* (top) and *p2* (bottom) in Brachypodium root. Promoter regions are fused to GFP in transgenic Brachypodium, with a constitutively expressed positive control (Ubi::GFP). Arrows show expression of GFP in root hairs of pGT61.9p2::GFP. Images captured by Kirstie Halsey.



pGT61.9p1::GFP

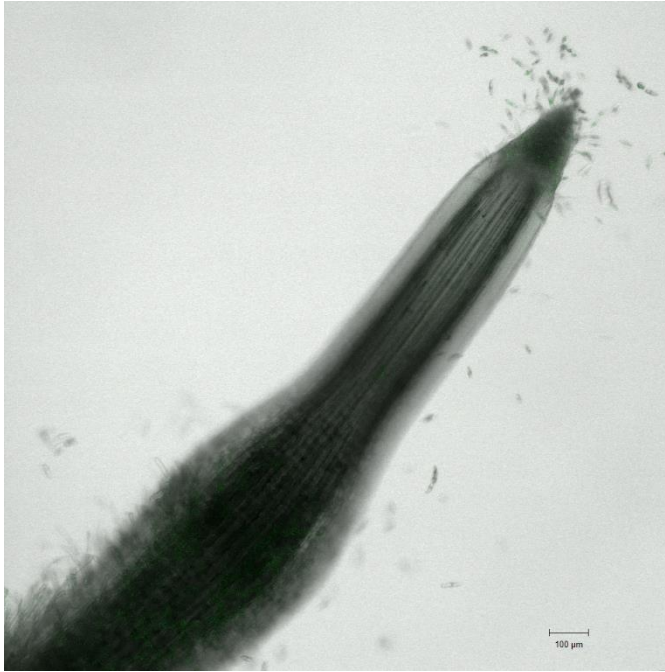


pGT61.9p2::GFP



Ubi::GFP

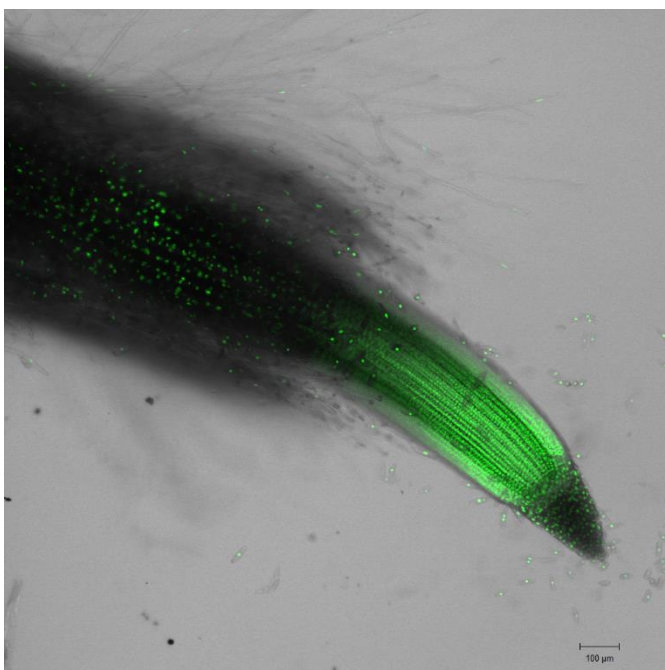
Figure 5.20 Confocal microscopy images of a section of the bottom (nearest the tip) quarter of the root. Differences in expression of the promoter regions (1500 bp upstream of start codon) of *GT61.9* paralogues *p1* (top) and *p2* (bottom) in Brachypodium root. Promoter regions are fused to GFP in transgenic Brachypodium, with a constitutively expressed positive control (Ubi::GFP). Arrows show expression of GFP in root hairs. Images captured by Kirstie Halsey.



pGT61.9p1::GFP



pGT61.9p2::GFP



Ubi::GFP

Figure 5.21 Confocal microscopy images of the root tip. Differences in expression of the promoter regions (1500 bp upstream of start codon) of *GT61.9* paralogues *p1* (top) and *p2* (bottom) in Brachypodium root. Promoter regions are fused to GFP in transgenic Brachypodium, with a constitutively expressed positive control (Ubi::GFP). Images captured by Kirstie Halsey.

5.4 Discussion

Brachypodium was successfully transformed with overexpression, RNAi and promoter-GFP fusion constructs using the Vogel and Hill (2008) transformation method, as shown by Western blot, PCR and microscopy images (**Figure 5.9**, **Figure 5.10**, **Figure 5.18**). Around 5% of calli generated viable transgenic plants, which was significantly under the 37% efficiency achieved by the original authors. This may have been dependent on a number of factors including the developmental stage of the immature embryos used to generate callus, and the environmental conditions for *Agrobacterium* infection of the callus (Vogel and Hill, 2008).

The experiments in this chapter aimed to investigate the function of GT61.9 in α -(1,3)-arabinoxyl-feruloyl transferase activity in AX synthesis in Brachypodium. Despite the successful generation of *GT61.9* overexpression lines driven by the ubiquitin promoter (**Figure 5.10**), there was no effect on total wall-bound FA or *pCA* in these lines (**Figure 5.11**), although there was a small significant increase in the diF8-8 dimer in leaves (**Figure 5.12**). It was notable that there was little variation in FA between lines, showing the reliability of the data collected from the randomised block design (**Figure 5.11**). The *GT61.9* overexpression lines that were driven by the *IRX5* promoter acquired a diseased phenotype and therefore were not further analysed. On their own, these results provide inconclusive evidence to neither support nor disprove the hypothesis that GT61.9 is an α -(1,3)-arabinoxyl-feruloyl transferase. All GT61 clade A and B proteins are predicted to be localised to the Golgi apparatus membrane; this has been shown for rice GT61 AX-synthesis proteins XAT and XAX1 (Anders et al., 2012, Chiniquy et al., 2012). One possible explanation is that GT61.9 has a limited number of specific binding sites at the Golgi membrane, and therefore excess protein may not have bound to the membrane. Secondly, it is

also possible that excess GT61.9 was recognised and degraded by the cell in a feedback mechanism. Transgenic Myc tagged protein may still have been detected by the Western blot as a mixture of transgenic and wild type protein may have been degraded and transgenic protein may have remained. Thirdly, the Myc tag may have interfered with GT61.9 enzymatic function at the active site or binding to the Golgi membrane, however this seems unlikely since C-terminal Myc tagged GT61 XAT proteins retained arabinosyl transferase activity (Anders et al., 2012).

Several cellular locations may be involved in cell wall-bound FA synthesis, including the Golgi, the cytoplasm and the cell wall, and it is possible that it is also necessary to upregulate helper proteins or transporters in conjunction with GT61.9 to induce increased cell wall-bound FA. In addition, the cellular pathway to synthesise wall-bound FA is complex, and, upstream of Golgi-bound GTs involves sugar synthesis pathways, which synthesise arabinose, and the phenylpropanoid pathway, which synthesises FA, among others. A likely explanation for lack of effect on cell wall-bound FA is therefore that, as these upstream components were not also upregulated, GT61.9 protein was increased at the Golgi membrane, but lacked sufficient arabinosyl-feruloyl substrate. In particular, it may be necessary to overexpress the BAHD acyl-transferases, which have been suggested to catalyse FA esterification to Ara in the cytoplasm (Molinari et al., 2013), in parallel with GT61.9, to induce an effect on wall-bound FA or *pCA*. In fact, upregulation of a member (*OsAT10*) of this BAHD clade was sufficient to increase amounts of *pCA* esterified to AX in rice (Bartley et al., 2013), suggesting that this may be the limiting step in the process, at least in the case of *pCA*. Notably, there was also no effect of overexpression of *GT61.9* on wall-bound sugars, including Ara (**Figure 5.13**), despite the fact that GT61 XAT proteins are responsible for addition of Ara to AX (Anders et al., 2012).

All *GT61.9p1* and *p2* RNAi knockdown lines showed moderate 5-6% decreases in cell wall-bound FA dimer in either leaf or stem compared to the null segregant controls. Where *GT61.9* suppression was driven by the ubiquitin promoter, individual FA dimers diF8-O-4 and diF8-5BF (summed due to overlapping peaks on HPLC chromatograph) were reduced in leaf (**Figure 5.15**). These individual dimers were also reduced in RNAi lines driven by the *IRX5* promoter, in both stem and leaf. In stem, diF5-5 was also significantly reduced in the *IRX5* promoter-driven RNAi lines (**Figure 5.17**). The *IRX5* promoter is secondary cell wall specific, and therefore the reduction of FA in secondary cell wall-rich stem tissue using the *IRX5* promoter, but not the ubiquitin promoter, may suggest that the reduction in FA is genuine. Further, the effects of *GT61.9* suppression on total cell wall-bound dimer were consistent across the transgenic lines. However, the reductions in FA dimer were small, and given genuine RNAi suppression of *GT61.9* genes, which was not measured, assumedly both monomer and dimer would be affected, as *GT61.9* protein would be expected to add monomeric FA to AX. Cell wall-bound FA monomer was significantly reduced by 9-27% in RNAi line (*IRX5* promoter) 9 in stem tissues, and in line 22 in stem and leaf tissues (**Figure 5.16**), which may be of interest to measure saccharification potential in these lines in future work. Taken together with the small opposite effect in increasing the diF8-8 dimer induced by over-expression, these results do provide some evidence that *GT61.9* may function in feruloylation of AX in grasses, however, the small magnitude of the effect makes it possible to interpret these as indirect consequences of altering gene expression.

These results were somewhat surprising given the marked effect of around 60% and 40% reduction of FA and *pCA* respectively in *GT61.9* knockout mutants in rice (Chiniquy et al., 2012). One possible reason for this discrepancy is the difference in experimental method between knockdown and knockout approaches. Whereas

knockout mutants completely effectively remove activity, even the best RNAi knock downs often leave some enzymatic activity of around 20%. Therefore, remaining *GT61.9* enzyme activity may have been sufficient to maintain cell wall-bound FA levels. A major drawback to testing this explanation is the lack of gene expression data for the *GT61.9* knock down lines, which was not collected due to time constraints. Assuming that *GT61.9* expression was successfully knocked down, it is further possible that, although rice and *Brachypodium* *GT61.9* genes are genetic orthologues, they may not be functional orthologues, however this seems unlikely given their sequence similarity (**Figure 5.1**). This could be investigated by complementation of the *xax1* rice mutant with the *GT61.9* overexpression constructs developed here.

Differences in expression patterns of the promoter regions were seen in leaf and root. Stem tissues were not analysed due to time constraints. The *GT61.9p2* promoter showed higher expression in leaf tissues (2.5 months old) than the *GT61.9p1* promoter, as visualised in GFP fusion transformants (**Figure 5.18**). This is in agreement with qRT-PCR data shown in **Appendix I** (Dr. Till Pellny, unpublished). Both the *GT61.9p2* and *GT61.9p1* promoters were expressed in guard cells surrounding stomata. This may be required for FA reinforcement of the cell walls in guard cells, presuming that *GT61.9* is involved in feruloylation. The *GT61.9p2* promoter also showed higher expression along the length of the root (4 days old) than *GT61.9p1*. The expression of the *GT61.9p1* promoter ceased at the root tip, and was not expressed in root hairs (**Figure 5.19, Figure 5.20, Figure 5.21**). This is in contrast with the qRT-PCR data (Dr. Till Pellny, unpublished, **Appendix I**), where *GT61.p1* expression is shown to be higher in root. However, root material was collected at 20 days after germination compared to 4 days after germination here, which may suggest that the two paralogues are differentially expressed at different

time points. These expression data provide further insight into the differential roles of *GT61.9* paralogues in Brachypodium. Other groups have previously shown that the amount of FA at the base of the root is greater than at the root tip (Locher et al., 1994), and the results presented here support this, where *GT61.9p1* and *GT61.9p2* are both expressed at the base of the root. FA is thought to decrease cell wall extensibility (MacAdam and Grabber, 2002), and therefore may be less highly expressed in the expanding cells at the root tip than at the base of the root.

In summary, the results from the overexpression and RNAi transgenic lines generated in this chapter provide some support for a role of two *GT61.9* paralogues in feruloylation in Brachypodium but were inconclusive due to the small size of effects. In addition, GFP fusion Brachypodium transformants show differential expression in leaf and root consistent with divergent roles for the two paralogues. The activity of these genes remains to be determined in future work (**Chapter 6.5**) and the transgenic lines generated here provide a useful starting point.

Chapter 6. General Discussion

6.1 Summary of results

This thesis investigated the roles of the glycosyltransferase (GT) 61 family and the Mitchell clade within the BAHD acyl transferases in the feruloylation and coumaroylation of arabinoxylan (AX) in the grasses, with particular interest in *GT61.9*.

A novel finding of this thesis was that cell wall-esterified *para*-coumaric acid (*pCA*) is dramatically induced in direct response to methyl-jasmonate (meJA) in the cell walls of *Brachypodium* callus. The results presented in **Chapter 4** report a 5-10 fold increase in cell wall-esterified *pCA* and at least a 50% increase in total cell wall-esterified FA after 2.5 weeks treatment with meJA. The finding that meJA induced increased cell wall-esterified hydroxycinnamic acids (HCAs) in callus provided a system in which to investigate the genes responsible for their synthesis on side chains of arabinoxylan (AX). The meJA induced increase in HCAs was accompanied by increased transcripts of candidate genes in the Mitchell clade within the BAHD family, and GT61 family, in response to meJA. Good candidates for involvement in the synthesis of *pCA* side chains of AX were *BAHD2p1* and *p2* and *GT61.21*; further, candidates for the synthesis of FA side chains of AX were *BAHD1*, and *GT61.5* and *GT61.10*.

An enzyme within the GT61 family, *GT61.9* (XAX1), has been characterised by previous authors as a xylosyl transferase (Chiniquy et al., 2012), however, other evidence suggests that *GT61.9* may be a feruloyl-arabinoxylan transferase (**Chapter 1.8.2**). In **Chapter 5**, *Brachypodium* was transformed with RNAi constructs designed to knock-down the expression of two *GT61.9* paralogues, resulting in a modest 4-6% decrease in FA dimers, and a 9-12% decrease in FA

monomer in some lines. The decreased FA in knock-down lines may be an indication that GT61.9 functions in FA esterification to AX, however care must be taken in interpreting these results as gene expression was not quantified due to time constraints. As the effect on cell wall-bound FA in knock-down lines was small, and overexpression of *GT61.9* did not result in increased FA monomer, nor significantly increased total dimer (although there was a small increase in leaf diF8-8), these results could not distinguish between two competing theories on the function of GT61.9. Further, the (1,2)-linked Xyl on AX side chains was not measured, and therefore the conclusions drawn by Chiniquy et al. (2012) could not be ruled out.

It was hypothesised in **Chapter 3** that mechanical stress may induce increased cell wall-bound FA due to the role of FA dimerisation in strengthening the cell wall (**Chapter 1.6.4**). There was some indication that mechanical stress induced tissue dependent increased cell wall-bound FA dimerisation in 10 week old *Brachypodium*, and also in younger plants to a greater extent. As these effects were small and inconsistent between tissues and developmental stages, this finding was not exploited further as a means of investigation into cell wall-bound FA synthesis genes. The large effects of mechanical stress on cellulose, AX and galactomannan in *Brachypodium* leaves, and in silica in leaves and stems, resulted in decreased cell wall digestibility. These findings contributed to an increased understanding of cell wall components which affect saccharification and may be of interest in second generation biofuel production or in lodging resistance applications.

6.2 BAHDs and GT61s in FA and *p*CA esterification to arabinoxylan

The BAHD and GT61 gene families have previously been implicated in the feruloylation of AX in grasses (Mitchell et al., 2007). Acyl transferases within the BAHD family of enzymes are hypothesised to catalyse the transfer of FA-CoA and

*p*CA-CoA to UDP-Araf (**Figure 1.6**). This reaction would most likely occur in the cytosol, as BAHD enzymes are localised here (D'Auria, 2006, Jackie Freeman, unpublished), as is the mutase which synthesises UDP-Araf (Konishi et al., 2007). BAHDs are likely to have high specificity for their substrate, as the enzymes from the Mitchell clade which have been characterised hitherto catalyse reactions involving *p*CA transfer, but not FA transfer (Bartley et al., 2013, Petrik et al., 2014, Withers et al., 2012). Furthermore, it is hypothesised that UDP-Ara-HCA is transported to the Golgi. At the Golgi, a GT61 enzyme may catalyse the addition of (1-3)-Ara-HCA side chains to the growing AX chain (**Figure 1.6**). There is a growing body of evidence to support this model for the feruloylation and coumaroylation of AX. GT61 enzymes are highly differently expressed in monocots and dicots (Mitchell et al., 2007). Additionally, *GT61.9* rice knock outs have approximately 50% less FA and *p*CA (Chiniquy et al., 2012), and RNAi knock-down of some genes within the BAHD family have resulted in reduced cell wall FA (Piston et al., 2010). Further, some GT61s are arabinosyl transferases (Anders et al., 2012), and are likely to therefore also be feruloyl/coumaroyl-arabinosyl transferases.

The results presented in **Chapter 4** provide some support for this model. Transcripts of genes within both the BAHD Mitchell clade and the GT61 family increased in *Brachypodium* callus when treated with meJA. This evidence supports the finding that *BAHD* and *GT61* genes are strongly coexpressed, which has previously been shown in the grasses, including in *Brachypodium* (Mitchell et al., 2007, Molinari et al., 2013). These findings are consistent with the hypothesis that these enzyme families function in the same molecular process. The most differentially expressed BAHD and GT61 genes within the Mitchell clade with meJA treatment in *Brachypodium* were *BAHD2p1* and *BAHD2p2* and *GT61.21*. This finding was correlated with a large increase in cell wall-esterified *p*CA in meJA treated callus.

Taken together, this evidence suggested that *BAHD2p1* and *p2* were the most likely candidates for the transfer of *pCA*-CoA to UDP-Ara in the cytosol, and *GT61.21* was the most likely candidate for the transfer of (1-3)-linked Ara-*pCA* side chains to AX at the Golgi, in this experiment.

AX-esterified FA is more abundant than AX-esterified *pCA* (Mueller-Harvey and Hartley, 1986); therefore, highly expressed genes within the candidate gene families are good candidates for the synthesis of FA. Out of the *GT61* and Mitchell clade *BAHD* genes that were significantly differentially expressed with meJA treatment, *GT61.5* and *BAHD1* were the most highly expressed in both the control and meJA treated samples. As FA also increased in meJA treated samples, and in the context of other evidence in support of this model, this may suggest a role for *BAHD1* in the transfer of FA-CoA to UDP-Ara-FA in the cytosol, and for *GT61.5* in the transfer of (1-3)-linked-Ara-FA side chains to AX at the Golgi in *Brachypodium* callus. The results presented in **Chapter 5** report a small decrease in cell wall-esterified FA in *GT61.9* RNAi knock-down *Brachypodium* lines. This supports a role for *GT61.9* in the transfer of (1-3)-linked-Ara-FA side chains to AX at the Golgi. It is also possible that *GT61* enzymes are non-specific for FA-Ara or *pCA*-Ara, as *xax1* (*BdGT61.9* orthologue) has decreased cell wall-bound FA and *pCA* (Chiniquy et al., 2012).

6.3 Functional redundancy with the BAHD and GT61 families

The β -(1-4)-linked AX backbone is synthesised by *IRX9/IRX9-L*, *IRX10/IRX10-L* and *IRX14/IRX14-L* and the respective pairs of genes are functionally redundant to each other (**Chapter 1.7.2**). It is therefore quite probable that there are also functionally redundant genes in AX side chain synthesis. In **Chapter 5**, there were small decreases in FA in *Brachypodium* transgenics designed to knock-down *GT61.9*; it is plausible that *GT61.9* is a feruloyl-arabinoxyl transferase and that an alternative

gene compensated for decreased GT61.9. A possible candidate for this may be the closely related GT61.10, which was upregulated in the primary cell walls of Brachypodium callus in response to meJA in **Chapter 4**. Also, *OsAt10* has been shown to be responsible for *pCA* addition to AX in rice (Bartley et al., 2013). Assumedly, the Brachypodium orthologue *BdBAHD10* has an equivalent function, although this has not been proven. *BdBAHD2p1* and *2p2* were strongly implicated in the addition of *pCA* to AX in **Chapter 4**, and therefore BAHD10, BAHD2p1 and 2p2 may have the same function.

Mortimer et al. (2015) suggested that pairs of closely related arabinoxylan synthesis genes *IRX9* and *IRX9-L*, *IRX10* and *IRX10-L*, and *IRX14* and *IRX14-L* are differently involved in primary and secondary cell wall synthesis using a callus system. *GUX* genes have also been shown to be differentially expressed in differing tissues within the stem (Lee et al., 2012). As the cell walls of callus tissue are mostly primary cell walls (Mortimer et al., 2015), it was hypothesised that *BAHD* and *GT61* genes expressed in Brachypodium callus (**Chapter 4**) may be primary cell wall specific. However, some of the identified genes are also relatively highly expressed in other tissues such as root and stem (**Appendix I**, Molinari et al., 2013), and may therefore also be important in some secondary cell wall formation. The BAHD and GT61 gene families are relatively large and the roles of each of the candidate genes for cell wall-bound FA and *pCA* synthesis within these families in differing plant tissues remains to be elucidated.

Given the importance of AX and FA in the plant cell wall, and considering that decreased xylan and FA result in severe morphological phenotypes (Brown et al., 2007, Chiniquy et al., 2012), functional redundancy within xylan, and xylan side chain, synthesis genes may be an evolutionary mechanism for protection against loss

of AX or FA. It may be required to target multiple genes to reduce FA cross-linking in grass cell walls in second generation biofuel and ruminant nutrition applications.

6.4 The difficulty in studying cell wall-bound FA and *pCA*

A portion of FA is integrally incorporated into grass cell walls through oxidatively-coupled, covalently bonded, dimers; also, FA cross-links to lignin by ether or C-C linkages in grasses (Grabber et al., 2004). The FA that is esterified to AX can be released by saponification, however, releasing ether-bonded FA is more difficult, requiring oxidation with 4 M KOH at 170 °C (Lam et al., 1990). There is no known method of reliably extracting FA cross-linked by C-C bonds and Grabber et al. (1995) estimate that approximately 60% of FA cross-linked to lignin is via C-C bonds. Alkali extractable ferulates decline in older tissues and in secondary cell walls as ether and C-C bonding increases (Grabber et al., 2004); therefore, in **Chapter 4**, the cell walls of callus, which are dominated by primary cell walls, were used to avoid this. In addition, tri- and tetraferulates may form in grass cell walls, and there is evidence that these make a major contribution to the total FA (Fry et al., 2000). Tri- and tetraferulates are difficult to measure because of the theoretical quantity of isomers. Therefore, FA is largely underestimated in grass cell walls when measuring alkali-labile FA and FA dimers. In addition, the majority of *pCA* in grass cell walls is ester-linked to lignin and remains difficult to separate from AX-esterified *pCA*. In *Brachypodium*, lignin-esterified *pCA* is four times that of AX-esterified *pCA* (Petrik et al., 2014). This difficulty was also avoided in **Chapter 4**, using a callus system which has almost no *pCA* ester linked to lignin, nor is *BdPMT* expressed in this tissue, which is responsible for the esterification of *pCA* to monolignols (Petrik et al., 2014, Withers et al., 2012).

6.5 Brachypodium as a model organism for the grasses

The work carried out in this thesis used *Brachypodium distachyon* inbred line Bd21 (Brachypodium) as a model organism for the grasses in order to study feruloylation in grass cell walls. Brachypodium proved to be a suitable model organism for this study. The short life cycle, short stature and ease of growth of the model organism were ideal for this project. In addition, the published diploid genome was advantageous in **Chapter 4**, where the newly published version 3 genome (Goodstein et al., 2012) was used as a reference in RNA sequencing analysis, and in **Chapter 5**, where it was used to obtain information on *GT61.9* genes in order to design transformation constructs. In addition, Brachypodium has a published transformation protocol (Vogel and Hill, 2008), which was used in **Chapter 5** to transform Brachypodium with overexpression and RNAi constructs. The primary cell walls of the Brachypodium callus generated using the Vogel and Hill (2008) transformation protocol also provided a useful system in order to study feruloylation and coumaroylation of cell walls in **Chapter 4**. In the future, the findings presented in this thesis in Brachypodium may be translatable to closely related, economically important crop species such as cereals, pasture grasses and bioenergy grasses.

6.6 Further work

The work presented in this thesis logically leads to a body of further work which should be undertaken in order to advance the knowledge described here. A limitation to drawing a conclusion in **Chapter 5** for the function of *GT61.9* in RNAi knock-down lines was the lack of data on expression levels of the gene due to time constraints. Therefore, quantitative-reverse transcription PCR (qRT-PCR) should be carried out to determine whether *GT61.9* gene expression was knocked down and if so, whether this correlated with the decrease in FA. Also, to distinguish between two competing

theories for the function of GT61.9 as a (1-2)-linked xylosyl side chain transferase, or alternatively a feruloyl-arabinosyl transferase, the fine structure of AX should be examined. This could be performed by enzymatic fingerprinting and further quantification by Polysaccharide Analysis using Gel Electrophoresis (PACE) as in Goubet et al. (2002), or HPAEC as in Chiniquy et al. (2012).

In **Chapter 5**, overexpression of *GT61.9* in *Brachypodium* did not induce increased FA. One possible reason for this was limited UDP-Ara-FA substrate for GT61.9 (**Figure 1.6**). As meJA was shown to induce increased FA in *Brachypodium* callus, and in enzymes in the phenylpropanoid pathway in **Chapter 4**, transforming *Brachypodium* callus with the *GT61.9* overexpression construct (**Figure 5.7**) may provide increased substrate and therefore may result in increased cell wall-esterified FA, and provide increased understanding of the function of GT61.9.

Additionally, it should be determined whether the increased *pCA* induced by meJA in **Chapter 4** is esterified to arabinoxylan or to lignin. Although mild acid hydrolysis followed by saponification of esterified phenolic acids indicated that most of the *pCA* was esterified to lignin, this should be unambiguously determined using liquid chromatography-mass spectrometry (LC-MS). Although no significant changes in cell wall-bound *pCA* were observed in *Brachypodium* in response to mechanical stress in **Chapter 3**, or in *GT61.9* transgenics in **Chapter 5**, it is possible that changes in *pCA* linked to AX occurred that were masked by the more abundant *pCA* esterified to lignin, so this technique could also be applied to these samples.

Chapter 4 highlighted a range of candidate genes for the feruloylation and coumaroylation of AX in response to meJA in *Brachypodium*. These genes could be studied further by measuring FA and *pCA* in knock out mutants. The CRISPR/Cas9 targeted genome editing approach has recently emerged as an effective method of

generating targeted mutations in plants (Jiang et al., 2013), which may be useful here.

6.7 Concluding remarks

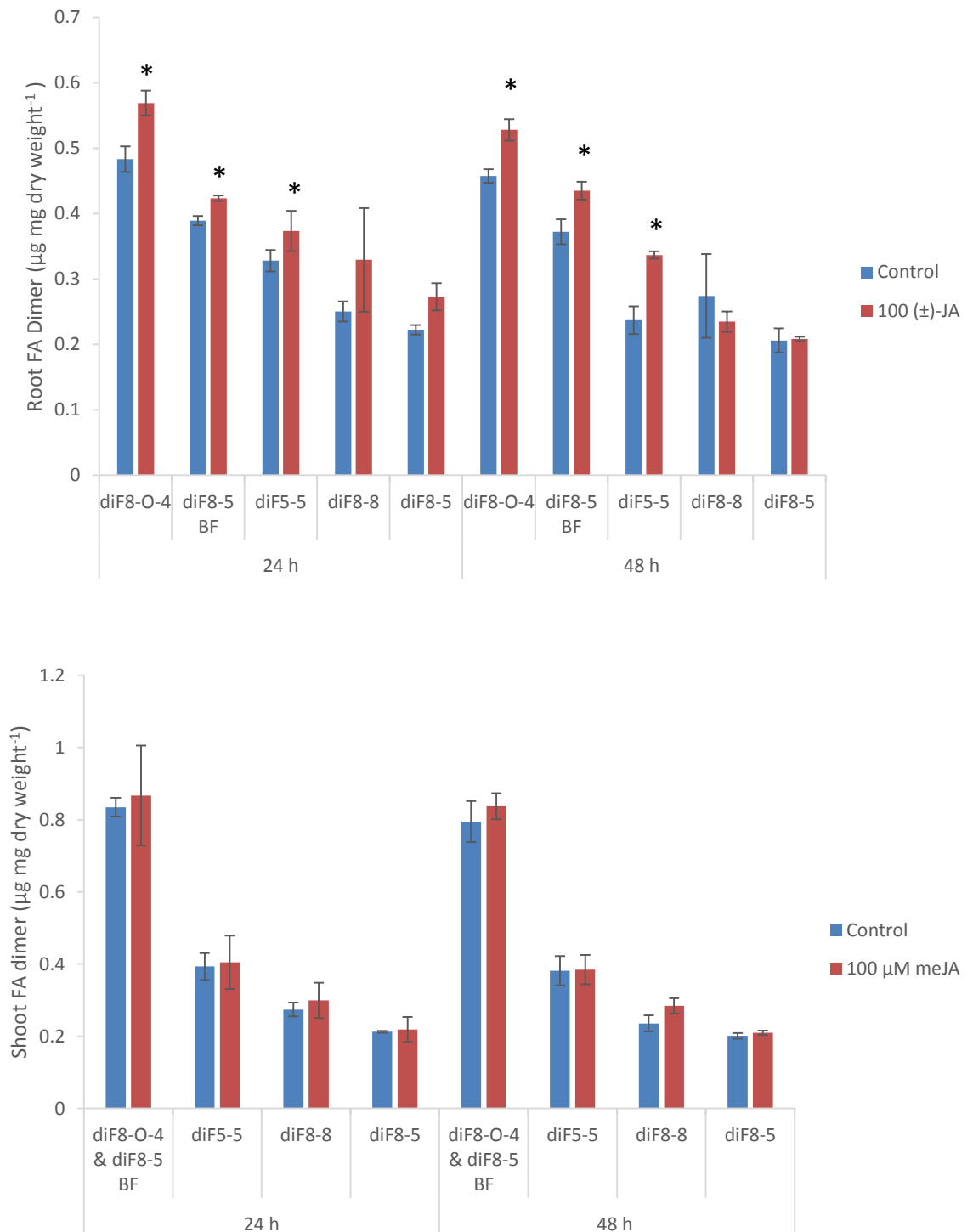
In conclusion, the results presented in this thesis enhance the existing knowledge on the genes and enzymes which may be involved in feruloylation and coumaroylation of AX. Candidate genes were identified by environmental stress, meJA treatment and transformation approaches. The candidate genes identified here could be targeted in further study. These findings may, in the future, have implications in improving the digestibility of grass cell walls for second generation biofuel and/or ruminant nutrition applications.

Appendices

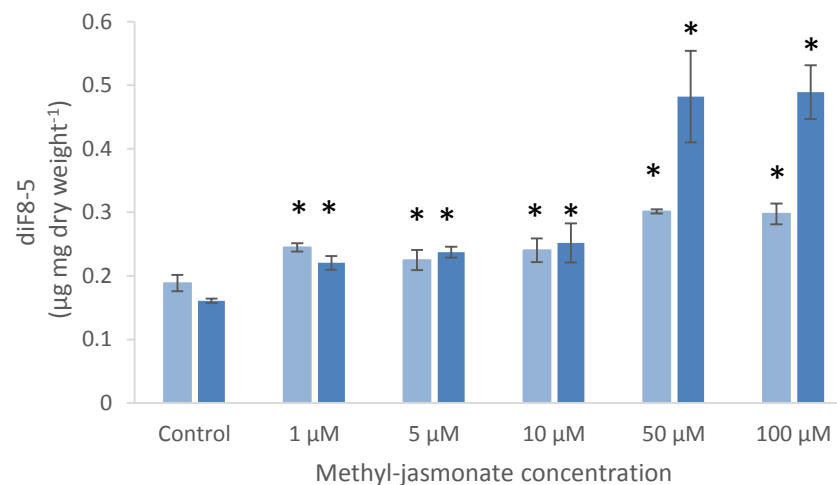
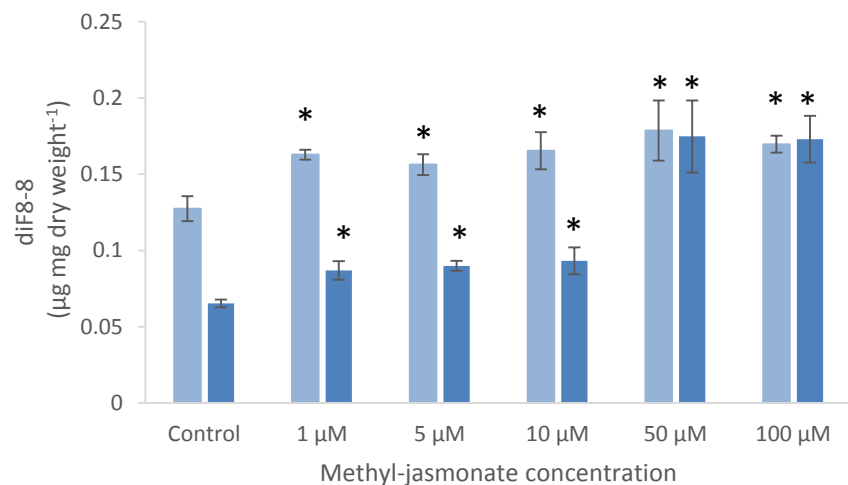
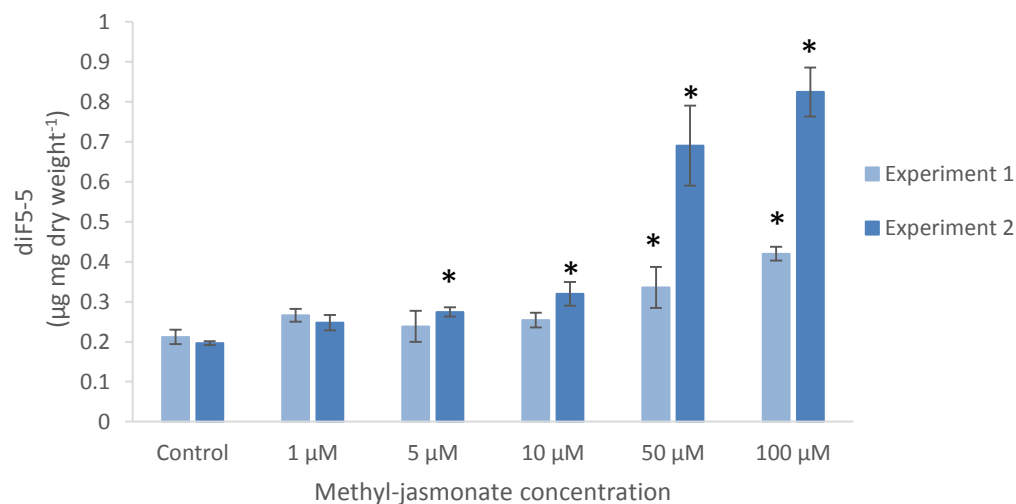
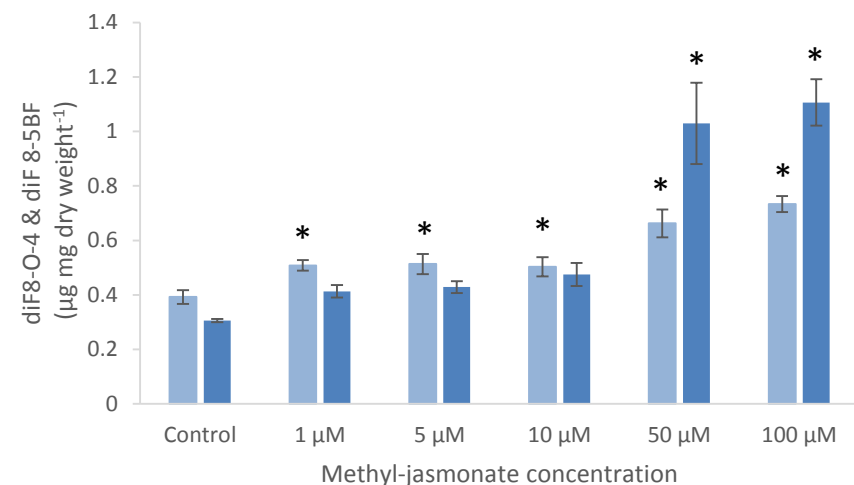
Appendix A The change in expression of genes within the GT61 and BAHD families in rice root and shoot when treated with 100 μ M (\pm)-JA for 12 h (shoot) or 6 h (root). Absolute expression and fold change (expression in JA treated samples divided by expression in control samples) are shown. Data sourced from RiceXPro (Sato et al., 2013).

MSU locus	gene family	Clade	Gene name	Root		Shoot	
				Abs cy3 signal	Fold Change	Abs cy3 signal	Fold Change
Os01g09010	BAHD Clade V	non-PMT	BAHD1	4	4	4	1.5
Os01g08380	BAHD Clade V	non-PMT	BAHD2	5	17	3	2
Os01g42870	BAHD Clade V	non-PMT	BAHD3	4	2	2	1.5
Os05g08640	BAHD Clade V	non-PMT	BAHD4	4	14	3	3
Os01g42880	BAHD Clade V	non-PMT	BAHD5	4	1.5	3	no change
Os06g39470	BAHD Clade V	non-PMT	BAHD8	3	2	2	1.5
Os01g18744	BAHD Clade V	PMT	BAHD6	4	no change	3	1.5
Os05g19910	BAHD Clade V	PMT	BAHD7	3	0.5	2	2
Os02g22650	GT family 61	A	GT61_1	3	no change	2	1.5
Os02g22480	GT family 61	A	GT61_2	1	no change	1	2
Os03g37010	GT family 61	A	GT61_3	3	1.5	low expression	1
Os01g02940	GT family 61	A	GT61_5	low expression	3	low expression	1.5
Os02g04250	GT family 61	A	GT61_7	3	2	2	3
Os02g22190	GT family 61	A	GT61_8	3	0.5	2	no change
Os02g22380	GT family 61	A	GT61_9	4	2	3	1.5
Os06g27560	GT family 61	A	GT61_10	4	2	3	2
Os06g28124	GT family 61	A	GT61_11	2	4	1	5
Os06g49320	GT family 61	A	GT61_12	3	no change	3	no change
Os10g35020	GT family 61	A	GT61_13	3	0.5	3	1.5
Os01g02920	GT family 61	A	GT61_15	1	0.5	1	1.5
Os01g02930	GT family 61	A	GT61_16	low expression	0.5	low expression	2
Os06g49300	GT family 61	A	GT61_17	low expression	0.5	low expression	2
Os04g12010	GT family 61	A	GT61_19	low expression	no change	low expression	2
Os01g02910	GT family 61	A	GT61_20	low expression	0.5	low expression	no change
Os01g02900	GT family 61	A	GT61_21	3	3.5	3	3
Os06g20570	GT family 61	A	GT61_22	low expression	0.5	low expression	0.5
Os12g13640	GT family 61	A	GT61_24	1	2.5	1	no change
Os07g46380	GT family 61	B	GT61_4	low expression	2	low expression	1.5
Os01g72610	GT family 61	B	GT61_6	3	8	2	3.5
Os05g32544	GT family 61	B	GT61_14	3	0.2	3	2
Os01g31370	GT family 61	B	GT61_18	low expression	12	low expression	3
Os11g36700	GT family 61	B	GT61_23	3	4	2	3

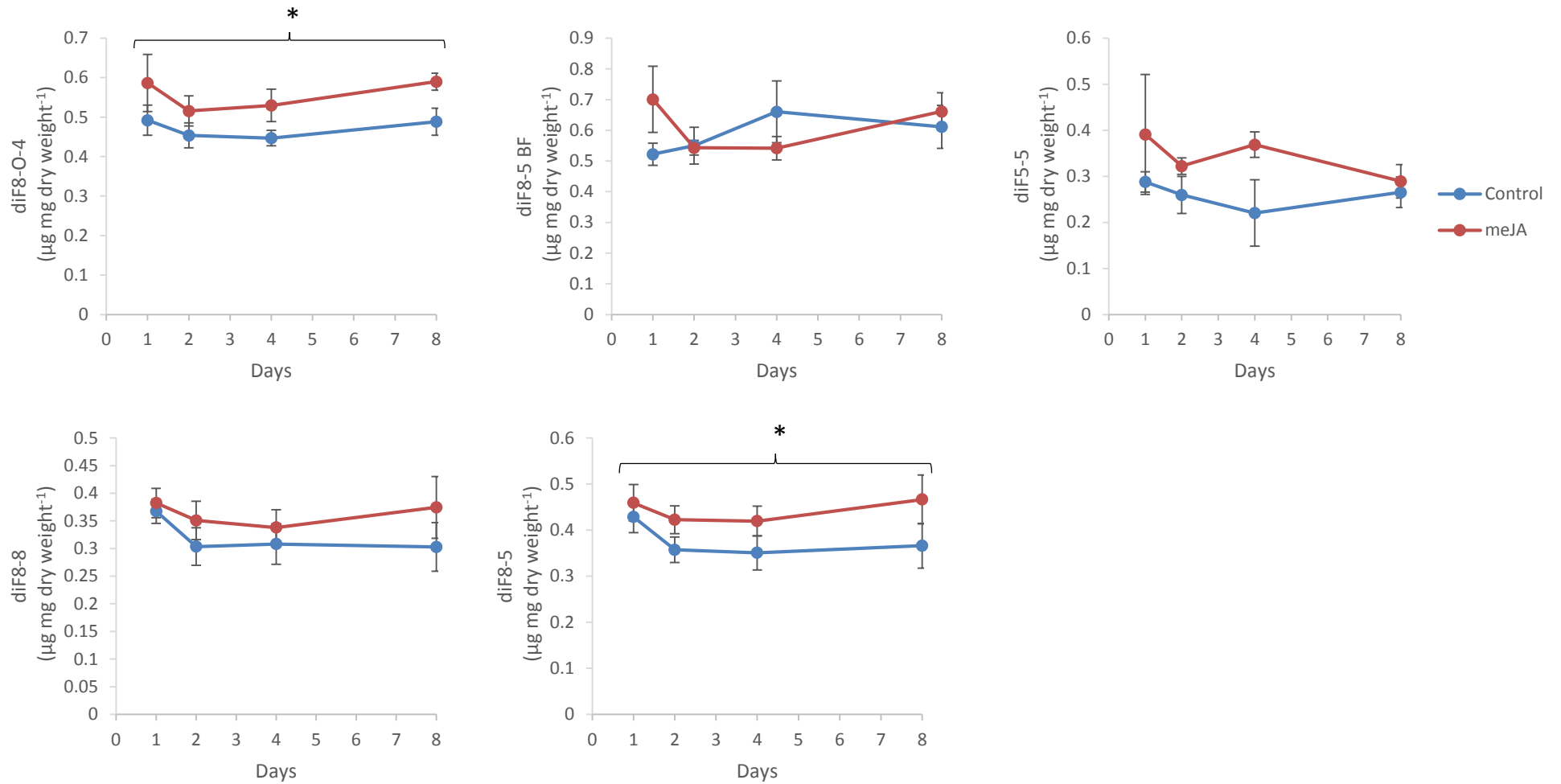
Appendix B The effect of 24 (\pm)-jasmonic acid (JA) on cell wall-bound ferulic acid dimers (\pm SE) in root (top) and shoot (bottom) of hydroponically grown *Brachypodium distachyon*. Asterisks represent statistically significant differences between control and (\pm)-JA treatment for main effect of treatment over time ($p < 0.05$, F-tests).



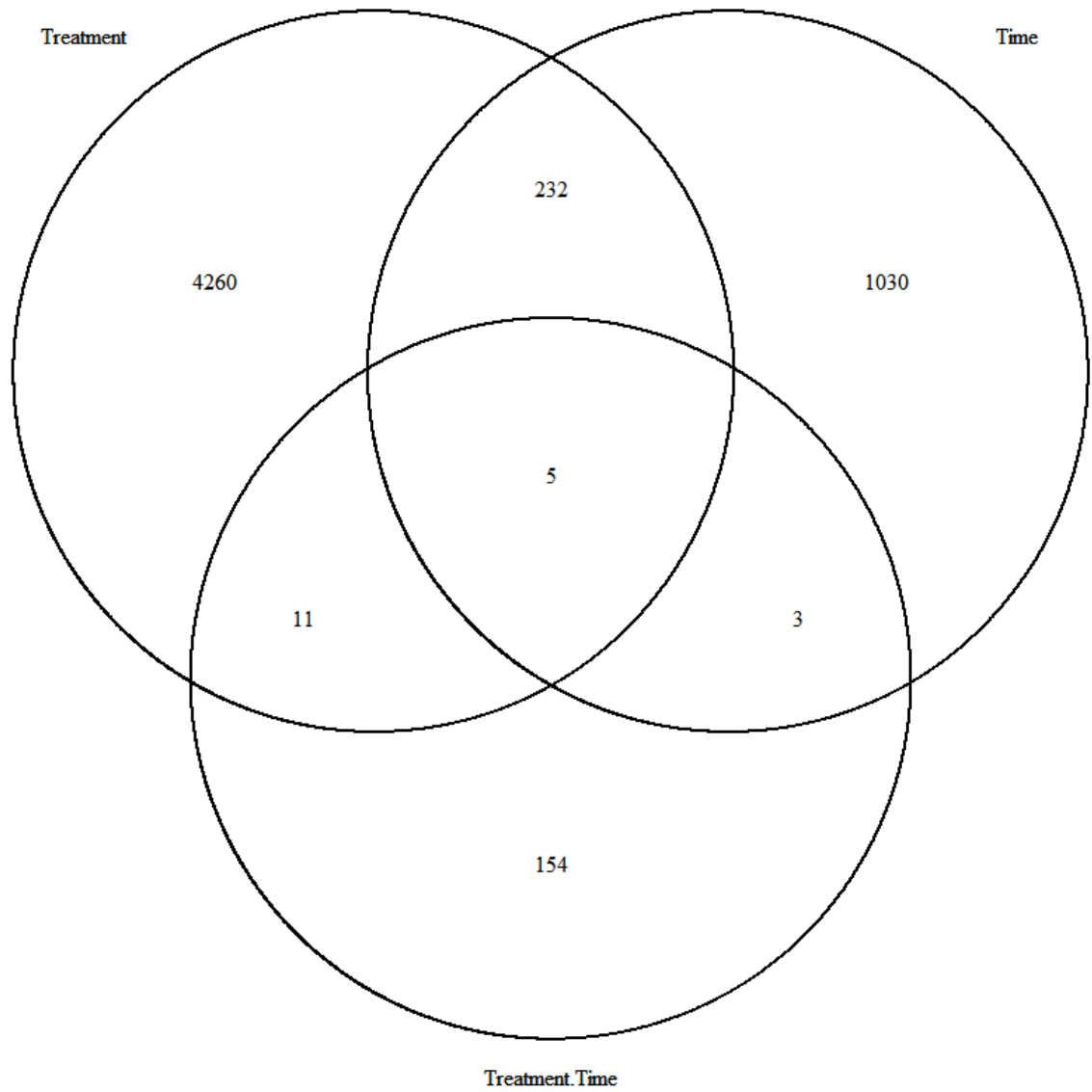
Appendix C The effect of 17 d treatment with increasing concentrations of methyl-jasmonate on individual cell wall-bound ferulic acid (F) dimer isomers (\pm SE) in *Brachypodium distachyon* callus, in two experiments. Asterisks represent statistically significant difference between meJA treated and control samples ($p < 0.05$ LSD).



Appendix D The effect of 1-8 d treatment with 50 μM methyl-jasmonate on individual cell wall-bound ferulic acid (F) dimer isomers (\pm SE) in *Brachypodium distachyon* callus (callus exp. 3). Asterisks represent statistically significant main effect of meJA treatment ($p < 0.05$, F-tests).



Appendix E Venn diagram showing counts of differentially expressed genes (DEGs) for ANOVA factors treatment (meJA), time (1-8 d) and the treatment.time interaction. Samples were treated with 50 μ M meJA or a mock control for 1, 2, 4 or 8 d.



Appendix F Changes in gene expression of statistically significant upregulated cell wall synthesis genes after 1, 2, 4 or 8 d treatment with 50 μ M meJA compared to a mock control, in *Brachypodium distachyon* callus. Fold changes are based on FPKM values from an RNAseq experiment and *p*-values (ANOVA) are corrected for FDR Benjamini-Hochberg. Candidate genes are arbitrarily numbered according to their rice orthologues, *p* = paralogue. Genes are ordered within families by average fold change over 4 time points.

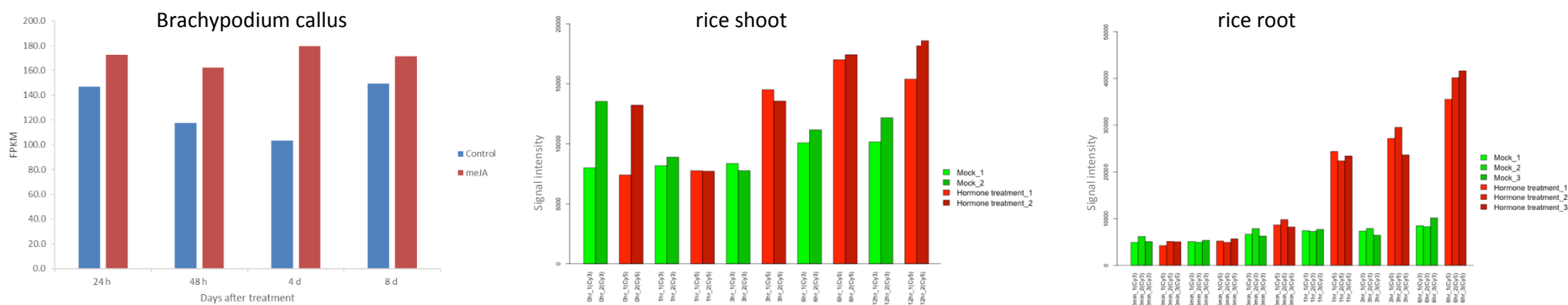
gene name	family	candidate	transcript abundance (FPKM)		24 h fold change	transcript abundance (FPKM)		48 h fold change	transcript abundance (FPKM)		4 d fold change	transcript abundance (FPKM)		8 d fold change	<i>p</i> -value
			24 h MC	24 h meJA	48 h MC	48 h meJA	4 d MC	4 d meJA	8 d MC	8 d meJA					
<i>Bradi3g37300</i>	4CL	lignin	2	9	483%	1	6	615%	1	7	594%	2	6	332%	1.03E-08
<i>Bradi2g04980</i>	BAHD2p2	BAHD Clade	0	2	774%	0	1	557%	0	1	300%	0	2	344%	2.26E-07
<i>Bradi2g04990</i>	BAHD2p1	BAHD Clade	1	6	536%	1	6	591%	1	6	422%	2	6	275%	2.49E-11
<i>Bradi2g01380</i>	GT61_21	GT family 61	0	1	458%	0	1	565%	1	1	251%	0	1	459%	1.95E-04
<i>Bradi2g58987</i>		GT family 77	1	4	386%	1	2	268%	1	2	268%	0	2	337%	4.13E-05
<i>Bradi1g15590</i>		GT family 31	0	2	423%	1	2	233%	1	2	164%	1	2	164%	7.75E-05
<i>Bradi2g23740</i>		lignin	1	2	196%	1	2	268%	1	3	184%	1	2	195%	5.52E-05
<i>Bradi1g76170</i>		lignin	14	27	197%	16	40	244%	19	35	184%	22	41	191%	1.78E-06
<i>Bradi1g34670</i>	GT61_12	GT family 61	1	2	187%	1	2	241%	1	3	183%	1	2	133%	1.45E-04
<i>Bradi2g55250</i>		lignin	3	4	127%	3	6	249%	3	7	215%	3	4	134%	2.19E-03
<i>Bradi2g33980</i>	BAHD4	BAHD Clade	21	38	176%	21	41	193%	20	40	201%	26	38	145%	2.51E-06
<i>Bradi4g04430</i>		GT family 31	3	4	132%	3	4	166%	3	7	200%	4	8	184%	6.89E-04
<i>Bradi4g27360</i>	GT61_10	GT family 61	21	31	151%	17	35	200%	19	33	172%	24	36	154%	1.33E-06
<i>Bradi2g01387</i>	GT61_15	GT family 61	26	39	151%	22	46	205%	23	39	168%	29	40	138%	2.69E-05
<i>Bradi1g76460</i>		GT family 77	4	7	151%	5	8	173%	4	7	175%	5	7	153%	2.25E-04
<i>Bradi1g35736</i>		lignin	7	12	158%	9	12	132%	9	15	166%	10	18	188%	4.98E-06
<i>Bradi2g61230</i>	GT61_6	GT family 61	3	4	135%	3	5	162%	3	5	160%	4	7	171%	3.67E-04
<i>Bradi3g16530</i>	CoMT	lignin	67	99	148%	60	110	184%	83	118	141%	94	118	125%	8.70E-05
<i>Bradi3g06480</i>	CAD	lignin	180	254	141%	163	261	160%	184	275	149%	211	311	148%	2.05E-04
<i>Bradi2g26590</i>	Gt61_14	GT family 61	13	18	132%	12	19	164%	13	19	147%	12	16	134%	4.34E-07
<i>Bradi1g01750</i>		GT family 77	30	36	123%	24	38	160%	29	42	148%	28	41	145%	5.04E-05
<i>Bradi1g64830</i>	AtGATL7	GT family 8	15	16	108%	11	18	157%	11	21	179%	13	15	120%	2.21E-04
<i>Bradi1g34550</i>		GT family 64	5	7	140%	5	6	132%	5	7	121%	5	9	170%	1.38E-03
<i>Bradi2g43510</i>	BAHD3p1	BAHD Clade	20	25	128%	18	28	155%	18	29	162%	22	25	114%	3.13E-04
<i>Bradi1g76260</i>		EXPANSIN	33	45	134%	41	50	123%	27	41	154%	31	45	146%	6.17E-03
<i>Bradi2g05480</i>	BAHD1	BAHD Clade	147	173	118%	118	162	138%	103	180	174%	149	171	115%	3.63E-03
<i>Bradi1g19160</i>	GT61_18	GT family 61	13	19	145%	15	22	150%	15	21	138%	19	19	104%	4.24E-03
<i>Bradi3g39420</i>	CCoAOMT	lignin	218	266	122%	189	274	145%	203	277	136%	203	268	132%	3.05E-04
<i>Bradi3g05750</i>	4CL	lignin	20	24	121%	14	22	153%	17	24	141%	19	23	118%	3.67E-05
<i>Bradi2g43520</i>	BAHD5	BAHD Clade	22	30	140%	21	29	138%	24	30	125%	25	30	120%	3.36E-04
<i>Bradi1g53207</i>	OsCESA6	GT family 2 CESA	12	17	133%	12	17	143%	13	15	118%	14	17	121%	2.48E-05
<i>Bradi2g34240</i>	OsCESA1	GT family 2 CESA	72	99	137%	71	101	143%	94	102	109%	90	108	121%	1.51E-05
<i>Bradi1g40997</i>		GT65R	8	11	145%	9	12	134%	8	10	122%	9	9	105%	6.40E-03
<i>Bradi2g04220</i>		GT65R	11	16	144%	10	15	149%	13	13	102%	13	14	107%	1.30E-03
<i>Bradi1g64950</i>		GT family 34	35	41	116%	29	40	135%	31	42	137%	35	39	111%	4.09E-04
<i>Bradi5g18377</i>		GT65R	22	29	135%	25	32	130%	25	29	117%	24	27	113%	1.23E-03
<i>Bradi2g37970</i>	GT43_6	GT family 43	18	23	127%	14	22	152%	19	21	111%	20	21	104%	3.72E-04
<i>Bradi5g24290</i>	GT43_5	GT family 43	31	34	108%	25	35	140%	32	41	128%	36	41	114%	6.97E-03
<i>Bradi2g01480</i>	GT61_5	GT family 61	61	70	115%	47	64	137%	53	64	122%	56	60	107%	1.71E-03
<i>Bradi2g43890</i>		GT4R	9	10	113%	8	10	127%	8	9	105%	8	10	117%	9.52E-03

Appendix G Changes in gene expression of statistically significant downregulated cell wall synthesis genes after 1, 2, 4 or 8 d treatment with 50 μ M meJA compared to a mock control, in *Brachypodium distachyon* callus. Fold changes are based on FPKM values from an RNAseq experiment and *p*-values (ANOVA) are corrected for FDR Benjamini-Hochberg. Candidate genes are arbitrarily numbered according to their rice orthologues, p = paralogue. Genes are ordered within families by average fold change over 4 time points.

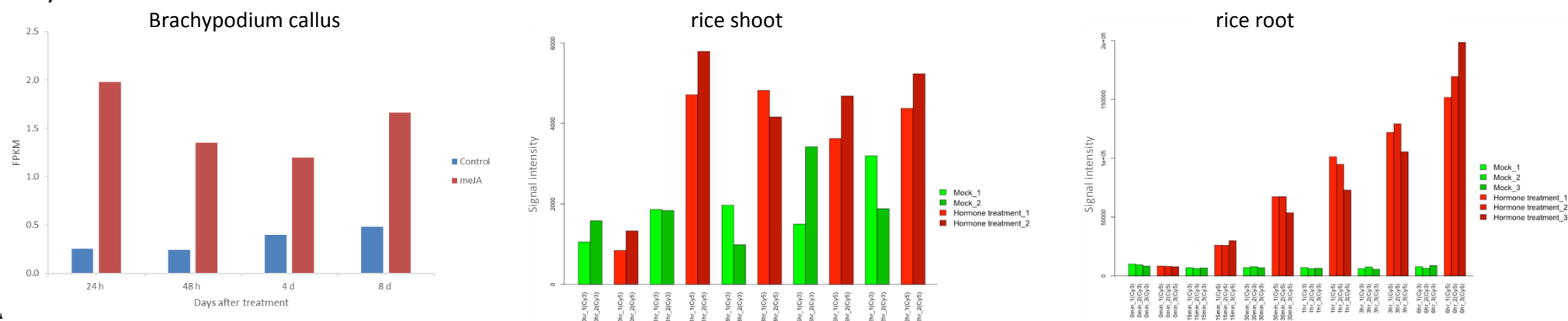
gene name	family	candidate	transcript abundance (FPKM)		24 h fold change	transcript abundance (FPKM)		48 h fold change	transcript abundance (FPKM)		4 d fold change	transcript abundance (FPKM)		8 d fold change	<i>p</i> -value
			24 h MC	24 h meJA	48 h MC	48 h meJA	4 d MC	4 d meJA	8 d MC	8 d meJA					
<i>Bradi3g14860</i>		GT family 31	19.7	15.8	80%	17.9	16.2	90%	18.8	15.1	80%	19.6	16.5	84%	7.88E-04
<i>Bradi3g14370</i>		GT family 31	3.6	3.1	87%	3.6	3.3	92%	4.0	3.0	75%	4.0	3.0	76%	6.13E-03
<i>Bradi3g25658</i>	OsCslA2	GT family 2	7.1	5.9	83%	8.4	6.5	77%	9.6	7.3	76%	8.8	6.7	77%	4.06E-03
<i>Bradi4g33090</i>	OsCslE6	GT family 2	8.3	5.7	69%	7.9	6.7	85%	8.9	5.4	61%	5.8	5.5	95%	9.73E-03
<i>Bradi2g33090</i>		GT family 31	7.0	6.0	86%	7.3	5.6	77%	7.7	4.9	64%	6.3	5.0	80%	2.23E-03
<i>Bradi3g44420</i>	GT47_16	GT family 47	36.1	31.1	86%	42.4	29.0	68%	48.6	31.2	64%	40.8	34.3	84%	5.31E-04
<i>Bradi5g10130</i>	OsCslH1	GT family 2	33.5	20.0	60%	33.6	24.8	74%	23.2	16.6	71%	21.4	16.4	77%	8.80E-03
<i>Bradi1g54620</i>		GT family 31	3.3	2.5	77%	3.3	2.4	72%	2.8	2.2	78%	3.4	1.7	51%	1.81E-03
<i>Bradi1g75450</i>	GT47_10	GT family 47	3.6	2.6	74%	3.4	2.5	74%	4.9	3.0	61%	3.9	2.6	67%	1.91E-03
<i>Bradi1g35830</i>		EXPANSIN	6.0	3.7	62%	4.3	3.6	83%	2.6	1.8	71%	3.4	1.8	55%	5.91E-03
<i>Bradi3g47480</i>		GT family 47	5.3	3.9	73%	4.6	3.3	73%	4.6	2.7	60%	4.6	2.5	55%	5.39E-03
<i>Bradi2g40460</i>		GT family 48	0.8	0.5	66%	0.7	0.5	67%	0.9	0.5	61%	0.7	0.4	51%	3.32E-04
<i>Bradi1g07890</i>		EXTENSIN	46.3	30.7	66%	42.8	23.8	56%	61.4	41.7	68%	73.5	31.3	43%	2.72E-03
<i>Bradi1g64560</i>		GT family 34	2.6	1.5	59%	1.6	1.0	61%	1.6	0.9	60%	1.4	0.7	51%	5.94E-03
<i>Bradi5g18927</i>		GT family 47	1.4	0.8	60%	1.5	0.7	47%	1.2	0.8	69%	1.0	0.6	54%	1.61E-03
<i>Bradi1g07900</i>		EXTENSIN	7.0	4.4	62%	5.2	4.3	83%	10.4	4.6	45%	10.5	3.6	35%	7.51E-04
<i>Bradi2g48710</i>	AtGAUT15	GT family 8	1.0	0.6	55%	0.8	0.3	38%	1.0	0.6	56%	1.2	0.7	57%	2.05E-03
<i>Bradi1g46037</i>		GT family 37	2.4	1.0	42%	1.7	1.1	67%	2.2	0.7	30%	1.2	0.8	64%	1.59E-03
<i>Bradi1g29515</i>		EXTENSIN	6.8	3.2	47%	4.4	2.7	61%	7.4	3.6	48%	6.4	2.4	38%	3.68E-04
<i>Bradi4g30955</i>		GT family 31	1.9	0.6	32%	1.4	0.5	37%	2.1	0.9	42%	1.4	0.8	56%	4.16E-03
<i>Bradi2g58994</i>	GT77_2	GT family 77	0.8	0.6	71%	1.2	0.6	49%	2.8	0.3	12%	2.6	0.9	34%	7.85E-06
<i>Bradi1g46030</i>		GT family 37	0.7	0.2	34%	0.6	0.3	59%	1.2	0.3	24%	1.0	0.04	4%	1.30E-03
<i>Bradi2g51360</i>		GT family 31	0.3	0.1	39%	0.5	0.1	18%	0.2	0.1	39%	0.3	0.02	7%	4.43E-03
<i>Bradi1g34647</i>		GT family 61	0.3	0.0	13%	0.2	0.1	60%	0.3	0.04	15%	0.2	0.02	13%	1.77E-03
<i>Bradi3g22875</i>		GT family 31	0.2	0.1	53%	0.4	0.1	13%	0.3	0.04	11%	0.4	0.1	16%	4.38E-03
<i>Bradi4g32160</i>		GT family 37	1.0	0.1	11%	0.9	0.1	8%	0.9	0.3	29%	0.6	0.1	23%	6.40E-05
<i>Bradi2g59017</i>	GT77_2	GT family 77	0.5	0.1	17%	0.4	0.04	9%	1.1	0.2	17%	1.1	0.2	15%	1.14E-03
<i>Bradi3g21365</i>		EXTENSIN	0.2	0.00	0.00%	0.00	0.00		0.3	0.00	0.00%	0.2	0.00	0.00%	4.36E-04

Appendix H Comparison of the effect of jasmonic acid on gene expression profiles of selected genes in *Brachypodium distachyon* callus, rice shoot and root (left to right) when treated with 50 μ M meJA for 24 h – 8 d (*Brachypodium distachyon* callus) or 100 μ M (\pm)-JA for 0 h – 12 h (rice shoot) or for 0 h – 6 h (rice root). Orthologues in *Brachypodium* and rice are a) *BAHD1*: *Bradi2g05480*, *Os01g09010*; b) *BAHD2*: *Bradi2g04980* (*BAHD2p2*), c) *Os01g08380*; *GT61_21*: *Bradi2g01380*, d) *Os01g02900*; *GT61_10*: *Bradi4g27360*, *Os06g27560*. Data obtained from RNA sequencing experiment in **Chapter 4**, or sourced from RiceXPro (Sato et al., 2013).

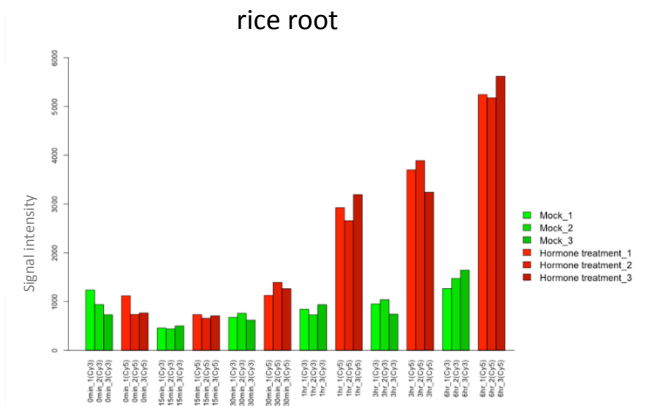
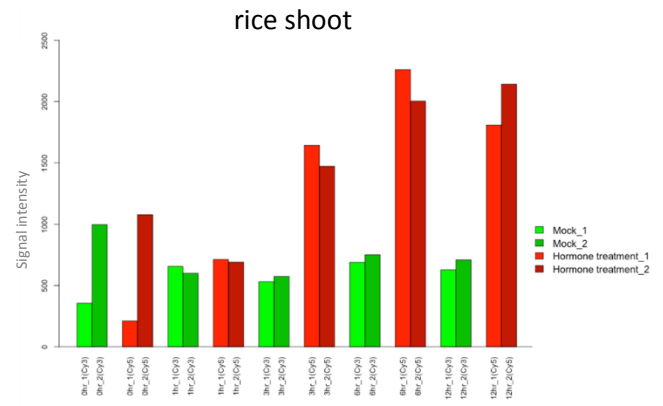
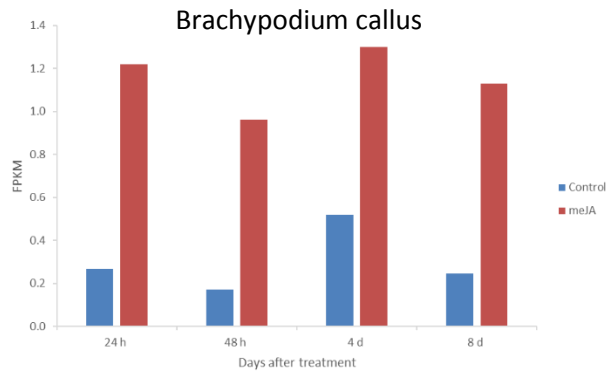
a) BAHD1



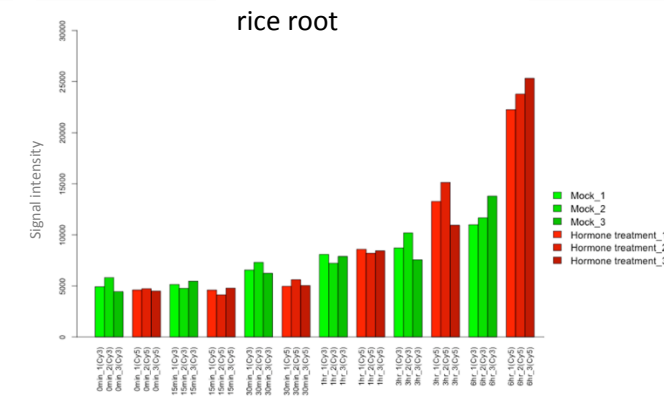
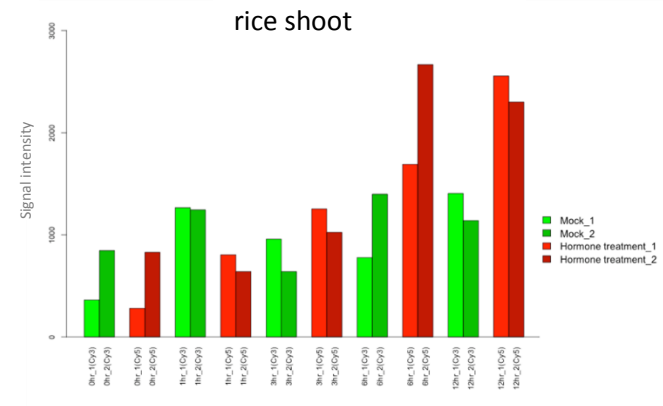
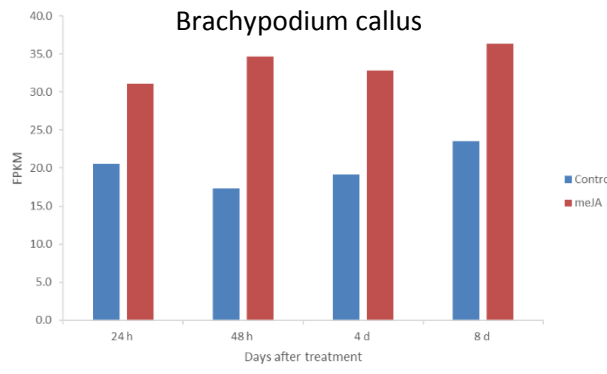
b) BAHD2



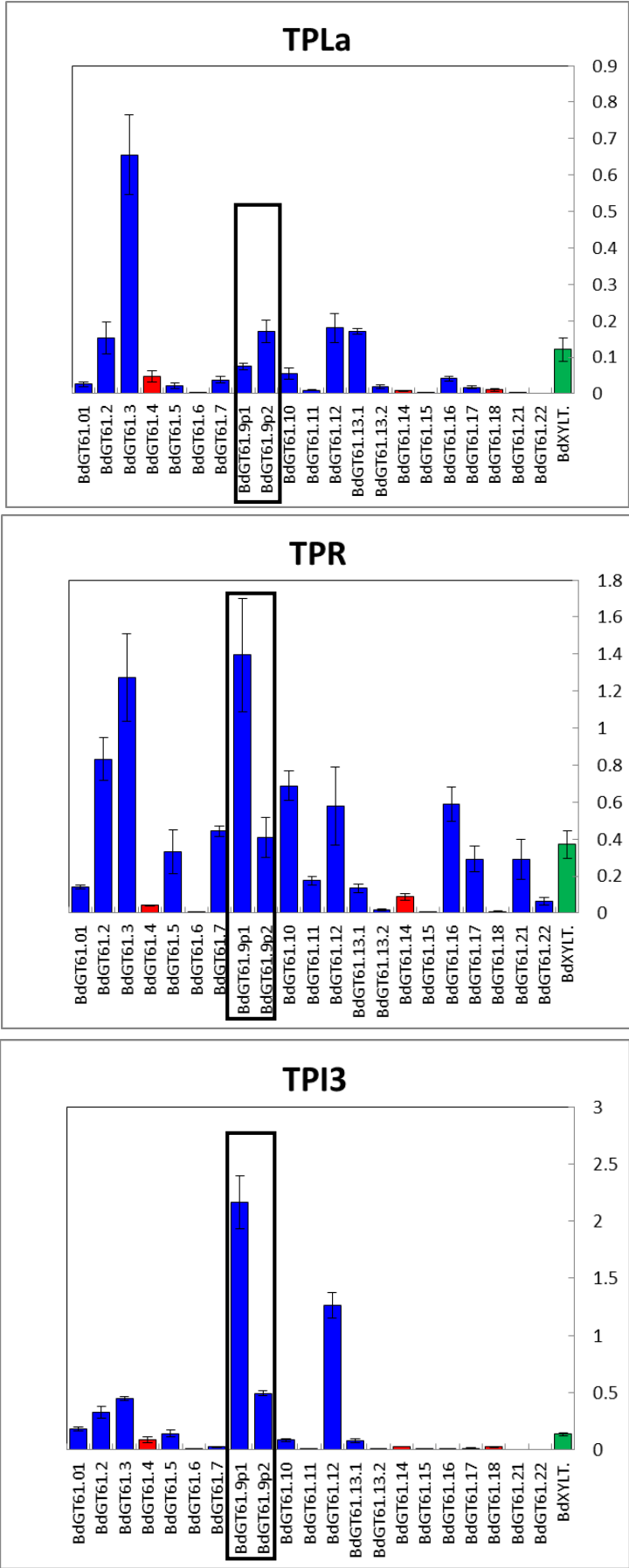
c) GT61_21



d) GT61_10



Appendix I Gene expression data highlighting the differences in gene expression of *Brachypodium distachyon* paralogues *GT61.9p1* (*Bradi1g06560*) and *p2* (*Bradi3g11337*) in TPL, TPR and TPI (transition phase (20 days after germination) leaves, roots and internodes). Samples are as described in Molinari et al. (2013), Dr. Till Pellny, unpublished data.



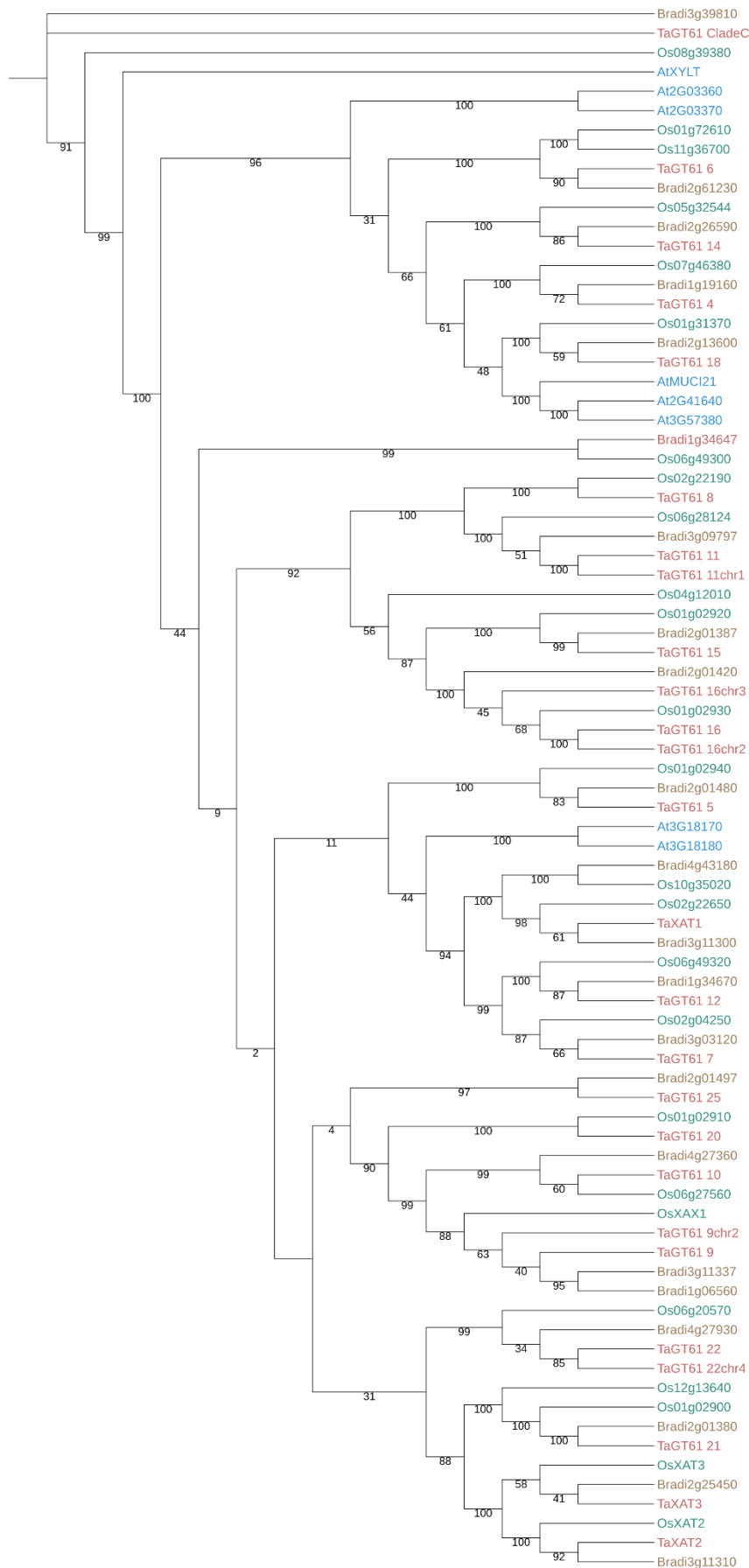
Appendix J RNAi sequence designed to simultaneously knock down the expression of *GT61.9p1* and *GT61.9p2* in *Brachypodium distachyon*. The RNAi sequence was used for transformation of *Brachypodium distachyon* in chapter 5.

```

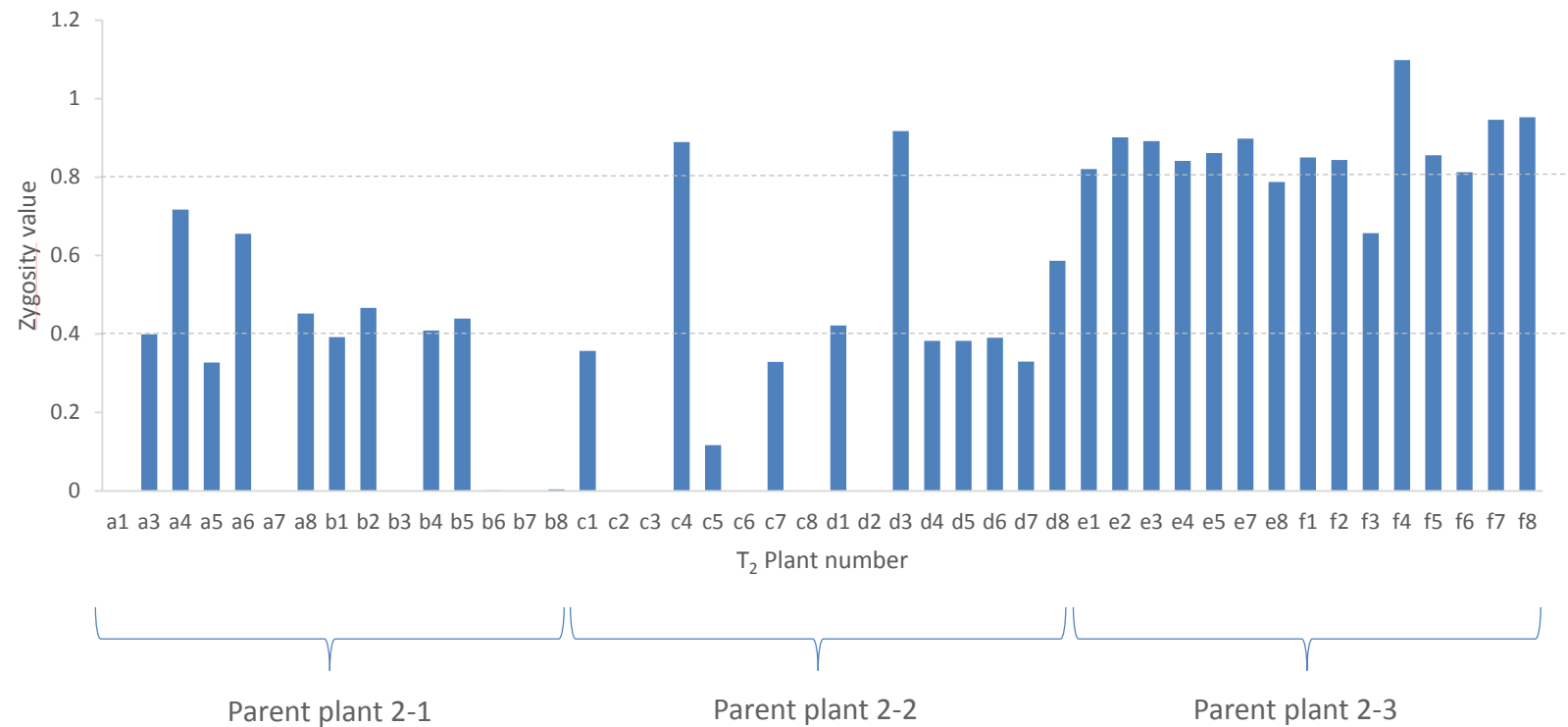
1      10      20      30      40      50
CCAAGAAGCTGGGCGCCGGCCTCCTCGCTGGCTGCTGCCTCGCGCTCCTC
60      70      80      90      100
ACCTACGTC TCCCTCGCCAAGCTCTTCGCCATCTACTCCCTGTATTTCGC
110     120     130     140     150
TAGCACGGCCAAACACGTCCGGCCTGCTGCAGAACTCCCCGCCCTCCTCCT
160     170     180     190     200
CCTCCGTGCCC GGAGACGACGGATGCCATTCCGGCCGAAGCAACA TTTGTT
210     220     230     240     250
GGCCGAAAGAACGACGACCCCGCGGCGGATCCCGTCGACTTCCCAGAGGA
260     270     280     290     300
GGGCCCGTCCATGGATGGGTCACAAGAACCCGGGTTGCCGGAGGTAGTCT
310     320     330     340     350
CGAGGAAGGAAGACGATGCAGAGAAGGCCGATCGCGGCGACCTCGCAGCCA
360     370     380     390     400
AAGCCATCTGAGGAGGATAGCGCCGCAGCCGGAGCCGGAGAGGGGACGCC
410
GCCGGCGAAG

```

Appendix K Phylogenetic tree of GT61 family genes in wheat (red), rice (green) and *Brachypodium distachyon* (brown) and *Arabidopsis thaliana* (blue) showing bootstrap values. Genes are numbered arbitrarily except characterised genes, which are named.



Appendix L An example of using qPCR to determine zygosity of T_2 generation *Brachypodium* transformants, as described in **Chapter 2.18**. Plants analysed (a1 – f8) are descendants of one independent primary transformant (line 2), and have 3 parent T_1 plants (2-1: plants a1-b8, 2-2: plants c1-d8, and 2-3: plants e1-f8). Heterozygous plants are shown with a relative zygosity value of around 0.4, and homozygous plants with a relative zygosity value of around 0.8. Null plants have a relative zygosity value of 0. Parent plants 2-1 and 2-2 are therefore segregating heterozygotes and plant 2-3 is a homozygous parent.



Definitions

4CL	4-coumarate:coenzyme A ligase
ABSL	acetyl bromide soluble lignin
AIR	alcohol insoluble residue
ANOVA	analysis of variance
Ara	arabinose
Araf	arabinofuranose
Arap	arabinopyranose
AX	arabinoxylan
BAHD	benzylalcohol acetyltransferase, anthocyanin hydroxycinnamoyl transferase, anthranilate hydroxycinnamoyl/benzoyl transferase, deacetylvindoline acetyltransferase
BF	benzofuran
bp	base pairs
BSA	bovine serum albumin
CaMV	cauliflower mosaic virus
Cas	CRISPR associated
CAD	cinnamyl alcohol dehydrogenase
CDS	coding sequence
CesA	cellulose synthase
CIM	callus initiation media
CoA	cinnamoyl CoA reductase
CoMT	caffeic acid O-methyl transferase
cpm	counts per million
CRISPR	clustered regularly interspaced short palindromic repeats
d	days
DEGs	differentially expressed genes
df	degrees of freedom
diF	ferulic acid dimer
DNA	deoxyribonucleic acid
DOE JGI	United States Department of Energy Joint Genome Institute
DTT	dithiothreitol
dw	dry weight
EDTA	Ethylenediaminetetraacetic acid

FA	ferulic acid
FPKM	fragments per kilobase of transcript per million mapped reads
<i>g</i>	g force
Gal	galactose
GalA	galacturonic acid
GAX	(glucurono)arabinoxylan
GFP	green fluorescent protein
GlcA	glucuronic acid
GO	gene ontology
GT	glycosyltransferase
GUX	glucuronic acid substitution of xylan
GX	glucuronoxylan
h	hours
HCA	hydroxycinnamic acid
hom	homozygous
HPLC	high performance liquid chromatography
hpt	hygromycin resistance gene
Ile	isoleucine
INRA	Institut National de la Recherche Agronomique
IRX	irregular xylem
JA	jasmonic acid
kDa	kilodalton
KEGG	Kyoto encyclopedia of genes and genomes
LC-MS	liquid chromatography - mass spectrometry
LSD	least significant difference
M	molar
MBTH	3-Methyl-2-benzothiazolinone hydrazone
MDS	multidimensional scaling
meGlcA	methyl glucuronic acid
meJA	methyl jasmonate
MES	2-(N-morpholino)ethanesulfonic acid
min	minute
mM	millimolar
MOPS	3-(N-morpholino)propanesulfonic acid
MS	Murashige and Skoog

NOS	nopaline synthase
PACE	polysaccharide analysis using gel electrophoresis
<i>p</i> CA	<i>para</i> -coumaric acid
PCR	polymerase chain reaction
Pfam	protein family
PMT	<i>p</i> -courmaroyl-CoA:monolignol transferase
qRT	quantitative-reverse transcription
Rha	rhamnose
RNA	ribonucleic acid
RNAi	ribonucleic acid interference
RNA-seq	ribonucleic acid sequencing
ROS	reactive oxygen species
SCF	Skp1-Cullin-F
SDS-PAGE	sodium dodecyl sulfate polyacrylamide gel electrophoresis
SE	standard error of the mean
SED	standard error of the difference between two means
Sm	streptomycin
Sp	spectinomycin
TAE	tris-acetate-EDTA
T-DNA	transfer deoxyribonucleic acid
TFA	trifluoroacetic acid
TILLING	targeting induced local lesions in genomes
TTBS	tris tween buffered saline
Ubi	ubiquitin
UDP	uridine diphosphate
UPLC	ultra performance liquid chromatography
v/v	volume/volume
w/v	weight/volume
XAT	xylan arabinosyl transferase
XAX	xylosyl arabinosyl substitution of xylan
Xyl	xylose
XylT	xylosyl transferase

Abbreviations included in the International System of Units are not listed

References

- ALLERDINGS, E., RALPH, J., SCHATZ, P. F., GNIECHWITZ, D., STEINHART, H. & BUNZEL, M. 2005. Isolation and structural identification of di-arabinosyl 8-O-4-dehydrodiferulate from maize bran insoluble fibre. *Phytochemistry*, 66, 113-124.
- ALMAGRO, L., ROS, L. V. G., BELCHI-NAVARRO, S., BRU, R., BARCELO, A. R. & PEDRENO, M. A. 2009. Class III peroxidases in plant defence reactions. *Journal of Experimental Botany* 60, 377-390.
- ANDERS, N., WILKINSON, M. D., LOVEGROVE, A., FREEMAN, J., TRYFONA, T., PELLNY, T. K., WEIMAR, T., MORTIMER, J. C., STOTT, K., BAKER, J. M., DEFOIN-PLATEL, M., SHEWRY, P. R., DUPREE, P. & MITCHELL, R. A. C. 2012. Glycosyl transferases in family 61 mediate arabinofuranosyl transfer onto xylan in grasses. *Proceedings of the National Academy of Sciences of the United States of America*, 109, 989-93.
- ANDERSSON-GUNNERAS, S., MELLEROWICZ, E. J., LOVE, J., SEGERMAN, B., OHMIYA, Y., COUTINHO, P. M., NILSSON, P., HENRISSAT, B., MORITZ, T. & SUNDBERG, B. 2006. Biosynthesis of cellulose-enriched tension wood in *Populus*: global analysis of transcripts and metabolites identifies biochemical and developmental regulators in secondary wall biosynthesis. *Plant Journal*, 45, 144-165.
- APG IV (ANGIOSPERM PHYLOGENY GROUP IV), BYNG, J. W., CHASE, M. W., CHRISTENHUSZ, M. J. M., FAY, M. F., JUDD, W. S., MABBERLEY, D. J., SENNIKOV, A. N., SOLTIS, D. E., SOLTIS, P. S., STEVENS, P. F., BRIGGS, B., BROCKINGTON, S., CHAUTEMS, A., CLARK, J. C., CONRAN, J., HASTON, E., MOLLER, M., MOORE, M., OLMSTEAD, R., PERRET, M., SKOG, L., SMITH, J., TANK, D., VORONTSOVA, M. & WEBER, A. 2016. An update of the Angiosperm Phylogeny Group classification for the orders and families of flowering plants: APG IV. *Botanical Journal of the Linnean Society*, 181, 1-20.
- ASHBURNER, M., BALL, C. A., BLAKE, J. A., BOTSTEIN, D., BUTLER, H., CHERRY, J. M., DAVIS, A. P., DOLINSKI, K., DWIGHT, S. S., EPPIG, J. T., HARRIS, M. A., HILL, D. P., ISSEL-TARVER, L., KASARSKIS, A., LEWIS, S., MATESE, J. C., RICHARDSON, J. E., RINGWALD, M., RUBIN, G. M. & SHERLOCK, G. 2000. Gene Ontology: tool for the unification of biology. *Nature Genetics*, 25, 25-29.
- AVANCI, N. C., LUCHE, D. D., GOLDMAN, G. H. & GOLDMAN, M. H. S. 2010. Jasmonates are phytohormones with multiple functions, including plant defense and reproduction. *Genetics and Molecular Research*, 9, 484-505.
- BACIC, A., HARRIS, P. J. & STONE, B. A. 1988. Structure and function of plant cell walls. In: PREISS, J. (ed.) *The Biochemistry of Plants*. San Diego, California: Academic Press, Inc.
- BACIC, A. & STONE, B. A. 1981. Chemistry and organization of aleurone cell wall components from wheat and barley. *Australian Journal of Plant Physiology*, 8, 475-495.
- BARRIERE, Y., MECHIN, V., LEFEVRE, B. & MALTESE, S. 2012. QTLs for agronomic and cell wall traits in a maize RIL progeny derived from a cross

between an old Minnesota13 line and a modern Iodent line. *Theoretical and Applied Genetics*, 125, 531-549.

- BARTLEY, L. E., PECK, M. L., KIM, S. R., EBERT, B., MANISSERI, C., CHINIQUEY, D. M., SYKES, R., GAO, L. F., RAUTENGARTEN, C., VEGASANCHEZ, M. E., BENKE, P. I., CANLAS, P. E., CAO, P. J., BREWER, S., LIN, F., SMITH, W. L., ZHANG, X. H., KEASLING, J. D., JENTOFF, R. E., FOSTER, S. B., ZHOU, J. Z., ZIEBELL, A., AN, G., SCHELLER, H. V. & RONALD, P. C. 2013. Overexpression of a BAHD acyltransferase, *OsAt10*, alters rice cell wall hydroxycinnamic acid content and saccharification. *Plant Physiology*, 161, 1615-1633.
- BENCUR, P., STEINKELLNER, H., SVOBODA, B., MUCHA, J., STRASSER, R., KOLARICH, D., HANN, S., KOLLENSPERGER, G., GLOSSL, J., ALTMANN, F. & MACH, L. 2005. *Arabidopsis thaliana* 81,2-xylosyltransferase: an unusual glycosyltransferase with the potential to act at multiple stages of the plant N-glycosylation pathway. *Biochemical Journal*, 388, 515-525.
- BERRY, P. M., STERLING, M., SPINK, J. H., BAKER, C. J., SYLVESTER-BRADLEY, R., MOONEY, S. J., TAMS, A. R. & ENNOS, A. R. 2004. Understanding and reducing lodging in cereals. *Advances in Agronomy*, 84, 217-271.
- BIDDINGTON, N. L. 1986. The effects of mechanically-induced stress in plants - a review. *Plant Growth Regulation*, 4, 103-123.
- BILY, A. C., REID, L. M., TAYLOR, J. H., JOHNSTON, D., MALOUIN, C., BURT, A. J., BAKAN, B., REGNAULT-ROGER, C., PAULS, K. P., ARNASON, J. T. & PHILOGENE, B. J. R. 2003. Dehydrodimers of ferulic acid in maize grain pericarp and aleurone: resistance factors to *Fusarium graminearum*. *Phytopathology*, 93, 712-719.
- BIRO, L. R. & JAFFE, M. J. 1984. Thigmomorphogenesis: ethylene evolution and its role in the changes observed in mechanically perturbed bean plants. *Physiologia Plantarum*, 62, 289-296.
- BOERJAN, W., RALPH, J. & BAUCHER, M. 2003. Lignin biosynthesis. *Annual Review of Plant Biology*, 54, 519-546.
- BRAAM, J. 2005. In touch: plant responses to mechanical stimuli. *New Phytologist*, 165, 373-389.
- BRAAM, J. & DAVIS, R. W. 1990. Rain-induced, wind-induced, and touch-induced expression of calmodulin and calmodulin-related genes in *Arabidopsis*. *Cell*, 60, 357-364.
- BRKLJACIC, J., GROTEWOLD, E., SCHOLL, R., MOCKLER, T., GARVIN, D. F., VAIN, P., BRUTNELL, T., SIBOUT, R., BEVAN, M., BUDAK, H., CAICEDO, A. L., GAO, C. X., GU, Y., HAZEN, S. P., HOLT, B. F., HONG, S. Y., JORDAN, M., MANZANEDA, A. J., MITCHELL-OLDS, T., MOCHIDA, K., MUR, L. A. J., PARK, C. M., SEDBROOK, J., WATT, M., ZHENG, S. J. & VOGEL, J. P. 2011. Brachypodium as a model for the grasses: today and the future. *Plant Physiology*, 157, 3-13.
- BROMLEY, J. R., BUSSE-WICHER, M., TRYFONA, T., MORTIMER, J. C., ZHANG, Z. N., BROWN, D. M. & DUPREE, P. 2013. GUX1 and GUX2 glucuronyltransferases decorate distinct domains of glucuronoxylan with different substitution patterns. *Plant Journal*, 74, 423-434.

- BROWN, D., WIGHTMAN, R., ZHANG, Z. N., GOMEZ, L. D., ATANASSOV, I., BUKOWSKI, J. P., TRYFONA, T., MCQUEEN-MASON, S. J., DUPREE, P. & TURNER, S. 2011. Arabidopsis genes *IRREGULAR XYLEM (IRX15)* and *IRX15L* encode DUF579-containing proteins that are essential for normal xylan deposition in the secondary cell wall. *Plant Journal*, 66, 401-413.
- BROWN, D. M., GOUBET, F., VICKY, W. W. A., GOODACRE, R., STEPHENS, E., DUPREE, P. & TURNER, S. R. 2007. Comparison of five xylan synthesis mutants reveals new insight into the mechanisms of xylan synthesis. *Plant Journal*, 52, 1154-1168.
- BROWN, D. M., ZHANG, Z. N., STEPHENS, E., DUPREE, P. & TURNER, S. R. 2009. Characterization of IRX10 and IRX10-like reveals an essential role in glucuronoxylan biosynthesis in Arabidopsis. *Plant Journal*, 57, 732-746.
- BROWN, S. A. 1966. Lignins. *Annual Review of Plant Physiology*, 17, 223-244.
- BUANAFINA, M. M. O. 2009. Feruloylation in grasses: current and future perspectives. *Mol Plant*, 2, 861-72.
- BUANAFINA, M. M. O., FESCEMYER, H. W., SHARMA, M. & SHEARER, E. A. 2016. Functional testing of a PF02458 homologue of putative rice arabinoxylan feruloyl transferase genes in *Brachypodium distachyon*. *Planta*, 243, 659-674.
- BUNZEL, M. 2010. Chemistry and occurrence of hydroxycinnamate oligomers. *Phytochemistry Reviews*, 9, 47-64.
- BUNZEL, M., ALLERDINGS, E., SINWELL, V., RALPH, J. & STEINHART, H. 2002. Cell wall hydroxycinnamates in wild rice (*Zizania aquatica* L.) insoluble dietary fibre. *European Food Research and Technology*, 214, 482-488.
- BUNZEL, M., RALPH, J., BRUNING, P. & STEINHART, H. 2006. Structural identification of dehydrotriferulic and dehydrotetraferulic acids isolated from insoluble maize bran fiber. *Journal of Agricultural and Food Chemistry*, 54, 6409-6418.
- BUNZEL, M., RALPH, J., KIM, H., LU, F. C., RALPH, S. A., MARITA, J. M., HATFIELD, R. D. & STEINHART, H. 2003. Sinapate dehydrodimers and sinapate-ferulate heterodimers in cereal dietary fiber. *Journal of Agricultural and Food Chemistry*, 51, 1427-1434.
- BUNZEL, M., RALPH, J., MARITA, J. & STEINHART, H. 2000. Identification of 4-O-5'-coupled diferulic acid from insoluble cereal fiber. *Journal of Agricultural and Food Chemistry*, 48, 3166-3169.
- BURR, S. J. & FRY, S. C. 2009. Feruloylated arabinoxylans are oxidatively cross-linked by extracellular maize peroxidase but not by horseradish peroxidase. *Molecular Plant*, 2, 883-892.
- BURTON, R. A. & FINCHER, G. B. 2012. Current challenges in cell wall biology in the cereals and grasses. *Frontiers in Plant Science*, 3, 6.
- BUSSE-WICHER, M., GRANTHAM, N. J., LYCZAKOWSKI, J. J., NIKOLOVSKI, N. & DUPREE, P. 2016. Xylan decoration patterns and the plant secondary cell wall molecular architecture. *Biochemical Society Transactions*, 44, 74-78.
- CARNACHAN, S. M. & HARRIS, P. J. 2000. Ferulic acid is bound to the primary cell walls of all gymnosperm families. *Biochemical Systematics and Ecology*, 28, 865-879.

- CARPITA, N. & MCCANN, M. 2000. The Cell Wall. *In*: BUCHANAN, B. B., GRUISSEM, W. & JONES, R. L. (eds.) *Biochemistry and molecular biology of plants*. USA: the American Society of Plant Physiologists.
- CHANG, S., PURYEAR, J. & CAIRNEY, J. 1993. A simple and efficient method for isolating RNA from pine trees. *Plant Molecular Biology Reporter*, 11, 113-116.
- CHEHAB, E. W., YAO, C., HENDERSON, Z., KIM, S. & BRAAM, J. 2012. Arabidopsis touch-induced morphogenesis is jasmonate mediated and protects against pests. *Current Biology*, 22, 701-706.
- CHINI, A., FONSECA, S., FERNANDEZ, G., ADIE, B., CHICO, J. M., LORENZO, O., GARCIA-CASADO, G., LOPEZ-VIDRIERO, I., LOZANO, F. M., PONCE, M. R., MICOL, J. L. & SOLANO, R. 2007. The JAZ family of repressors is the missing link in jasmonate signalling. *Nature*, 448, 666-U4.
- CHINIQUY, D., SHARMA, V., SCHULTINK, A., BAIDOO, E. E., RAUTENGARTEN, C., CHENG, K., CARROLL, A., ULVSKOV, P., HARHOLT, J., KEASLING, J. D., PAULY, M., SCHELLER, H. V. & RONALD, P. C. 2012. XAX1 from glycosyltransferase family 61 mediates xylosyltransfer to rice xylan. *Proceedings of the National Academy of Sciences of the United States of America*, 109, 17117-22.
- CHINIQUY, D., VARANASI, P., OH, T., HARHOLT, J., KATNELSON, J., SINGH, S., AUER, M., SIMMONS, B., ADAMS, P. D., SCHELLER, H. V. & RONALD, P. C. 2013. Three novel rice genes closely related to the *Arabidopsis* *IRX9*, *IRX9L*, and *IRX14* genes and their roles in xylan biosynthesis. *Frontiers in Plant Science*, 4, 83.
- COLQUHOUN, I. J., RALET, M. C., THIBAUT, J. F., FAULDS, C. B. & WILLIAMSON, G. 1994. Structure identification of feruloylated oligosaccharides from sugar-beet pulp by NMR spectroscopy. *Carbohydrate Research*, 263, 243-256.
- CONESA, A., GOTZ, S., GARCIA-GOMEZ, J. M., TEROL, J., TALON, M. & ROBLES, M. 2005. Blast2GO: a universal tool for annotation, visualization and analysis in functional genomics research. *Bioinformatics*, 21, 3674-3676.
- COUTINHO, P. M., DELEURY, E., DAVIES, G. J. & HENRISSAT, B. 2003. An evolving hierarchical family classification for glycosyltransferases. *Journal of Molecular Biology*, 328, 307-317.
- CREELMAN, R. A. & MULLET, J. E. 1995. Jasmonic acid distribution and action in plants: regulation during development and response to biotic and abiotic stress. *Proceedings of the National Academy of Sciences of the United States of America*, 92, 4114-4119.
- D'AURIA, J. C. 2006. Acyltransferases in plants: a good time to be BAHD. *Current Opinion in Plant Biology*, 9, 331-340.
- DE ASCENSAO, A. & DUBERY, I. A. 2003. Soluble and wall-bound phenolics and phenolic polymers in *Musa acuminata* roots exposed to elicitors from *Fusarium oxysporum* f.sp. *cubense*. *Phytochemistry*, 63, 679-686.
- DE OLIVEIRA, D. M., FINGER-TEIXEIRA, A., MOTA, T. R., SALVADOR, V. H., MOREIRA-VILAR, F. C., MOLINARI, H. B. C., MITCHELL, R. A. C., MARCHIOSI, R., FERRARESE, O. & DOS SANTOS, W. D. 2015. Ferulic acid: a key component in grass lignocellulose recalcitrance to hydrolysis. *Plant Biotechnology Journal*, 13, 1224-1232.

- DHUGGA, K. S. 2007. Maize biomass yield and composition for biofuels. *Crop Science*, 47, 2211-2227.
- DOBBERSTEIN, D. & BUNZEL, M. 2010a. Identification of ferulate oligomers from corn stover. *Journal of the Science of Food and Agriculture*, 90, 1802-1810.
- DOBBERSTEIN, D. & BUNZEL, M. 2010b. Separation and detection of cell wall-bound ferulic acid dehydrodimers and dehydrotrimers in cereals and other plant materials by reversed phase high-performance liquid chromatography with ultraviolet detection. *Journal of Agricultural and Food Chemistry*, 58, 8927-8935.
- DRAPER, J., MUR, L. A. J., JENKINS, G., GHOSH-BISWAS, G. C., BABLAK, P., HASTEROK, R. & ROUTLEDGE, A. P. M. 2001. *Brachypodium distachyon*. A new model system for functional genomics in grasses. *Plant Physiology*, 127, 1539-1555.
- EBRINGEROVA, A. 2006. Structural diversity and application potential of hemicelluloses. *Macromolecular Symposia*, 232, 1-12.
- EBRINGEROVA, A. & HEINZE, T. 2000. Naturally occurring xylans structures, isolation procedures and properties. *Macromolecular Rapid Communications*, 21, 542-556.
- ECKARDT, N. A. 2004. What makes a grass? Drooping leaf influences flower and leaf development in rice *The Plant Cell*, 16, 291-293.
- EDGAR, R. C. 2004. MUSCLE: multiple sequence alignment with high accuracy and high throughput. *Nucleic Acids Research*, 32, 1792-1797.
- ENGLYST, H. N., QUIGLEY, M. E. & HUDSON, G. J. 1994. Determination of dietary fibre as non-starch polysaccharides with gas-liquid chromatographic, high-performance liquid chromatographic or spectrophotometric measurement of constituent sugars. *Analyst*, 119, 1497-509.
- ERNER, Y. & JAFFE, M. J. 1982. Thigmomorphogenesis: the involvement of auxin and abscisic acid in growth retardation due to mechanical perturbation. *Plant and Cell Physiology*, 23, 935-941.
- FAO 2013. Food and agriculture organisation of the united nations statistics division, available at: <http://faostat3.fao.org/>. Last accessed Sep 2016.
- FINCHER, G. B. 2009. Revolutionary times in our understanding of cell wall biosynthesis and remodeling in the grasses. *Plant Physiology*, 149, 27-37.
- FISCHER, M. H., YU, N. X., GRAY, G. R., RALPH, J., ANDERSON, L. & MARLETT, J. A. 2004. The gel-forming polysaccharide of psyllium husk (*Plantago ovata* Forsk). *Carbohydrate Research*, 339, 2009-2017.
- FLINT-GARCIA, S. A., JAMPATONG, C., DARRAH, L. L. & MCMULLEN, M. D. 2003. Quantitative trait locus analysis of stalk strength in four maize populations. *Crop Science*, 43, 13-22.
- FOSTER, C. E., MARTIN, T. M. & PAULY, M. 2010. Comprehensive compositional analysis of plant cell walls (lignocellulosic biomass) part I: lignin. *Journal of visualized experiments : JoVE*, e1745.
- FRY, S. C. 1982. Phenolic components of the primary cell wall: feruloylated disaccharides of D-galactose and L-arabinose from spinach polysaccharide. *Biochemical Journal*, 203, 493-504.

- FRY, S. C., WILLIS, S. C. & PATERSON, A. E. J. 2000. Intraprotoplasmic and wall-localised formation of arabinoxylan-bound diferulates and larger ferulate coupling-products in maize cell-suspension cultures. *Planta*, 211, 679-692.
- GARVIN, D. F., GU, Y. Q., HASTEROK, R., HAZEN, S. P., JENKINS, G., MOCKLER, T. C., MUR, L. A. J. & VOGEL, J. P. 2008. Development of genetic and genomic research resources for *Brachypodium distachyon*, a new model system for grass crop research. *Crop Science*, 48, S-69-S-84.
- GIARDINE, B., RIEMER, C., HARDISON, R. C., BURHANS, R., ELNITSKI, L., SHAH, P., ZHANG, Y., BLANKENBERG, D., ALBERT, I., TAYLOR, J., MILLER, W., KENT, W. J. & NEKRUTENKO, A. 2005. Galaxy: A platform for interactive large-scale genome analysis. *Genome Research*, 15, 1451-1455.
- GIRIN, T., DAVID, L. C., CHARDIN, C., SIBOUT, R., KRAPP, A., FERRARIO-MERY, S. & DANIEL-VEDELE, F. 2014. *Brachypodium*: a promising hub between model species and cereals. *Journal of Experimental Botany*, 65, 5683-5696.
- GOMEZ, L. D., WHITEHEAD, C., ROBERTS, P. & MCQUEEN-MASON, S. J. 2011. High-throughput Saccharification assay for lignocellulosic materials. *Journal of Visualized Experiments : JoVE*, 53, e3240.
- GOODSTEIN, D. M., SHU, S. Q., HOWSON, R., NEUPANE, R., HAYES, R. D., FAZO, J., MITROS, T., DIRKS, W., HELLSTEN, U., PUTNAM, N. & ROKHSAR, D. S. 2012. Phytozome: a comparative platform for green plant genomics. *Nucleic Acids Research*, 40, D1178-D1186.
- GOUBET, F., BARTON, C. J., MORTIMER, J. C., YU, X., ZHANG, Z., MILES, G. P., RICHENS, J., LIEPMAN, A. H., SEFFEN, K. & DUPREE, P. 2009. Cell wall glucomannan in Arabidopsis is synthesised by CSLA glycosyltransferases, and influences the progression of embryogenesis. *The Plant Journal*, 60, 527-38.
- GOUBET, F., JACKSON, P., DEERY, M. J. & DUPREE, P. 2002. Polysaccharide analysis using carbohydrate gel electrophoresis: A method to study plant cell wall polysaccharides and polysaccharide hydrolases. *Analytical Biochemistry*, 300, 53-68.
- GRABBER, J. H. 2005. How do lignin composition, structure, and cross-linking affect degradability? A review of cell wall model studies. *Crop Science*, 45, 820-831.
- GRABBER, J. H., HATFIELD, R. D. & RALPH, J. 1998a. Diferulate cross-links impede the enzymatic degradation of non-lignified maize walls. *Journal of the Science of Food and Agriculture*, 77, 193-200.
- GRABBER, J. H., HATFIELD, R. D., RALPH, J., ZON, J. & AMRHEIN, N. 1995. Ferulate cross-linking in cell-walls isolated from maize cell-suspensions. *Phytochemistry*, 40, 1077-1082.
- GRABBER, J. H., RALPH, J. & HATFIELD, R. D. 1998b. Ferulate cross-links limit the enzymatic degradation of synthetically lignified primary walls of maize. *Journal of Agricultural and Food Chemistry*, 46, 2609-2614.
- GRABBER, J. H., RALPH, J. & HATFIELD, R. D. 2000. Cross-linking of maize walls by ferulate dimerization and incorporation into lignin. *Journal of Agricultural and Food Chemistry*, 48, 6106-6113.
- GRABBER, J. H., RALPH, J. & HATFIELD, R. D. 2002. Model studies of ferulate-coniferyl alcohol cross-product formation in primary maize walls: Implications

- for lignification in grasses. *Journal of Agricultural and Food Chemistry*, 50, 6008-6016.
- GRABBER, J. H., RALPH, J., LAPIERRE, C. & BARRIERE, Y. 2004. Genetic and molecular basis of grass cell-wall degradability. I. Lignin-cell wall matrix interactions. *Comptes Rendus Biologies*, 327, 455-465.
- GUERRIERO, G., HAUSMAN, J. F. & LEGAY, S. 2016. Silicon and the plant extracellular matrix. *Frontiers in Plant Science*, 7, 463.
- GUINDON, S. & GASCUEL, O. 2003. A simple, fast, and accurate algorithm to estimate large phylogenies by maximum likelihood. *Systematic Biology*, 52, 696-704.
- GUO, Q., CUI, S. W., WANG, Q. & YOUNG, J. C. 2008. Fractionation and physicochemical characterization of psyllium gum. *Carbohydrate Polymers*, 73, 35-43.
- HARHOLT, J., JENSEN, J. K., SORENSEN, S. O., ORFILA, C., PAULY, M. & SCHELLER, H. V. 2006. ARABINAN DEFICIENT 1 is a putative arabinosyltransferase involved in biosynthesis of pectic arabinan in arabidopsis. *Plant Physiology*, 140, 49-58.
- HARHOLT, J., SORENSEN, I., FANGEL, J., ROBERTS, A., WILLATS, W. G. T., SCHELLER, H. V., PETERSEN, B. L., BANKS, A. & ULVSKOV, P. 2012. The glycosyltransferase repertoire of the spikemoss *Selaginella moellendorffii* and a comparative study of its cell wall. *Plos One*, 7, e35846.
- HARRIS, P. J. & HARTLEY, R. D. 1976. Detection of bound ferulic acid in cell-walls of Gramineae by ultraviolet fluorescence microscopy. *Nature*, 259, 508-510.
- HARTLEY, R. D. 1972. *p*-coumaric and ferulic acid components of cell-walls of ryegrass and their relationships with lignin and digestibility. *Journal of the Science of Food and Agriculture*, 23, 1347-1354.
- HATCHER, P. E., PAUL, N. D., AYRES, P. G. & WHITTAKER, J. B. 1994. Interactions between *Rumex* spp., herbivores and a rust fungus: *Gastrophysa viridula* grazing reduces subsequent infection by *Uromyces rumicis*. *Functional Ecology*, 8, 265-272.
- HATFIELD, R., RALPH, J. & GRABBER, J. H. 2008. A potential role for sinapyl *p*-coumarate as a radical transfer mechanism in grass lignin formation. *Planta*, 228, 919-928.
- HATFIELD, R. D., RALPH, J. & GRABBER, J. H. 1999. Cell wall cross-linking by ferulates and diferulates in grasses. *Journal of the Science of Food and Agriculture*, 79, 403-407.
- HORNBLAD, E., ULFSTEDT, M., RONNE, H. & MARCHANT, A. 2013. Partial functional conservation of IRX10 homologs in *Physcomitrella patens* and *Arabidopsis thaliana* indicates an evolutionary step contributing to vascular formation in land plants. *Bmc Plant Biology*, 13, 3.
- HUBBARD, T., BARKER, D., BIRNEY, E., CAMERON, G., CHEN, Y., CLARK, L., COX, T., CUFF, J., CURWEN, V., DOWN, T., DURBIN, R., EYRAS, E., GILBERT, J., HAMMOND, M., HUMINIECKI, L., KASPRZYK, A., LEHVASLAIHO, H., LIJNZAAD, P., MELSOPP, C., MONGIN, E., PETTETT, R., POCOCK, M., POTTER, S., RUST, A., SCHMIDT, E., SEARLE, S., SLATER, G., SMITH, J., SPOONER, W., STABENAU, A., STALKER, J.,

- STUPKA, E., URETA-VIDAL, A., VASTRIK, I. & CLAMP, M. 2002. The Ensembl genome database project. *Nucleic Acids Research*, 30, 38-41.
- IYAMA, K., LAM, T. B. T. & STONE, B. A. 1990. Phenolic-acid bridges between polysaccharides and lignin in wheat internodes. *Phytochemistry*, 29, 733-737.
- INTERNATIONAL BRACHYPODIUM INITIATIVE 2010. Genome sequencing and analysis of the model grass *Brachypodium distachyon*. *Nature*, 463, 763-768.
- IPCC 2014. *Climate Change 2014: Synthesis Report. Contribution of Working Groups I, II and III to the Fifth Assessment Report of the Intergovernmental Panel on Climate Change [Core Writing Team, R.K. Pachauri and L.A. Meyer (eds.)]*. , Geneva, Switzerland, IPCC.
- ISHII, T. 1991. Isolation and characterisation of a diferuloyl arabinoxylan hexasaccharide from bamboo shoot cell-walls. *Carbohydrate Research*, 219, 15-22.
- ISHII, T. 1997. Structure and functions of feruloylated polysaccharides. *Plant Science*, 127, 111-127.
- ISHII, T. & HIROI, T. 1990. Isolation and characterization of feruloylated arabinoxylan oligosaccharides from bamboo shoot cell-walls. *Carbohydrate Research*, 196, 175-183.
- ISHII, T., HIROI, T. & THOMAS, J. R. 1990. Feruloylated xyloglucan and *para*-coumaroyl arabinoxylan oligosaccharides from bamboo shoot cell-walls. *Phytochemistry*, 29, 1999-2003.
- IZYDORCZYK, M. S. & BILIADERIS, C. G. 1995. Cereal arabinoxylans: Advances in structure and physicochemical properties. *Carbohydrate Polymers*, 28, 33-48.
- JACQUET, G., POLLET, B. & LAPIERRE, C. 1995. New ether-linked ferulic acid-coniferyl alcohol dimers identified in grass straws. *Journal of Agricultural and Food Chemistry*, 43, 2746-2751.
- JAFFE, M. J. 1973. Thigmomorphogenesis: The response of plant growth and development to mechanical stimulation. With special reference to *Bryonia dioica*. *Planta*, 114, 143-157.
- JAFFE, M. J. & FORBES, S. 1993. Thigmomorphogenesis: the effect of mechanical perturbation on plants. *Plant Growth Regulation*, 12, 313-324.
- JENSEN, J. K., JOHNSON, N. & WILKERSON, C. G. 2013. Discovery of diversity in xylan biosynthetic genes by transcriptional profiling of a heteroxylan containing mucilaginous tissue. *Frontiers in Plant Science*, 4, 183.
- JENSEN, J. K., JOHNSON, N. R. & WILKERSON, C. G. 2014. *Arabidopsis thaliana* IRX10 and two related proteins from psyllium and *Physcomitrella patens* are xylan xylosyltransferases. *Plant Journal*, 80, 207-215.
- JENSEN, J. K., KIM, H., COCUNON, J. C., ORLER, R., RALPH, J. & WILKERSON, C. G. 2011. The DUF579 domain containing proteins IRX15 and IRX15-L affect xylan synthesis in *Arabidopsis*. *Plant Journal*, 66, 387-400.
- JIANG, N., WIEMELS, R. E., SOYA, A., WHITLEY, R., HELD, M. & FAIK, A. 2016. Composition, assembly, and trafficking of a wheat xylan synthase complex. *Plant Physiology*, 170, 1999-2023.
- JIANG, W. Z., ZHOU, H. B., BI, H. H., FROMM, M., YANG, B. & WEEKS, D. P. 2013. Demonstration of CRISPR/Cas9/sgRNA-mediated targeted gene

- modification in Arabidopsis, tobacco, sorghum and rice. *Nucleic Acids Research*, 41.
- JONES, L., MILNE, J. L., ASHFORD, D. & MCQUEEN-MASON, S. J. 2003. Cell wall arabinan is essential for guard cell function. *Proceedings of the National Academy of Sciences of the United States of America*, 100, 11783-11788.
- JONES, R. S. & MITCHELL, C. A. 1989. Calcium-ion involvement in growth-inhibition of mechanically stressed soybean (*Glycine max*) seedlings. *Physiologia Plantarum*, 76, 598-602.
- JUNG, H. G., MERTENS, D. R. & PHILLIPS, R. L. 2011. Effect of reduced ferulate-mediated lignin/arabinoxylan cross-linking in corn silage on feed intake, digestibility, and milk production. *Journal of Dairy Science*, 94, 5124-5137.
- JUNG, H. J. G., SAMAC, D. A. & SARATH, G. 2012. Modifying crops to increase cell wall digestibility. *Plant Science*, 185, 65-77.
- KAHN-JETTER, Z., EVANS, L. S., GRZAN, J. & FRENZ, C. 2000. Compressive/tensile stresses and lignified cells as resistance components in joints between cladodes of *Opuntia laevis* (Cactaceae). *International Journal of Plant Sciences*, 161, 447-462.
- KANEHISA, M., SATO, Y., KAWASHIMA, M., FURUMICHI, M. & TANABE, M. 2016. KEGG as a reference resource for gene and protein annotation. *Nucleic Acids Research*, 44, D457-D462.
- KASHIWAGI, T., MUNAKATA, J. & ISHIMARU, K. 2016. Functional analysis of the lodging resistance QTL *BSUC11* on morphological and chemical characteristics in upper culms of rice. *Euphytica*, 210, 233-243.
- KEARSE, M., MOIR, R., WILSON, A., STONES-HAVAS, S., CHEUNG, M., STURROCK, S., BUXTON, S., COOPER, A., MARKOWITZ, S., DURAN, C., THIERER, T., ASHTON, B., MEINTJES, P. & DRUMMOND, A. 2012. Geneious Basic: An integrated and extendable desktop software platform for the organization and analysis of sequence data. *Bioinformatics*, 28, 1647-1649.
- KELLOGG, E. A. 2001. Evolutionary history of the grasses. *Plant Physiology*, 125, 1198-1205.
- KEPPLER, B. D. & SHOWALTER, A. M. 2010. IRX14 and IRX14-LIKE, two glycosyl transferases involved in glucuronoxylan biosynthesis and drought tolerance in *Arabidopsis*. *Molecular Plant*, 3, 834-841.
- KERSEY, P. J., ALLEN, J. E., ARMEAN, I., BODDU, S., BOLT, B. J., CARVALHO-SILVA, D., CHRISTENSEN, M., DAVIS, P., FALIN, L. J., GRABMUELLER, C., HUMPHREY, J., KERHORNOU, A., KHOBOVA, J., ARANGANATHAN, N. K., LANGRIDGE, N., LOWY, E., MCDOWALL, M. D., MAHESWARI, U., NUHN, M., ONG, C. K., OVERDUIN, B., PAULINI, M., PEDRO, H., PERRY, E., SPUDICH, G., TAPANARI, E., WALTZ, B., WILLIAMS, G., TELLO-RUIZ, M., STEIN, J., WEI, S., WARE, D., BOLSER, D. M., HOWE, K. L., KULESHA, E., LAWSON, D., MASLEN, G. & STAINES, D. M. 2016. Ensembl Genomes 2016: more genomes, more complexity. *Nucleic Acids Research*, 44, D574-D580.
- KNIGHT, M. R., SMITH, S. M. & TREWAVAS, A. J. 1992. Wind-induced plant motion immediately increases cytosolic calcium. *Proceedings of the National Academy of Sciences of the United States of America*, 89, 4967-4971.

- KONISHI, T., TAKEDA, T., MIYAZAKI, Y., OHNISHI-KAMEYAMA, M., HAYASHI, T., O'NEILL, M. A. & ISHII, T. 2007. A plant mutase that interconverts UDP-arabinofuranose and UDP-arabinopyranose. *Glycobiology*, 17, 345-354.
- KROON, P. A. & WILLIAMSON, G. 1996. Release of ferulic acid from sugar-beet pulp by using arabinanase, arabinofuranosidase and an esterase from *Aspergillus niger*. *Biotechnology and Applied Biochemistry*, 23, 263-267.
- KUMAR, P., BARRETT, D. M., DELWICHE, M. J. & STROEVE, P. 2009. Methods for pretreatment of lignocellulosic biomass for efficient hydrolysis and biofuel production. *Industrial & Engineering Chemistry Research*, 48, 3713-3729.
- LAM, T. B. T., IYAMA, K. & STONE, B. A. 1990. Distribution of free and combined phenolic acids in wheat internodes. *Phytochemistry*, 29, 429-433.
- LANGE, M. J. P. & LANGE, T. 2015. Touch-induced changes in Arabidopsis morphology dependent on gibberellin breakdown. *Nature Plants*, 1, Article number: 14025.
- LEE, C., O'NEILL, M. A., TSUMURAYA, Y., DARVILL, A. G. & YE, Z. H. 2007a. The *irregular xylem 9* mutant is deficient in xylan xylosyltransferase activity. *Plant and Cell Physiology*, 48, 1624-1634.
- LEE, C., TENG, Q., ZHONG, R. Q. & YE, Z. H. 2012. Arabidopsis GUX proteins are glucuronyltransferases responsible for the addition of glucuronic acid side chains onto xylan. *Plant and Cell Physiology*, 53, 1204-1216.
- LEE, C. H., TENG, Q., HUANG, W. L., ZHONG, R. Q. & YE, Z. H. 2009. The F8H glycosyltransferase is a functional paralog of FRA8 involved in glucuronoxylan biosynthesis in arabidopsis. *Plant and Cell Physiology*, 50, 812-827.
- LEE, C. H., ZHONG, R. Q., RICHARDSON, E. A., HIMMELSBACH, D. S., MCPHAIL, B. T. & YE, Z. H. 2007b. The *PARVUS* gene is expressed in cells undergoing secondary wall thickening and is essential for glucuronoxylan biosynthesis. *Plant and Cell Physiology*, 48, 1659-1672.
- LEE, D., POLISENSKY, D. H. & BRAAM, J. 2005. Genome-wide identification of touch- and darkness-regulated Arabidopsis genes: a focus on calmodulin-like and *XTH* genes. *New Phytologist*, 165, 429-444.
- LEE, H. Y., SEO, J. S., CHO, J. H., JUNG, H., KIM, J. K., LEE, J. S., RHEE, S. & CHOI, Y. D. 2013. *Oryza sativa* *COI* homologues restore jasmonate signal transduction in *Arabidopsis coi1-1* mutants. *Plos One*, 8, 9.
- LEE, J. E., VOGT, T., HAUSE, B. & LOBLER, M. 1997. Methyl jasmonate induces an *O*-Methyltransferase in barley. *Plant and Cell Physiology*, 38, 851-862.
- LI, F. C., ZHANG, M. L., GUO, K., HU, Z., ZHANG, R., FENG, Y. Q., YI, X. Y., ZOU, W. H., WANG, L. Q., WU, C. Y., TIAN, J. S., LU, T. G., XIE, G. S. & PENG, L. C. 2015. High-level hemicellulosic arabinose predominately affects lignocellulose crystallinity for genetically enhancing both plant lodging resistance and biomass enzymatic digestibility in rice mutants. *Plant Biotechnology Journal*, 13, 514-525.
- LI, L., SHEWRY, P. R. & WARD, J. L. 2008. Phenolic Acids in Wheat Varieties in the HEALTHGRAIN Diversity Screen. *Journal of Agricultural and Food Chemistry*, 56, 9732-9739.

- LOCHER, R., MARTIN, H. V., GRISON, R. & PILET, P. E. 1994. Cell wall-bound *trans*-ferulic and *cis*-ferulic acids in growing maize roots. *Physiologia Plantarum*, 90, 734-738.
- LOVEGROVE, A., WILKINSON, M. D., FREEMAN, J., PELLNY, T. K., TOSI, P., SAULNIER, L., SHEWRY, P. R. & MITCHELL, R. A. C. 2013. RNA interference suppression of genes in glycosyl transferase families 43 and 47 in wheat starchy endosperm causes large decreases in arabinoxylan content. *Plant Physiology*, 163, 95-107.
- MA, J. F. 2004. Role of silicon in enhancing the resistance of plants to biotic and abiotic stresses. *Soil Science and Plant Nutrition*, 50, 11-18.
- MA, J. F. & YAMAJI, N. 2006. Silicon uptake and accumulation in higher plants. *Trends in Plant Science*, 11, 392-397.
- MACADAM, J. W. & GRABBER, J. H. 2002. Relationship of growth cessation with the formation of diferulate cross-links and *p*-coumaroylated lignins in tall fescue leaf blades. *Planta*, 215, 785-793.
- MARKWALDER, H. U. & NEUKOM, H. 1976. Diferulic acid as a possible crosslink in hemicelluloses from wheat-germ. *Phytochemistry*, 15, 836-837.
- MARRIOTT, P. E., GOMEZ, L. D. & MCQUEEN-MASON, S. J. 2016. Unlocking the potential of lignocellulosic biomass through plant science. *New Phytologist*, 209, 1366-1381.
- MASSEY, F. P., ENNOS, A. R. & HARTLEY, S. E. 2007. Herbivore specific induction of silica-based plant defences. *Oecologia*, 152, 677-683.
- MASTRANGELO, L., LENUCCI, M., PIRO, G. & DALESSANDRO, G. 2009. Evidence for intra- and extra-protoplasmic feruloylation and cross-linking in wheat seedling roots. *Planta*, 229, 343-355.
- MELIDA, H., LARGO-GOSENS, A., NOVO-UZAL, E., SANTIAGO, R., POMAR, F., GARCIA, P., GARCIA-ANGULO, P., ACEBES, J. L., ALVAREZ, J. & ENCINA, A. 2015. Ectopic lignification in primary cellulose-deficient cell walls of maize cell suspension cultures. *Journal of Integrative Plant Biology*, 57, 357-372.
- MERALI, Z., MAYER, M. J., PARKER, M. L., MICHAEL, A. J., SMITH, A. C. & WALDRON, K. W. 2007. Metabolic diversion of the phenylpropanoid pathway causes cell wall and morphological changes in transgenic tobacco stems. *Planta*, 225, 1165-1178.
- MEYER, K., KOHLER, A. & KAUSS, H. 1991. Biosynthesis of ferulic acid esters of plant cell wall polysaccharides in endomembranes from parsley cells. *FEBS Letters*, 290, 209-212.
- MIKKELSEN, M. D., HARHOLT, J., ULVSKOV, P., JOHANSEN, I. E., FANGEL, J. U., DOBLIN, M. S., BACIC, A. & WILLATS, W. G. T. 2014. Evidence for land plant cell wall biosynthetic mechanisms in charophyte green algae. *Annals of Botany*, 114, 1217-1236.
- MITCHELL, C. A. 1996. Recent advances in plant response to mechanical stress: Theory and application. *Hortscience*, 31, 31-35.
- MITCHELL, C. A., SEVERSON, C. J., WOTT, J. A. & HAMMER, P. A. 1975. SEISMOMORPHOGENIC REGULATION OF PLANT-GROWTH. *Journal of the American Society for Horticultural Science*, 100, 161-165.

- MITCHELL, R. A. C., DUPREE, P. & SHEWRY, P. R. 2007. A novel bioinformatics approach identifies candidate genes for the synthesis and feruloylation of arabinoxylan. *Plant Physiology*, 144, 43-53.
- MOLINARI, H. B., PELLNY, T. K., FREEMAN, J., SHEWRY, P. R. & MITCHELL, R. A. 2013. Grass cell wall feruloylation: distribution of bound ferulate and candidate gene expression in *Brachypodium distachyon*. *Frontiers in Plant Science*, 4, 50.
- MOORE, J. P., PAUL, N. D., WHITTAKER, J. B. & TAYLOR, J. E. 2003. Exogenous jasmonic acid mimics herbivore-induced systemic increase in cell wall bound peroxidase activity and reduction in leaf expansion. *Functional Ecology*, 14, 549-554.
- MORTIMER, J. C., FARIA-BLANC, N., YU, X. L., TRYFONA, T., SORIEUL, M., NG, Y. Z., ZHANG, Z. N., STOTT, K., ANDERS, N. & DUPREE, P. 2015. An unusual xylan in Arabidopsis primary cell walls is synthesised by GUX3, IRX9L, IRX10L and IRX14. *Plant Journal*, 83, 413-527.
- MORTIMER, J. C., MILES, G. P., BROWN, D. M., ZHANG, Z. N., SEGURA, M. P., WEIMAR, T., YU, X. L., SEFFEN, K. A., STEPHENS, E., TURNER, S. R. & DUPREE, P. 2010. Absence of branches from xylan in Arabidopsis *gux* mutants reveals potential for simplification of lignocellulosic biomass. *Proceedings of the National Academy of Sciences of the United States of America*, 107, 17409-17414.
- MUELLER-HARVEY, I. & HARTLEY, R. D. 1986. Linkage of *p*-coumaroyl and feruloyl groups to cell wall polysaccharides of barley straw. *Carbohydrate research*, 148, 71-85.
- MYTON, K. E. & FRY, S. C. 1994. Intraprotoplasmic feruloylation of arabinoxylans in *Festuca arundinacea* cell cultures. *Planta*, 193, 326-330.
- NIGAM, P. S. & SINGH, A. 2011. Production of liquid biofuels from renewable resources. *Progress in Energy and Combustion Science*, 37, 52-68.
- OPANOWICZ, M., VAIN, P., DRAPER, J., PARKER, D. & DOONAN, J. H. 2008. *Brachypodium distachyon*: making hay with a wild grass. *Trends in Plant Science*, 13, 172-177.
- PARR, A. J., NG, A. & WALDRON, K. W. 1997. Ester-linked phenolic components of carrot cell walls. *Journal of Agricultural and Food Chemistry*, 45, 2468-2471.
- PARR, A. J., WALDRON, K. W., NG, A. & PARKER, M. L. 1996. The wall-bound phenolics of Chinese water chestnut (*Eleocharis dulcis*). *Journal of the Science of Food and Agriculture*, 71, 501-507.
- PAUWELS, L., MORREEL, K., DE WITTE, E., LAMMERTYN, F., VAN MONTAGU, M., BOERJAN, W., INZE, D. & GOOSSENS, A. 2008. Mapping methyl jasmonate-mediated transcriptional reprogramming of metabolism and cell cycle progression in cultured *Arabidopsis* cells. *Proceedings of the National Academy of Sciences of the United States of America*, 105, 1380-1385.
- PEAR, J. R., KAWAGOE, Y., SCHRECKENGOST, W. E., DELMER, D. P. & STALKER, D. M. 1996. Higher plants contain homologs of the bacterial *celA* genes encoding the catalytic subunit of cellulose synthase. *Proceedings of the National Academy of Sciences of the United States of America*, 93, 12637-12642.

- PELLNY, T. K., LOVEGROVE, A., FREEMAN, J., TOSI, P., LOVE, C. G., KNOX, J. P., SHEWRY, P. R. & MITCHELL, R. A. C. 2012. Cell walls of developing wheat starchy endosperm: comparison of composition and RNA-seq transcriptome. *Plant Physiology*, 158, 612-627.
- PENA, M. J., ZHONG, R. Q., ZHOU, G. K., RICHARDSON, E. A., O'NEILL, M. A., DARVILL, A. G., YORK, W. S. & YE, Z. H. 2007. *Arabidopsis irregular xylem8* and *irregular xylem9*: Implications for the complexity of glucuronoxyylan biosynthesis. *Plant Cell*, 19, 549-563.
- PERSSON, S., CAFFALL, K. H., FRESHOUR, G., HILLEY, M. T., BAUER, S., POINDEXTER, P., HAHN, M. G., MOHNEN, D. & SOMERVILLE, C. 2007. The *Arabidopsis irregular xylem8* mutant is deficient in glucuronoxyylan and homogalacturonan, which are essential for secondary cell wall integrity. *Plant Cell*, 19, 237-255.
- PETRIK, D. L., KARLEN, S. D., CASS, C. L., PADMAKSHAN, D., LU, F. C., LIU, S., LE BRIS, P., ANTELME, S., SANTORO, N., WILKERSON, C. G., SIBOUT, R., LAPIERRE, C., RALPH, J. & SEDBROOK, J. C. 2014. *p*-Coumaroyl-CoA:monolignol transferase (PMT) acts specifically in the lignin biosynthetic pathway in *Brachypodium distachyon*. *Plant Journal*, 77, 713-726.
- PISTON, F., UAUY, C., FU, L. H., LANGSTON, J., LABAVITCH, J. & DUBCOVSKY, J. 2010. Down-regulation of four putative arabinoxyylan feruloyl transferase genes from family PF02458 reduces ester-linked ferulate content in rice cell walls. *Planta*, 231, 677-691.
- POPPER, Z. A., MICHEL, G., HERVE, C., DOMOZYCH, D. S., WILLATS, W. G. T., TUOHY, M. G., KLOAREG, B. & STENGEL, D. B. 2011. Evolution and diversity of plant cell walls: from algae to flowering plants. *Annual Review of Plant Biology*, 62, 567-588.
- RALPH, J. 2010. Hydroxycinnamates in lignification. *Phytochemistry Reviews*, 9, 65-83.
- RALPH, J., BUNZEL, M., MARITA, J. M., HATFIELD, R. D., LU, F., KIM, H., SCHATZ, P. F., GRABBER, J. H. & STEINHART, H. 2004. Peroxidase-dependent cross-linking reactions of *p*-hydroxycinnamates in plant cell walls. *Phytochemistry Reviews*, 3, 79-96.
- RALPH, J., GRABBER, J. H. & HATFIELD, R. D. 1995. Lignin-ferulate cross-links in grasses: active incorporation of ferulate polysaccharide esters into ryegrass lignins. *Carbohydrate Research*, 275, 167-178.
- RALPH, J., QUIDEAU, S., GRABBER, J. H. & HATFIELD, R. D. 1994. Identification and synthesis of new ferulic acid dehydrodimers present in grass cell-walls. *Journal of the Chemical Society-Perkin Transactions 1*, 3485-3498.
- RANCOUR, D. M., MARITA, J. M. & HATFIELD, R. D. 2012. Cell wall composition throughout development for the model grass *Brachypodium distachyon*. *Frontiers in Plant Science*, 3, 266.
- RATKE, C., PAWAR, P. M. A., BALASUBRAMANIAN, V. K., NAUMANN, M., DUNCRANZ, M. L., DERBA-MACELUCH, M., GORZASAS, A., ENDO, S., EZCURRA, I. & MELLEROWICZ, E. J. 2015. *Populus GT43* family members group into distinct sets required for primary and secondary wall xylan biosynthesis and include useful promoters for wood modification. *Plant Biotechnology Journal*, 13, 26-37.

- REIDINGER, S., RAMSEY, M. H. & HARTLEY, S. E. 2012. Rapid and accurate analyses of silicon and phosphorus in plants using a portable X-ray fluorescence spectrometer. *New Phytologist*, 195, 699-706.
- REN, Y. F., HANSEN, S. F., EBERT, B., LAU, J. & SCHELLER, H. V. 2014. Site-directed mutagenesis of IRX9, IRX9L and IRX14 proteins involved in xylan biosynthesis: glycosyltransferase activity is not required for IRX9 function in Arabidopsis. *Plos One*, 9, e105014.
- RENARD, C., WENDE, G. & BOOTH, E. J. 1999. Cell wall phenolics and polysaccharides in different tissues of quinoa (*Chenopodium quinoa* Willd). *Journal of the Science of Food and Agriculture*, 79, 2029-2034.
- RENNIE, E. A., HANSEN, S. F., BAIDOO, E. E. K., HADI, M. Z., KEASLING, J. D. & SCHELLER, H. V. 2012. Three members of the Arabidopsis glycosyltransferase family 8 are xylan glucuronosyltransferases. *Plant Physiology*, 159, 1408-1417.
- RENNIE, E. A. & SCHELLER, H. V. 2014. Xylan biosynthesis. *Current Opinion in Biotechnology*, 26, 100-107.
- RODRIGUEZ-ARCOS, R. C., SMITH, A. C. & WALDRON, K. W. 2004. Ferulic acid crosslinks in asparagus cell walls in relation to texture. *Journal of Agricultural and Food Chemistry*, 52, 4740-4750.
- ROUAU, X., CHEYNIER, V., SURGET, A., GLOUX, D., BARRON, C., MEUDEEC, E., LOUIS-MONTERO, J. & CRITON, M. 2003. A dehydrotrimer of ferulic acid from maize bran. *Phytochemistry*, 63, 899-903.
- SALZMAN, R. A., BRADY, J. A., FINLAYSON, S. A., BUCHANAN, C. D., SUMMER, E. J., SUN, F., KLEIN, P. E., KLEIN, R. R., PRATT, L. H., CORDONNIER-PRATT, M. M. & MULLET, J. E. 2005. Transcriptional profiling of sorghum induced by methyl jasmonate, salicylic acid, and aminocyclopropane carboxylic acid reveals cooperative regulation and novel gene responses. *Plant Physiology*, 138, 352-368.
- SANTIAGO, R., BUTRON, A., ARNASON, J. T., REID, L. M., SOUTO, X. C. & MALVAR, R. A. 2006. Putative role of pith cell wall phenylpropanoids in *Sesamia nonagrioides* (Lepidoptera : Noctuidae) resistance. *Journal of Agricultural and Food Chemistry*, 54, 2274-2279.
- SANTIAGO, R., SANDOYA, G., BUTRON, A., BARROS, J. & MALVAR, R. A. 2008. Changes in phenolic concentrations during recurrent selection for resistance to the Mediterranean corn borer (*Sesamia nonagrioides* Lef.). *Journal of Agricultural and Food Chemistry*, 56, 8017-8022.
- SATO, Y., TAKEHISA, H., KAMATSUKI, K., MINAMI, H., NAMIKI, N., IKAWA, H., OHYANAGI, H., SUGIMOTO, K., ANTONIO, B. A. & NAGAMURA, Y. 2013. RiceXPro Version 3.0: expanding the informatics resource for rice transcriptome. *Nucleic Acids Research*, 41, D1206-D1213.
- SAULNIER, L., SADO, P. E., BRANLARD, G., CHARMET, G. & GUILLON, F. 2007. Wheat arabinoxylans: Exploiting variation in amount and composition to develop enhanced varieties. *Journal of Cereal Science*, 46, 261-281.
- SAULNIER, L. & THIBAUT, J. F. 1999. Ferulic acid and diferulic acids as components of sugar-beet pectins and maize bran heteroxylans. *Journal of the Science of Food and Agriculture*, 79, 396-402.

- SAULNIER, L., VIGOUROUX, J. & THIBAUT, J. F. 1995. Isolation and partial characterization of feruloylated oligosaccharides from maize bran. *Carbohydrate Research*, 272, 241-253.
- SCALBERT, A., MONTIES, B., LALLEMAND, J. Y., GUITTET, E. & ROLANDO, C. 1985. Ether linkage between phenolic acids and lignin fractions from wheat straw. *Phytochemistry*, 24, 1359-1362.
- SCHELLER, H. V. & ULVSKOV, P. 2010. Hemicelluloses. *Annual Review of Plant Biology*, 61, 263-89.
- SCHOELYNCK, J., PUIJALON, S., MEIRE, P. & STRUYF, E. 2015. Thigmomorphogenetic responses of an aquatic macrophyte to hydrodynamic stress. *Frontiers in Plant Science*, 6, 43.
- SHETTY, N. P., KRISTENSEN, B. K., NEWMAN, M. A., MOLLER, K., GREGERSEN, P. L. & JORGENSEN, H. J. L. 2003. Association of hydrogen peroxide with restriction of *Septoria tritici* in resistant wheat. *Physiological and Molecular Plant Pathology*, 62, 333-346.
- SHEWRY, P. R. 2009. Wheat. *Journal of Experimental Botany*, 60, 1537-1553.
- SMITH, B. G. & HARRIS, P. J. 2001. Ferulic acid is esterified to glucuronoarabinoxylans in pineapple cell walls. *Phytochemistry*, 56, 513-519.
- SMITH, M. M. & HARTLEY, R. D. 1983. Occurrence and nature of ferulic acid substitution of cell-wall polysaccharides in Gramineous plants. *Carbohydrate Research*, 118, 65-80.
- SOCCOL, C. R., VANDENBERGHE, L. P. D., MEDEIROS, A. B. P., KARP, S. G., BUCKERIDGE, M., RAMOS, L. P., PITARELO, A. P., FERREIRA-LEITAO, V., GOTTSCHALK, L. M. F., FERRARA, M. A., BON, E. P. D., DE MORAES, L. M. P., ARAUJO, J. D. & TORRES, F. A. G. 2010. Bioethanol from lignocelluloses: Status and perspectives in Brazil. *Bioresource Technology*, 101, 4820-4825.
- SUGE, H. 1978. Growth and gibberellin production in *Phaseolus vulgaris* as affected by mechanical stress. *Plant and Cell Physiology*, 19, 1557-1560.
- TAKAHAMA, U., ONIKI, T. & SHIMOKAWA, H. 1996. A possible mechanism for the oxidation of sinapyl alcohol by peroxidase-dependent reactions in the apoplast: Enhancement of the oxidation by hydroxycinnamic acids and components of the apoplast. *Plant and Cell Physiology*, 37, 499-504.
- THINES, B., KATSIR, L., MELOTTO, M., NIU, Y., MANDAOKAR, A., LIU, G. H., NOMURA, K., HE, S. Y., HOWE, G. A. & BROWSE, J. 2007. JAZ repressor proteins are targets of the SCFCO11 complex during jasmonate signalling. *Nature*, 448, 661-665.
- TRAVIS, A. J., MURISON, S. D., HIRST, D. J., WALKER, K. C. & CHESSON, A. 1996. Comparison of the anatomy and degradability of straw from varieties of wheat and barley that differ in susceptibility to lodging. *Journal of Agricultural Science*, 127, 1-10.
- UDDIN, N., HANSTEIN, S., FAUST, F., EITENMULLER, P. T., PITANN, B. & SCHUBERT, S. 2014. Diferulic acids in the cell wall may contribute to the suppression of shoot growth in the first phase of salt stress in maize. *Phytochemistry*, 102, 126-136.

- URBANOWICZ, B. R., PENA, M. J., MONIZ, H. A., MOREMEN, K. W. & YORK, W. S. 2014. Two Arabidopsis proteins synthesize acetylated xylan *in vitro*. *Plant Journal*, 80, 197-206.
- VAIN, P. 2011. *Brachypodium* as a model system for grass research. *Journal of Cereal Science*, 54, 1-7.
- VAN CRAEYVELD, V., DELCOUR, J. A. & COURTIN, C. M. 2009. Extractability and chemical and enzymic degradation of psyllium (*Plantago ovata* Forsk) seed husk arabinoxylans. *Food Chemistry*, 112, 812-819.
- VERBRUGGEN, M. A., SPRONK, B. A., SCHOLS, H. A., BELDMAN, G., VORAGEN, A. G. J., THOMAS, J. R., KAMERLING, J. P. & VLIEGENTHART, J. F. G. 1998. Structures of enzymically derived oligosaccharides from sorghum glucuronoarabinoxylan. *Carbohydrate Research*, 306, 265-274.
- VERHERTBRUGGEN, Y., MARCUS, S. E., CHEN, J. & KNOX, P. 2013. Cell wall pectin arabinans influence the mechanical properties of *Arabidopsis thaliana* inflorescence stems and their response to mechanical stress. *Plant and Cell Physiology*, 54, 1278-1288.
- VILES, F. J. & SILVERMAN, L. 1949. Determination of starch and cellulose with anthrone. *Analytical Chemistry*, 21, 950-953.
- VOGEL, J. 2008. Unique aspects of the grass cell wall. *Current Opinion in Plant Biology*, 11, 301-307.
- VOGEL, J. & HILL, T. 2008. High-efficiency *Agrobacterium*-mediated transformation of *Brachypodium distachyon* inbred line Bd21-3. *Plant Cell Reports*, 27, 471-8.
- VOINICIUC, C., GUNL, M., SCHMIDT, M. H. W. & USADEL, B. 2015. Highly branched xylan made by IRREGULAR XYLEM14 and MUCILAGE-RELATED21 links mucilage to Arabidopsis seeds. *Plant Physiology*, 169, 2481-2495.
- VULETIC, M., SUKALOVIC, V. H. T., MARKOVIC, K., KRAVIC, N., VUCINIC, Z. & MAKSIMOVIC, V. 2014. Differential response of antioxidative systems of maize (*Zea mays* L.) roots cell walls to osmotic and heavy metal stress. *Plant Biology*, 16, 88-96.
- WALDRON, K. W., PARR, A. J., NG, A. & RALPH, J. 1996. Cell wall esterified phenolic dimers: Identification and quantification by reverse phase high performance liquid chromatography and diode array detection. *Phytochemical Analysis*, 7, 305-312.
- WALLACE, G. & FRY, S. C. 1995. *In vitro* peroxidase-catalysed oxidation of ferulic acid esters. *Phytochemistry*, 39, 1293-1299.
- WAN, Y. F., GRITSCH, C., TRYFONA, T., RAY, M. J., ANDONGABO, A., HASSANI-PAK, K., JONES, H. D., DUPREE, P., KARP, A., SHEWRY, P. R. & MITCHELL, R. A. C. 2014. Secondary cell wall composition and candidate gene expression in developing willow (*Salix purpurea*) stems. *Planta*, 239, 1041-1053.
- WASTERNAK, C. & HAUSE, B. 2013. Jasmonates: biosynthesis, perception, signal transduction and action in plant stress response, growth and development. An update to the 2007 review in *Annals of Botany*. *Annals of Botany*, 111, 1021-58.

- WENDE, G. & FRY, S. C. 1997. 2-*O*- β -D-xylopyranosyl-(5-*O*-feruloyl)-L-arabinose, a widespread component of grass cell walls. *Phytochemistry*, 44, 1019-1030.
- WHELAN, S. & GOLDMAN, N. 2001. A general empirical model of protein evolution derived from multiple protein families using a maximum-likelihood approach. *Molecular Biology and Evolution*, 18, 691-699.
- WHITMORE, F. W. 1974. Phenolic acids in wheat coleoptile cell walls. *Plant Physiology*, 53, 728-731.
- WILSON, J. R. & MERTENS, D. R. 1995. Cell wall accessibility and cell structure limitations to microbial digestion of forage. *Crop Science*, 35, 251-259.
- WITHERS, S., LU, F. C., KIM, H., ZHU, Y. M., RALPH, J. & WILKERSON, C. G. 2012. Identification of grass-specific enzyme that acylates monolignols with *p*-coumarate. *Journal of Biological Chemistry*, 287, 8347-8355.
- WORLD RESOURCES INSTITUTE 2000. *A guide to world resources 2000-2001: people and ecosystems: the fraying web of life*, Washington, D.C., USA, World Resources Institute.
- WU, A. M., HORNBLAD, E., VOXEUR, A., GERBER, L., RIHOUEY, C., LEROUGE, P. & MARCHANT, A. 2010. Analysis of the Arabidopsis *IRX9/IRX9-L* and *IRX14/IRX14-L* pairs of glycosyltransferase genes reveals critical contributions to biosynthesis of the hemicellulose glucuronoxylan. *Plant Physiology*, 153, 542-554.
- WU, A. M., RIHOUEY, C., SEVENO, M., HORNBLAD, E., SINGH, S. K., MATSUNAGA, T., ISHII, T., LEROUGE, P. & MARCHANT, A. 2009. The Arabidopsis *IRX10* and *IRX10-LIKE* glycosyltransferases are critical for glucuronoxylan biosynthesis during secondary cell wall formation. *Plant Journal*, 57, 718-731.
- WU, J. S., WANG, L. & BALDWIN, I. T. 2008. Methyl jasmonate-elicited herbivore resistance: does MeJA function as a signal without being hydrolyzed to JA? *Planta*, 227, 1161-1168.
- YAHRAUS, T., CHANDRA, S., LEGENDRE, L. & LOW, P. S. 1995. Evidence for a mechanically induced oxidative burst. *Plant Physiology*, 109, 1259-1266.
- YAMASHITA, S., YOSHIDA, M., TAKAYAMA, S. & OKUYAMA, T. 2007. Stem-righting mechanism in gymnosperm trees deduced from limitations in compression wood development. *Annals of Botany*, 99, 487-493.
- YANG, F., ZHANG, Y., HUANG, Q., YIN, G., PENNERMAN, K. K., YU, J., LI, D. & GUO, A. 2015. Analysis of key genes of jasmonic acid mediated signal pathway for defense against insect damages by comparative transcriptome sequencing. *Scientific Reports*, 5, article no: 16500.
- YORK, W. S. & O'NEILL, M. A. 2008. Biochemical control of xylan biosynthesis - which end is up? *Current Opinion in Plant Biology*, 11, 258-265.
- YUAN, Y., TENG, Q., ZHONG, R. & YE, Z. H. 2015. TBL3 and TBL31, two Arabidopsis DUF231 domain proteins, are required for 3-*O*-monoacetylation of xylan. *Plant and Cell Physiology*, 57, 35-45.
- YUAN, Y. X., TENG, Q., ZHONG, R. Q. & YE, Z. H. 2013. The Arabidopsis DUF231 domain-containing protein ESK1 mediates 2-*O*- and 3-*O*-acetylation of xylosyl residues in xylan. *Plant and Cell Physiology*, 54, 1186-1199.

- ZENG, W., JIANG, N., NADELLA, R., KILLEN, T. L., NADELLA, V. & FAIK, A. 2010. A glucurono(arabino)xylan synthase complex from wheat contains members of the GT43, GT47, and GT75 families and functions cooperatively. *Plant Physiology*, 154, 78-97.
- ZENG, W., LAMPUGNANI, E. R., PICARD, K. L., SONG, L. L., WU, A. M., FARION, I. M., ZHAO, J., FORD, K., DOBLIN, M. S. & BACIC, A. 2016. Asparagus IRX9, IRX10, and IRX14A are components of an active xylan backbone synthase complex that forms in the Golgi apparatus. *Plant Physiology*, 171, 93-109.
- ZHANG, B. L., ZHAO, T. M., YU, W. G., KUANG, B. Q., YAO, Y., LIU, T. L., CHEN, X. Y., ZHANG, W. H. & WU, A. M. 2014. Functional conservation of the glycosyltransferase gene *GT47A* in the monocot rice. *Journal of Plant Research*, 127, 423-432.
- ZHONG, R. Q., PENA, M. J., ZHOU, G. K., NAIRN, C. J., WOOD-JONES, A., RICHARDSON, E. A., MORRISON, W. H., DARVILL, A. G., YORK, W. S. & YE, Z. H. 2005. *Arabidopsis fragile fiber8*, which encodes a putative glucuronyltransferase, is essential for normal secondary wall synthesis. *Plant Cell*, 17, 3390-3408.